



Water Supply Potential of the
Charlestown State Park Aquifer

2011

Prepared by
Layne Hydro
a division of Layne Christensen Company
Bloomington, Indiana

Contents

1	Introduction	1
1.1	Study Purpose	3
1.2	Study Approach	3
1.3	Previous Studies	5
2	Regional Setting	9
2.1	Geology	9
2.1.1	Bedrock	9
2.1.2	Unconsolidated deposits	10
2.2	Groundwater	10
2.3	Surface Water	13
3	Field Investigation	14
3.1	Geophysical Survey	14
3.1.1	Methodology	14
3.1.2	Data analysis	17
3.1.3	Results	21
3.2	Water-level Measurements	21
3.3	Infrastructure Assessment	27
4	Well Field Capacity Evaluation	33
4.1	Mechanical Capacity Estimation	35
4.2	Groundwater Flow Model Development	37
4.2.1	Revised conceptual model of the Aquifer	38
4.2.2	Model features	38
4.2.3	Calibration	45
4.2.4	Comparison of calibrated properties with previous studies	51
4.3	Predictive Modeling and Uncertainty Analysis	58

4.3.1	Preliminary theoretical yield predictions	59
4.3.2	Predictive uncertainty analysis	60
4.3.3	Results of predictive modeling and predictive uncertainty analysis	64
4.4	Conclusions	65
5	Water Quality and Implications for Treatment	67
5.1	Source-Water Quality	67
5.1.1	Iron and manganese	68
5.1.2	Hardness	69
5.1.3	Potential legacy contaminants	69
5.1.4	Mercury	71
5.2	Source-Water Classification	73
5.3	Treatment Recommendations	76
6	Alternative Analysis	78
6.1	Conceptual Design of Alternatives	78
6.2	Alternative Analysis	78
6.3	Conceptual Cost Estimates	82
7	Conclusions and Recommendations	84
7.1	Yield	84
7.1.1	Sustainable Capacity	84
7.1.2	Further evaluation of the south end of Well Field	84
7.2	Water Quality and Treatment Requirements	85
7.2.1	Water origin	85
7.2.2	Source water classification	86
7.2.3	Riverbank filtration	86
7.2.4	Engineered treatment requirements	86
7.3	Water Supply Development and Operation	87

7.3.1	Infrastructure	87
7.3.2	Water demand	88
7.3.3	Collector well improvement alternatives	88
7.3.4	Water quality monitoring & protection	88
7.3.5	Impacts on neighboring wells	89
7.3.6	Well field performance monitoring	90
7.3.7	Optimization of collector well design	90
7.3.8	Optimization of collector well operation	91
References		92
Appendix A - Supplemental Geophysical Survey Information		95
Appendix B - Predicting Collector Well Yields with MODFLOW		108
Appendix C - Comparison with Kazmann Yield Model		124
Appendix D - Alternative Analysis		126
Appendix E - Infrastructure Evaluation		154

List of Figures

1	Location of the Charlestown State Park Well Field in southern Indiana.	2
2	Aquifer cross section that runs the length of the project site and along the Ohio River.	11
3	Generalized cross section of the Aquifer perpendicular to the Ohio River.	12
4	Location of the land electrical resistivity profiles R1 through R8 and seismic lines SL1 and SL2.	16
5	Location of the 6-meter marine electrical resistivity profiles.	18
6	Location of the 12-meter marine electrical resistivity profiles.	19
7	Elevation of the top of the aquifer under the Ohio River along the study site in Charlestown State Park.	22
8	Elevation of the bottom of the aquifer under the Ohio River along the study site in Charlestown State Park.	23
9	Thickness of the aquifer under the Ohio River along the study site in Charlestown State Park.	24
10	Bathymetry of the Ohio River along the Charlestown State Park.	25
11	Thickness of the riverbed sediment in the Ohio River along the study area in Charlestown State Park.	26
12	Location of the monitoring wells and stilling well in the study area along the Ohio River.	28
13	Water levels in the Ohio River during monitoring period. The USGS gaging station (blue line) shows that the river level varied less than 1 ft except during the flood pulse from December 4 to 6, 2010.	29
14	Domain boundary and zones of hydraulic conductivity, as represented in the groundwater flow model.	41
15	River reaches as represented in the groundwater flow model.	42
16	Plot of modeled versus observed heads for all observation data used in the model calibration.	50
17	Results from the calibrated groundwater model. Computed (blue line) and observed (red cross) hydrographs at the monitoring wells during the South Site pumping test.	52

18	Results from the calibrated groundwater model. Computed (blue line) and observed (red cross) hydrographs at the monitoring wells during the North Site pumping test.	53
19	Results from the calibrated groundwater model. Computed (blue line) and observed (red cross) hydrographs at the monitoring wells during the pumping test of CW-5.	54
20	Results from the calibrated groundwater model. Computed (blue line) and observed (red cross) hydrographs at the monitoring wells prior to and during the passing of a flood wave on the Ohio River.	55
21	Contour plot of the objective function Φ for a calibration problem with two parameters, P_1 and P_2 (Doherty, 2000).	62
22	Contour plot of a model-predicted value, for example, the simulated yield of a well, for the two-parameter problem (Doherty, 2000).	62
23	Identifying the maximum predicted value at the desired confidence level (Doherty, 2000).	63
24	Comparison between groundwater (WHPA, 2010) and filtered river samples (ORSANCO, 2011) of A) iron, B) manganese, and C) total hardness concentrations. . .	70
25	URS's conceptual hydrogeologic model at the Indiana Army Ammunition Plant (URS, 2003).	72
26	Observed 2009 mercury concentrations in the study area (WHPA, 2010).	74
27	Comparison of observed mercury concentrations in Indiana groundwater (USGS, 2011), in the Aquifer at the Park (WHPA, 2010), and the Ohio River (ORSANCO, 2011).	75
28	Equipping existing collector well.	79
29	Improving existing collector well.	80
30	General layout of collector wells and raw water transmission main.	81
31	Land survey profile R1.	97
32	Land survey profile R2.	98
33	Land survey profile R3.	99
34	Land survey profile R4.	100
35	Land survey profile R5.	101
36	Land survey profile R6.	102
37	Land survey profile R7.	103

38	Land survey profile R8.	104
39	Seismic line SL2.	105
40	Seismic line SL1.	105
41	Marine survey 2-D sections of the 6-meter profile lines.	106
42	Marine survey 2-D sections of the 12-meter profile lines.	107
43	(a) Plan view of a collector well with six laterals. (b) Detail of a lateral m , divided into segments; each segment j may have a different sink density σ_j	111
44	Resistance c [d] as a function of the elevation of a lateral with radius $r_w = 0.5$ m in an aquifer of thickness 100 m, where $\bar{K} = 100$ m/d.	114
45	Selecting cells for a coarse representation (top) and a finer resolution (bottom) of a collector well lateral using the MODFLOW MNW package. Note that the aquifer would require detailed vertical discretization, with the cells all lying within the layer that contains the lateral.	115
46	Calculating drain conductances for the collector well model.	116
47	Input file for collector wells.	119
48	The validation model domain. Ambient groundwater flow is from left to right. The collector well is installed with the orientation of the laterals 30 degrees counter-clockwise of the grid orientation.	120
49	Conceptual layout of Alternative 10-A	128
50	Conceptual layout of Alternative 10-B	129
51	Conceptual layout of Alternative 20-A	131
52	Conceptual layout of Alternative 20-B	132
53	Conceptual layout of Alternative 30-A	134
54	Conceptual layout of Alternative 30-B	135
55	Conceptual layout of Alternative 30-C	137
56	Conceptual layout of Alternative 40-A	138
57	Conceptual layout of Alternative 40-B	140
58	Conceptual layout of Alternative 50-A	142
59	Conceptual layout of Alternative 50-B	143
60	Conceptual layout of Alternative 50-C	145

61	Conceptual layout of Alternative 60-A	146
62	Conceptual layout of Alternative 60-B	148
63	Conceptual layout of Alternative 70-A	149
64	Conceptual layout of Alternative 80-A	151
65	Collector Well CW-1	155
66	CW-1 Plan & Section (Ranney, 1979)	156
67	Collector Well CW-2	157
68	CW-2 Plan & Section (Ranney, 1979)	158
69	Collector Well CW-3	159
70	CW-3 Plan & Section (Ranney, 1979)	160
71	Collector Well CW-4	161
72	CW-4 Plan & Section (Ranney, 1979)	162
73	Collector Well CW-5	163
74	CW-5 Plan & Section (Ranney, 1979)	164
75	Collector Well CW-6	165
76	CW-6 Plan & Section (Ranney, 1979)	166
77	Collector Well CW-7	167
78	CW-7 Plan & Section (Ranney, 1979)	168

List of Tables

1	The RMS and L2 results for the the marine and land ERI profiles.	20
2	Interpretation of resistivity values delineated using results from ERI surveys along the Ohio River.	27
3	Monitoring well locations and synoptic water-level measurements.	30
4	Mechanical capacity of the existing collector wells.	36
5	Additional 170 ft-long laterals required to increase the mechanical capacity of collector wells to 15 mgd.	37
6	Water wells in the bedrock formations within five miles of Charlestown State Park (IDNR, 2009).	44
7	Weight assigned to observation data sets for model calibration.	46
8	PEST-calibrated values of hydraulic conductivity with approximate 95% confidence intervals.	47
9	PEST-calibrated values of riverbed leakance and approximate 95% confidence intervals.	48
10	PEST-calibrated aquifer storage parameters and approximate 95% confidence intervals.	49
11	Calibration statistics.	49
12	Properties at the South Site for evaluating equivalent transmissivities. Average values for each zone were estimated from the model data sets.	57
13	Properties at the North Site for evaluating equivalent transmissivities. Average values for each zone were estimated from the model data sets.	58
14	Predicted yields with all wells operating: (column 2) the seven existing wells, and (column 3) the seven existing wells augmented with two additional wells south of CW-7.	59
15	Development alternatives that were considered using the groundwater flow model.	60
16	Results of predictive modeling and summary of sustainable capacity for each alternative. All values are in millions of gallons per day (mgd) and represent the yield of the entire well field for each alternative.	64
17	Summary of alternatives: included wells, sustainable capacity, and estimated conceptual cost.	83

18	Relationship between the simulated collector well yield and cell size, as compared to the 3D analytic element solution.	121
19	Kazmann's linear model. Drawdown (ft) caused by pumping each collector well individually at 10 mgd.	125
20	Comparison of results from the Predictive Model and Kazmann's linear model. . .	125
21	Results of modeling for 10 mgd, alternative A. All values are in millions of gallons per day (mgd).	127
22	Results of modeling for 10 mgd, scenario B. All values are in millions of gallons per day (mgd).	130
23	Results of modeling for 20 mgd, scenario A. All values are in millions of gallons per day (mgd).	130
24	Results of modeling for 20 mgd, scenario B. All values are in millions of gallons per day (mgd).	133
25	Results of modeling for 30 mgd, scenario A. All values are in millions of gallons per day (mgd).	133
26	Results of modeling for 30 mgd, scenario B. All values are in millions of gallons per day (mgd).	136
27	Results of modeling for 30 mgd, scenario C. All values are in millions of gallons per day (mgd).	136
28	Results of modeling for 40 mgd, scenario A. All values are in millions of gallons per day (mgd).	139
29	Results of modeling for 40 mgd, scenario B. All values are in millions of gallons per day (mgd).	141
30	Results of modeling for 50 mgd, scenario A. All values are in millions of gallons per day (mgd).	141
31	Results of modeling for 50 mgd, scenario B. All values are in millions of gallons per day (mgd).	144
32	Results of modeling for 50 mgd, scenario C. All values are in millions of gallons per day (mgd).	144
33	Results of modeling for 60 mgd, scenario A. All values are in millions of gallons per day (mgd).	147

34	Results of modeling for 60 mgd, scenario B. All values are in millions of gallons per day (mgd).	147
35	Results of modeling for 70 mgd, scenario A. All values are in millions of gallons per day (mgd).	150
36	Results of modeling for 80 mgd, scenario A. All values are in millions of gallons per day (mgd).	150

Acronyms

$\mu\text{g/L}$	micrograms per liter
AGI	Advanced Geosciences Inc.
CRP	continuous resistivity profiling
DBP	disinfection by-product precursors
DOC	dissolved organic carbon
ERI	electrical resistivity imaging
ft	feet
ft amsl	feet above mean sea level
ft/day	feet per day
ft/min	feet per minute
ft/sec	feet per second
ft ² /day	squared foot per day
gpm	gallons per minute
GPS	global positioning system
GWUDISW	groundwater under the direct influence of surface water
IDEM	Indiana Department of Environmental Management
IDNR	Indiana Department of Natural Resources
IESWTR	Interim Enhanced Surface Water Treatment Rules
IFA	Indiana Finance Authority
IGS	Indiana Geological Survey
INAAP	Indiana Army Ammunition Plant
LT2ESWTR	Long Term 2 Enhanced Surface Water Treatment Rule
m	meter

MCL	maximum contaminant level
mgd	million gallons per day
mg/L	milligrams per liter
mi	mile
MPA	microparticulate analysis
mph	miles per hour
MRL	method reporting limit
NADP	National Atmospheric Deposition Program
NTU	Nephelometric Turbidity Unit
ORSANCO	Ohio River Valley Water Sanitation Commission
PCS	potential contaminant source
PWS	public water systems
RBF	river bank filtration
RCRA	Resource Conservation and Recovery Act
RMS	root mean square
RRCC	River Ridge Commerce Center
SMCL	secondary maximum contaminant level
SWTR	Surface Water Treatment Rule
USACE	U.S. Army Corps of Engineers
USEPA	U.S. Environmental Protection Agency
USGS	U.S. Geological Survey
WHPA	wellhead protection area
WHPP	wellhead protection plan

Executive Summary

Water supplies in Southern Indiana are vulnerable to drought. There are only a few large rivers separated by rocky forested hills and many communities depend on small surface water reservoirs for their drinking water. A tenuous water supply makes it more difficult to attract manufacturing businesses which in turn suppresses the economic vitality of the region. A regional water supply would support economic development in southeastern and central Indiana. As one alternative, the State has invested in understanding the water supply potential of the aquifer in Charlestown State Park. In the 1940s, this narrow but prolific aquifer produced an average of over 50 million gallons per day (mgd) to wells that supplied water to an ammunition plant. The mechanical components of the remaining water supply infrastructure are old and now defunct but the aquifer could still deliver abundant, sustainable and effectively drought-proof supplies. The analysis described in this report was done to estimate the potential capacity of a redeveloped, modern and optimized high capacity new well field at the Park. This report answers the following questions:

- How much water can be produced from the aquifer?
- Is water quality in the aquifer adequate for drinking water – what treatment could be required for this to be used as a source?
- How should the well field be developed to maximize its value as a regional water supply?

Findings

Based upon our assessment of the Charlestown State Park Aquifer, it is clear that this groundwater supply could produce enough high quality water to be a valuable asset for regional economic development. The following are key findings:

- A redeveloped well field on this property could pump approximately 75 mgd, with the addition of new wells at the downstream end of the aquifer.
- The source of water pumped from wells on this property will be infiltration into the aquifer from the Ohio River. Riverbank filtration provides natural, partial treatment of source water, resulting in lower infrastructure and operating costs.
- Until the well field is producing large volumes of water, it will most likely be regulated as a groundwater supply. As the system grows and pumping rates increase, the raw water will eventually be classified as Groundwater Under the Direct Influence (of Surface Water), which requires additional treatment.

- The existing collector well caissons appear to be in good condition, and suitable for reuse. Unfortunately, the well houses and electrical, pumping and mechanical equipment are in poor condition and need to be demolished and removed.

A reliable water supply is needed for economic development in southern Indiana. The State has the potential to provide 75 mgd of drought-proof water to southern and central Indiana. Planning for the use of this valuable resource today will build the foundation needed to promote and sustain economic growth in the future. This report is intended to inform investment decisions that may turn this resource into an important new regional water supply.

1 Introduction

Southern Indiana is naturally a water-poor landscape. The hills that lie between the Ohio River and Indianapolis have no natural lakes, and there are few water-supply aquifers of significant regional extent. Thus, runoff from precipitation rapidly migrates to the East Fork White River, Whitewater River, Patoka River, Muscatatuck River, and a number of smaller rivers and creeks, all of which ultimately discharge into the Ohio River. The lack of reliable water supplies has constrained economic development in southern Indiana since European settlement. Consequently, in the 1960s, the U.S. Army Corps of Engineers (USACE) constructed Lake Monroe (near Bloomington) and Patoka Lake (near Jasper). The economic impact of these two reservoirs has been profound, and Hoosiers in these localities no longer fear short-term droughts. Nonetheless, there are many areas within southeastern Indiana that are economically depressed and lack adequate water supplies.

Besides the USACE lakes, southern Indiana has one other reliable source for significant water supply withdrawals: the Ohio River with its localized aquifer systems that lie adjacent to it. Charlestown State Park (Park) overlies a prolific two-mile long outwash aquifer (Aquifer) along the Ohio River near Louisville, Kentucky (Figure 1). During World War II, the U.S. Army constructed a major well field at what is now the Park as a source of water for the former Indiana Army Ammunition Plant (INAAP). The well field included seven Ranney collector wells and two tubular wells. When constructed, the INAAP facility was one of the largest single well fields ever operated in the Midwest, with production rates averaging over 50 million gallons per day (mgd) during 1942 and 1943. After the war, some wells were used intermittently for operations at the site and for public water supply, but withdrawal rates that never approached those achieved during the war.

In 1996, ownership of a portion of the INAAP facility was transferred to the state of Indiana (State) and the Park was established. At that time, the Indiana Department of Natural Resources (IDNR) acquired ownership of the land and other INAAP facilities. Later, IDNR also assumed operation of the original INAAP water-supply infrastructure. Two of the existing wells, tubular well TW-6001 and collector well CW-1, are now used to supply water to the Park and to the River Ridge Commerce Center (RRCC).

IDNR has recently constructed a new water-supply well field at the Park to replace the aging infrastructure that serves the Park and the RRCC. Furthermore, IDNR identified the aquifer at the Park as a potential water-supply resource for the future of southern, and ultimately central Indiana. Consequently, the Indiana Finance Authority (IFA) contracted Layne Hydro to evaluate the long-term potential for regional water-supply development at the Park.

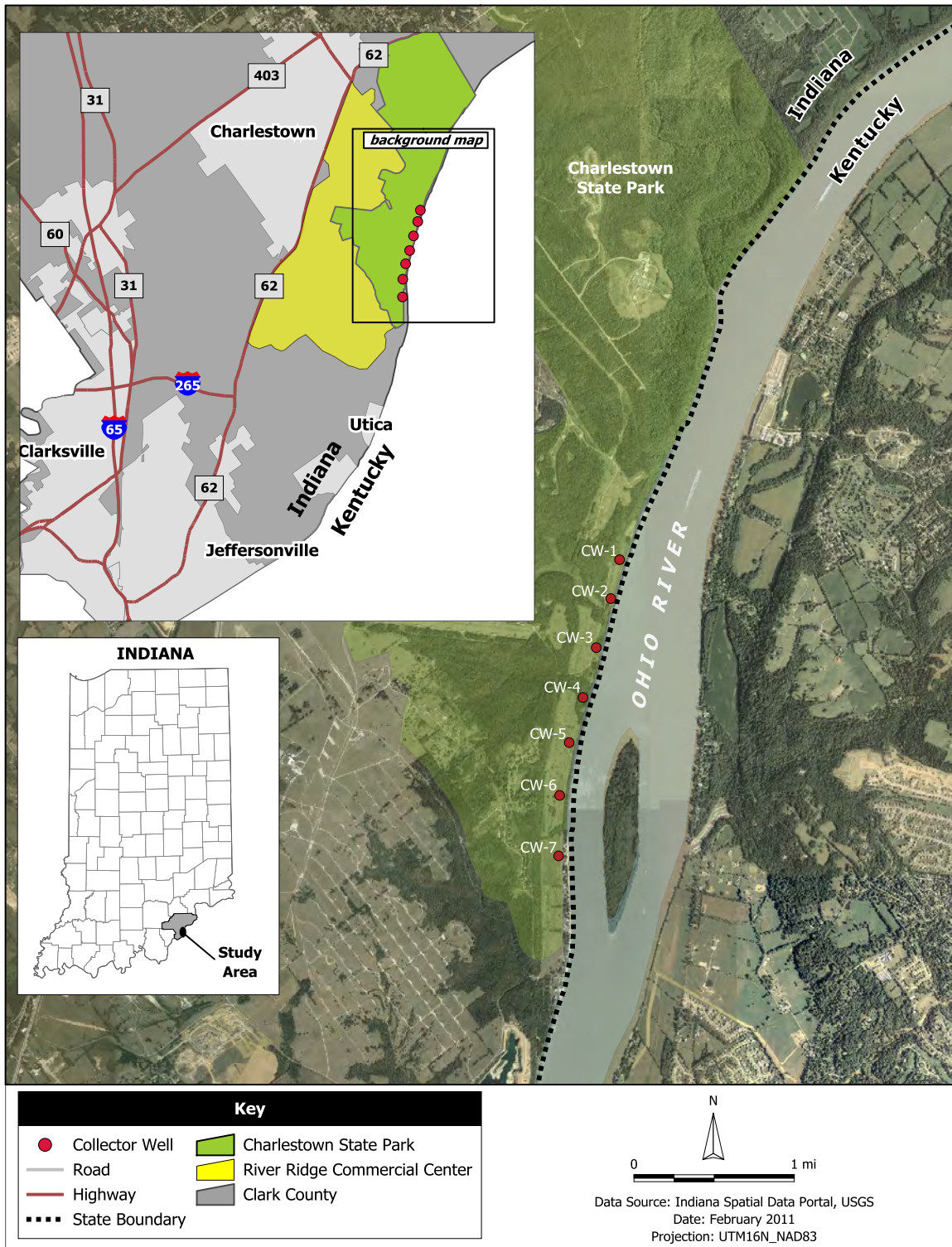


Figure 1: Location of the Charlestown State Park Well Field in southern Indiana.

1.1 Study Purpose

The central purpose of this study was to estimate the potential of a re-developed, modern, and optimized well field at the Park. We estimated the quantity of water available for a water supply, evaluated anticipated water quality, and developed conceptual cost estimates for multiple development alternatives. The study answers these questions:

- How much water can be produced from the aquifer?
- Is water quality in the aquifer adequate for drinking water – what treatment could be required for this to be used as a source?
- How should the well field be developed to maximize its value as a regional water supply?

A regional water supply could support economic development in southeastern and central Indiana but will require significant investment. Our analysis is intended to support decisions regarding potential investments in regional water supply infrastructure. To inform investment decisions, the long-term value of a regional water supply must be assessed with a greater level of confidence than that which exists today. For this purpose, our estimates of the sustainable capacity of the Well Field include a rigorous assessment of their certainty.

1.2 Study Approach

This report provides estimates of the sustainable capacity of a re-developed well field, recommendations regarding water quality and treatment, and an evaluation of alternatives for development. Our approach included

- analyzing existing data and reports
- conducting field investigations including geophysical surveys, water-level measurements, and limited inspection of infrastructure
- developing and calibrating a groundwater flow model
- evaluating existing water quality data and probable treatment requirements
- analyzing predicted performance and conceptual cost estimates of alternatives

Analyzing Existing Data We reviewed data on the Aquifer published by the United States Geological Survey (USGS), engineering consultants, and local public water suppliers, including the Louisville Water Company. Our objective was to consolidate the existing data and establish what is known and, where possible, convert that data into a digital format. The digital data and visualization tools provided new insights into the aquifer boundaries and properties.

Field Investigation To fill in gaps in our knowledge about the aquifer, land and marine geophysical surveys were conducted. For the land survey we used electrical resistivity imaging and seismic refraction to determine the bedrock surface elevation and the thickness and lateral extent of sand, gravel, and clay layers overlying the bedrock. The marine geophysical survey helped define the bathymetry of the riverbed and the thickness and composition of the riverbed sediments that control the hydraulic connection between the Aquifer and the river. This was important because riverbank filtration relies on the ability of a well to induce recharge from a nearby surface water source. The degree of hydraulic connection between the surface water body and the Aquifer affects well field capacity.

In addition to the geometry of the Aquifer, the data synthesis helped us map other hydraulic properties needed to determine aquifer yield. To determine these additional aquifer properties, we analyzed synoptic water-level measurements and groundwater and river stage data collected during previous pumping tests at the north and south ends of the Park (WHPA, 2010), and from a previous pumping test conducted by Burgess and Niple (1995) at CW-5. These data sets were also used to calibrate the groundwater flow model.

In a previous inspection, pitting and a crack were observed in the concrete caisson of CW-6. Layne Christensen's Ranney Collector Wells division investigated the reported crack for this study, using a commercial diving service that visually inspected the interior of the caisson and collected concrete cores from the affected area for laboratory testing. This information provided a preliminary assessment of the suitability of the existing caisson for use in a re-developed well field.

Groundwater Flow Modeling We developed a groundwater flow model for the Aquifer adjacent to and beneath the Ohio River at the Park. We created a new, more detailed conceptual model of the Aquifer using data collected during the geophysical surveys, pump tests, and data review. The model was used to estimate aquifer yield and to assess the effects of high pumping rates on regional and local groundwater flow.

The model was calibrated using the inverse model code PEST (Doherty, 2004). Collector wells were simulated using the MODFLOW DRN (drain) package and included in the calibrated model.

Evaluating Water Quality and Treatment Requirements The treatment required for water pumped from the Aquifer depends on the quality of the source water (especially iron and manganese concentrations) and whether the source water is classified by the Indiana Department of Environmental Management (IDEM) as groundwater under the direct influence of surface water (GWUDISW). We estimated the relative contributions of induced recharge from the river and recharge from precipitation. We used this knowledge, in conjunction with our understanding of the site and the new and previously collected data, to determine recommended planning-level assumptions for treatment in this setting.

Analyzing Alternatives After calibration, the groundwater flow model was used to evaluate multiple well field designs. We identified 16 well field development alternatives using both the existing collector well lateral layouts and re-designed lateral layouts. We evaluated each alternative on the basis of simulated yield and conceptual cost estimates and used the calibrated model to estimate the level of uncertainty in the yield estimates.

1.3 Previous Studies

This site has been the subject of many previous studies and analysis. Previous findings and conclusions relevant to our study are briefly summarized below.

Analysis of collector well yields - Kazmann (1948) Kazmann investigated the yield of the seven collector wells based on four years of water pumping data from 1941 to 1945. 10 mgd pump tests were performed in each collector well, with steady-state drawdown measurements recorded in the other wells. Based on the data, Kazmann developed a linear model of well drawdown for the Well Field and estimated the firm yield of each collector well with all wells pumping. CW-1, CW-6, and CW-7 were identified as having the highest potential capacity.

Collector well evaluation - Ranney (1965) Ranney Water Systems and a professional diver conducted an inspection of the seven collector wells. Each well, except CW-5, was pumped to evaluate flow and drawdown. The condition of the collector wells was recorded, flow and drawdown were measured in the pumping wells, and water quality samples were collected and analyzed from CW-2. Slimes were observed in all of the wells and may be caused by the presence of iron bacteria. In CW-2, rotifers were identified indicating the presence of contamination by surface sewage.

Collector well evaluation - Ranney (1979) The Ranney Company and a professional diver conducted another inspection of the seven collector wells in 1979. Only CW-1 and CW-4 were observed under pumping conditions. Water-level measurements were collected in the wells and the

Ohio River. In CW-1 and CW-4, individual lateral flow was measured. The general condition of the collector wells was described as fair. Samples of water and encrustations were collected and analyzed, and the water entering the wells was determined to be fairly corrosive. A full video inspection of the laterals was recommended because the laterals were at the end of the average screen life.

Collector well evaluation - Burgess & Niple (1995) In 1994 and 1995, Burgess & Niple investigated the condition and performance of CW-4, CW-5, and CW-6. They performed two separate pumping tests. During the first test in July 1994, all three wells were pumped at a combined rate of 22 mgd for four days. During the second test in March and April 1995, CW-4 and CW-6 were pumped individually at 10 mgd and 4 mgd, respectively for four consecutive days. Water samples were collected from the pumping wells and the Ohio River and analyzed for general groundwater-quality parameters. There were no indications of groundwater contamination from VOCs, metals, dioxin, enterovirus, or radionuclides. However, manganese concentrations in CW-4 and CW-6 were above the secondary maximum contaminant level (SMCL). The wells were evaluated for surface water influence risk factors using microparticulate analysis (MPA) and the U.S. Environmental Protection Agency's (USEPA) relative-risk rating tables. The analysis indicated that CW-4 and CW-5 had a moderate risk of surface water influence and CW-6 had a low risk. Because the risk scoring of CW-4 and CW-5 was related to a type of algae that occurs in groundwater wells, and based on the evaluated data, it was concluded that none of the wells exhibited characteristics of GWUDISW. A professional diver observed a crack and pitting of the concrete in CW-6.

Assessment of hydrogeologically significant solution and fracture features - Indiana Geological Survey (1995) The Indiana Geological Survey (IGS) studied the karst features of the INAAP property to evaluate the impacts of historical acidic wastewater discharges from the INAAP to Jenny Lind Run. The conclusions of the study were that by virtue of their mineralogy, the natural tendency for dissolution of the Jefferson Limestone and Louisville Limestone was accelerated by the wastewater discharges. The study concluded that while the underlying Waldron Shale presents a barrier to downward migration of water, it was subjected to weathering in areas of high flows resulting in the emergence of springs at the top of the underlying Laurel Member of the Salamonie Dolomite. The Osgood and Laurel Members of the Salamonie Dolomite and the Saluda Member of the Whitewater Formation are all resistant to karst processes and are important aquitards, precluding the downward migration of groundwater contaminants. The study concluded that other than surficial dissolution, the wastewater effects along Jenny Lind Run were relatively minor and that no significant linkage was found between the upland bedrock aquifer and the Ohio River (Hendricks, 1995).

Collector well evaluation - Reynolds, Inc. (2000) In 2000, Reynolds investigated the collector wells, with the support of a professional diver. The general condition of the collector wells was described as fair to good with the potential for successful rehabilitation. The exterior concrete was tested for surface hardness and compressive strength using a Type N Schmidt Hammer. The report concluded that the caissons were competent and able to withstand coring for installation of additional laterals (Reynolds, 2000).

Phase II RCRA Facility Investigation for Installation Groundwater - URS Corporation (2003) URS studied the groundwater at the former INAAP property as part of a Phase II RCRA Facility Investigation. Monitoring wells and springs were sampled to characterize groundwater. Temporary wells were sampled to determine if the groundwater in the local epikarst contained chemicals that could adversely impact groundwater in the karst or alluvial groundwater and surface water flow systems. Permanent monitoring wells were sampled to determine if chemicals had entered the slow flow portion of the karst groundwater flow system of the lowland alluvial aquifer. Springs were sampled to determine if chemicals had entered the rapid flow part of the karst groundwater flow system. It was concluded that there was no apparent impact to the lowland outwash aquifer from groundwater/surface water at INAAP and it was recommended that no additional characterization of installation water quality was necessary.

City of Charlestown Well Field Study - WHPA (2009) Layne Hydro (formerly Wittman Hydro Planning Associates) performed an investigation of the water quality at the City of Charlestown (City) Well Field. The purpose of the study was to evaluate the origin of elevated manganese concentrations in the City's wells. A three-day pump test was performed with three of the City's wells during which water samples were collected from the production wells, monitoring wells completed in the Aquifer, and the Ohio River. The investigation demonstrated that the source of manganese in the supply wells is the result of redox processes in the riverbed and unconsolidated deposits under the river. Manganese concentrations on the river side of the well field are 10 times greater than those upgradient of the wells. Observed manganese concentrations in production well #2 were over 0.5 mg/L, an order of magnitude higher than the SMCL.

Charlestown State Park, IFA preliminary options, IFA well design - WHPA (2010) Layne Hydro evaluated the development of a proposed two mgd well field at the southern end of the Park. We performed exploratory drilling and construction of test production and monitoring wells at the proposed site and at a second site at the north end of the Aquifer. At both sites, we performed extended pump tests and collected samples for analysis of water quality. We used groundwater modeling to develop the design of the proposed well field. We installed additional monitoring wells

along the full length of the Aquifer and collected samples for a longitudinal study of the water quality in the Aquifer. Elevated levels of iron and manganese were observed in most of the sampled wells, and we recommended that design of the proposed well field and treatment facility provide for removal of iron and manganese.

2 Regional Setting

The project site lies within the Ohio River Basin, which is the fourth largest drainage basin in Indiana. It encompasses 4,224 mi² and extends approximately 200 mi across southern Indiana. The physiography of the basin is controlled by bedrock topography, which strongly influenced the deposition of the overlying alluvial deposits. The basin's shape was affected by the relocation of the pre-Pleistocene Teays River drainage into the Ohio River Valley during the Pleistocene. Stream erosion and weathering left considerable topographic relief that can be seen at the Park. The Ohio River Valley varies in width from a few hundred feet wide near Leavenworth, Indiana, to about six miles wide near Evansville, Indiana. In addition to the Ohio River, smaller tributary systems drain the valley, depositing fine-grained alluvium (mainly silt and clay) over coarse-grained glacial outwash deposits (mainly sand and gravel) that form the Aquifer (Fenelon and Bobay, 1994).

2.1 Geology

The Park is located in Clark County, Indiana, which is located along the western flank of the Cincinnati Arch, a northwest trending anticline that separates the Michigan Basin to the north and the Illinois Basin to the southwest. Rocks of Ordovician, Silurian, Devonian, and Mississippian age are either exposed at the surface or buried. The older rocks are typically present at the crest of the arch in southeastern to central Indiana, where the younger rock units have eroded away.

The local geology at the site consists of two hydrologically distinct units: a predominantly carbonate bedrock overlain by approximately 100 ft of unconsolidated glacial sediments. The Ohio River Valley formed where the bedrock was eroded by glacial melt water. This bedrock valley was filled with up to 80 ft of sand and gravel. As the glaciers retreated and the stream load diminished, up to 30 ft of finer-grained materials (clays, silts, and fine sand) were deposited on top of the sand and gravel. These two layers of unconsolidated sediment form the terrace and flood plain areas along the Ohio River (URS, 2003).

2.1.1 Bedrock

Along the Ohio River within Clark County, bedrock ranges from Ordovician shale and limestone to the northeast, Silurian dolomite and limestone in the central part, to Devonian shale, limestone, and dolomite in the west (Fenelon and Bobay, 1994). Karst features including sinkholes and springs are common in some of the limestone formations. Near the study area, the bedrock is the Ordovician Whitewater Formation, which consists primarily of skeletal limestone and calcareous shale with dolomitic mudstone at the base. The bedrock dips very gently to the west-southwest. The Whitewater Formation is unconformably overlain by the Silurian Brassfield Limestone.

2.1.2 Unconsolidated deposits

Regionally, the bedrock is covered by as much as 100 ft of till, silt, clay, and alluvium overlying the outwash sand and gravel deposits (Fenelon and Bobay, 1994). The Aquifer is composed of highly permeable sand and gravel deposits. However, in the terrace areas, finer-grained (less permeable) material is deposited on top of the Aquifer and restricts recharge.

Within the Park, the Aquifer varies in thickness from 40 ft to 90 ft and is overlain by 20 ft to 35 ft of Recent alluvium (Figure 2). The Recent alluvium consists of glacial till, silt, and clay that is thickest longitudinally and thins along the margins of the Aquifer to the west (Figure 3).

Our characterization of the unconsolidated deposits of the Aquifer is based on local geologic information from the following sources:

- the planning and installing of INAAP collector wells in the 1940s (Kazmann, 1948)
- borings drilled by URS, Inc. during an investigation related to base closure (URS, 2003)
- borings and test wells drilled during a study of the City of Charlestown Well Field (WHPA, 2009)
- well logs in the State Well Log Database (IDNR, 2009)
- borings and monitoring wells drilled by Layne at the site (WHPA, 2010)

2.2 Groundwater

Groundwater in Clark County can be pumped either from bedrock aquifers or from unconsolidated deposits. Bedrock aquifers within the county typically yield 0 to 20 gallons per minute (gpm) at individual wells (IDNR, 1980). Several hydrogeologic features within Clark County limit the use of bedrock as a large production water-supply source:

1. the bedrock formations are neither thick nor transmissive
2. water levels in the bedrock are too far below the land surface
3. water quality from the bedrock aquifer is poor

Unconsolidated aquifers in Clark County are much more productive than the bedrock aquifers and have been used for public water supply. The aquifer is composed of clean, well-rounded, poorly-sorted sands, gravels, and pebbles of glacial origin. Wells tapping the unconsolidated deposits provide yields in the range of 10 gpm to 1,000 gpm (IDNR, 1980). The highest yields are found where

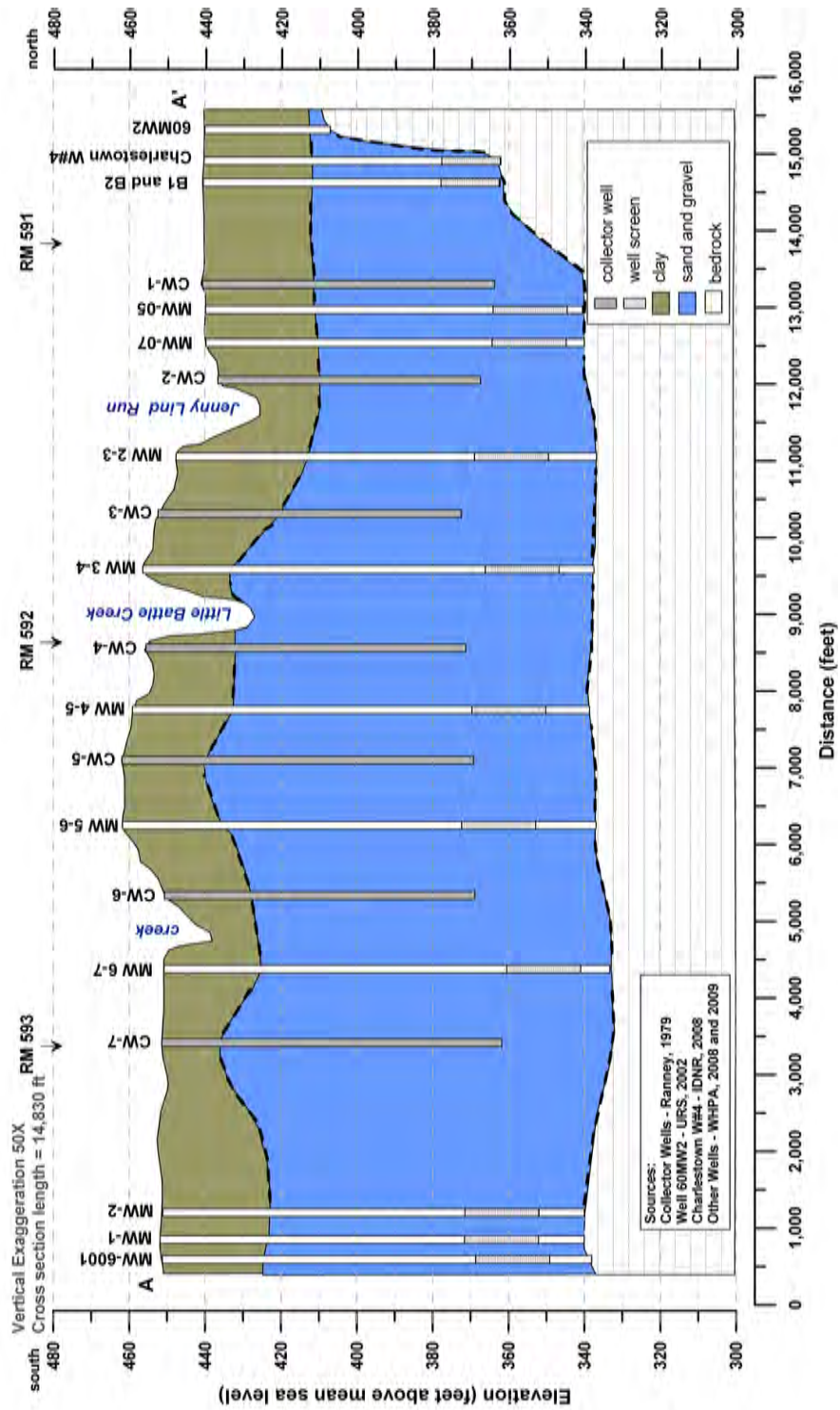


Figure 2: Aquifer cross section that runs the length of the project site and along the Ohio River.

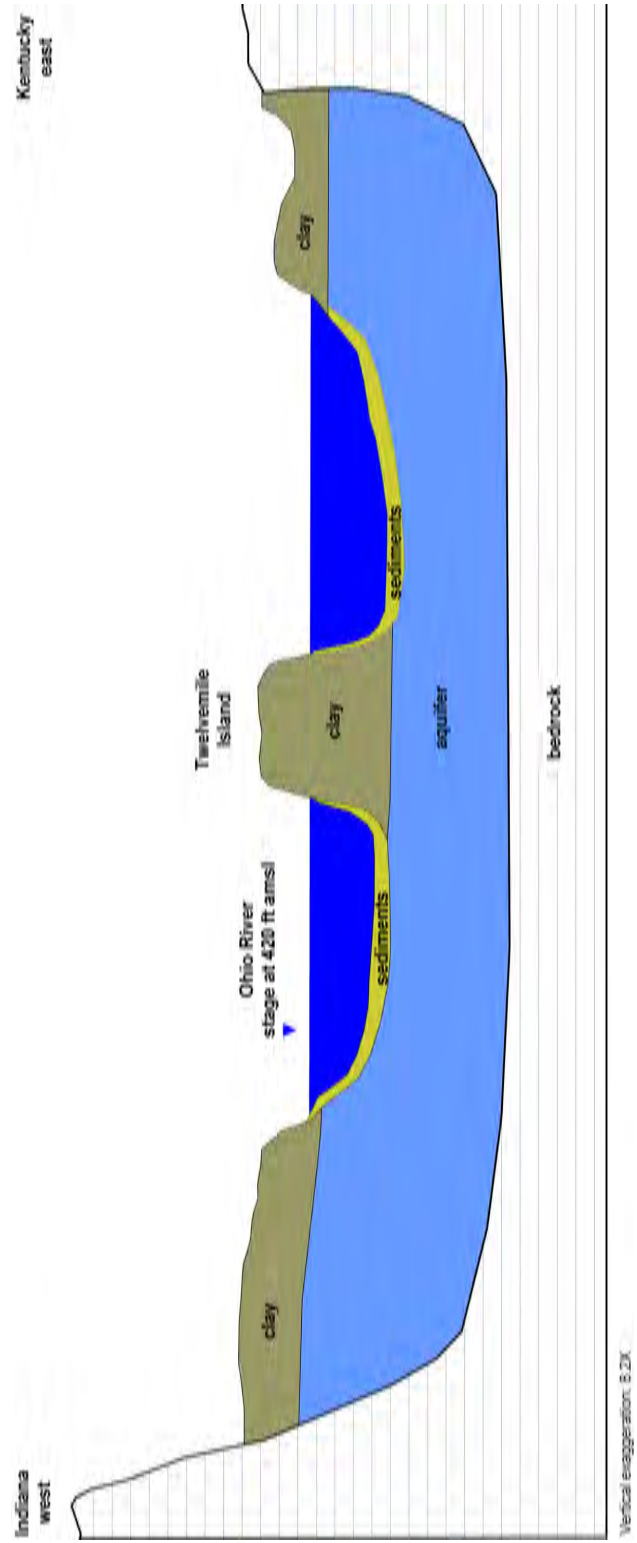


Figure 3: Generalized cross section of the Aquifer perpendicular to the Ohio River.

the unconsolidated deposits are hydraulically connected to surface water (Planert and Williams, 1995). Although the unconsolidated aquifer is prolific, high concentrations of naturally occurring metals, especially manganese and iron, are present in many wells.

Within the Park, the Aquifer is a narrow strip of highly permeable outwash material filling the bedrock valley adjacent to and underlying the Ohio River. It extends south along the Ohio River from north of the City of Charlestown Well Field to just north of Utica, Indiana. The Aquifer has a saturated thickness of up to 100 ft near the river. Its width between the western valley wall and the west bank of the Ohio River, varies from 0 to 1,000 ft. The Ohio River is the primary recharge source for water pumped from the Aquifer and is the primary control on ambient groundwater levels. The river cuts into the Aquifer but is locally separated from the Aquifer by a layer of silt and organic material lying along the riverbed (Figure 3).

2.3 Surface Water

The Ohio River is the primary eastern tributary of the Mississippi River and flows in a southwesterly direction for 357 mi along the state line between Indiana and Kentucky. Flow in the Ohio River is controlled by a series of dams operated by the USACE. The McAlpine Dam, located south of the Park in Louisville, Kentucky, controls the river stage along the Park.

Two major streams, Fourteen Mile Creek and Silver Creek, cross Clark County flowing east and southeast and discharge into the Ohio River. Fourteen Mile Creek drains an area of 101 mi² on the eastern side of the county while Silver Creek drains 219 mi² drains the western side. The Park lies between these two streams. Within the Park, minor streams cross the Ohio River floodplain, including Jenny Lind Run and Little Battle Creek.

This page intentionally left blank

3 Field Investigation

A detailed field investigation was conducted to refine the characterization of the Aquifer and riverbed sediments. The investigation included a geophysical survey, measurements of water levels in the Aquifer and the River, and an investigation of the condition of selected existing infrastructure in the well field.

3.1 Geophysical Survey

We performed two geophysical surveys: a land survey and a marine survey. The objective of these surveys was to collect more detailed information about the physical properties and distribution of unconsolidated materials in the subsurface. The land geophysical survey defined the geometry and composition of the aquifer, the overlying confining layer, and the depth to bedrock in the survey area. The marine geophysical survey defined the bathymetry of the riverbed and characterized the underlying sediments that control the hydraulic connection between the aquifer and the river.

3.1.1 Methodology

We used electrical resistivity imaging (ERI) and seismic refraction techniques to complete the land and marine surveys. These techniques are discussed below.

Land ERI survey

For the land survey, eight ERI profile lines (R1 through R8) were used to collect geophysical data in the study area (Figure 4). The profile lines were positioned to characterize the subsurface geology in areas where only limited information was available. The land survey was conducted using the Advanced Geosciences Inc. (AGI) Super Sting R8 IP eight-channel automatic multi-electrode system.

Data collection was automated, and each individual measurement involved four electrodes along the profile line (two current electrodes and two potential electrodes). A series of measurements were made using various current and potential electrode pairings along the profile line. As electrode spacing was increased with each successive measurement, overall electrical current penetration depth increased.

Electrode spacing used for each profile line varied because of site constraints. Profile lines R1, R3, R4, R6, R7, and R8 were surveyed with a 4.6 meter (m) (15 ft) electrode spacing, whereas profile lines R2 and R5 were surveyed with 6.1 m (20 ft) electrode spacing. For each profile line, we

collected the geographical location of select electrodes with a hand-held global positioning system (GPS).

Seismic refraction survey

We completed seismic refraction surveys to corroborate the depth to bedrock results calculated in the land ERI survey. The method of seismic refraction uses propagation of sound waves through the earth to determine the geologic structure beneath the seismic line. Two seismic refraction profile lines were surveyed in the study area, Line SL1 (coinciding with ERI line R4) and line SL2 (coinciding with ERI line R3) (Figure 4). Seismic data were collected using a Geometrics Geode 24-channel digital signal enhancement seismograph. We generated sound waves by striking a steel plate with a sledge hammer. A line of motion detectors (geophones) was spread along the ground to record the time required for the sound energy to reach each geophone. Geophones closest to the sound source recorded the arrival of sound energy traveling directly through near surface material. Geophones farther from the sound source recorded the sound energy traveling at faster velocities in deeper layers.

The geophone spacing for both seismic lines was 30 ft. Multiple hammer shots were recorded at each location to improve the signal-noise ratio. Forward and reverse shots were also collected with the seismic source positioned approximately 10 ft and 75 ft from the last geophone at the end of each line.

Marine ERI survey

For the marine ERI survey, we surveyed six profiles in the Ohio River that were roughly parallel to the Park shoreline to map riverbed sediment thickness. The distribution of these sediments affects the hydraulic connection between the river and the aquifer (Figures 5 and 6). Penetration depth and overall resolution were determined by electrode spacing. Increasing the spacing between electrode pairs resulted in an increase in signal penetration but a loss in resolution. Tighter electrode pair spacing increased the resolution but decreased signal penetration. For this survey, electrode spacings of 6 m (approximately 19.7 ft) and 12 m (approximately 39.4 ft) were used to characterize the riverbed and underlying unconsolidated deposits.

We employed a technique called continuous resistivity profiling (CRP) using the Advanced Geosciences Inc. Supersting Marine ERI System. This system uses a boat-towed electrode array that simultaneously injects current and measures voltage. The voltage measurements yielded information about different depths and locations during each measurement cycle.

The towed electrode array consisted of 11 electrodes (2 current electrodes and 9 potential electrodes) that allowed for the collection of 8 voltage measurements during each measurement cycle. The



Figure 4: Location of the land electrical resistivity profiles R1 through R8 and seismic lines SL1 and SL2.

electrode cable was configured for a dipole-dipole array in which the electrodes were equally spaced and the first two electrodes (closest to the tow boat) were designated as the current electrodes. Data collection speed is a function of boat speed, which is typically between two and three miles per hour (mph). Our average boat speed for each profile line was approximately 2.5 mph. We also used a GPS and sonar system to record location and water column depth for each measurement cycle. Water temperature data were also recorded to aid in modeling the marine electrical resistivity survey data.

3.1.2 Data analysis

The ERI and seismic field data were analyzed and the results were used together to delineate the geologic variations in the subsurface. The data analysis techniques are described below.

Land and marine ERI surveys

For the land ERI survey, we plotted the calculated apparent resistivity values as a contoured depth section to show spatial variations. The data were first processed to remove noise. We then calculated the resistivity changes in both vertical and lateral directions along the profile lines, which allowed for developing a continuous 2D geo-electrical cross section along each profile line.

The marine electrical resistivity data were modeled using the EarthImager software with the CRP module to construct continuous inverted resistivity depth sections (similar to the land ERI profile models) along each profile line. Recorded water column depth, surface water temperature, and corresponding GPS coordinates were also incorporated into the model.

The difference between the ERI model data for the land and marine surveys and the field data was measured as a fitting error (i.e., RMS), which is a relative measure of field data quality and model reliability. Also, a normalized L2 factor - which is the square of the weighted data errors between the calculated and measured apparent resistivity data - was used to gauge model accuracy. An electrical resistivity model with RMS and normalized L2 values less than 10% is considered a good fit. The model RMS and L2 values for all the land and marine ERI profile lines were below 10%, which suggests that the model results accurately reflect the subsurface geologic conditions in the study area (Table 1). Compared to the land ERI L2 results, marine ERI L2 results generally have higher noise levels because of variations in water-column temperature and turbidity. Overall, we considered the marine model results to accurately reflect the subsurface below the Ohio River. We are confident in our estimates of riverbed depth and the variation in thickness of riverbed sediments.

The ERI survey and modeling software measures and interprets, respectively, the electrical properties of the subsurface to delineate the types of geologic materials present. Weathered, unsaturated

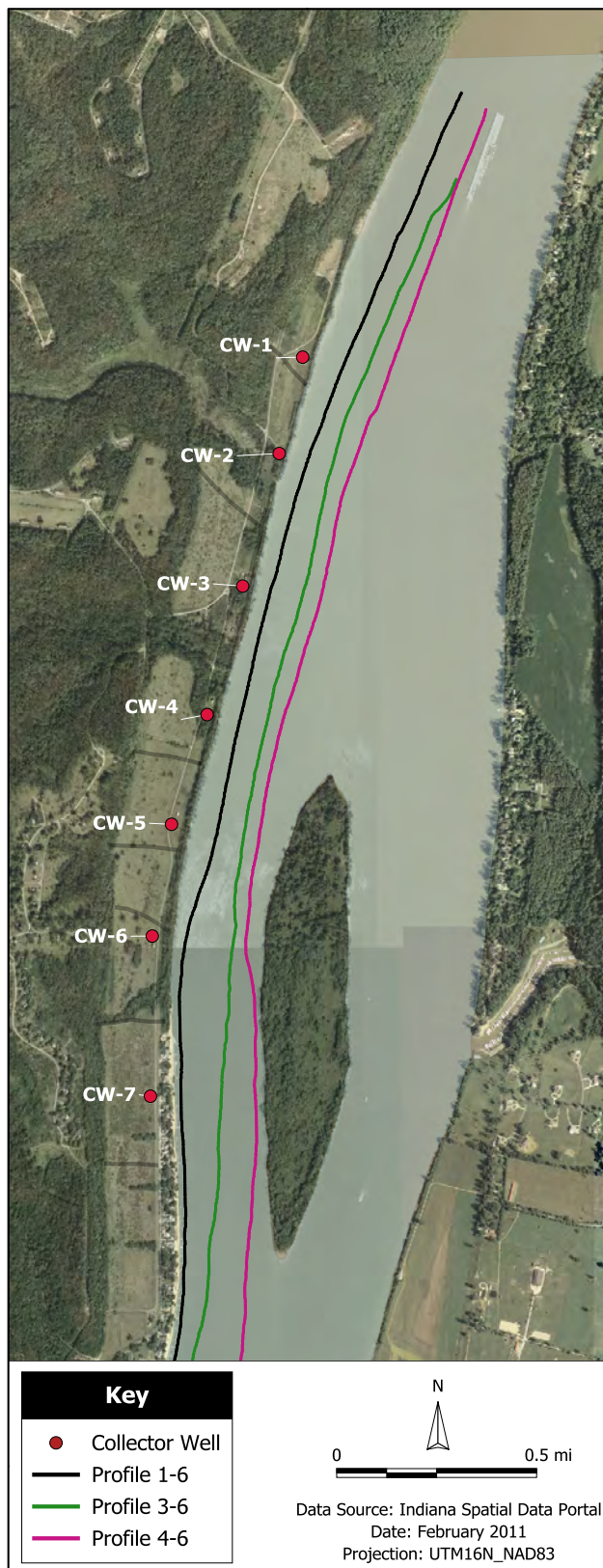


Figure 5: Location of the 6-meter marine electrical resistivity profiles.

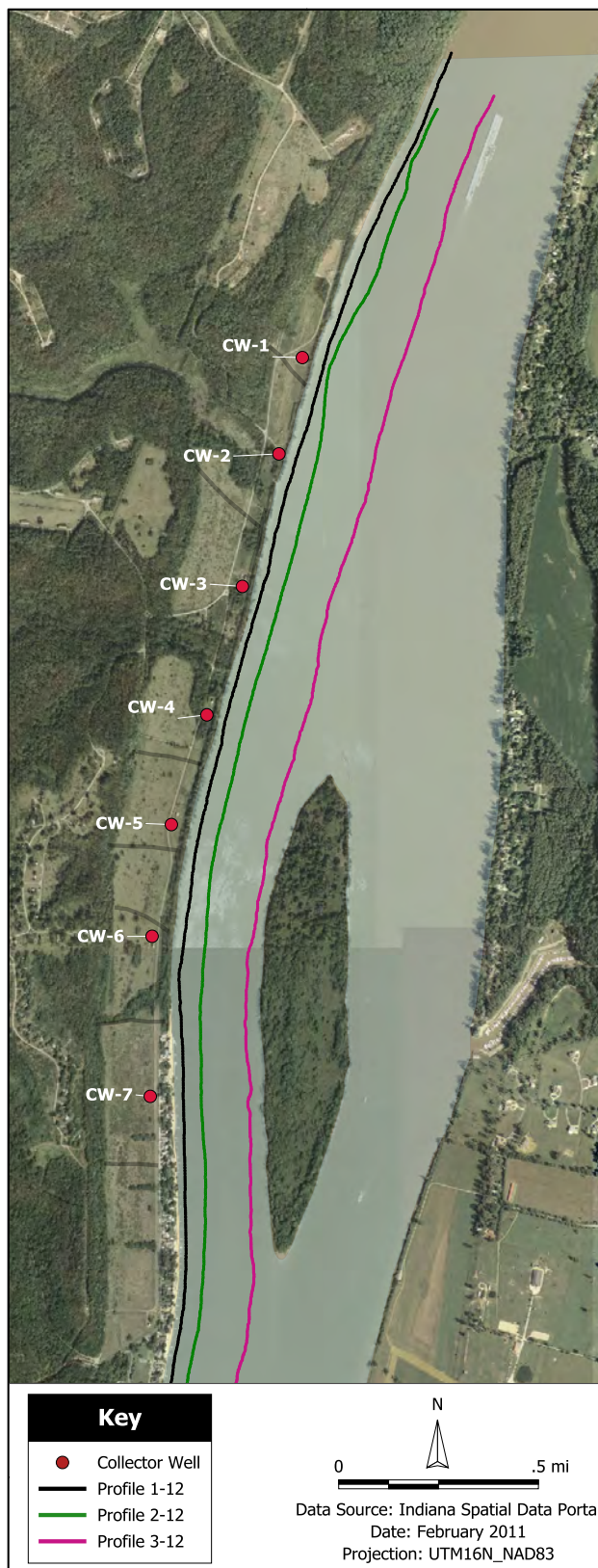


Figure 6: Location of the 12-meter marine electrical resistivity profiles.

Table 1: The RMS and L2 results for the the marine and land ERI profiles.

Marine profile	RMS (%)	L2	Land profile	RMS (%)	L2
6-meter spacing			R1	2.97	0.98
1-6	7.92	6.95	R2	5.86	0.80
3-6	9.87	9.8	R3	7.77	0.93
4-6	3.11	1.07	R4	7.28	0.68
12-meter spacing			R5	5.05	0.87
1-12	3.67	1.49	R6	4.70	0.62
2-12	7.29	5.89	R7	4.07	0.70
3-16	3.10	1.06	R8	1.62	0.29

Note. RMS = root mean square, L2 = square of the weighted data errors between the calculated and measured apparent resistivity data.

material has a higher resistivity value when compared to saturated material. Also, sand and gravel deposits have higher resistivity values than material of silt, clay, and fine sand. The modeled resistivity values were used to map the permeable materials in the subsurface. Areas with resistivity values between 10-ohm meters and 50-ohm meters were interpreted either as clay/silt or as bedrock. These materials have low hydraulic conductivity and porosity, and therefore are not considered aquifer materials. Areas with resistivity between 100-ohm meters and 1,000-ohm meters were classified as sand and gravel in the Aquifer. Using this classification scheme, we characterized the land and marine ERI profiles into four types: bedrock, aquifer material, confining unit in the land area, or streambed sediment under the river. These data were used to estimate the elevation of the top and base of the aquifer and the thickness of the riverbed sediment.

Land seismic survey

The seismic data were interpreted using the delay-time analysis technique with the WINSIP software package from Rimrock Geophysics, Inc. With the delay-time analysis technique, depths are calculated under each geophone, thereby accounting for irregular refracting surfaces (i.e., irregular bedrock surface).

Using the seismic refraction data for profile lines SL1 and SL2, we created velocity-depth section models, which illustrated three distinct layers:

- an upper, unsaturated, weathered soil layer
- an intermediate, saturated unconsolidated material layer

- an underlying bedrock layer

The modeled seismic velocity-depth sections for both profile lines are included in Appendix A - Supplemental Geophysical Survey Information.

3.1.3 Results

Using the results of the ERI and seismic surveys, we delineated

- aquifer top elevation (Figure 7)
- aquifer base elevation (Figure 8)
- aquifer thickness (Figure 9)
- river bottom elevation(Figure 10)
- riverbed sediment thickness (Figure 11)

Each of these different data sets were converted into GIS grids or surfaces. Each grid was incorporated into the groundwater flow model to accurately reflect the geometry and boundaries of the aquifer and the hydraulic connection between the river and the aquifer. Appendix A - Supplemental Geophysical Survey Information includes a detailed description of the geophysical surveys and modeling.

In addition to the grids, three aquifer transmissivity zones were delineated based on resistivity values calculated from the ERI profile results (Table 2). Regions with resistivity values between 200 and 320 ohm-meters are found mostly away from the river, towards the west side of the study area where the aquifer thins with the rise of the bedrock. Zones with resistivity values between 320 and 600 ohm-meters and 600 and 1,00 ohm-meters are generally closer to the river where aquifer material is larger and the Aquifer is thicker. These transmissivity zones were used to discretize 12 zones of constant hydraulic conductivity during the initial stages of groundwater flow modeling (Section 4).

3.2 Water-level Measurements

During this study, we collected synoptic and continuous water-level measurements in monitoring wells and the Ohio River. These measurements were used to calibrate the groundwater flow model. Blankenbeker & Son Land Surveyors Inc. surveyed the location and elevation of 14 monitoring wells to use as the reference elevation for water-level measurements. A USGS benchmark on the boat ramp was used as the reference elevation for the river stage measurements (Figure 12).

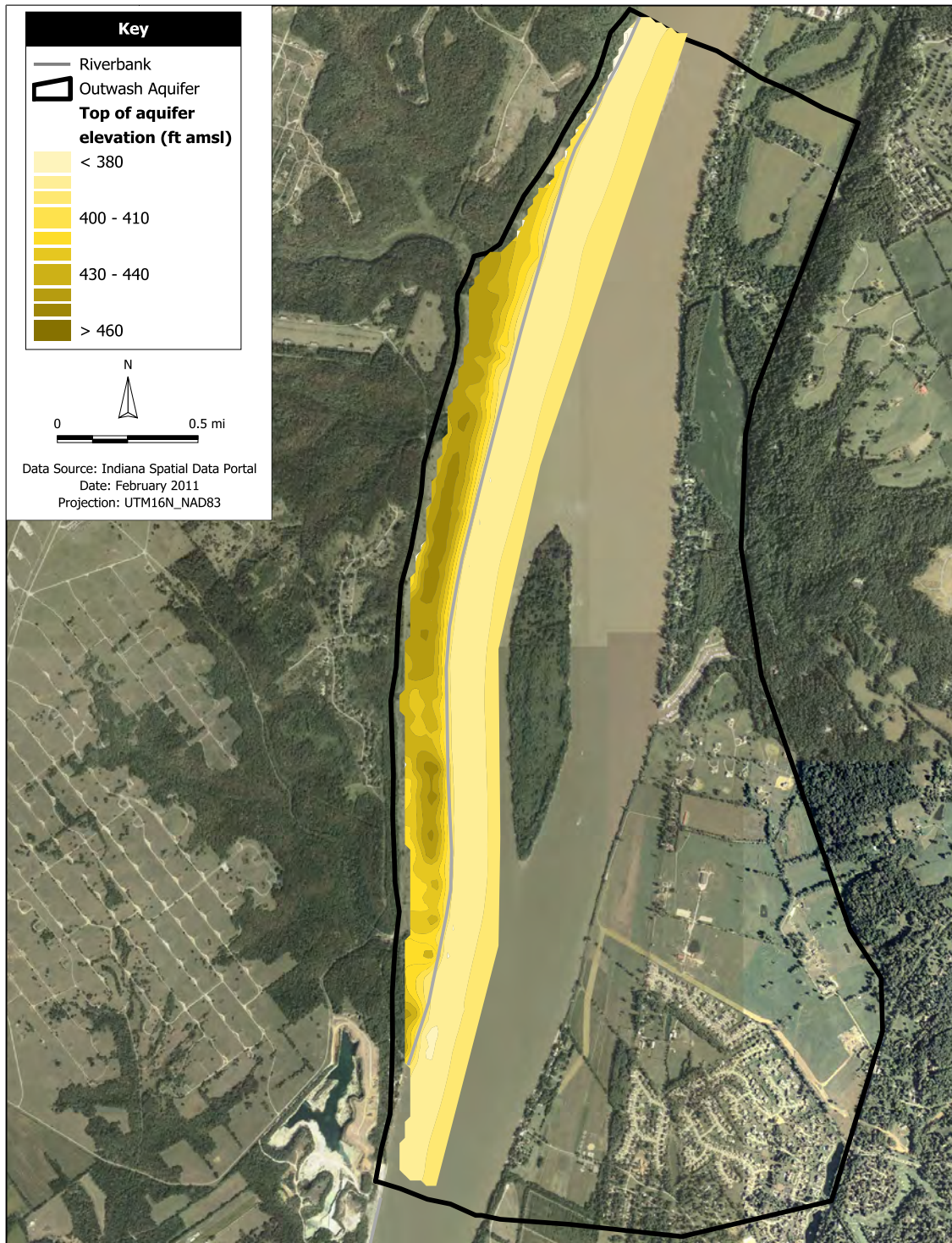


Figure 7: Elevation of the top of the aquifer under the Ohio River along the study site in Charlestown State Park.

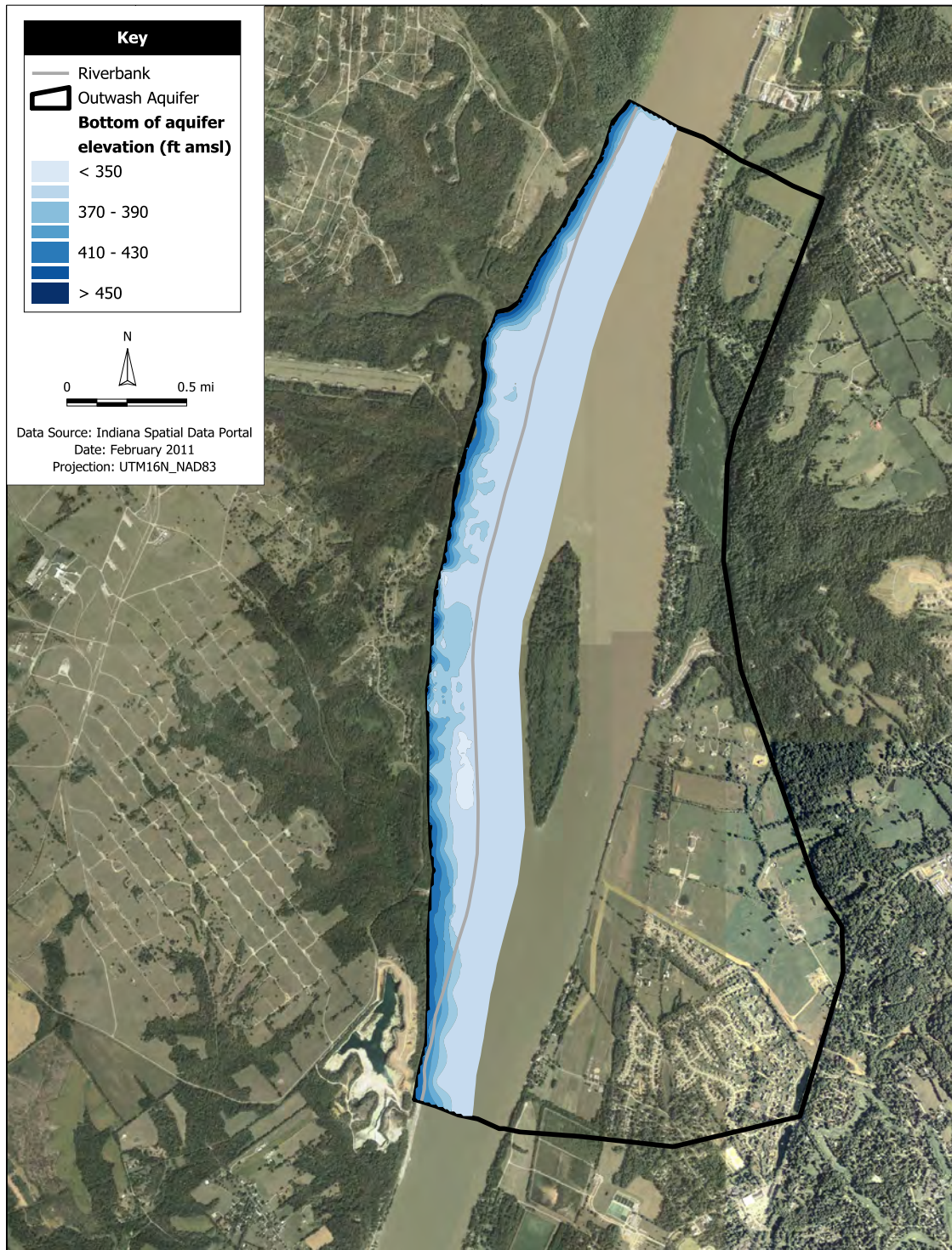


Figure 8: Elevation of the bottom of the aquifer under the Ohio River along the study site in Charlestown State Park.

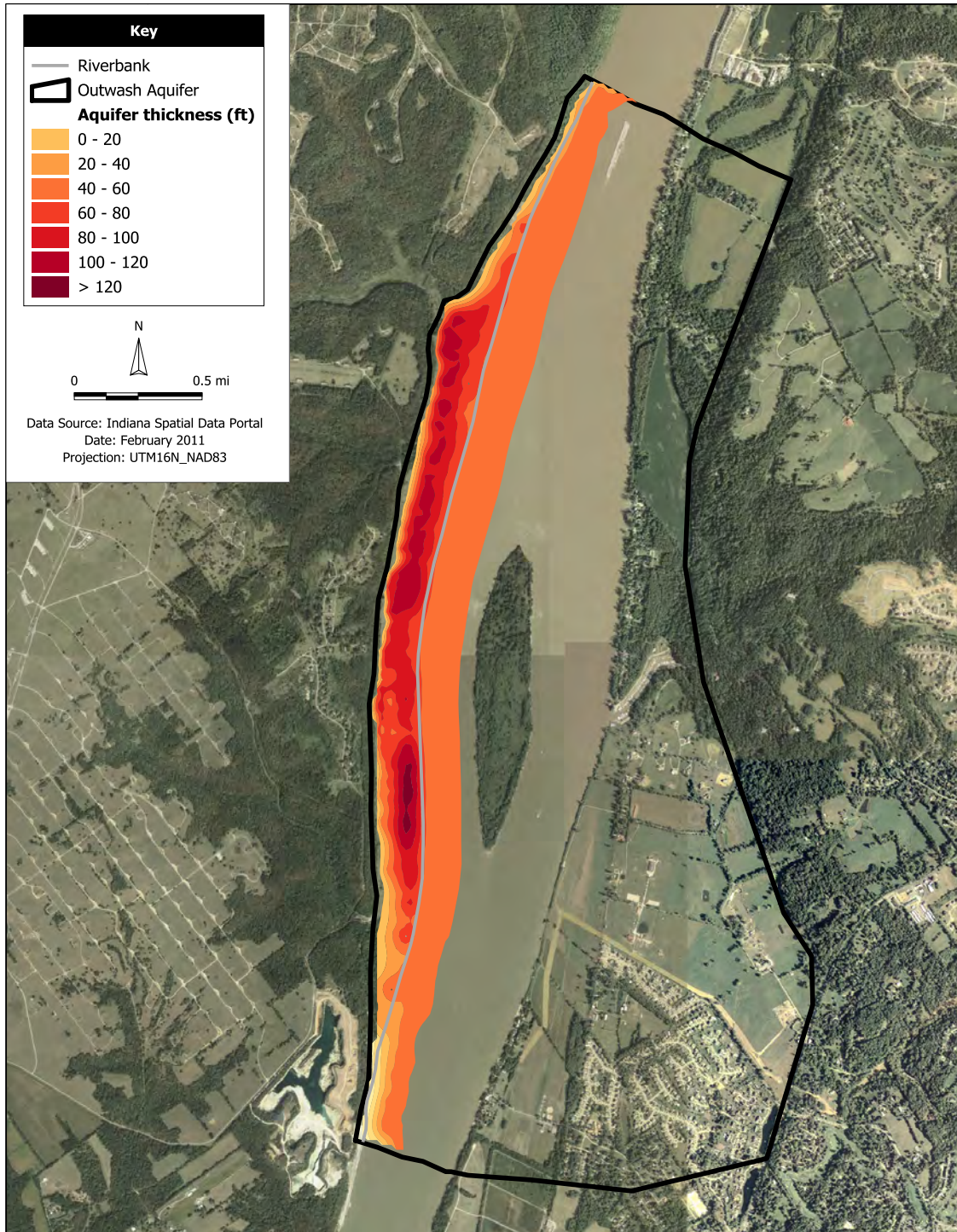


Figure 9: Thickness of the aquifer under the Ohio River along the study site in Charlestown State Park.

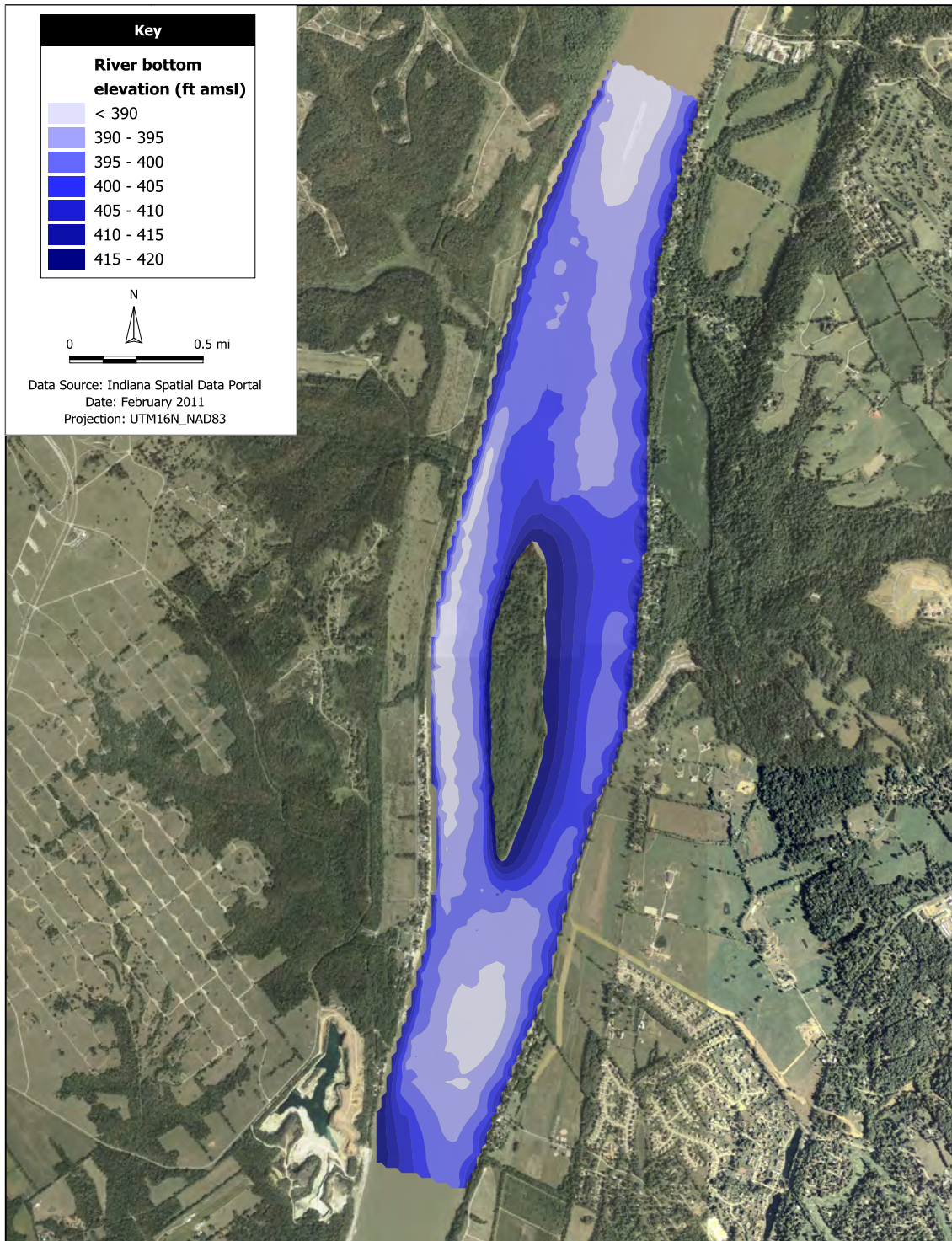


Figure 10: Bathymetry of the Ohio River along the Charlestown State Park.

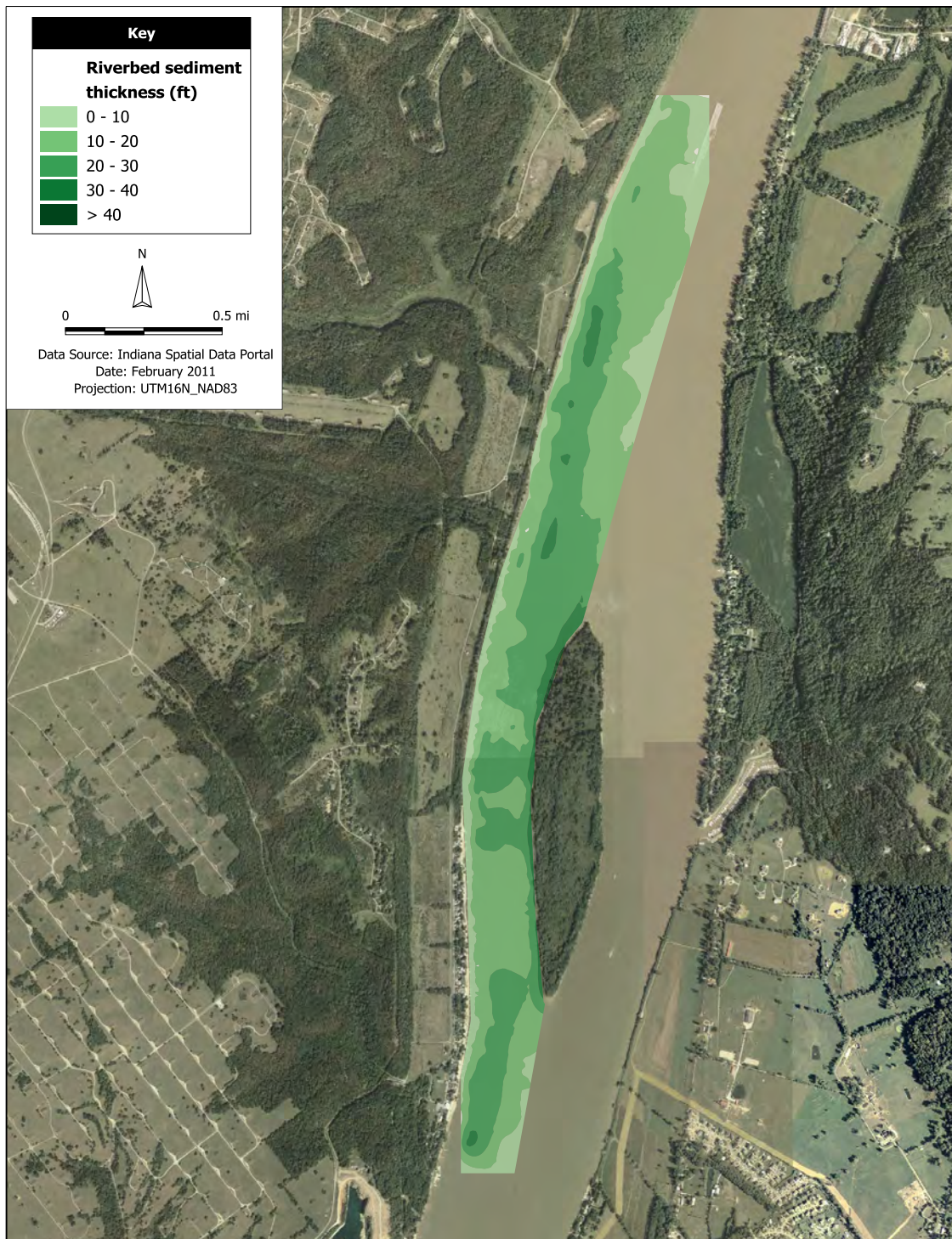


Figure 11: Thickness of the riverbed sediment in the Ohio River along the study area in Charlestown State Park.

Table 2: Interpretation of resistivity values delineated using results from ERI surveys along the Ohio River.

Reading <i>ohm meters</i>	Aquifer material characteristics	Transmissivity
200-300	fine-grain	low
320-600	fine- to coarse-grain	medium
600-1,000	coarse-grain	high

Synoptic water-level measurements were taken from the 14 monitoring wells on October 20, 2010, during a period when the river level did not fluctuate significantly and prior conditions were dry (Table 3). These measurements were taken to get a snapshot of the aquifer water levels during a period of constant stage on the Ohio River. Water levels were manually measured using an electronic water-level meter with a precision of 0.01 ft. The results show that water levels in the aquifer throughout the Park are nearly constant, and approximately 0.4 ft lower than the river stage when the measurements were taken.

Continuous water-level measurements were recorded from October 20, 2010 to December 7, 2010, every half hour in wells MW-3, MW3-4, MW-6, MW-8, and a stilling well located on the bank of the Ohio River (Figure 12). The four data loggers installed in the monitoring wells recorded changes in the aquifer’s water level, while the stilling well was used to record water levels in the Ohio River. Typically, water levels along the Ohio River fluctuate little because of dams; the closest dam to the study site is McAlpine Locks and Dam, which is approximately 11 mi downstream at River Mile 606.8. However, during the study period (October 20, 2010 to January 7, 2011) a flood pulse was recorded (December 4, 2010 to December 6, 2010) that raised the river’s stage six feet and increased groundwater levels (Figure 13). The continuous monitoring allowed us to record changes in the aquifer over time caused by the changing stage of the Ohio River and to demonstrate the the river’s influence on the aquifer. A calibration data set was developed from the monitoring data and used in developing and calibrating the groundwater flow model.

3.3 Infrastructure Assessment

Our field assessment of infrastructure was limited to a paper review of previous inspection reports of the collector wells (Ranney, 1965, 1979; Burgess and Niple, 1995; Reynolds, 2000) and an inspection of collector well CW-6.

The Well Field contains a great deal of existing water supply infrastructure, not all of it is useful. However, there may be opportunities to reuse some assets in the redevelopment of the Well Field.

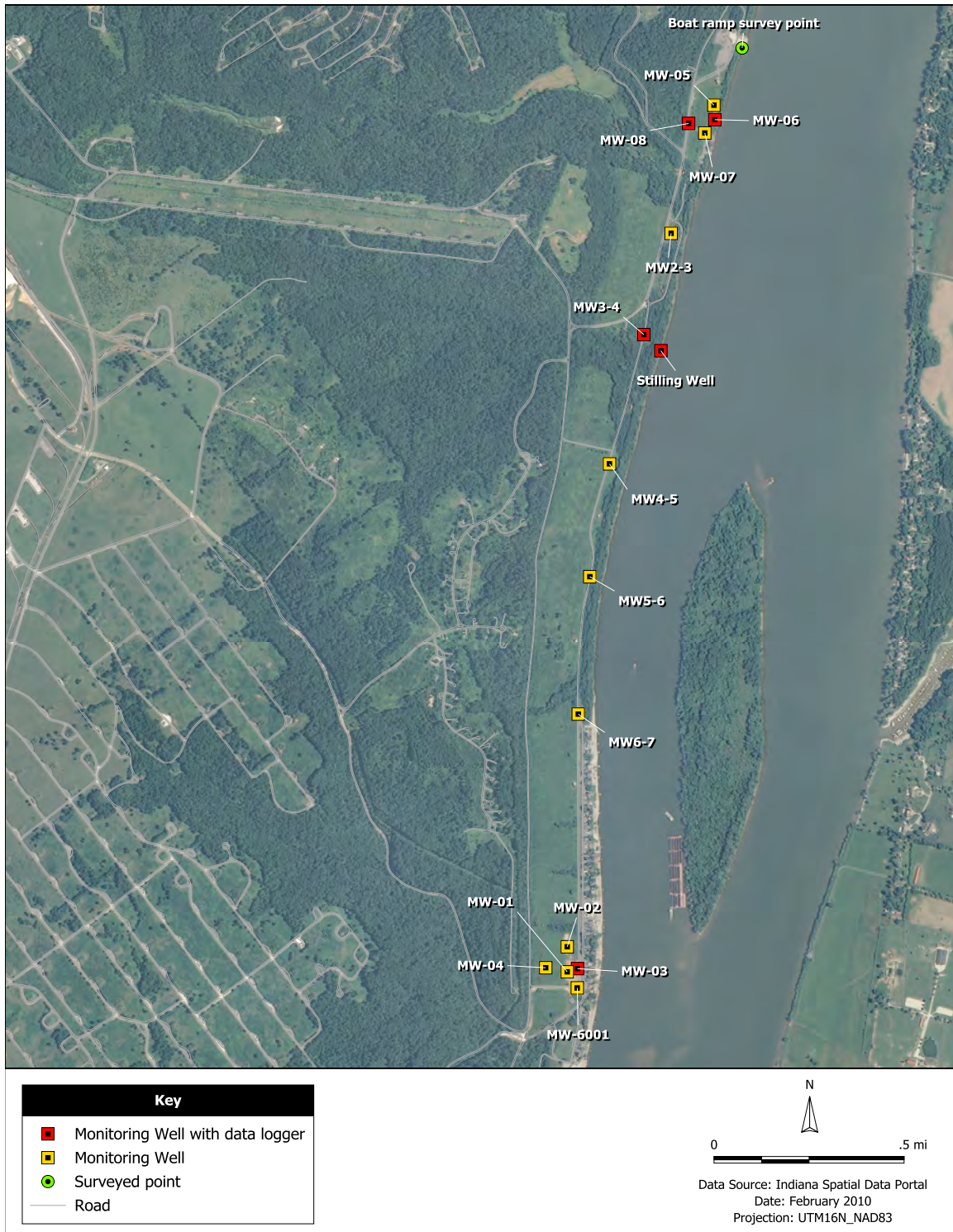


Figure 12: Location of the monitoring wells and stilling well in the study area along the Ohio River.

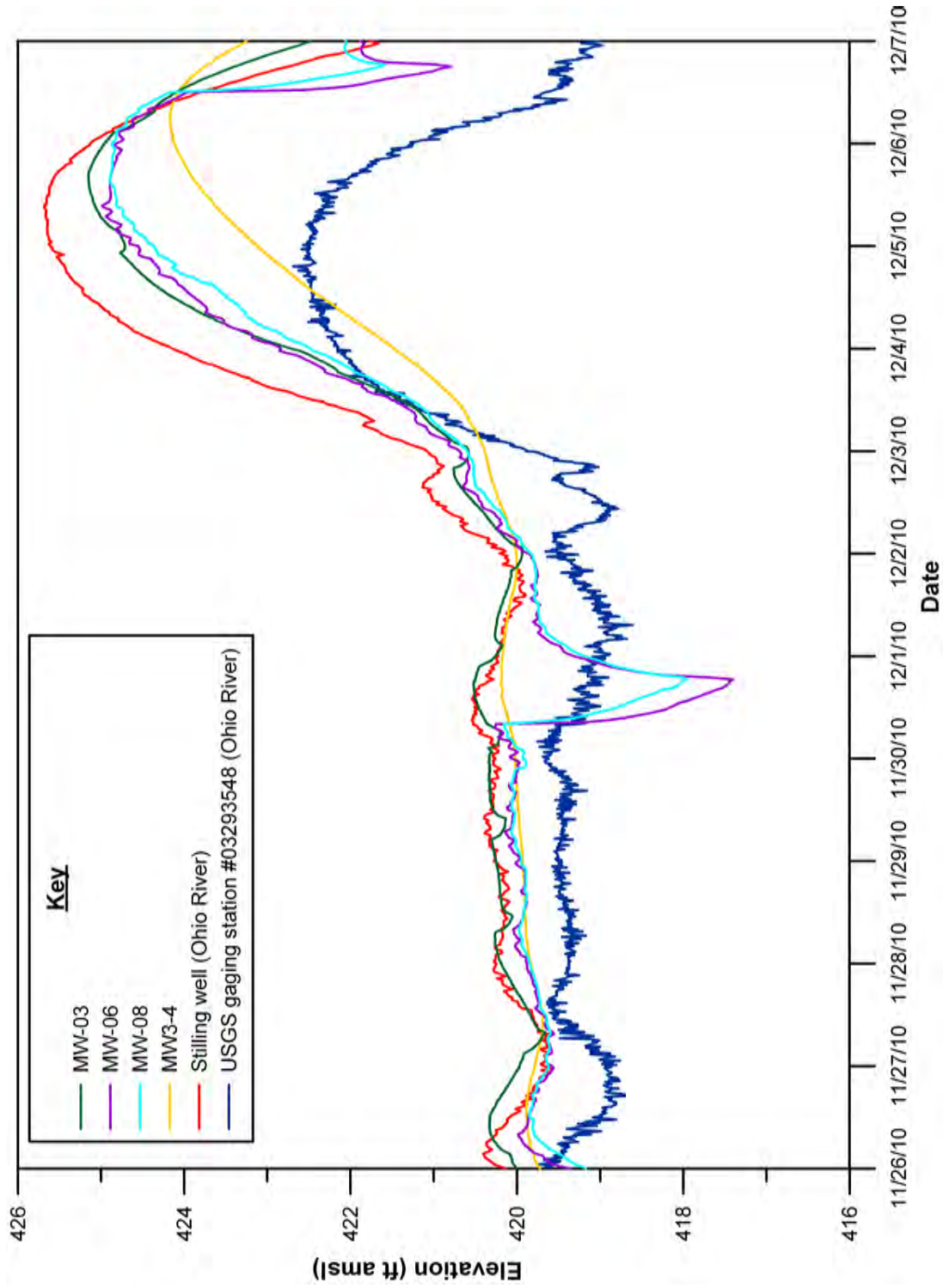


Figure 13: Water levels in the Ohio River during monitoring period. The USGS gaging station (blue line) shows that the river level varied less than 1 ft except during the flood pulse from December 4 to 6, 2010.

Table 3: Monitoring well locations and synoptic water-level measurements.

Monitoring Well	Coordinates		Date: 10/20/2010	
	Latitude	Longitude	Time	Water elevation (ft amsl)
MW-6001	38° 21.883' N	-85° 38.403' W	12:06 PM	419.61
MW-01	38° 21.920' N	-85° 38.431' W	12:23 PM	419.56
MW-02	38° 21.977' N	85° 38.430' W	12:32 PM	419.55
MW-03 ^a	38° 21.927' N	-85° 38.402' W	12:16 PM	419.65
MW-04	38° 21.930' N	-85° 38.494' W	12:27 PM	419.67
MW-05	38° 23.899' N	-85° 37.968' W	2:10 PM	419.50
MW-06 ^a	38° 23.866' N	-85° 37.966' W	2:02 PM	419.60
MW-07	38° 23.836' N	-85° 37.995' W	2:10 PM	419.56
MW-08 ^a	38° 23.858' N	-85° 38.042' W	1:52 PM	419.53
MW2-3	38° 23.607' N	-85° 38.098' W	1:39 PM	419.62
MW3-4 ^a	38° 23.376' N	-85° 38.181' W	1:06 PM	419.59
MW4-5	38° 23.081' N	-85° 38.207' W	12:51 PM	419.65
MW5-6	38° 22.824' N	-85° 38.347' W	12:46 PM	419.60
MW6-7	38° 22.509' N	-85° 38.349' W	12:43 PM	419.62
Stilling Well ^a	38° 23.338' N	-85° 38.133' W	1:36 PM	419.98
Boat ramp survey point	38° 24.029' N	-85° 37.883' W	-	-

Note. ft amsl = feet above mean level. .

^aWell was used in the continuous ambient water-level monitoring.

Existing water supply facilities include the seven collector wells, two vertical wells, pumping equipment, water transmission mains, multiple storage tanks, and distribution networks. Relatively little of the original infrastructure remains in service.

Wells CW-1 is operated periodically to supply water to the north end of the RRCC and is the only collector well in operating condition. The other collector wells have been out of service for up to 40 years. The collector wells have been inspected previously (Ranney, 1965, 1979; Burgess and Niple, 1995; Reynolds, 2000). Photographs and additional information on the collector wells is provided in Appendix E - Infrastructure Evaluation.

On the south end of the system, tubular well TW-6001 is currently operated to supply water to the south end of the RRCC. A new water supply facility nearing completion at the south end of the Well Field will eliminate the current need for supplies from CW-1 and TW-6001 (WHPA, 2010). It is anticipated by IDNR that both CW-1 and TW-6001 will be shut down when the new supply and treatment facilities are placed in service.

Collector well caissons and laterals The concrete caissons were reported in 2000 to be in condition suitable for rehabilitation. Concrete tests conducted at that time with a Type N Schmidt Hammer determined that the compressive strength of the concrete was from 3,000 psi to 8,500 psi (Reynolds, 2000).

During a 1995 inspection of CW-6 by Burgess & Niple, extensive pitting was observed in the interior concrete wall of the caisson below the water line. Additionally, a crack was observed in the caisson wall, estimated to be 3 ft long, up to 1½ in wide, and 3 in deep (Burgess and Niple, 1995). CW-6 is the only well where potential structural issues were previously identified. As part of our study, a commercial diving firm performed a visual inspection of the well and collected concrete cores to determine the preliminary feasibility of reusing CW-6's caisson. The inspection was overseen by Ranney Collector Wells. A temporary generator-powered pump was installed in CW-6 and pumped for an extended period to clear the water prior to entry for inspection. Pumping continued during the inspection to minimize the impact of disturbed sediments on diver's visibility and movement. On February 17, 2011, the diver made a video recording of his inspection of the interior of the collector well, observing the previously reported pitting and cracking in the concrete. The diver collected concrete cores from pitted and cracked areas for laboratory testing of concrete strength. The report describing the results of the inspection is included in Appendix E - Infrastructure Evaluation. The inspection and results of the laboratory tests confirmed that the previously reported crack was in fact a construction joint and that the compressive strength of the concrete was very high. Based on the evaluation, it was determined that the structural integrity of the concrete caisson of CW-6 appears to be adequate for rehabilitation.

Pump houses The pump houses of the existing collector wells appear to be in generally poor condition. Doors, siding, hatches, and other metal have corroded, in many cases severely. Sanitary conditions appear to be generally poor. Bird and rodent infestation is evident. Tanks and pumping equipment previously used for oil lubrication of the collector well pumps present a potential source of contamination. Many of the pump houses have been broken into, vandalized, and stripped of salvageable metals.

Pumping equipment and switchgear The only collector well known to have operable pumping equipment is CW-1. Wiring and other salvageable metal has been stripped from the switchgear and control panels of many of the collector wells.

Electrical service The condition of electrical service lines supplying power to the Well Field and to individual collector wells is unknown. Existing high voltage transformers installed at each collector well are assumed to be inoperable or non-compliant with current electrical codes.

Pipelines The majority of existing pipelines in the well field were installed in the 1940s. They are believed to be primarily composed of cast iron with leadite joints, and are as large as 36-inches in diameter. With the exception of the main between CW-1 and the north portion of the RRCC, the existing water mains in the well field have been removed from service. Water loss is believed to be very high, typical of cast iron pipe with leadite joints. As recently as 2006, water loss was reported to be 65% to 80% in portions of the system (Curry, 2006).

A thorough inspection of existing water supply infrastructure was outside of the scope of our study. Specific decisions made regarding the reuse, repair, or replacement of existing structures and equipment should be preceded by a thorough inspection.

This page intentionally left blank

4 Well Field Capacity Evaluation

Predicting the overall capacity of a well field that includes collector wells is complicated by many physical and operational factors. There are the usual hydraulic constraints that affect groundwater flow and limit the amount of water that can move through the aquifer to the well, such as aquifer properties and the hydraulic connection between groundwater and surface waters. However, the structural design of the well itself often is the limiting factor that determines well capacity. At Charlestown, the design is further limited because seven collector wells already exist and their construction details can not be easily changed. Operational interference with neighboring wells, excessive drawdown in the well caissons, and reduction in yield during the “break-in period” of a well field must also be taken into consideration when multiple wells are running. These physical and operational factors that affect yield were included in this study when estimating a sustainable capacity of the well field.

In discussing and evaluating the various constraints on the well field, several different terms relating to well and well field yield are used. All of these terms contain the words *capacity* or *yield*; for clarity we define each measure of yield used in this report.

mechanical capacity - the capacity that is based on the ability of a well to deliver water.

theoretical yield -the amount of water entering a well at a specified drawdown in the caisson, as determined by a calibrated groundwater flow model.

design capacity -the lesser of the mechanical capacity and the theoretical yield.

sustainable capacity -a value equal to or less than the design capacity. A 25% reduction in design capacity is applied to the largest producing collector wells if the design capacity of that well is based on the theoretical yield.

The *sustainable capacity* of the well field reported in this study is the capacity that should be used for planning and development of the well field. To estimate sustainable capacity, it is necessary to first estimate the mechanical capacity, the theoretical yield, and the design capacity of the individual wells within the field.

Physical constraints on yield Several physical constraints on the yield of the well field exist, affecting both the mechanical capacity and theoretical yield of the wells. Physical constraints affecting the mechanical capacity of a well include the ability of the filters and screens on the lateral arms to pass water without clogging or degrading, and the ability of the lateral arms to conduct water safely to the caisson without developing excessive velocities. These factors limit a well’s ability

to transmit water to the water supply system. Physical constraints affecting the theoretical yield of the wells include the aquifer's hydraulic conductivity and the degree of connection between the Aquifer and the Ohio River. These properties impact the ability of the Aquifer to transmit water to the wells. In this analysis, we computed the well field capacity based on each potentially limiting factor, then defined the design capacity as the smallest of the various estimates. For example, if the well screens and caisson were capable of delivering 5 mgd but the groundwater flow model only estimated a yield of 4.6 mgd, we estimated the well's yield to be 4.6 mgd.

Operational constraints on yield Operation constraints primarily impact the theoretical yield of collector wells. Two operational issues were investigated in the yield analysis.

1. The operating water level in each well caisson must lie sufficiently (e.g., 5 ft or more) above the top tier of the lateral screen openings to prevent accelerated fouling of the screens. This impacts the theoretical yield of each collector well.
2. Water levels beneath the streambed must not fall to a level that threatens to induce plugging or compaction of the streambed sediments, reducing long-term yield. This constraint also impacts the theoretical yield of each collector well.

Streambed compaction is critical because it can reduce long-term yields. The elevation of the streambed on the west side of the river is approximately 385 to 390 feet above mean sea level (ft amsl); fixing the minimum head in the caisson of each well at 399.5 ft amsl is intended to safely prevent dewatering of the Aquifer beneath the streambed. This will limit the potential for streambed sediments to plug or compact because of over pumping. Therefore, the maximum allowable drawdown in the caisson is fixed at 20 ft (399.5 ft amsl); this value was specified in all predictive calculations.

Approach Our approach for predicting the sustainable capacity of a redeveloped well field at the Park explicitly accounted for each of the physical and operational constraints on the design.

1. The mechanical capacity for each well was estimated based on the as-built drawings and collector well design guidelines provided by Ranney Collector Wells. The design guidelines were then used to specify additional laterals for some wells to increase their mechanical capacity. The original as-built design and the modified designs were used in predictive model simulations.
2. A new groundwater flow model of the entire site was developed and calibrated. This model was based on the conceptual model derived from the newly acquired geophysical data. The

model was calibrated with new water-level data collected during this study, water-level data collected during pumping tests in 2009 (WHPA, 2010), and water-level data from a 1995 aquifer test (Burgess and Niple, 1995).

3. The calibrated model was then used to predict the theoretical yield of collector wells at the site for each of 16 Well Field development alternatives. Depending on the design configuration for each alternative, the as-built lateral layout or the modified layout was selected for each well. The predictive model runs were configured in a manner that accounted for the operational constraints identified above.
4. The theoretical yield and mechanical capacity results for all alternatives were tabulated. For each well in each alternative, the design capacity was determined as the lesser of the theoretical yield and mechanical capacity.
5. Finally, the sustainable capacity of the Well Field was determined by reducing some of the well design capacities by 25%. The decrease in theoretical yield is used to reflect changes in aquifer conditions that often occur during the “breaking-in period” of a well field. No reduction is made to the theoretical yields of the existing, low-producing collector wells because those wells were pumped at higher levels for extended periods of time during the 1940s. We anticipate that there will be no reduction in yield for those wells when operation resumes.

After the sustainable capacity for each alternative was evaluated, an additional set of model runs was performed to assess the degree of uncertainty in the model predictions.

4.1 Mechanical Capacity Estimation

The mechanical capacity of a collector well is the well’s maximum hydraulic capacity based solely on its design and construction characteristics. Therefore, the mechanical capacity of a well is independent of the ability of the aquifer to deliver water to the well, which is the aquifer yield. To compute mechanical capacity, maximum allowable design values were specified for the lateral screen entrance velocity, the velocity of groundwater approaching the screen from the aquifer (the approach velocity), and the in-line flow velocity (water velocity inside the lateral). The mechanical capacity was the largest well discharge that satisfied all of the design criteria.

The approach velocity is the velocity at the interface between the aquifer and the screen in a naturally developed well. The maximum allowable approach velocity is calculated as

$$V = 35.5\sqrt{K} \tag{1}$$

Table 4: Mechanical capacity of the existing collector wells.

	Total screen length (<i>ft</i>)	Maximum capacity based on		
		Approach velocity (<i>mgd</i>)	Entrance velocity (<i>mgd</i>)	In-line velocity ^a (<i>mgd</i>)
CW-1	1,204	24.2	4.9	7.1
CW-2	1,202	16.8	4.9	7.1
CW-3	1,382	19.3	5.6	11.0
CW-4	1,231	20.4	5.0	7.9
CW-5	1,423	23.6	5.8	7.9
CW-6	1,111	18.4	4.5	7.9
CW-7	1,246	36.9	5.1	5.5
Total			35.7	

^aIn-line velocity is the velocity within the collector well's lateral arm.

where K is the hydraulic conductivity of the aquifer in ft/d, and V is the approach velocity (actually, the specific discharge, in ft/day) (Williams, 1981). This is an empirical equation. It has been observed that exceeding the maximum approach velocity may lead to clogging of the aquifer material around the well screen.

The entrance velocity depends on the slot size and transmitting capacity of the lateral screen. The maximum design value for a horizontal lateral is 1 ft/min (0.017 ft/sec). The in-line velocity is based on the number and diameter of the lateral screens and has a maximum design value of 3.5 ft/sec.

Estimates of the mechanical capacity were made for each of the existing collector wells at the Park. The estimates are based on information in an inspection report for the well field (Ranney, 1979), information in Burgess and Niple (1995), and estimates of hydraulic conductivity obtained from calibration of the groundwater flow model. The Ranney inspection report provides as-built drawings for each collector well including lateral lengths, orientations, and elevations. The report states that all laterals are 8 inch inside diameter slotted pipe with 18% open area for inflow. During the 1979 inspection, the valves of several laterals were shut; the capacity calculations presented here assume all laterals are open and in operating condition. The screen entrance velocity is the limiting factor for all of the collector wells (Table 4); therefore the mechanical capacity of the individual wells and the well field is based on the maximum allowable entrance velocity.

Estimates were also made of the additional number of laterals that would need to be added to collector wells CW-1, CW-6, and CW-7 to increase their mechanical capacity to 15 mgd (Table 5). In retrofitting the wells, we assume that a third tier of laterals is added 5 ft above the centerline

Table 5: Additional 170 ft-long laterals required to increase the mechanical capacity of collector wells to 15 mgd.

Well	Existing capacity (<i>mgd</i>)	Additional capacity (<i>mgd</i>)	Additional length of screen (<i>ft</i>)	Additional lateral arms
CW-1	4.9	10.1	905	6
CW-6	4.5	10.5	940	7
CW-7	5.1	9.9	887	6

of the highest existing laterals. Additionally, we assumed the new laterals would be constructed of 12 inch inside diameter continuous-slot screen with an average open area of 33%. The screen would be installed in 10-ft sections with 9.5 ft of screened length per section, and a 10-ft long blank (unscreened) section at the caisson. All new laterals are assumed to be 170 ft in length (approximately 152 ft of screened length).

4.2 Groundwater Flow Model Development

We developed a new groundwater flow model of the Aquifer lying adjacent to and beneath the Ohio River at the Park. The modeling objectives were: 1) estimate the theoretical yield of the well field; and 2) assess the effects of high pumping rates on regional conditions in the Aquifer.

The groundwater flow model was developed for MODFLOW 2000 (Harbaugh et al., 2000) using the Groundwater Vistas pre- and post-processor (Rumbaugh and Rumbaugh, 2007). Two models of the Aquifer were developed for separate purposes: (1) a transient model with a coarse grid was developed and used for calibration (the Calibration Model); and (2) a steady-state, fine-grid model was developed for predictive modeling to evaluate aquifer yield (the Predictive Model). A coarse grid was necessary to minimize the computational burden while calibrating the model, which requires multiple, repetitive model runs. The fine grid was necessary in the Predictive Model to accurately represent the collector well laterals and to evaluate their yield. The computational burden caused by the fine grid of the Predictive Model was acceptable because it was a steady-state model and repetitive model runs were not necessary. Both models consist of a single layer with identical parameter zones; parameter values obtained from the Calibration Model were specified in the Predictive Model. The only difference between the two aquifer models was grid spacing, and the two are referred to collectively in this report as *the model*.

4.2.1 Revised conceptual model of the Aquifer

A revised conceptual model of the Aquifer was the basis for the groundwater flow model. The revised conceptual model is consistent with the previous study of the Aquifer (WHPA, 2010), but includes additional details that were identified during the geophysical study. The Aquifer is bounded laterally and below by bedrock that is assumed to be impermeable for the purposes of the model. It extends from bedrock outcrops on the Indiana side beneath the Ohio River and ends to the east at bedrock outcrops in Kentucky. Recharge to and discharge from the Aquifer is primarily due to fluctuations of river water levels, which controls groundwater elevations in the Aquifer. A thick layer of till, silt, and clay overlying the outwash materials limits recharge to the Aquifer from precipitation, and acts as a confining unit for the Aquifer where water levels in the river are above the bottom of the clay. Pumping from existing and proposed wells may lead to locally unconfined flow conditions when the potentiometric head falls below the bottom of the confining layer. In other areas, the confining unit is above the normal pool level of the river and unconfined flow conditions exist during most of the year. In the conceptual model, the river was the source of all recharge to the Aquifer. Neglecting recharge from precipitation and from the bedrock provides a conservative model for use in well field design because drawdown may be overestimated.

4.2.2 Model features

After review of the geophysical data and existing boring logs, it was determined that the aquifer properties do not vary significantly over the depth of the Aquifer. Flow in the Aquifer may be described as “shallow flow” suggesting that a single-layer groundwater flow model would be appropriate for this study. The complex, 3D flow near the lateral arms of collector wells is approximated in the single-layer model using a new approach, described in Appendix B - Predicting Collector Well Yields with MODFLOW. As the purpose of the model is to evaluate the theoretical yield of the well field rather than the local details of the groundwater flow field, this approach is adequate and greatly reduces the computational times required for each simulation.

The following computational features were used in the development of the model in MODFLOW.

- The Aquifer top and bottom elevations and thickness vary as the Aquifer extends from the walls of the bedrock valley to areas beneath the Ohio River.
- No-Flow Boundaries completely enclose the model.
- RIV (MODFLOW river package) cells overlie the Aquifer wherever the Ohio River is present. The riverbed conductance varies spatially according to the results of the marine geophysical survey.

- Vertical wells used for the pumping tests were represented as single-cell boundary conditions with a given, time-varying pumping rate using the MODFLOW WEL package.
- The existing collector wells (CW-1 through CW-7) were represented differently in the Calibration Model and the Predictive Model, as discussed in following sections of this report.

The details and features of the groundwater flow model are discussed below in more detail.

Spatial extent of the Aquifer The Aquifer extends over the entire portion of the Park that is on the Ohio River floodplain, and lies beneath the entire extent of the river within the Park. The Aquifer is limited in its extent perpendicular to the river; the bedrock crops out along a line of bluffs ranging from 400 ft to 1,000 ft from the river. In the model, this bedrock outcrop, and the corresponding outcrop east of the river in Kentucky, were represented as no-flow boundaries. North and south of the Park, the western river bank meets the bedrock outcrop, and the Aquifer is absent. These are located far from the existing well locations, and we chose these points as the northern and southern limits of our model.

It is assumed that nearly all the water moving to the wells will enter the aquifer as induced recharge from the overlying river. Thus, we imposed a no-flow boundary that joins the east and west bedrock boundaries, perpendicular to the river at the north and south ends of the model. The active perimeter of the model is illustrated in Figure 14.

Aquifer top and bottom elevations The Aquifer is bounded above by a thick layer of clay and silt that varies from 10 ft to 35 ft thick and below by bedrock consisting of limestone and siltstone. The elevations of the bedrock underlying the Aquifer and the top of the Aquifer also vary spatially, and were determined from the geophysical survey. Contour maps of the Aquifer top and bottom elevations and Aquifer thickness used in the model are presented in Section 3. The surfaces were imported into the groundwater model as GIS grids. The MODFLOW model is flexible enough to switch from confined conditions to unconfined conditions during flow simulations, as heads fall below the specified Aquifer top elevation.

Aquifer heterogeneity Previous studies indicate that the transmissivity of the Aquifer is large and varies within the Park; previous estimates of hydraulic conductivity range from 560 ft/day to 1,270 ft/day and the saturated aquifer thickness ranges from 50 ft to 85 ft (WHPA, 2010). In the current study, the model aquifer was divided into 12 zones of hydraulic conductivity (Figure 14). The zone boundaries are based on results of the geophysical survey, previous studies, and preliminary model calibration tests. Initially, the Aquifer was divided into three transmissivity zones, with boundaries approximately parallel to the river. The boundaries were chosen based on trends in

the resistivity of aquifer materials identified from the geophysical survey. A further subdivision of the zones was then made by adding two straight boundaries normal to the river; these boundaries are easily identified in Figure 14. This subdivision was based upon results from previous studies (WHPA, 2010; Burgess and Niple, 1995) which indicate that the aquifer transmissivity varies along the river as you move from the south end of the Park to the north end. Finally, the location of the boundaries normal to the river were adjusted based upon preliminary results of model calibration.

Surface water Interactions between the Aquifer and the Ohio River were simulated using the MODFLOW RIV (river) package in both the transient calibration model and the steady predictive model. The RIV package treats surface waters as head-dependent flux boundaries, in which the rate of groundwater infiltration from the river is related to the difference between the (modeler-specified) head in the river and the simulated head in the Aquifer,

$$Q_{river} = COND \times (H_{river} - H_{aquifer}) \quad (2)$$

where the *conductance* parameter is defined as

$$COND = A \times \frac{K_v}{D} \quad (3)$$

where A is the area of overlap between the surface waters and the cell, K_v is the vertical hydraulic conductivity of the streambed sediments and D is the thickness of the sediments. The rate of inflow to the Aquifer is rate-limited if the head in the Aquifer falls below the bottom of the riverbed sediments.

In the model, the River cells were divided into seven reaches of different properties, displayed in Figure 15. Streambed thickness was estimated for each reach based on the geophysical survey data. In the groundwater flow model, Reaches 1 through 3 have thicknesses of 20 ft, and Reaches 4 through 7 have thicknesses of 10 ft. The division of the river into reaches initially contained two zones based on streambed thickness: the first consisted of an approximately a 300 ft wide strip along the west bank with sediment thickness of 10 ft; the second zone consisted of the remainder of the streambed. Those two zones were further subdivided using the same boundaries normal to the river that were used to subdivide the transmissivity zones, allowing for variations in streambed properties along the Ohio River.

The vertical hydraulic conductivity of the riverbed sediments in each reach were allowed to vary during model calibration. During calibration, we specified a lumped *leakance* parameter

$$LEAKANCE = \frac{K_v}{D} \quad (4)$$

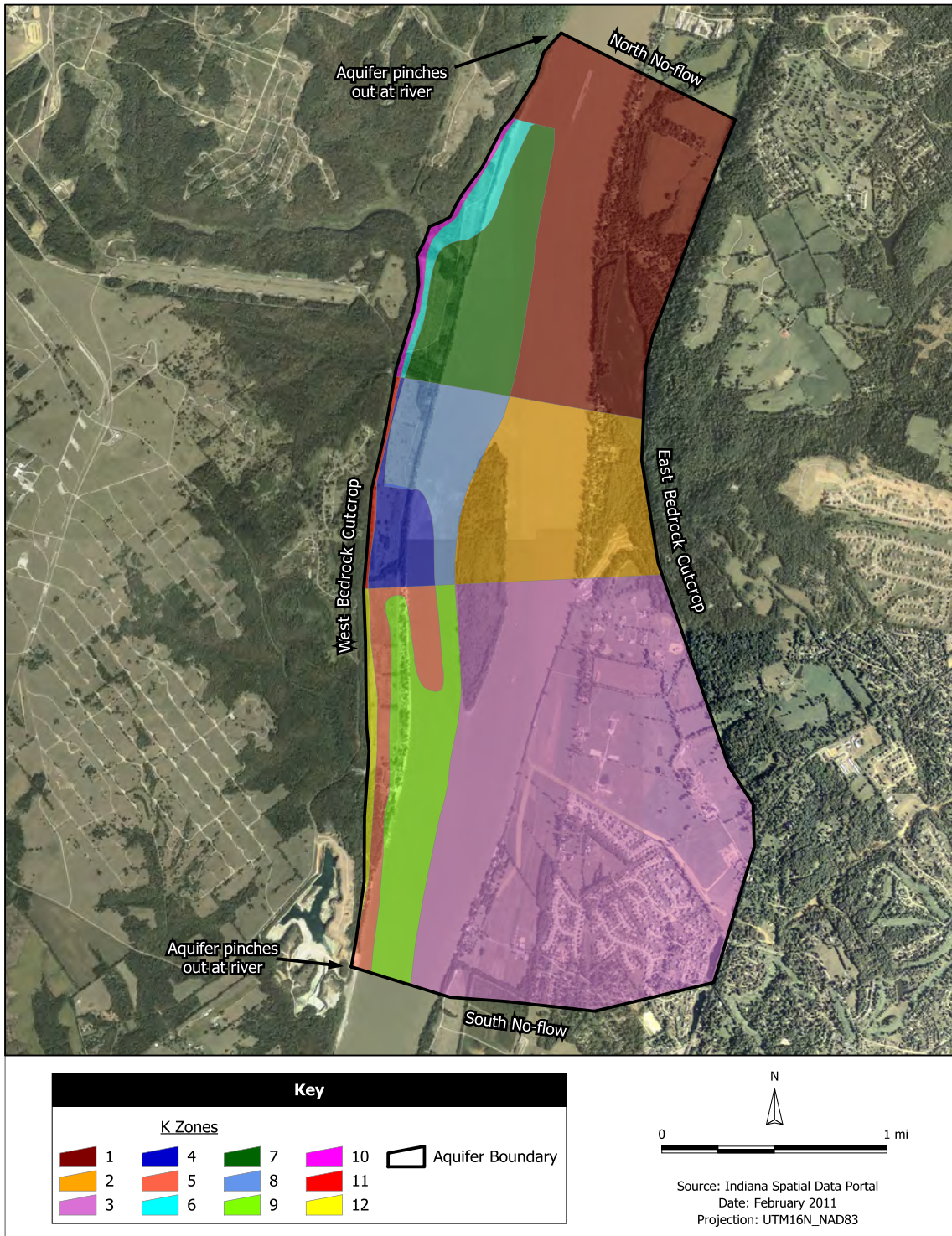


Figure 14: Domain boundary and zones of hydraulic conductivity, as represented in the groundwater flow model.

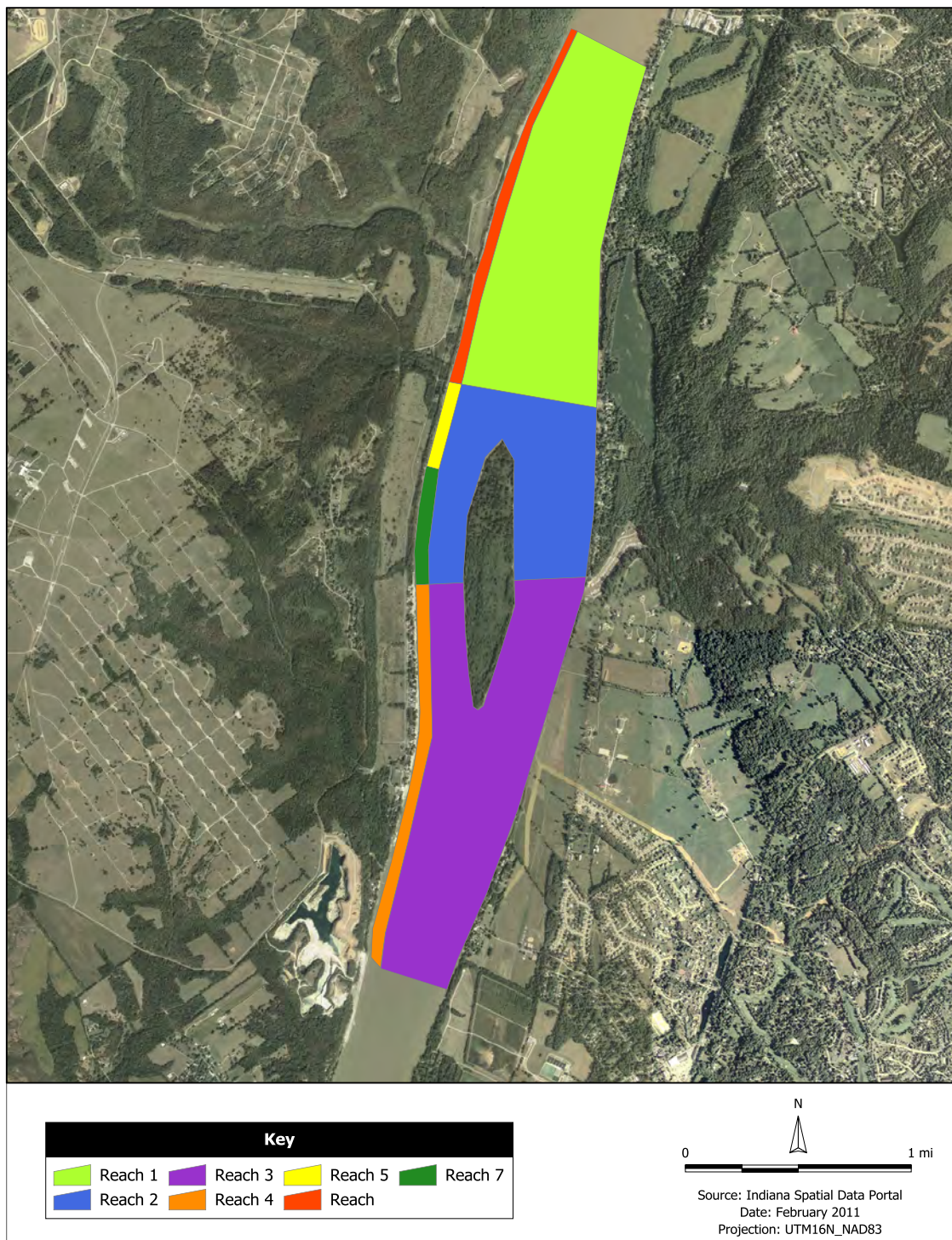


Figure 15: River reaches as represented in the groundwater flow model.

which was allowed to vary among the reaches. In both the calibration model and the predictive model, the river was sufficiently wide that entire cells were inundated; the area of overlap was the same as the cell area. During model calibration, we adjusted the leakance of the river reaches and developed a pre-processor that converted the leakance to RIV conductance values for each model run,

$$COND = AREA \times LEAKANCE \quad (5)$$

where *AREA* is the cell area.

Small surface-water features, including Jenny Lind Run, cross the Aquifer and discharge to the Ohio River. No surface-water features other than the Ohio River are represented in the model because there is no hydrologic evidence that they cut through the overlying clay confining unit at the site. Neglecting the potential for aquifer recharge from small surface water features is a conservative assumption when estimating the well yields.

Aquifer recharge Examination of the overall water budget at the site demonstrated that nearly all the water entering wells at a high-capacity well field will come from the Ohio River. Such a well field will potentially receive water from three sources:

- recharge to the Aquifer from precipitation at the site
- recharge to the Aquifer from the adjoining bedrock
- induced recharge from the river

Annual recharge due to precipitation is estimated to be 3.9 in/yr, which is approximately 9% of the 43 in/yr average precipitation for the region (Clark and Larrison, 1980). The thick layer of clay and silt overlying the entire Aquifer limits the amount of precipitation that infiltrates to the Aquifer. Additionally, the Aquifer covers an areal extent of 0.58 square miles. At a rate of 3.9 in/yr, this equates to 0.11 mgd, a negligibly small amount compared to the likely production rate of a well field at the Park. Indeed, even if all of the annual precipitation at the site were to reach the wells, it would only account for 1.2 mgd. Thus, we have made the conservative assumption to ignore areal recharge due to precipitation in the groundwater flow model.

Recharge from the fractured bedrock north and west of the site is also assumed to be negligibly small. This assumption is based on the fact that few, if any, high-capacity wells or homeowner wells are located near the site (Table 6). A study by the IGS found no significant leakage between the upland bedrock aquifer and the river (Hendricks, 1995).

Since other sources are negligibly small, the primary control on aquifer water levels is the Ohio River (Figure 13). We concluded that the only significant source of aquifer recharge to the wells is induced recharge from the Ohio River.

Table 6: Water wells in the bedrock formations within five miles of Charlestown State Park (IDNR, 2009).

IDNR reference number	Easting (<i>m</i>)	Northing (<i>m</i>)	Depth (<i>ft</i>)	Reported capacity (<i>gpm</i>)
195670	613676	4253060	100	-
195675	611077	4249783	85	1
195680	611937	4250791	75	30
195690	612411	4249644	85	4
195800	619331	4256995	80	5
195805	619928	4255423	125	-
201421	614493	4245685	69	4
201422	611903	4245806	80	1
201426	613112	4243902	45	7.5
201427	611772	4245679	51	2
201431	613547	4244995	95	10
201441	613516	4244981	100	15
201446	612962	4243836	67	1
201454	616613	4244548	55	-
201459	617055	4244707	124	-
201462	611930	4245928	65	45
201467	611796	4245826	31	3
201484	617232	4243773	65	10
201489	617437	4244667	50	-

Note. Spatial coordinates are UTM, zone 16 North, NAD 27

Wells In the Calibration Model, withdrawals at vertical wells and collector wells were simulated using the MODFLOW WEL (well) package. Each vertical well used for the pumping tests was represented in the model as a single WEL boundary condition with a given pumping rate. Similarly, since the production rate of the collector wells was known in the Calibration Model, each collector well was modeled as a collection of WEL boundary conditions with the total well discharge distributed among the cells. This is appropriate since only observation wells distant from the pumping center were used in the calibration data sets; therefore, it was not necessary to model details of the complex local flow field near the collector wells to calibrate the model.

In the Predictive Model, it was necessary to simulate each well's *theoretical yield*, which is the amount of water that will enter the well based on an assumed drawdown in the caisson. This can only be achieved by having the collector well appropriately represented as a head-dependent feature in the groundwater flow model. Thus, collector wells in the Predictive Model were simulated in the single layer model using the MODFLOW DRN (drain) package. The modeled flux into the drain cells was computed similarly as the RIV package,

$$Q_{drain} = COND \times (h_{drain} - h_{aquifer}) \quad (6)$$

where the head in the drain h_{drain} is provided by the modeler. In MODFLOW, DRN boundary conditions can never lose water to the Aquifer; thus the flux to a drain is always less than or equal to zero (water is removed from the Aquifer).

Simulation of collector well yields using the DRN package is not a new idea. Schafer (2006) used the DRN package in a model of proposed collector wells in Louisville, Kentucky. However, the literature currently offers no guidance as to the computation of the conductance value or how to arrange the DRN cells in the model. We developed a new formulation for collector wells in single-layer MODFLOW models that was fully validated by comparisons with the published 3D, analytic element collector well formulation (Bakker et al., 2005). The complete details of the new formulation are provided in Appendix B - Predicting Collector Well Yields with MODFLOW.

4.2.3 Calibration

As described above, zones of aquifer and streambed properties in the model were created based on the geophysical survey, previous knowledge of the Aquifer, and preliminary calibration results. The properties of each zone were calibrated to match water-level observations. Water-level measurements came from the following sources:

- Transient water-level measurements were collected during a previous analysis at the Park during two aquifer tests (WHPA, 2010).

Table 7: Weight assigned to observation data sets for model calibration.

Data set	Max. head	
	change (ft)	Weight
South Site pumping test	1.7	1.0
North Site pumping test	5.5	0.4
CW5 pumping test	2.5	1.0
Ambient monitoring	7.0	0.25

- Transient drawdown data from a test of collector well CW-5 were extracted from the report by Burgess and Niple (1995).
- Synoptic water-level measurements were made by Layne Hydro on October 20, 2010, as part of this study.
- Continuous monitoring of water-level changes in the Aquifer were made for this study. The measurements were made during the passing of a flood wave on the Ohio River.

Four calibration data sets were incorporated into a single transient model of the Aquifer, with each transient data set separated by a steady-state stress period. The data sets include

- pumping tests at the north and south ends of the Park (WHPA, 2010)
- a pumping test conducted by Burgess and Niple (1995) at CW-5
- continuous monitoring of water levels in selected monitoring wells made during the present study

Calibration of model parameters was achieved using the inverse model code PEST (Doherty, 2004). Model parameters included the hydraulic conductivity (12 zones), river bed leakance (7 zones), specific yield (constant throughout the model), and specific storage (constant throughout the model). Prior to running PEST, the target heads for each data set were weighted inversely proportional to the maximum change in head observed in each data set (Table 7). In this weighting scheme, the pumping test data is considered more important than the ambient data during calibration. The ambient data is considered less important because no measurements of groundwater discharge were made during the passing of the flood wave. While the ambient data is important for determining spatial variations in the diffusivity of the Aquifer and the resistance of the river bed, it cannot be used to evaluate the hydraulic conductivity of the Aquifer.

Table 8: PEST-calibrated values of hydraulic conductivity with approximate 95% confidence intervals.

Zone	Best-fit value (ft/day)	95% confidence interval (ft/day)
1	900	–
2	900	–
3	550	–
4	890	488 - 1,622
5	182	152 - 219
6	1,157	1,036 - 1,291
7	628	480 - 823
8	294	262 - 331
9	2,764	2,576 - 2,967
10	1,155	–
11	682	–
12	1,100	–

Along with best-fit parameter values, PEST provides approximate confidence intervals for these same parameters. The range of a parameter’s confidence interval is, in large part, determined by the sensitivity of the model predictions (in this case, modeled heads in monitoring wells) to the parameter. The confidence interval is typically smaller for a parameter that has a strong influence on model predictions than for a parameter whose influence is less. For parameters that have little or no influence on the model, PEST reports a very large confidence interval of many orders of magnitude. This indicates that nearly any value may be entered for the parameter without affecting the quality of fit between the model and observed data. Consequently, confidence intervals are not provided for those parameters to which the model is insensitive. The best-fit value listed for those parameters are based on PEST results, parameter values in adjacent zones or reaches, results of the geophysical survey, and engineering judgment.

Calibration indicates that model results are insensitive to the conductivity of zones 1 through 3 and zones 10 through 12 (Table 8) . Zones 1 through 3 are the eastern-most zones in the model where significant portions lie beneath RIV cells and are farthest from the influence of the pumping tests. Zones 10 through 12 are thin strips of aquifer material that lie adjacent to the western bedrock wall; much of this area becomes unsaturated during pumping in the Aquifer.

Table 9: PEST-calibrated values of riverbed leakance and approximate 95% confidence intervals.

Reach	Sediment thickness (<i>ft</i>)	Best-fit value (<i>day</i> ⁻¹)	95% confidence interval (<i>ft/day</i>)
1	20	5.52E-3	–
2	20	6.91E-2	–
3	20	3.33E-3	–
4	10	0.512	0.426 - 0.614
5	10	0.151	0.138 - 0.165
6	10	0.200	0.159 - 0.252
7	10	0.391	0.298 - 0.514

Model results are insensitive to the riverbed leakance values specified for reaches 1 through 3 (Table 9) . These reaches represent the eastern-most portion of the riverbed that are furthest from the influence of the pumping tests. This is an expected outcome because when a well is pumped near a river, the drawdown beneath the river is largest near the bank closest to the well. As a result, the rate of induced recharge from the river becomes smaller as one looks farther from the riverbank. At a point that is approximately $3 \times \lambda$ or farther away from the riverbank the rate of induced recharge approaches zero (Haitjema, 1995). λ is defined as

$$\lambda = \sqrt{\frac{\text{Aquifer Transmissivity}}{\text{River Leakance}}} \quad (7)$$

If the river is hydraulically connected to the Aquifer, the leakance is large, λ is small, and induced recharge will tend to be concentrated at the riverbank. Thus, calibration to an aquifer test is expected to offer little information about the properties of the riverbed on the opposite side of the river and PEST will report a large confidence interval. The remaining reaches (4 through 7) lie along a relatively thin strip adjacent to the western bank of the Ohio River. The geophysical survey data suggests that the thickness of the streambed sediment in reaches 4 through 7 is approximately half that of the rest of the river and the results suggest that yield is sensitive to sediment thickness.

The calibrated aquifer storage parameters are presented in Table 10. The specific storage is only used in model cells where the calculated head is greater than the elevation of the Aquifer top. Model results indicate that such confined flow regions lie mainly beneath the Ohio River and in a narrow strip adjacent to the Ohio River, while the majority of the flow in the Aquifer is unconfined. The calibrated values indicate that the specific storage is very small, but model results are insensitive to this parameter. By comparison, the specific yield, used by the model wherever flow is unconfined, has a very small range for the 95% confidence interval. This is expected. Confined storage is due

Table 10: PEST-calibrated aquifer storage parameters and approximate 95% confidence intervals.

Parameter	Best-fit value	95% confidence interval
Specific storage, Ss	1.0E-8	–
Specific yield, Sy	0.0487	0.0462 - 0.0513

Table 11: Calibration statistics.

Residual statistic	Value
Minimum (<i>ft</i>)	-1.14
Maximum (<i>ft</i>)	1.28
Range (<i>ft</i>)	10.70
Mean	-0.11
Standard deviation	0.32
Absolute mean	0.23
Sum of squares	1.24E+2
RMS error	0.34
Scaled st. dev.	0.030
Scaled abs. mean	0.022
Scaled RMS	0.032

to the compressibility of water and the aquifer material itself, while unconfined storage is due to the dewatering of the Aquifer and related to the porosity of the aquifer material. At the spatial and temporal scales of an aquifer test (a few hundred feet and two to three days), confined responses take place very rapidly and cannot be represented accurately with a finite-difference model like MODFLOW, but the unconfined response over a several-day aquifer test is well-represented.

Table 11 provides the statistics for the residuals (observed minus computed heads) of the calibrated model. A comparison of observed heads versus computed heads shows that the model provides a good fit to observed heads (Figure 16). A perfect fit of the model to observations would be indicated if all data plotted along the line of slope 1 as in Figure 16. Each calibration data set is described in more detail in the following sections where hydrographs are presented comparing computed heads and target heads at each monitoring well.

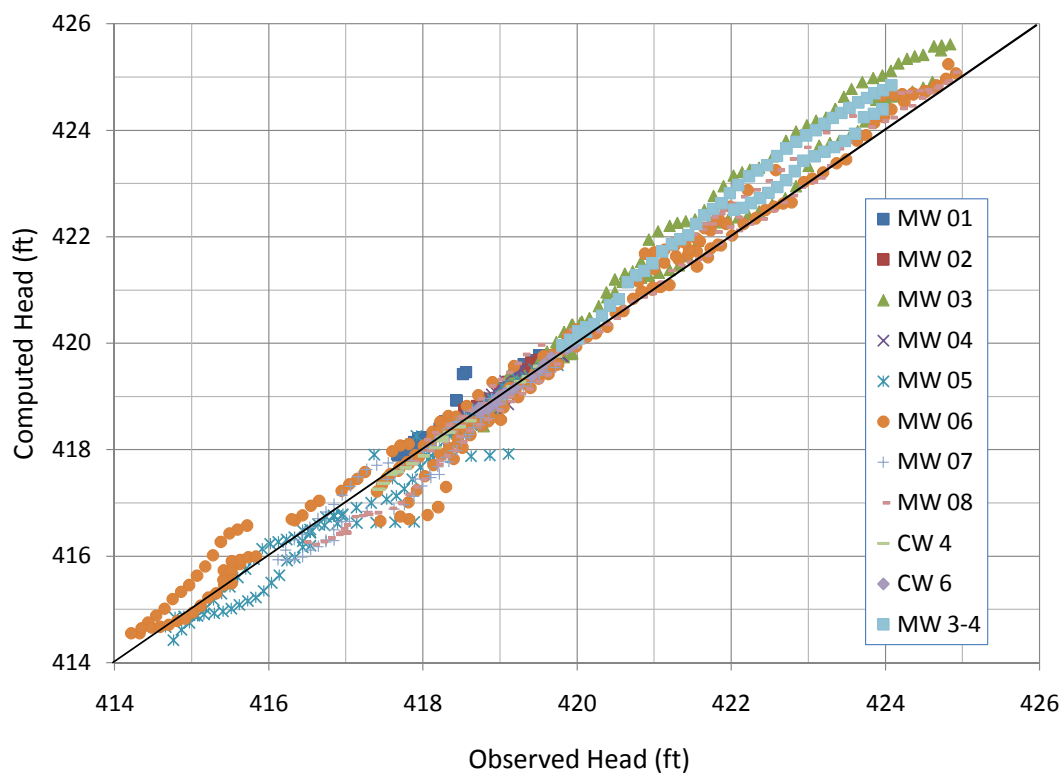


Figure 16: Plot of modeled versus observed heads for all observation data used in the model calibration.

South Site aquifer test The time-versus-drawdown data collected during the September, 2009 constant-rate test for PW-01 was converted to elevation at each monitoring well, and used as calibration targets in the groundwater flow model (WHPA, 2010). Stage data for the Ohio River was obtained from the USGS gaging station downstream in Louisville, Kentucky; the stage data was increased 0.3 ft, based on estimates of the hydraulic gradient in the river, to represent river stage near the Park in the simulation of the pumping test. Hydrographs simulated at each monitoring well obtained from the final Calibration Model demonstrate a good fit between modeled and observed water level elevations (Figure 17).

North Site aquifer test The time-versus-drawdown data sets obtained from the North Site testing (WHPA, 2010) were used as calibration targets in the Calibration Model. The model included the step test and constant-rate test, the effects of pumping at PW-02, variations in river stage, and the cyclic pumping of CW-1. The pumping rate of CW-1 was estimated based upon the capacity of the pump to be 3,500 gpm, and the timing of pumping was taken directly from the hydrographs recorded at MW-05, the nearest observation point to the collector well. The continuously monitored drawdown data was converted to elevation data and sampled to provide a representative set of discrete observation data for calibration of the groundwater flow model. Hydrographs simulated at each monitoring well obtained from the final Calibration Model demonstrate a good fit between modeled and observed water level elevations (Figure 18).

Test of Collector Well 5 Burgess and Niple (1995) reported data for a pumping test conducted on CW-5 from March 26-30, 1995. During the test, the well was pumped at a nearly constant rate of 10.1 mgd, groundwater levels were monitored near CW-4 and CW-6, and river stage was monitored. The observation data were digitized from graphs appearing in the report for use in the groundwater flow model. Hydrographs simulated at each monitoring well obtained from the final Calibration Model demonstrate a good fit between modeled and observed water level elevations (Figure 19).

Continuous monitoring Continuous head measurements were collected from October 20, 2010 to January 7, 2010. During this time a flood pulse moved through the Ohio River from December 4, 2010 to December 7, 2010 (see Section 3). Hydrographs simulated at each monitoring well obtained from the final Calibration Model demonstrate a good fit between modeled and observed water level elevations (Figure 20).

4.2.4 Comparison of calibrated properties with previous studies

Knowledge of aquifer properties from previous studies was used as a guide for subdivision of the aquifer into zones of constant properties and in specifying initial aquifer parameters. It is useful to

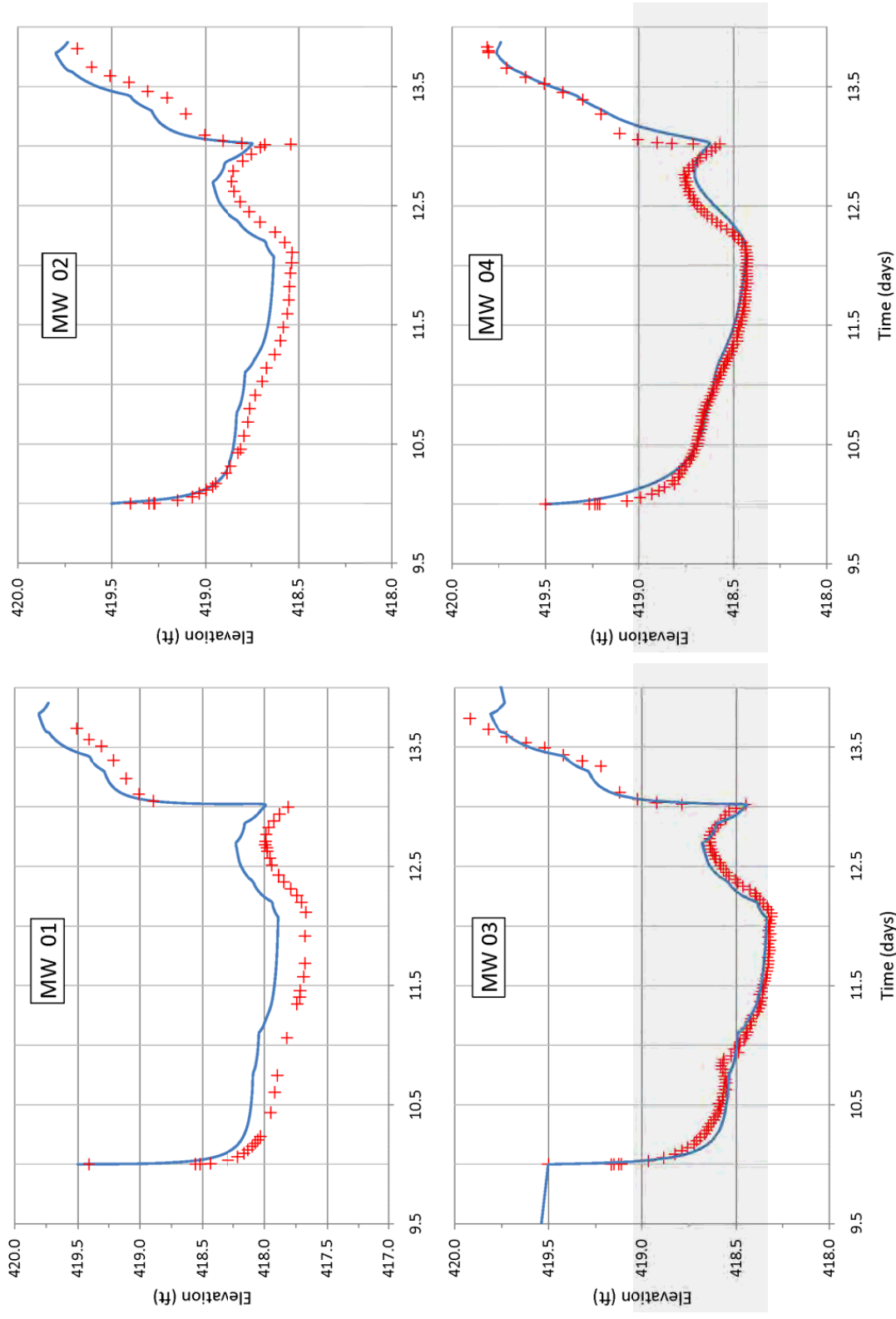


Figure 17: Results from the calibrated groundwater model. Computed (blue line) and observed (red cross) hydrographs at the monitoring wells during the South Site pumping test.

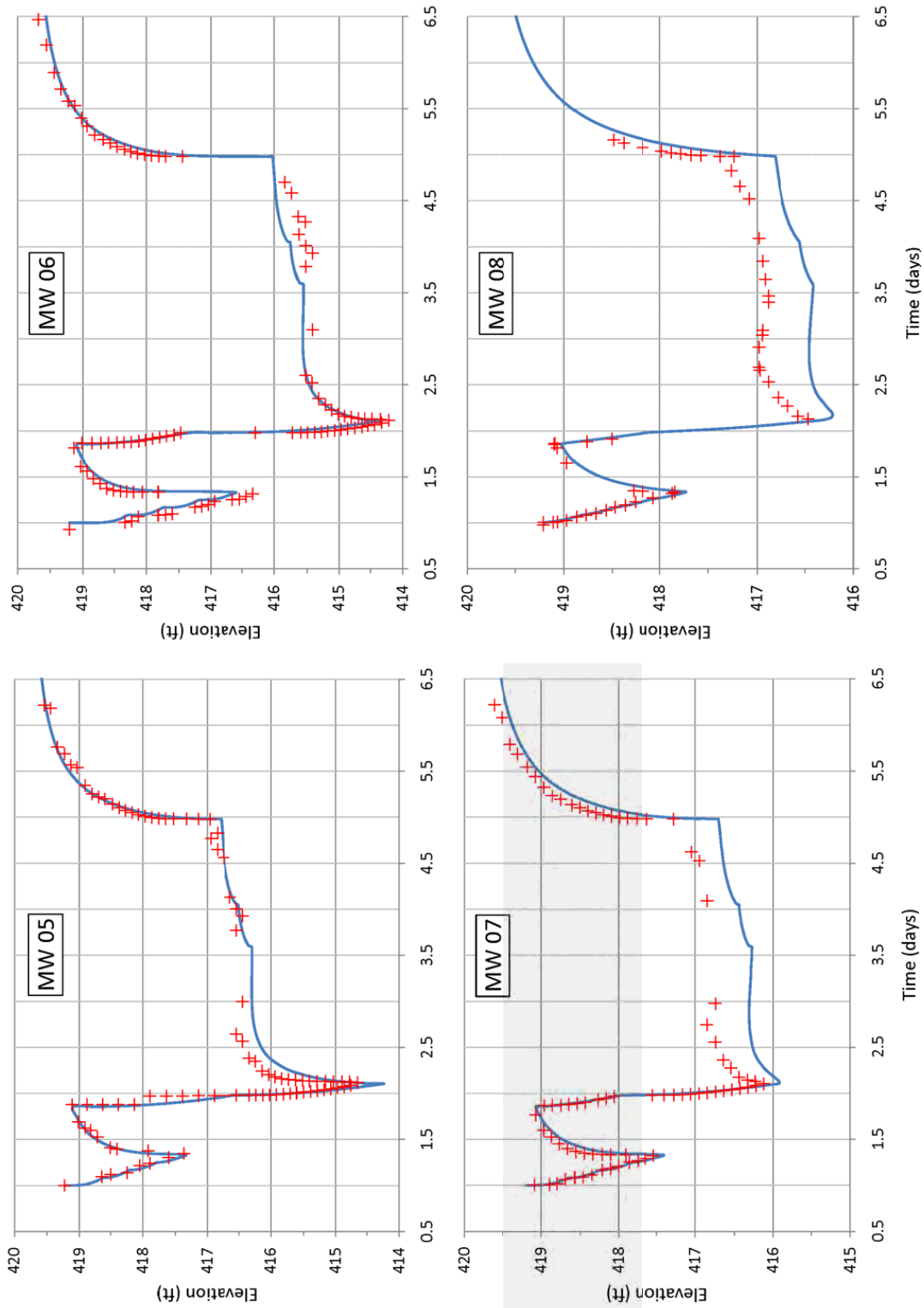


Figure 18: Results from the calibrated groundwater model. Computed (blue line) and observed (red cross) hydrographs at the monitoring wells during the North Site pumping test.

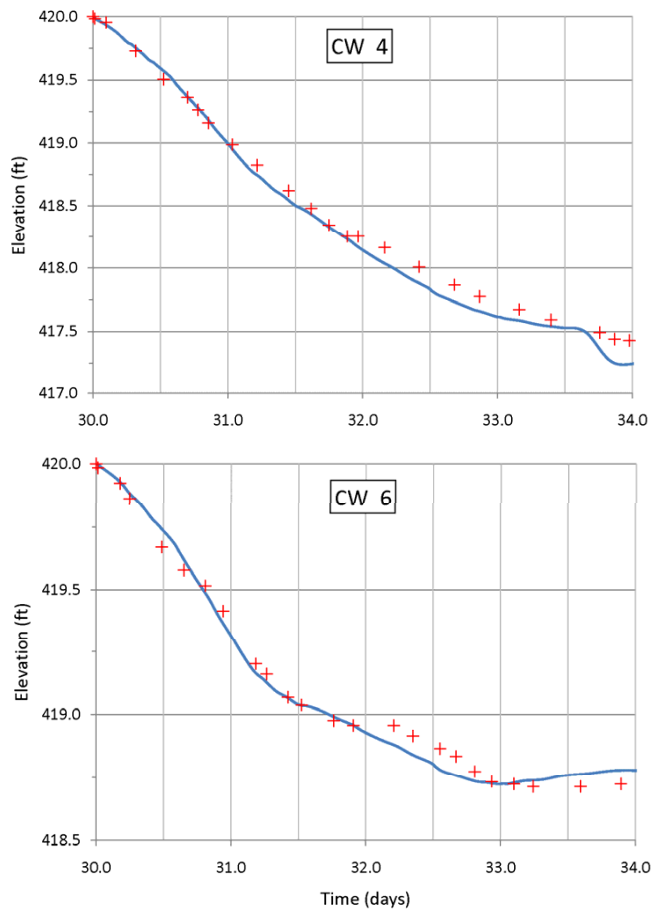


Figure 19: Results from the calibrated groundwater model. Computed (blue line) and observed (red cross) hydrographs at the monitoring wells during the pumping test of CW-5.

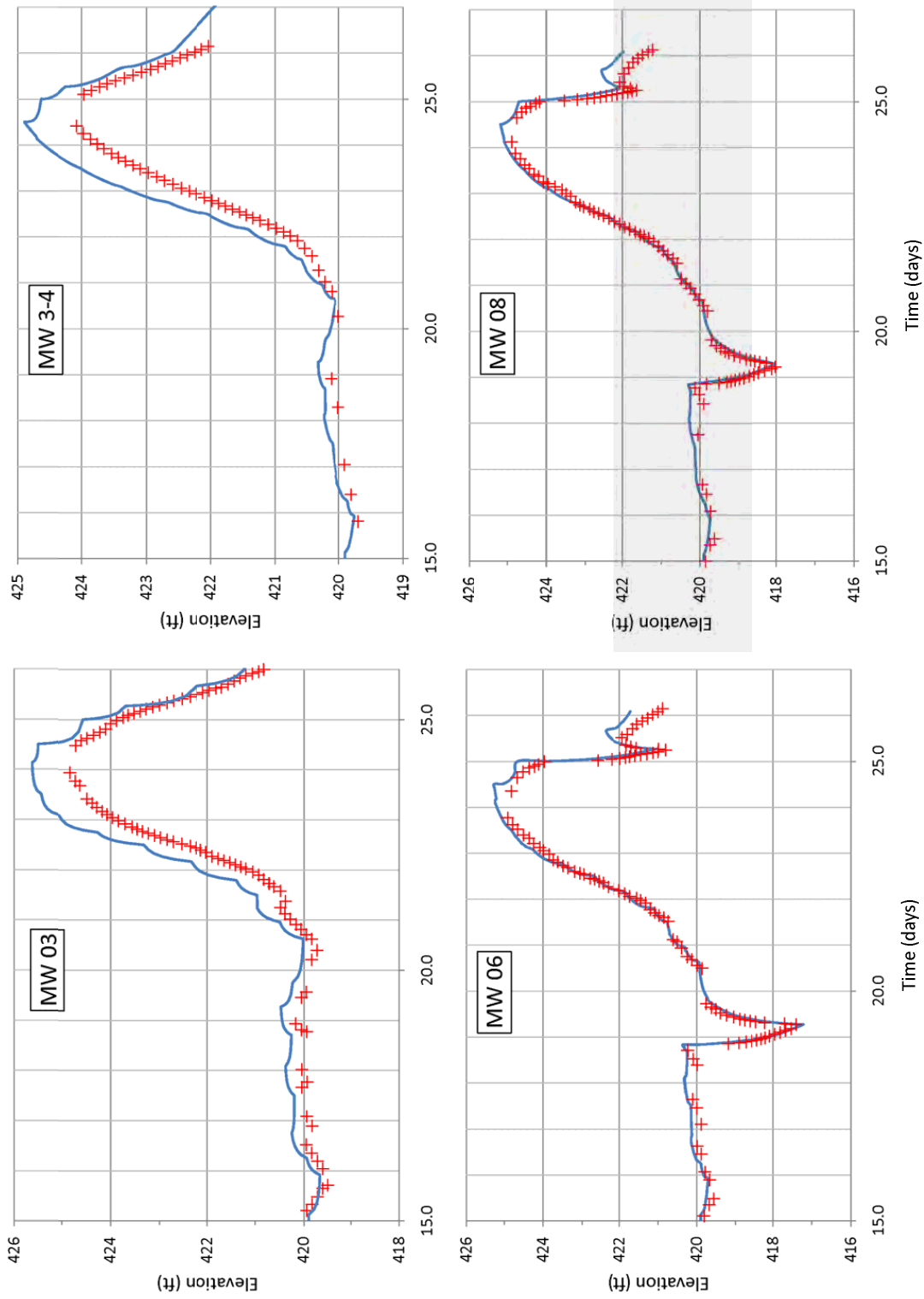


Figure 20: Results from the calibrated groundwater model. Computed (blue line) and observed (red cross) hydrographs at the monitoring wells prior to and during the passing of a flood wave on the Ohio River.

compare the final PEST-calibrated values with the results from previous studies. We provide this comparison at the South Site, the North Site, and at CW-4.

South Site The data collected during aquifer testing at the South Site was analyzed and reported by WHPA (2010). The pumping test was simulated using wigaem, a transient analytic element code, and the best-fit parameters were evaluated using PEST. Details of the analysis are presented in the report by WHPA (2010). Results include the following:

- Riverbed resistance parameter = 0.00765 ft/day
- Specific yield = 0.0233
- Transmissivity = 101,500 ft²/day

For comparison with the riverbed leakance obtained from the current study, we multiplied the above riverbed resistance parameter by 300 ft – the width of River Reach 4 – and invert the results to obtain 0.435 day⁻¹. This compares well with the leakance of Reach 4 of 0.512 day⁻¹ estimated in the current study (Table 9). The specific yield of 0.0233 also compares well with the calibrated value of 0.0487 (Table 10).

The local transmissivity of the Aquifer is difficult to compare with results of the current study, as the groundwater flow model includes varying aquifer thickness and multiple hydraulic conductivity zones at the South Site (Figure 14 and Table 8). Furthermore, the calibrated values indicate large contrasts in hydraulic conductivity between Zones 2, 5, and 9. As the hydraulic conductivity zones at the South Site run parallel to the river, one approach for comparison is to evaluate equivalent, in directions normal to the river and parallel to the river. The expression for the equivalent transmissivity parallel to the river is

$$T_{NS} = \frac{1}{W} (T_2 W_2 + T_5 W_5 + T_9 W_9) \quad (8)$$

where T_{NS} is the equivalent transmissivity of the Aquifer in the north-south direction (parallel to the river), T_2 and W_2 are the transmissivity and width of Zone 2, and W is the total width of Zones 2, 5, and 9. The expression for the equivalent transmissivity normal to the river is

$$T_{EW} = \frac{W}{\frac{W_2}{T_2} + \frac{W_5}{T_5} + \frac{W_9}{T_9}} \quad (9)$$

where T_{EW} is the equivalent transmissivity of the Aquifer in the east-west direction (normal to the river). Properties of the three zones at the South Site were taken from the model and are included in Table 12, along with the results of equations (8) and (9). The reported width of Zone 9 is taken to be

Table 12: Properties at the South Site for evaluating equivalent transmissivities. Average values for each zone were estimated from the model data sets.

Zone	Average		Average		Average	
	k (ft/day)	H (ft)	T (ft ² /day)	W (ft)	T_{NS} (ft ² /day)	T_{EW} (ft ² /day)
2	900	24	21,600	150		
5	184	77	14,000	290	161,100	40,800
9	2764	86	237,700	830		

the width that extends from the boundary of Zone 2 to the eastern edge of River Reach 4. The transmissivity from the previous study of 101,500 ft²/day falls within the two equivalent transmissivities of 40,800 ft²/day and 161,100 ft²/day.

The hydraulic conductivity of 2,764 ft/day (Zone 9) is very large for an outwash aquifer. This large value is supported by calibration of the groundwater flow model, as well as by data not included in the model calibration. After the aquifer study conducted by WHPA (2010), two additional production wells were placed at the South Site and subsequently tested by IDNR. These unpublished data were not included in the calibration data set as it included only drawdown measurements in the production wells. Well 2 was placed 200 ft north of PW-01 and Well 3 placed 200 ft north of Well 2. Well 2 was test pumped at a rate of 2,060 gpm for 24 hours. At the end of the test, the drawdown in the pumping well was 6.0 ft. Similarly, Well 3 was tested at 2,060 gpm with a measured drawdown of 5.4 ft after 24 hours of pumping. For comparison, PW-01 was pumped for 72 hours at a rate of 1,600 gpm during testing of the South Site (WHPA, 2010); the drawdown measured at the pumping well after 24 hours was 10.4 ft. The IDNR tests indicate that the Aquifer at the South Site is even more productive than the data included in the calibration data set indicates. There is no doubt that the Aquifer is highly productive and highly transmissive at the South Site.

North Site Data from the aquifer testing of the North Site were analyzed and reported in WHPA (2010). The Cooper-Jacob straight line method was used to estimate the following aquifer properties:

- Transmissivity = 42,200 ft²/day
- Specific yield = 0.0258

The specific yield compares well with the calibrated value from the groundwater flow model. A comparison of the transmissivity results from the calibrated model and previous analysis of aquifer

Table 13: Properties at the North Site for evaluating equivalent transmissivities. Average values for each zone were estimated from the model data sets.

Zone	Average		Average	Average		
	k (ft/day)	H (ft)	T (ft ² /day)	W (ft)	T_{NS} (ft ² /day)	T_{EW} (ft ² /day)
1	1155	10	11,600	130		
6	1157	78	90,200	640	62,000	37,300
7	628	48	30,100	360		

testing at the North Site was made, as was done at the South Site. Properties of the three zones at the North Site were taken from the model and are included in Table 13, along with the results of equations (8) and (9). The reported width of Zone 7 is taken to be the width that extends to the eastern edge of River Reach 6. The transmissivity from pumping test analysis of 42,000 ft²/day compares well with the directional transmissivities.

Testing of Collector Wells 5 and 6 Burgess and Niple (1995) performed pumping tests on CW-4, CW-5, and CW-6. Data from testing of CW-5 was incorporated into the calibration data set of the groundwater flow model. Burgess and Niple analyzed the data and estimated aquifer transmissivities at the wells ranging from 142,000 ft²/day to 207,400 ft²/day. WHPA (2010) analyzed the late-time drawdown data with a steady-state, analytic element model of the Aquifer, and estimated a smaller transmissivity of 100,300 ft²/day. Results from the current study indicate average transmissivities of Zones 4 and 8 to be 80,100 ft²/day and 26,500 ft²/day. The current results are smaller, but are based on transient modeling with realistic boundary conditions; the match of model drawdowns to observed data at CW-4 and CW-6 when pumping CW-5 is excellent.

4.3 Predictive Modeling and Uncertainty Analysis

The calibrated model was used to predict the theoretical groundwater yields of collector wells at the site. As previously discussed, theoretical yields are strongly influenced by local and regional hydraulic factors such as the aquifer transmissivity and the degree of connection between the river and the Aquifer. It is therefore necessary to explicitly represent collector well hydraulics within the calibrated regional flow model. No off-the-shelf computer codes were available for this task, so we developed a new model code that is based on our patented analytic element collector well model (Appendix B - Predicting Collector Well Yields with MODFLOW).

There are many options for future development at the site, and our objective was to consider the long-term potential. We used a two-step procedure to predict the well field capacity. We first ran

Table 14: Predicted yields with all wells operating: (column 2) the seven existing wells, and (column 3) the seven existing wells augmented with two additional wells south of CW-7.

Well	Theoretical yield (mgd) with 7 wells	Theoretical yield (mgd) with 9 wells
CW-1	10.2	10.2
CW-2	6.5	6.5
CW-3	6.4	6.4
CW-4	4.2	4.6
CW-5	4.6	4.6
CW-6	10.1	10.1
CW-7	21.3	15.2
CW-8	—	22.1
CW-9	—	26.4
Total	63.3	105.3

Note. Column 3 includes the seven existing wells augmented with two additional wells south of CW-7.

the model with all wells in operation in order to predict the theoretical yield for each well while all are operating. These yield estimates were used to create 16 development alternatives for design production rates ranging from 10 mgd to 80 mgd. We then re-ran the predictive model to predict the capacity for each alternative. This procedure accounts for the fact that the influence of well interference on each well’s simulated yield is dependent on the configuration of the well field.

4.3.1 Preliminary theoretical yield predictions

We used the model to predict the theoretical yield for all seven existing wells, and for a nine-well configuration in which hypothetical wells CW-8 and CW-9 are added south of CW-7, where the Aquifer is predicted to be most productive (Table 14). Recalling the above discussion of the effect of well interference, note that the hypothetical addition of wells CW-8 and CW-9 results in a reduction of 6.1 mgd in the yield of CW-7. The results compare favorably with data that were collected while the site was in operation during World War II (Appendix C - Comparison with Kazmann Yield Model).

The re-development of the Well Field could occur in a single large effort or in a phased approach to develop capacity as demands increase. It is therefore useful to consider more than one alternative for site development that allows engineers to find the most cost-effective approach to achieve a desired

Table 15: Development alternatives that were considered using the groundwater flow model.

Alternative	Target rate (mgd)	Collector Well								
		1	2	3	4	5	6	7	8	9
10-A	10	E	E	-	-	-	-	-	-	-
10-B	10	-	-	-	-	-	-	I	-	-
20-A	20	E	E	E	-	E	-	-	-	-
20-B	20	-	-	-	-	E	-	I	-	-
30-A	30	I	E	E	E	-	-	-	-	-
30-B	30	E	E	E	E	E	E	E	-	-
30-C	30	-	-	-	-	-	-	I	-	N
40-A	40	E	E	E	E	E	-	I	-	-
40-B	40	-	-	-	-	E	-	-	N	N
50-A	50	I	E	E	E	E	I	I	-	-
50-B	50	-	-	-	-	E	-	I	N	N
50-C	50	-	-	-	-	-	I	I	N	N
60-A	60	I	-	-	-	-	I	I	N	N
60-B	60	-	-	E	E	E	-	I	N	N
70-A	70	I	E	E	E	-	-	I	N	N
80-A	80	I	E	E	E	E	I	I	N	N

Note. Wells marked with *E* are considered to be *equipped* with new pumping equipment to produce their existing mechanical capacity. Wells marked with *I* are considered to be *improved* and their mechanical capacity raised to 15 mgd. Construction of *new* wells CW-8 and CW-9 are marked with *N*, assuming a mechanical capacity of 15 mgd for each.

production rate. We evaluated 16 alternatives that align with production rates ranging from 10 mgd to 80 mgd. Table 15 describes the simulated alternatives and results are provided in Section 4.3.3.

4.3.2 Predictive uncertainty analysis

During the development of a groundwater model, the modeler makes simplifying assumptions about the conceptual model and approximates the likely values of the hydraulic properties, pumping rates, surface water levels, and other data in the model. Additionally, the hydraulic properties of geologic materials vary over the area being modeled, and it is not possible to have complete understanding of that variability. For this study, our model was calibrated to match several sets of field measurements; this was done by the use of the computer code PEST, which automatically adjusted parameters in the model to match the observations. However, as discussed in Section 4.2.3, some parameters have

a strong influence on the calibration while others have little or no influence. This is demonstrated by the uncertainty associated with each model parameter. However, at the end of the calibration process, it was possible to assess our confidence in the parameters in the model, and our ability to re-create the field observations.

Uncertainty in the model parameters (e.g., transmissivity) and incomplete information (e.g., geologic variation across the site) affect our confidence in the predictions made when simulating the yield of a well field at the Park. An obvious question arises: How confident are we that the theoretical yield values computed by the model will actually be achieved when the wells are placed in service? Below we describe the process that was used to determine confidence intervals for model predictions.

What does it mean for the model to be calibrated? As discussed previously, the inverse model PEST modifies the model parameters and determines the set of parameter values that minimizes an objective function, which is related to the difference between field observations and the corresponding modeled values. That is, PEST makes the model fit the real-world data and the resulting value of the objective function is a measure of how well it fits. However, it is likely that there are many sets of parameter values that will yield a value for the objective function that is close to the minimum value. Put another way, the parameter set that yields the best fit with the model lies within a “neighborhood” of parameter sets that *nearly* minimize the objective function.

It is therefore useful to think of calibration not in terms of a single set of best-fit parameters, but rather as all the sets of model parameters that yield a value close to the minimum objective function. This is illustrated by the contour plot in Figure 21. For the two-parameter problem illustrated, the model is considered to be calibrated at a particular confidence level for all values of the two parameters that lie within the shaded area. For all values of the objective function between the minimum value Φ_{min} and $\Phi_{min} + \delta$, the model is considered to be in calibration with the field data. Details about the determination of the value δ are provided in the PEST manual and will not be discussed here (Doherty, 2004).

Effects of parameter values on model predictions Armed with the understanding that the model may be considered to be in calibration for a variety of parameter values, it is intuitive to ask how predictions (e.g., well yields), made with the model might vary in a calibrated model. This is graphically illustrated in Figure 22.

Recalling that the model has 12 adjustable parameters, it is likely that there can be a substantial variation in model predictions over the calibrated region (Figure 23). The model is considered calibrated at the desired confidence level for all parameter values within the shaded area, however, the predicted value varies within the shaded region. In this case, the critical point is the parameter set

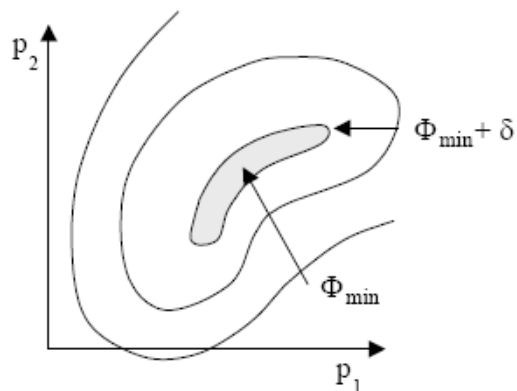


Figure 21: Contour plot of the objective function Φ for a calibration problem with two parameters, P_1 and P_2 (Doherty, 2000).

The minimum objective function is located at the point labeled Φ_{min} . However, the model is considered for all pairs of parameters P_1 and P_2 that lie within the shaded region. Within the shaded area, the objective function is smaller than $\Phi_{min} + \delta$, where the value of δ is chosen based on the level of confidence in the prediction that is desired, for example, 95%.

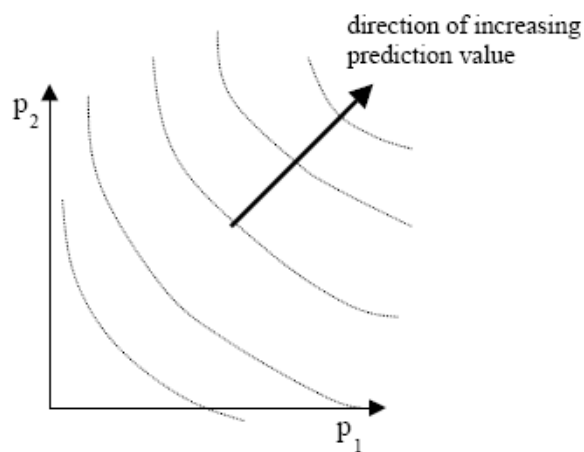


Figure 22: Contour plot of a model-predicted value, for example, the simulated yield of a well, for the two-parameter problem (Doherty, 2000).

The model prediction varies as shown in the figure. Along each contour line, the predicted value is constant.

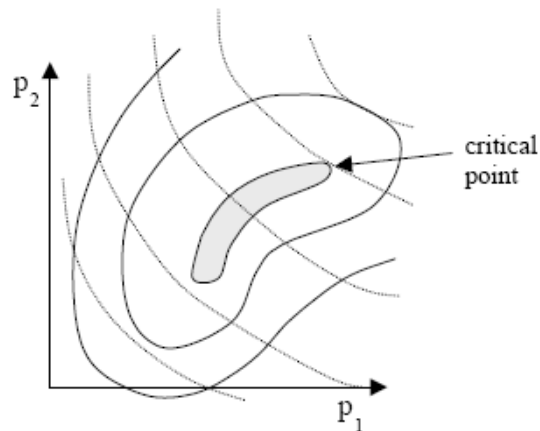


Figure 23: Identifying the maximum predicted value at the desired confidence level (Doherty, 2000).

The contours of the predicted value are overlaid upon the contours of the objective function. The model is considered calibrated everywhere within the shaded region; at the critical point, the predicted value is maximized under the condition that the model remains in calibration.

that produces the largest value of the model prediction subject to the constraint that the model remains calibrated. There is similarly a critical point for the smallest model prediction. The predicted values at the minimum and maximum critical points define the confidence interval for the model prediction.

Advantages of the predictive uncertainty methodology The use of predictive uncertainty analysis is preferred over more traditional methods of assessing confidence in model predictions. Traditionally, modelers often adjust model parameters, either one parameter at a time or in groups of parameters, and then report the sensitivity of critical model predictions to the parameters. This traditional approach has several shortcomings. When adjusting a single parameter, there is no guarantee that the model will remain in calibration. In that case, predictions made with the perturbed model may not be representative of the system as a whole. More importantly, parameters that have no effect on the calibration results may have a large effect on model predictions. By examining the range of predicted values that are possible while maintaining model calibration, our method achieves a more reliable result and our confidence in the range of possible yields is quantifiable.

Table 16: Results of predictive modeling and summary of sustainable capacity for each alternative. All values are in millions of gallons per day (mgd) and represent the yield of the entire well field for each alternative.

Alternative	Theoretical yield			Sustainable capacity
	Minimum	Best-fit	Maximum	
10-A	16.6	17.9	19.3	9.8
10-B	18.7	22.1	27.1	15.0
20-A	27.2	28.2	31.1	20.0
20-B	23.1	26.8	32.3	19.7
30-A	33.7	40.0	45.6	30.4
30-B	53.5	59.3	63.9	32.6
30-C	44.6	51.0	58.0	30.0
40-A	52.8	53.2	59.0	38.4
40-B	52.1	58.4	69.7	34.7
50-A	54.2	62.4	88.3	48.5
50-B	59.5	69.2	91.4	46.6
50-C	64.2	74.5	81.4	49.5
60-A	76.1	86.3	94.0	58.4
60-B	89.6	90.9	101.8	55.5
70-A	81.6	91.7	114.0	64.1
80-A	90.2	104.7	144.0	74.8

4.3.3 Results of predictive modeling and predictive uncertainty analysis

We ran the predictive model for each of the 16 alternatives and the results are summarized in Table 16. Appendix D - Alternative Analysis provides the detailed results for each alternative. For each model we used PEST in predictive uncertainty mode to find the 95% confidence interval for the theoretical yield of the well field; the theoretical well field yield (i.e., the individual well yields summed over all wells) was minimized and maximized during the uncertainty analysis. For each alternative, we also report in Appendix D - Alternative Analysis the *mechanical capacity* and the *design capacity* for each well. As discussed previously, the *design capacity* is smaller than the *mechanical capacity* and the *theoretical yield*. Note that the values presented in Table 16 represent the yield for the entire well field, while tables in Appendix D - Alternative Analysis provide values for each alternative and for each individual well in the well field. While the theoretical yield was evaluated for the entire well field, the *design capacity* and *sustainable capacity* were based on the values obtained for individual wells, as reported in Appendix D - Alternative Analysis.

The *sustainable capacity* is reported in the last column of Table 16 and in each table in Appendix D - Alternative Analysis. When large volumes of water are pumped near the river, the potentiometric head beneath the river sediments may fall to a level that is sufficient to cause plugging or compaction of the riverbed sediments. This plugging and compaction reduces the hydraulic conductivity and induced recharge rate and thus reduces the well yields. This effect has been studied across the river and southwest of the Park site at a collector well operated by Louisville (KY) Water Works and at other sites. Hubbs, et al. (2006) indicated that the reduction in yield due to sediment plugging can be expected to be in the range of 65 to 80% when the Aquifer is over pumped. We have limited the possibility of over pumping by imposing the operational constraint of a minimum head in the caisson of 399.5 ft amsl for each collector well. As discussed previously, this minimum elevation represents a 20 ft drawdown in the Aquifer and is approximately 10 ft to 15 ft above the streambed. This prevents the possibility of the heads beneath the river being drawn down below the elevation of the streambed. Further, each of the existing collector wells in the Park were historically pumped to levels significantly below 399.5 ft. Both the operational constraint and the historical record at the site provide confidence that the effects of plugging and compaction of the streambed sediments can be minimized. For our purposes, we assume that there is the potential for plugging that would lead to a reduction of 25% in the capacity of the largest wells at the Park – the wells for which the theoretical yield is greater than 10 mgd. Therefore, we define the *sustainable capacity* to be an adjusted design capacity based on a 25% reduction in theoretical yield for collector wells 1, 6, 7, 8, and 9.

4.4 Conclusions

Well field capacity Based on a combination of groundwater flow modeling and an assessment of the mechanical capacity of the wells in the Park, we conclude that a sustainable capacity of 48.5 mgd or more can be achieved by renovating existing wells at the Park. Furthermore, the available data suggest that it is possible to construct one or two additional collector wells south of CW-7 with capacities that exceed that of CW-7. If so, we estimate that a sustainable well field capacity of 74.8 mgd is feasible.

Confidence in estimates of well field capacity In general, our analysis of predictive uncertainty in the theoretical well field yield suggests a 10 to 15% uncertainty in predictions for each alternative investigated. It is noted that our *sustainable capacity* estimates are based on a 25% reduction in the values of theoretical yield of selected wells, owing to the possibility of plugging in the riverbed. Furthermore, in most cases, the mechanical capacity of the collector well was the limiting factor in the predicted capacity of the wells. Thus, we have a high degree of confidence in our overall conclusions.

The Ohio River is the source of water An analysis of the potential sources of recharge to the Aquifer concludes that ambient recharge from precipitation and from the nearby bedrock is negligible. Thus, it is safely assumed that all, or very nearly all, of the water that will enter wells in the Park originated as induced recharge from the Ohio River. Thus, over the long term, after years of high-yield operation, water quality in the wells is expected to be comparable to that of infiltrated river water.

5 Water Quality and Implications for Treatment

A well pumping near a river captures some fraction of ambient groundwater, some fraction of surface water, and some fraction of upgradient recharge. For wells next to a river, a gradient is produced by pumping groundwater to a point where the zone of contribution intersects the river and thus causes induced infiltration of surface water. As discussed previously, most of the source water from a new well field at the Park would come from the Ohio River.

New or re-developed collector wells constructed in the Park would induce infiltration of water from the river and take advantage of a natural filtering process referred to as Riverbank Filtration (RBF). Riverbank filtration has been demonstrated to provide reliable, albeit partial, treatment of surface water (Weiss et al., 2003; Schmidt et al., 2003; Kelly and Rylund, 2006; Gollnitz et al., 2003, 2004, 2005). Natural filtration that occurs along the flowpath between the riverbed and the collector wells provides treatment benefits unavailable to a direct surface-water intake, such as reduced turbidity, lower suspended solids, less risk of microbial contamination, buffering from potential spills in the river, and fewer temperature fluctuations. Compared to surface water, RBF systems use less chemicals for treatment, resulting in lower operating costs. The higher quality of raw water produced by RBF reduces the volume of residuals generated by the treatment process, which reduces the disposal costs.

The type and level of treatment required depends on the classification of the source under the Surface Water Treatment Rule (SWTR). Water produced by new or re-developed wells will be classified by the state of Indiana as either as groundwater or groundwater under the direct influence of surface water (GWUDISW). This classification determines the treatment that will be required to comply with safe drinking water rules. The criteria for determining the classification includes the location of wells relative to the river, well construction features, evaluation of pathogen contamination from the river, and the response of groundwater to temperature and turbidity changes in the river. Through evaluation and demonstration of RBF performance, credit for pathogen removal may be achieved under current drinking-water regulations. The demonstrated performance of RBF may be sufficient to reduce requirements for engineered treatment, and in turn, the amount of investment required for treatment infrastructure.

5.1 Source-Water Quality

In 2009, Layne Hydro characterized the quality of the Aquifer by sampling wells located along the length of the Aquifer from the southern to northern Park boundary (WHPA, 2010). The results of the investigation were compared to drinking-water standards established by the USEPA. These enforceable standards, called maximum contaminant levels (MCL), are established to protect the public from consuming drinking water contaminants that present a risk to human health. The MCL

is the maximum concentration allowed in water delivered to the public. SMCLs are non-enforceable guidelines for contaminants that may cause unwanted cosmetic or aesthetic effects to water such as taste, color, and odor problems.

The 2009 results showed that groundwater in the Aquifer can be generally classified as a calcium-magnesium bicarbonate type. No VOCs were detected and no MCLs were exceeded for any constituent in any sample. However, observed iron and manganese concentrations were above the respective SMCL in most of the samples. Based on data from other well fields along the Ohio River, the iron and manganese concentrations observed in the Aquifer are consistent with the regional setting (WHPA, 2010). At the observed concentrations of iron and manganese, treatment is required to prevent precipitation of metals in the transmission and distribution system. However, the long-term water quality characteristics of an RBF system at the Park will be dominated by river chemistry, which is lower in hardness and dissolved iron and manganese.

Predicting the likely composition of water from the collector wells is complex for several reasons. Water-quality in the river varies through time. Also, the chemical evolution of surface water as it travels to the well depends on redox conditions, specific reaction rates, the chemical properties of the aquifer matrix, and the residence time between the river and the well. Water induced through the riverbed and into a well includes a wide variety of residence times. Some of the pathlines from the river to the well will be short; other pathlines are long enough that water composition will resemble ambient groundwater.

Despite these difficulties, source-water quality can be estimated if the quality of the groundwater and surface water is understood. The water pumped from an RBF well will lie somewhere between that of the ambient groundwater and that of filtered surface water. Available water-quality data from the Ohio River in the Louisville area is limited, particularly for filtered constituents. However, the Ohio River Valley Water Sanitation Commission (ORSANCO) monitors water quality in the river to help manage the resource for public supply, industrial supply, and recreation. The data collected by ORSANCO includes results from filtered river samples for hardness and metals collected between 2001 and 2009 (ORSANCO, 2011).

In the following sub-sections we compare analytical results from filtered river samples to the observed iron and manganese concentrations in groundwater at the Park. We also summarize Phase II results from URS (2003) regarding potential impacts to the Aquifer from historic activities at INAAP, and discuss mercury results from the 2009 investigation.

5.1.1 Iron and manganese

Iron and manganese concentrations in the Aquifer are high enough to require removal by filtration WHPA (2010). The distribution of iron and manganese concentrations observed in groundwater at

the Park in 2009 are shown in Figure 24. Nineteen of 24 samples analyzed for iron were above the SMCL (0.3 mg/L). Observed iron concentrations ranged from 0.08 to 3.8 mg/L, with a median concentration of 0.91 mg/L. All 25 samples analyzed for manganese were above the SMCL (0.05 mg/L). Observed manganese concentrations ranged from 0.06 to 0.44 mg/L, with a median concentration of 0.24 mg/L. The riverbed and the aquifer underlying the river are sources of iron and manganese in the Aquifer (WHPA, 2009). This is consistent with low dissolved oxygen observed in the Aquifer (WHPA, 2010) and the general redox chemistry of iron and manganese.

Iron and manganese concentrations in new or re-developed collector wells will likely decrease over time if the wells are pumped consistently at capacity. Iron and manganese in surface water is typically associated with metal hydroxide particulates (total iron and manganese). Surface water is low in dissolved iron and manganese because it is well-aerated. The natural filtration provided by the aquifer removes the metal oxide particulates. Consistent pumping will oxygenate the aquifer, decreasing the mobilization of iron and manganese in the sediment. Over time, iron and manganese concentrations in the source water will trend toward that of the river. Figure 24 shows iron and manganese concentrations observed in filtered samples from the river (ORSANCO, 2011). The median concentrations in the river are far below the respective SMCLs. The median concentration for iron is at the method reporting limit (MRL) of 0.05 mg/L and the median concentration of manganese is 0.01 mg/L.

5.1.2 Hardness

Hardness levels in the Aquifer are classified as *very hard* (Scharfenaker et al., 2006). Observed hardness in the groundwater ranged from 249 to 465 mg/L, with a median of 319 mg/L. Surface water is typically lower in hardness than groundwater. For comparison, Figure 24 shows hardness from filtered river samples. The median hardness observed in the river is 134 mg/L. Similar to iron and manganese, hardness in the source water should, over time, trend toward the hardness levels observed in the river.

5.1.3 Potential legacy contaminants

URS (2003) performed a groundwater investigation of the former INAAP property as part of a Phase II RCRA Facility Investigation. Water samples were taken from springs, temporary shallow wells, new monitoring wells in the upland bedrock, and new monitoring wells in the unconsolidated deposits that form the lowland Aquifer. A total of 11 monitoring wells, some of which were multi-depth wells, were installed in the Aquifer. Sample locations were near known or suspected sources of contamination or were representative of groundwater discharge near the INAAP boundaries at locations potentially impacted by groundwater transport from INAAP.

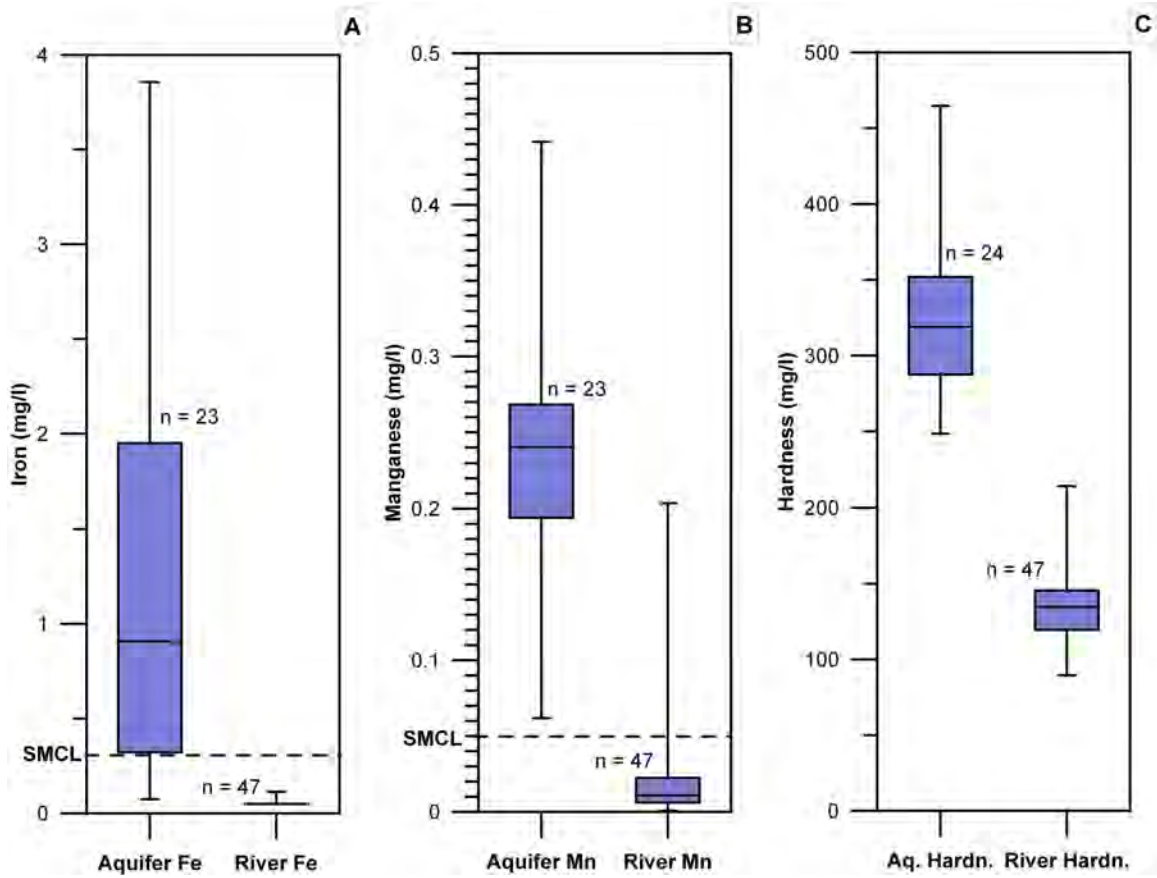


Figure 24: Comparison between groundwater (WHPA, 2010) and filtered river samples (OR-SANCO, 2011) of A) iron, B) manganese, and C) total hardness concentrations.

In the process of developing a conceptual hydrogeologic model of INAAP, URS concluded that groundwater flow from the upland bedrock is primarily lateral through karst features above the Waldron Shale. Groundwater flows along the shale unit to springs that emerge where the shale outcrops at the bluff above the lowland (Figure 25). The springs feed surface water that ultimately flows to the Ohio River. Therefore, URS concluded that most surface water from INAAP probably does not infiltrate the aquifer sediments but flows directly to the river as surface water. URS also concluded that little water moves vertically below the Waldron Shale because springs below the shale unit are uncommon and water in the deeper bedrock units underlying parts of INAAP is saline in some areas.

URS (2003) also concluded that the potential impact of historic activities at INAAP on the Aquifer was *little to none*. The sampling results from the bedrock upland indicated the presence of low concentrations of compounds related to minor releases of fuels, solvents, and nitroaromatic/nitramine compounds, but showed no evidence of existing contaminant plumes. URS also reported that mercury may be the only contaminant present in groundwater as a result of operations at INAAP. However, they concluded that the mercury that was released into the shallow bedrock groundwater as a result of operations at INAAP had not been transported to the Aquifer (URS, 2003). Below we discuss the URS mercury results and conclusions in the context of WHPA (2010) results.

5.1.4 Mercury

Mercury was detected in the shallow karst system and in some springs at a maximum concentration of 2.9 $\mu\text{g/L}$. However, no mercury was detected in any of the monitoring wells, including all of the monitoring wells in the lowland Aquifer (reporting limit was 0.5 $\mu\text{g/L}$). URS concluded that mercury has not been transported into the deeper karst flow system intercepted by the bedrock monitoring wells nor has it been transported into the lowland Aquifer.

WHPA (2010) detected mercury in 13 of 20 samples collected from monitoring wells in the Aquifer (Figure 26). The higher level of detections in this more recent investigation is most likely due to a lower MRL (0.1 $\mu\text{g/L}$ as compared to 0.5 $\mu\text{g/L}$) because most of the detections were near the MRL. All of the detections were well below the MCL for mercury (2 $\mu\text{g/L}$).

The recent mercury results could be indicative of contamination from historic activities at INAAP or could be due to non-point sources. The USEPA reports that the Ohio River Valley has one of the highest rates of mercury deposition in the continental United States (USEPA, 1997). The USGS operates a mercury monitoring station in Clifty Falls State Park (Clifty Falls) as part of the National Atmospheric Deposition Program (NADP). The annual mercury depositions at Clifty Falls in 2004 and 2005 were in the top 25% of all NADP stations in eastern North America (Risch and Fowler, 2008).

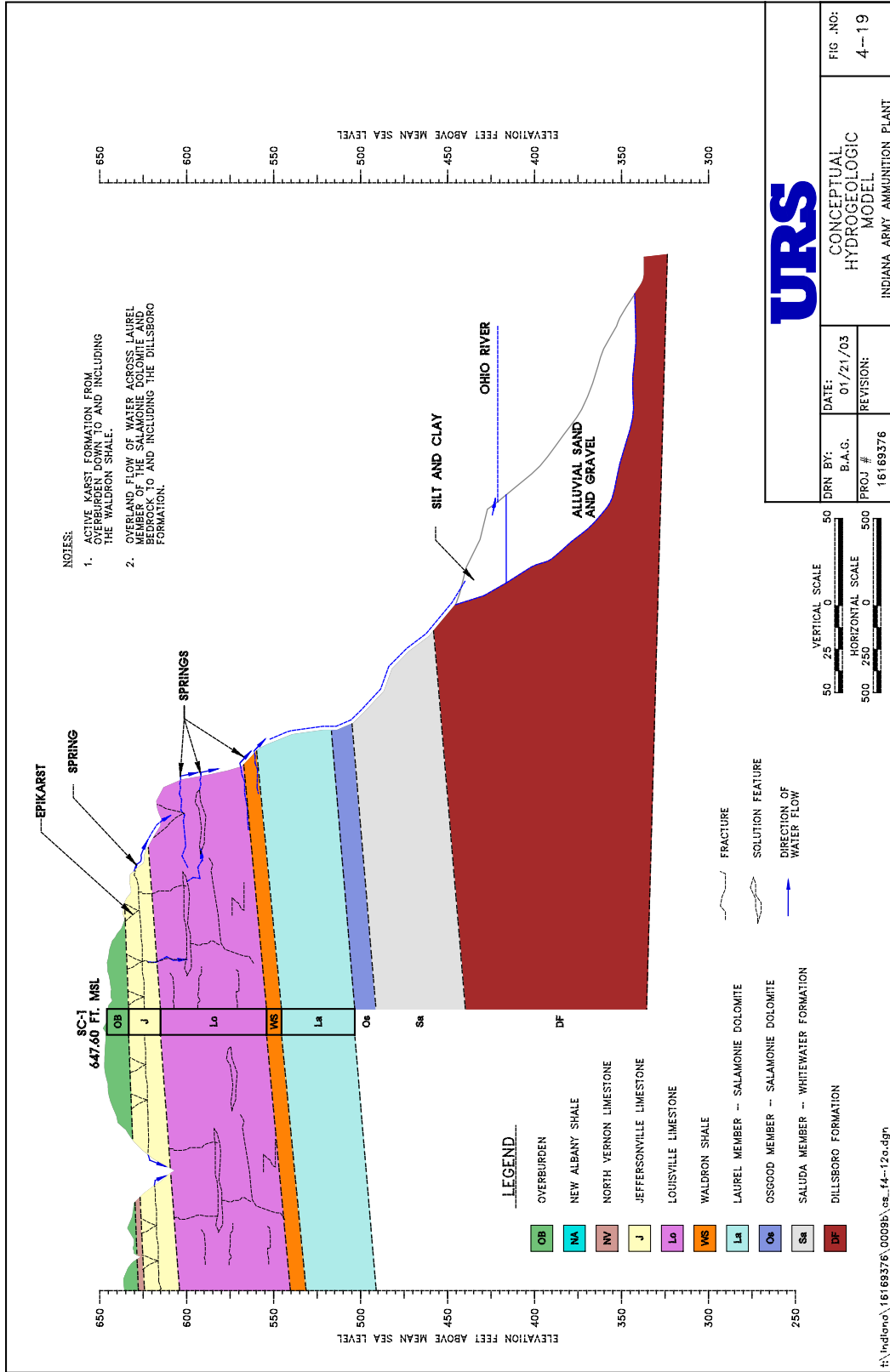


Figure 25: URS's conceptual hydrogeologic model at the Indiana Army Ammunition Plant (URS, 2003).

None of the observed groundwater mercury concentrations were high compared to observations from other sites in Indiana. Figure 27 compares the observed mercury concentrations in the Aquifer to results from an IDEM groundwater investigation that included wells in different locations and hydrogeologic settings in Indiana (USGS, 2011). The MRLs from the two groundwater data sets are different, but we can conclude that the results from the Aquifer are within the range of general observations from Indiana groundwater.

Despite the low concentrations of mercury in the Aquifer, the river will control source water mercury concentration in a re-developed RBF system. For comparison, Figure 27 shows mercury concentrations in the Ohio River for filtered and unfiltered water samples (ORSANCO, 2011). Unfiltered samples from the river are generally near the MRL of 0.0015 $\mu\text{g/L}$ but are elevated during significant precipitation events. Filtered samples from the river are rarely detected above the MRL. Given the low concentrations of mercury in the river, mercury concentrations in a RBF source water Well Field are expected to satisfy current drinking water regulations.

5.2 Source-Water Classification

Under the SWTR, source water is classified as one of the following:

- Groundwater (GW)
- Groundwater under the direct influence of surface water (GWUDISW) or
- Surface water (SW)

Treatment requirements are determined based on the source-water classification.

Indiana's GWUDISW Protocol The federal definition of GWUDISW is

any water beneath the surface of the ground with significant occurrence of insects or other macroorganisms, algae, or large-diameter pathogens such as *Giardia* or *Cryptosporidium*; or significant and relatively rapid shifts in water characteristics such as turbidity, temperature, conductivity, or pH which closely correlate to climatological or surface water conditions. (Scharfenaker et al., 2006)

The intent of the SWTR is to determine if there is a possibility for a direct connection between the well and the surface water body that would allow surface water to enter the well without adequate filtration.

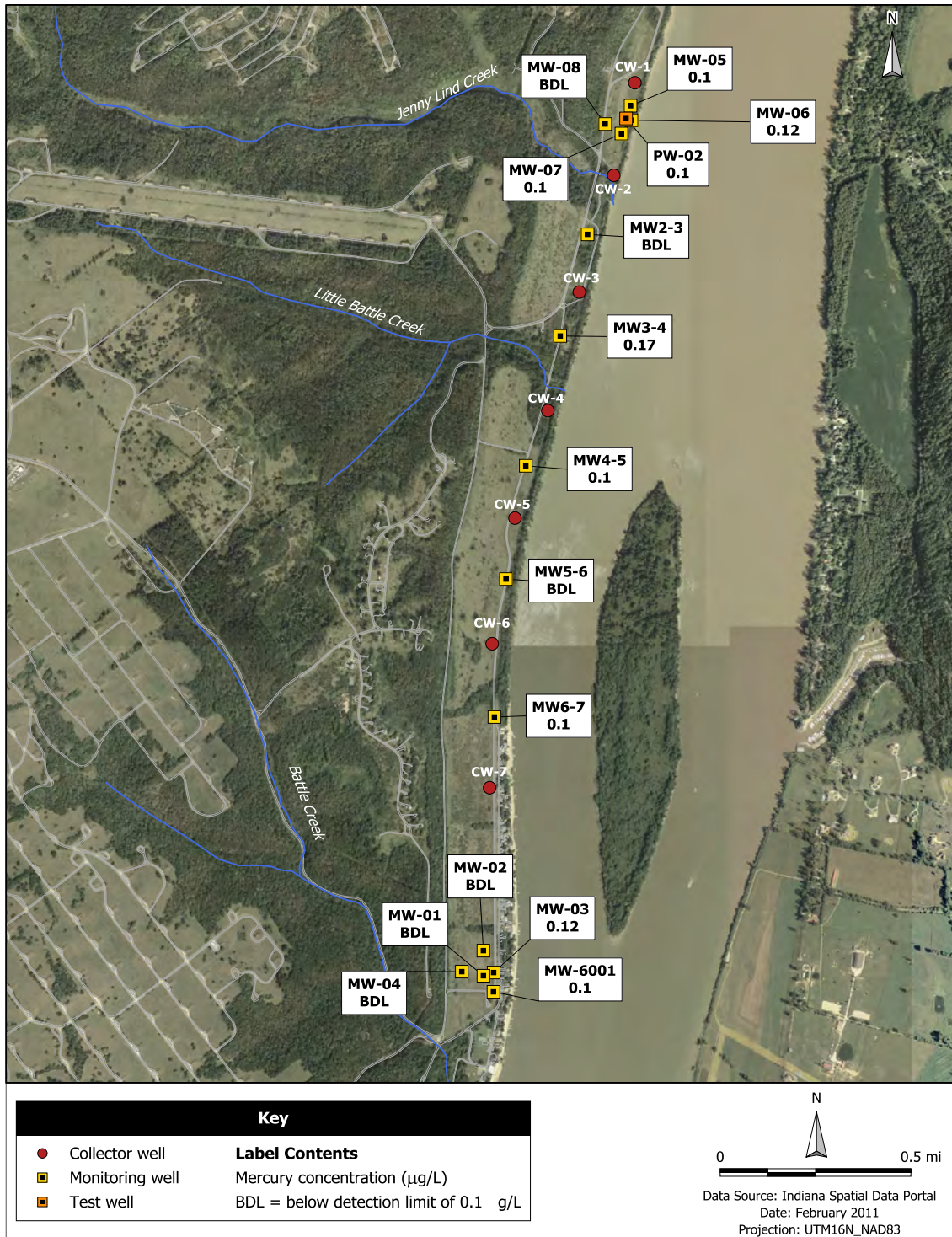


Figure 26: Observed 2009 mercury concentrations in the study area (WHPA, 2010).

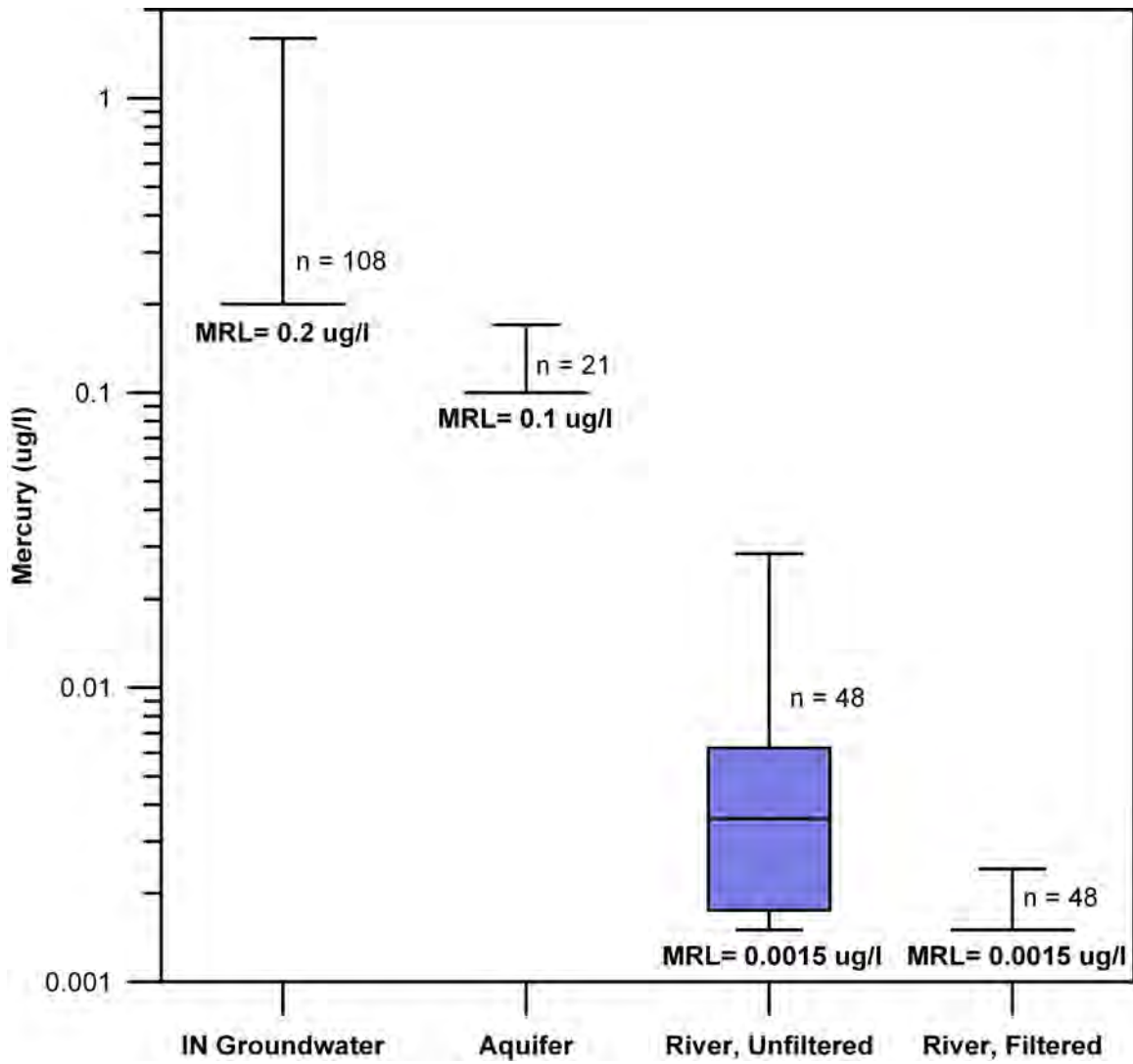


Figure 27: Comparison of observed mercury concentrations in Indiana groundwater (USGS, 2011), in the Aquifer at the Park (WHPA, 2010), and the Ohio River (ORSANCO, 2011).

In the early 1990s, IDEM developed a protocol for evaluating groundwater sources with respect to GWUDISW. The protocol is similar to one provided in the Surface Water Treatment Rule Guidance Manual (AWWA, 1991). IDEM's protocol is a three-step process that, in summary, looks at well construction, well depth, and distance from a surface water source. It also includes select water quality parameters such as turbidity and temperature. Arbitrary decisions incorporated into the protocol assume that certain depths and distances from surface water provide protection from contamination by pathogenic protozoa. The protocol does not provide any quantification as to how much temperature or turbidity variation is representative of surface water. Groundwater systems that may be GWUDISW are required to be evaluated for the occurrence of surface water indicators using Microscopic Particulate Analysis (MPA). The data generated is evaluated using a set of relative risk tables created by a consensus committee working under the USEPA.

The 1994-95 GWUDISW Evaluation Burgess and Niple (1995) evaluated the potential source designation for three of the existing collector wells in 1995 (CW-4, CW-5, and CW-6). Water-quality characteristics were monitored or analyzed from the river and the wells during pumping tests, including physical parameters, MPA, and enteroviruses. No viruses were detected in any of the well samples. Some biological indicators were present in the MPA results, but the counts were low. CW-4 was categorized as *low risk* according to the USEPA relative risk table. CW-5 and CW-6 were categorized as *moderate risk* according to the relative risk table. However, for CW-5 and CW-6 most of the relative risk scoring was due to a common chlorella algae.

5.3 Treatment Recommendations

At lower pumping rates (5 to 10 mgd), it is expected that the water will be classified as groundwater. However, at higher pumping rates we recommend assuming that the water will be classified as GWUDISW. Treatment requirements will depend on whether the regional water supply delivers potable water or partially-treated water. If the purpose of the regional supply is to provide potable water, all drinking water regulations that govern surface water supplies will apply and engineered treatment must be designed accordingly. If the purpose is to provide partially-treated water for subsequent treatment by others, treatment for the regional supply should result in the highest water quality that is economically feasible. This will minimize costs for wholesale customers and maximize the value of the regional water supply.

While the USEPA had previously recognized RBF as a technology that can achieve pathogen removal, the LT2ESWTR was the first United States drinking-water regulation that specifically recognized RBF as a compliance technology option. The LT2ESWTR recognizes RBF as a "toolbox" pretreatment technique that can provide a system 0.5- or 1.0-log additional pretreatment credit, if it

meets specified design and monitoring criteria. For RBF to be eligible for credit as a pretreatment technique, the following criteria must be met.

- Wells must be drilled in an unconsolidated, predominantly sandy aquifer, as determined by grain-size analysis of recovered core material — the recovered core must contain greater than 10% fine-grained material (grains less than 1.0-millimeter diameter) in at least 90% of its length.
- Wells must be located at least 25 ft (in any direction) from the surface-water source to be eligible for 0.5-log credit; wells located at least 50 ft from surface water are eligible for 1.0-log credit.
- The wellhead must be continuously monitored for turbidity to ensure that no system failure is occurring. If the monthly average of daily maximum turbidity values exceeds 1 Nephelometric Turbidity Unit (NTU), the system must report this finding to IDEM. The system must also conduct an assessment to determine the cause of high turbidity levels in the well and consult with IDEM to determine whether the previously allowed credit is still appropriate.

We strongly recommend that prior to planning and design of treatment facilities, a demonstration of performance study be performed to evaluate the level of treatment that can reliably be expected from natural RBF in the well field.

This page intentionally left blank

6 Alternative Analysis

Because specific regional water demands have not been determined, and those demands will vary in quantity, location, and timing, we evaluated a range of development alternatives. Conceptual layouts and estimated costs are provided for 16 alternatives covering water demand scenarios from 10 mgd to 80 mgd. This information is intended to inform planning and investment decisions related to the development of a regional water supply.

6.1 Conceptual Design of Alternatives

The alternatives are comprised of varying configurations of collector wells, pipelines, and treatment for demand scenarios ranging from 10 mgd to 80 mgd. We considered two options for reuse of the seven existing collector wells, each applicable depending on the available or required capacity. The first option consists of equipping the existing collector well with new pumps and other equipment, and constructing a new pump house (Figure 28). The second option consists of the same, but in addition includes increasing the capacity of the existing collector well by installing additional laterals (Figure 29). We also determined that there is sufficient land area to construct two additional collector wells (CW-8 and CW-9) on Park property, south of existing CW-7.

We assumed that new pipelines would be constructed along the well field for connection to the collector wells, and from the well field to State Roads 3 and 62 in the City of Charlestown (Figure 30). We assumed that the most likely route for a pipeline from the well field would begin near CW-2 and follow a path through the RRCC toward the intersection of State Roads 3 and 62. We determined the size of the pipeline based on the estimated capacity of each scenario.

The conceptual layout and cost of each alternative includes the cost to equip, improve, or construct the included collector wells. Because the location of included wells determines the length of pipeline required to deliver the water, and the cost of pipe is significant, we consider its cost in the analysis. In the conceptual cost estimates, we included the cost to construct a new pipeline from the collector wells to the intersection of State Roads 3 and 62. The conceptual cost estimates also include the cost of treatment. The layouts and estimates for each alternative are detailed in Appendix D - Alternative Analysis.

6.2 Alternative Analysis

As described in Section 4, we used the calibrated groundwater flow model to obtain preliminary estimates of the theoretical yields of the well field in two configurations: one consisting of the seven existing collector wells; and the other consisting of nine wells - the seven existing collector

Equip existing collector well

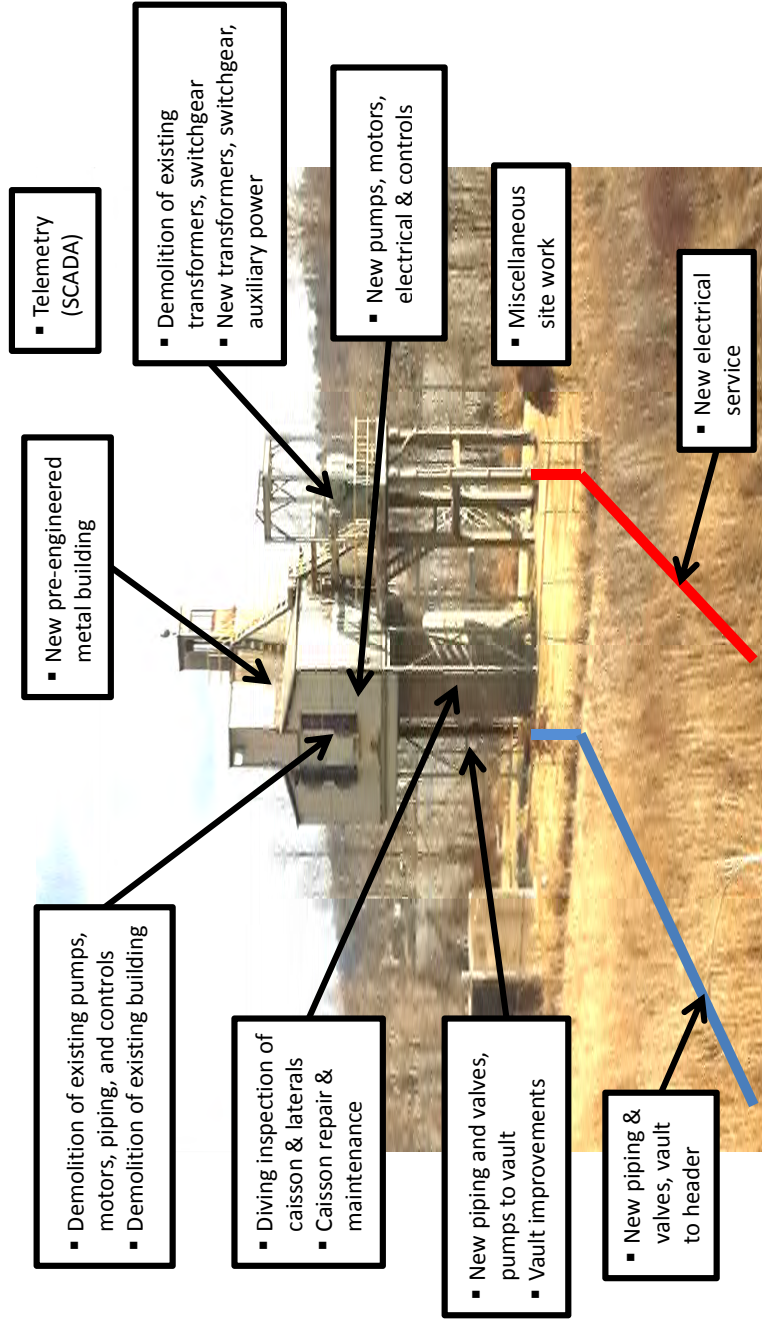


Figure 28: Equipping existing collector well.

Improve existing collector well

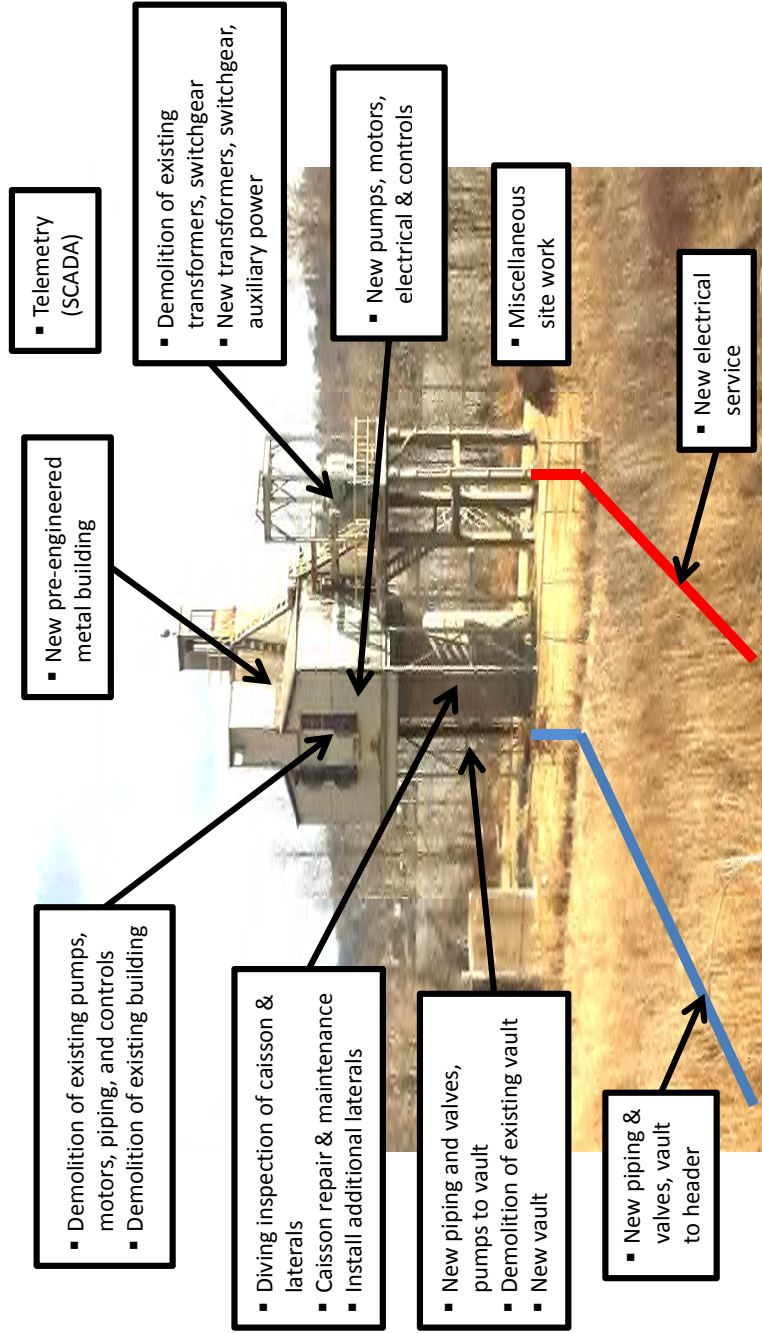


Figure 29: Improving existing collector well.

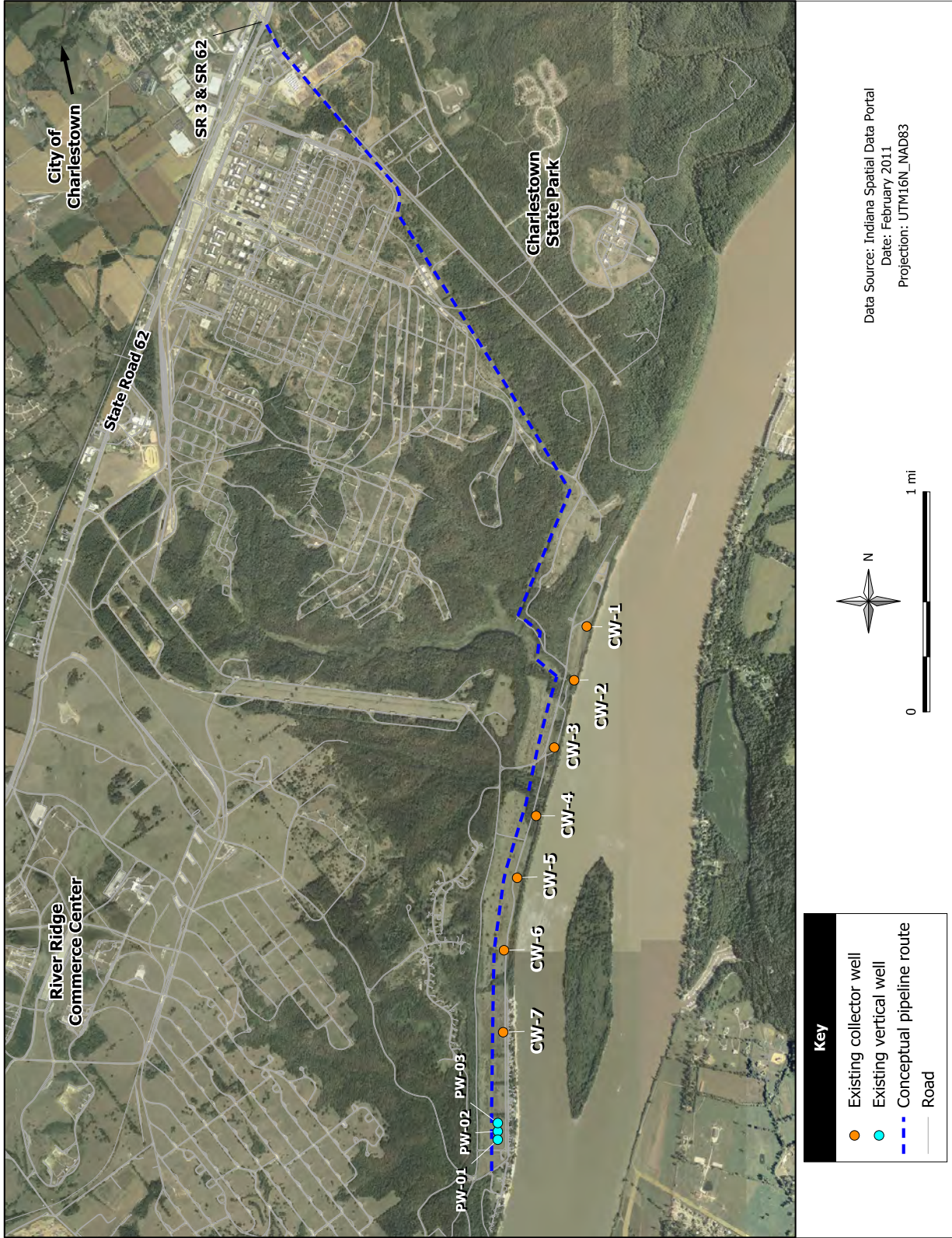


Figure 30: General layout of collector wells and raw water transmission main.

wells plus two new wells. The theoretical yields were adjusted downward to account for riverbed clogging. We also calculated the mechanical capacity of the existing collector wells and laterals based on current design standards. Based on the adjusted theoretical yields of the collector wells, and the mechanical capacities of the existing laterals, we developed multiple alternatives consisting of conceptual layouts for well field capacities ranging from 10 mgd to 80 mgd.

Based on our estimates of theoretical yields, we identified the existing collector wells for which the installation of additional laterals is unlikely to result in significant gains in capacity. CW-2 through CW-5 are located in a portion of the Aquifer in which the theoretical yield is not appreciably higher than the mechanical capacity of the existing collector well. Therefore, for these wells we only recommend improvements in pumping equipment and other facilities necessary for production equivalent to the mechanical capacity of the existing laterals. Existing CW-1, CW-6, and CW-7 are located in areas of the Aquifer that have properties conducive to producing more water than the current mechanical capacity of the wells. For these wells, we either recommended equipping them with pumps, or improving them with new laterals and pumps. For each alternative, we identified

- which wells would be re-equipped with new pumps
- which wells would be re-equipped and improved with new laterals
- where new collector wells would be constructed

6.3 Conceptual Cost Estimates

For each alternative, we estimated the conceptual costs of the collector wells and pipelines, and calculated the cost per mgd of capacity. The results of the evaluation of all alternatives is presented in Table 17 and the conceptual layout for each alternative and basis for cost estimates is included in Appendix D - Alternative Analysis. Conceptual cost estimates include design and construction and are accurate to +40%/-20%.

The cost of raw water transmission pipelines is significant. If future expansion of initial facilities is likely, we advise consideration of the cost and potential future savings realized by installing mains with greater capacity than initially required.

Decisions regarding investments in equipping or improving collector wells should also consider all likely paths of system development. The alternatives developed for the full development of the well field provide insight into which initial investments would most likely continue to be useful as part of an expanded regional supply.

Table 17: Summary of alternatives: included wells, sustainable capacity, and estimated conceptual cost.

Alternative	Equipped wells CW-#	Improved wells CW-#	New wells CW-#	Sustainable capacity (mgd)	Estimated conceptual cost			Total (millions)	Cost per mgd (millions)
					Wells (millions)	Pipeline (millions)	Treatment (millions)		
10-A	1,2	-	-	9.8	\$9.9	\$2.8	\$35.0	\$47.7	\$4.87
10-B	-	7	-	15.0	\$6.7	\$3.8	\$35.0	\$45.6	\$3.04
20-A	1,2,3,5	-	-	20.0	\$19.8	\$5.2	\$66.0	\$91.0	\$4.55
20-B	5	7	-	19.7	\$11.7	\$5.9	\$66.0	\$83.5	\$4.24
30-A	2,3,4	1	-	30.4	\$20.4	\$7.1	\$96.0	\$123.5	\$4.06
30-B	1,2,3,4,5,6,7	-	-	32.6	\$34.7	\$7.6	\$96.0	\$138.3	\$4.24
30-C	-	7	9	30.0	\$13.7	\$8.3	\$96.0	\$118.0	\$3.93
40-A	1,2,3,4,5	7	-	38.4	\$31.5	\$9.2	\$120.0	\$160.7	\$4.19
40-B	5	-	8,9	34.7	\$18.9	\$10.1	\$120.0	\$149.0	\$4.29
50-A	2,3,4,5	1,6,7	-	48.5	\$37.6	\$10.0	\$137.5	\$185.1	\$3.82
50-B	5	7	8,9	46.6	\$25.6	\$11.0	\$137.5	\$174.1	\$3.74
50-C	-	6,7	8,9	49.5	\$26.2	\$11.0	\$137.5	\$174.7	\$3.53
60-A	-	1,6,7	8,9	58.3	\$31.7	\$12.1	\$150.0	\$193.8	\$3.32
60-B	3,4,5	7	8,9	55.5	\$35.5	\$11.9	\$150.0	\$197.4	\$3.56
70-A	2,3,4	1,7	8,9	64.1	\$41.1	\$13.5	\$157.5	\$212.1	\$3.31
80-A	2,3,4,5	1,6,7	8,9	74.8	\$51.5	\$15.5	\$160.0	\$227.0	\$3.03

Note. Names of alternatives are based on the target, not estimated production capacity.

7 Conclusions and Recommendations

Properly developed and managed, the Charlestown State Park Aquifer represents a valuable asset for economic development in southern and central Indiana. The work described in this report was done to estimate the potential yield of the Outwash Aquifer, to evaluate the implications of RBF on water quality and treatment, and to recommend a plan for development.

7.1 Yield

How much water can be produced from the Aquifer?

To answer this question we use conservative estimates of the sustainable capacity of the Well Field. Also, we recommend further evaluation of the most productive area of the Well Field, in order to improve estimates of its potential contribution to a high-capacity regional water supply.

7.1.1 Sustainable Capacity

Based on a configuration of 9 collector wells, we conservatively estimate the sustainable capacity of the Well Field to be 74.8 mgd. The actual sustainable capacity would be greater if it is determined, based on a site-specific evaluation, that it is feasible to construct some of the collector wells with mechanical capacities greater than 15 mgd, or if it is determined, through water-level monitoring, that greater drawdowns are permissible without dewatering riverbed sediments.

We defined the sustainable capacity of the Well Field as the volume of water that can be consistently produced overtime from constructed wells subject to multiple constraints. As described in Section 4, we limited the permissible drawdown in the wells to prevent dewatering of riverbed sediments overlying the Aquifer. We reduced aquifer yield estimates by 25% to allow for a decline in specific capacity that may result from partial clogging and compaction of riverbed sediments in areas with the highest initial rates of induced recharge (Hubbs et al., 2006). Also, we limited the maximum mechanical capacity of a collector well to 15 mgd. Aquifer yields are greater at the north and south ends of the Aquifer than in the middle. The south end of the Aquifer is highly productive.

7.1.2 Further evaluation of the south end of Well Field

As discussed in Section 4, the south end of the Well Field is highly productive with theoretical aquifer yields in excess of 20 mgd per collector well. Pumping tests performed to date at the south end of the Aquifer have been limited. To fully evaluate the potential of the south end of the Aquifer, a high-rate pumping test is required. We recommend that CW-7 be equipped for an extended test at

a minimum pumping rate of 14,000 gpm (approximately 20 mgd). Piezometers should be installed between CW-7 and the riverbank and into the river. During the pump test and recovery, water levels should be continuously monitored in nearby IDNR production wells and in existing monitoring and collector wells.

Additionally, it is recommended that nearby private residential wells be inspected and equipped to monitor water levels. Based on the inspection of private wells, it may be determined that alternate water supply arrangements would be necessary for some residents during the pump test. Private wells south of the Park property also should be monitored to evaluate the potential for construction of an additional future collector well at the south end of the Aquifer, outside the current Park property.

For the purposes of this study, estimates of the Well Field's long-term capacity have been intentionally conservative. With the additional data from a high-rate pump test of CW-7, our estimates of long-term capacity of the Aquifer could be reviewed and revised.

7.2 Water Quality and Treatment Requirements

Is water quality in the Aquifer adequate for drinking water – what treatment could be required for this to be used as a source?

To answer these questions we provide conclusions regarding the anticipated general long-term water quality in the Well Field. We recommend planning assumptions related to source water classification and treatment requirements. We also identify the value of RBF for improving the quality of source water and the potential of RBF to reduce the cost of infrastructure and operations.

7.2.1 Water origin

As described in Section 5, we determined that the river is the origin of the majority of water pumped from the Well Field. Previous investigation of the bedrock geology, karst features, and joints of the upland bedrock of the former INAAP site found no significant, direct hydrogeological linkage with the Ohio River (Hendricks, 1995). Some recharge to the Aquifer does result from precipitation at the Well Field, however, we estimate that the recharge from the entire land surface to the Aquifer averages 0.11 mgd (Section 5). At an average pumping rate of 50 mgd, the percentages of water originating from surface recharge and induced recharge from the river are 0.2% and 99.8%, respectively. In the long term, we believe that the quality of water produced from the Well Field will be predominantly influenced by the water quality of the river.

7.2.2 Source water classification

As described in Section 5, the water produced by wells constructed in the Park may be either classified as groundwater (GW) or groundwater under the direct influence of surface water (GWUDISW). The criteria for determining the source water classification include evidence of pathogen contamination from the river, and response of groundwater to changes in temperature and turbidity of river water (Section 5). While it is possible that the water could be initially classified as groundwater, particularly at lower pumping rates, for planning purposes we recommend assuming that the water will eventually be classified as GWUDISW.

7.2.3 Riverbank filtration

Water that is recharged to the Aquifer from the river benefits from natural filtration through the riverbed sediments and the riverbank itself. As discussed in Section 5, RBF can provide partial, but reliable treatment of surface water. The natural filtration that occurs with RBF can reduce suspended solids and organic matter to levels consistently lower than those in surface water. As a result,

- less chemical treatment is required, resulting in lower operating costs
- fewer residuals are generated by the treatment process, reducing the cost to construct and operate infrastructure for their handling
- residual disposal costs are significantly lower
- the impact of future regulations related to residuals management and disposal will be minimized

Through evaluation and demonstration of the performance of RBF, credit under current drinking water regulations may be achieved for pathogen removal. The demonstrated performance of RBF may be sufficient to reduce requirements for engineered treatment and in turn, the amount of investment required for treatment infrastructure.

We recommend that a demonstration-of-performance study be performed in conjunction with the development of a regional water supply to obtain regulatory credit for RBF at the Well Field. In terms of reduced infrastructure and operational requirements, the return on investment for this study could be significant.

7.2.4 Engineered treatment requirements

Treatment requirements will depend on whether the regional water supply is intended to deliver potable water or partially treated water intended for use as a raw water source. If the purpose is

to provide a source of raw water for subsequent treatment by others, the cost of treatment may be slightly less costly than treatment to potable standards. However, treatment for raw water supply must consider the cost of operating and maintaining transmission mains that will be impacted by deposition of materials not removed by the treatment process, corrosion, or biological growth.

If the regional water supply will be delivered as potable water, treatment requirements will be determined by the classification of the source water and current safe drinking water regulations. We recommend assuming that the source will be classified as GWUDISW and that surface water treatment requirements will apply. As discussed above, we strongly recommend that prior to planning and design of treatment facilities, a demonstration-of-performance study be performed to evaluate the level of treatment that can reliably be expected from natural RBF in the Well Field.

7.3 Water Supply Development and Operation

How should the well field be developed to maximize its value as a regional water supply?

7.3.1 Infrastructure

The Well Field contains a great deal of existing water supply infrastructure, although much of it is in poor condition and no longer useful. However, there may be opportunities to reuse some existing assets in the redevelopment of the Well Field. Specific decisions regarding the reuse, repair, or replacement of existing structures and equipment should be preceded by a thorough inspection.

Collector wells If use of the existing caissons is considered, we recommend that they first be inspected by a qualified structural engineer to determine if the concrete is in adequate condition to allow the installation of new laterals and to bear the load of a new well house. The structural engineer should assess the remaining useful life of the caissons for an economic analysis of reuse or replacement.

For our conceptual cost estimates, we assumed that the existing well houses will be demolished and replaced. We recommend that the existing well houses and equipment be inspected prior to demolition to identify any building or other materials that will require special precautions for removal and disposal.

Electrical service For our conceptual cost estimates, we assumed that the existing electrical services are not usable and will be demolished or abandoned and replaced with new wiring, conduit, and equipment. We recommend that the existing high voltage transformers and other equipment be inspected prior to demolition to identify any materials that will require special precautions for removal and disposal.

Pipelines For our conceptual cost estimates, we assumed that none of the existing cast iron pipelines can economically be used. We recommend installing new pipelines for the redevelopment of the well field. To minimize water loss and optimize the use of the resource, we recommend that high standards be established for pressure and leakage testing of new mains, and that they be equipped with provisions for accurate accounting of water and early detection of leaks. We also recommend that the existing cast iron mains be abandoned in a manner that physically interrupts the continuity of the original pipelines to prevent them from serving as conduits for any future sources of contamination.

7.3.2 Water demand

We recommend that a study be performed to assess potential demand for a regional water supply. The location, magnitude, and timing of these demands will be critical for the economic analysis of a regional water supply.

7.3.3 Collector well improvement alternatives

Based on our estimates of theoretical yields, we identified the existing collector wells for which the installation of additional laterals is unlikely to result in significant gains in capacity. CW-2 through CW-5 are located in a portion of the Aquifer in which the theoretical yield is not appreciably higher than the mechanical capacity of the existing collector well. Therefore, for these wells we only recommend improvements in pumping equipment and other facilities necessary for production equivalent to the mechanical capacity of the existing laterals. Existing wells CW-1, CW-6, and CW-7 are located in areas of the Aquifer that are conducive to producing more water than the current mechanical capacity of the wells. For these wells, we recommend either equipping them with pumps or improving them with new laterals and pumps.

7.3.4 Water quality monitoring & protection

River water quality monitoring As discussed in Section 4, the predominant source of recharge to the Aquifer is the Ohio River. Barge traffic on the river presents a contaminant risk because of spills. In the event of a spill, the potential impact to the Aquifer could be significantly reduced by promptly stopping pumping operations to avoid inducing recharge of contaminated surface water into the Aquifer. For planning purposes we recommend initial contact with the authorities responsible for alerting communities of emergencies and potential hazards affecting the Ohio River.

Groundwater quality monitoring For previous studies, a network of monitoring wells were constructed in the Aquifer (URS, 2003; WHPA, 2010). These monitoring wells provide the means for periodically evaluating water quality in the Aquifer in order to further develop baseline water-quality data, and to identify and monitor potential trends in specific contaminants. Monitoring wells were installed during our previous study (WHPA, 2010) for the purpose of continued monitoring. Because they were installed recently, these monitoring wells are easily located and are in excellent condition. Monitoring wells installed in the course of work performed by URS are documented (URS, 2003), but have not been located and inspected. For the purposes of long-term monitoring of water quality in the Aquifer, we recommend that the URS wells be located, inspected, and cleaned in order to add them to the network of wells available for periodic sampling. We also recommend initiating a monitoring program, and that water-quality samples from representative monitoring wells be collected and analyzed annually at a minimum.

Wellhead protection A wellhead protection plan (WHPP) exists for the current operating wells at the Park, and an updated WHPP is in development for the new wells in construction at the south end of the Well Field. As part of the WHPP, potential contaminant sources (PCS) are identified, and activities are developed to promote the protection of the wellhead protection area (WHPA) from current and future PCS. We recommend that current WHPP activities be expanded to include the full Well Field in anticipation of the development of a regional water supply.

Abandonment of unused wells We recommend that any wells that are not used in the re-developed water supply should be properly abandoned in order to eliminate a potential contaminant source.

Monitoring of INAAP remediation activities Monitoring activities continue at the former INAAP for the Jenny Lind Pond site. These activities include sampling of surface water and sediments (BRAC, 2010). The remedial action phase for the Jenny Lind Pond site will be completed in 2011 and the USACE will request final approval from IDEM. We recommend monitoring of the status of activities related to sites previously identified as potential contaminant sources.

7.3.5 Impacts on neighboring wells

If large quantities of water are pumped for a regional water supply, we anticipate that there will be impacts on the water levels in existing wells currently in operation for the Park, the City of Charlestown, and private residences. In Alternative 80-A, representing full development of the Aquifer, we predict that water levels in the vicinity of the City of Charlestown Well Field may decline by approximately 15 ft. In the same alternative, at the south end of the Aquifer in the

vicinity of IDNR's new well field and treatment facility we predict an average water level decline of approximately 15 ft. At less than full development of the Well Field, impacts to existing well fields will be less than 15 ft but will depend on their proximity to pumping wells.

In the planning and design of well field infrastructure for a regional water supply, we recommend that the impacts to existing wells be evaluated for a full range of anticipated operating conditions and that cost-effective measures be implemented to mitigate those impacts. Mitigation may include compensation for improvements necessary to restore well function, modification of existing wells to ensure adequate performance, or connection to an alternative water supply.

7.3.6 Well field performance monitoring

As discussed in Section 4, the long-term performance of the Well Field is impacted in part by the efficiency of induced recharge from the river. In our analysis, we established constraints intended to minimize the occurrence of clogging and compaction of riverbed sediments as observed by the Louisville Water Company (Hubbs et al., 2006). Clogging and compaction results in reduced transmissivity of riverbed sediments that in turn causes the area of induced recharge to extend further and further away from the well. Specific capacity and overall well field efficiency are reduced as a result. In our conservative estimates of aquifer yield, we limited drawdown to prevent dewatering of the Aquifer below the riverbed sediments *and* assumed that some clogging and resulting reduction in specific capacity would occur.

To optimize the long-term capacity of the Well Field, we recommend monitoring the Well Field's performance to evaluate the effectiveness of drawdown management in minimizing the occurrence of clogging and compaction of riverbed sediments. Therefore, piezometers should be installed between collector wells and the river to monitor water levels in response to varying pumping rates and in relation to the depth of riverbed sediments. We also recommend that the collected data be used to monitor changes in transmissivity of riverbed sediments and to adjust operating constraints to optimize capacity while minimizing the risk of compaction of sediments and long-term loss of well field efficiency.

7.3.7 Optimization of collector well design

The capacity of a collector well is determined both by the yield of the Aquifer and by the mechanical capacity of the collector well laterals. Maximum mechanical capacity is constrained by the number, orientation, and slot size of laterals that can be installed at the location of the collector well. In our analysis, we have conservatively assumed that the maximum mechanical capacity of a collector well constructed in this Aquifer will be 15 mgd. For Alternative 80-A, this conservative assumption

reduced our estimate of well field capacity by 6.5 mgd. Collector wells have been constructed with individual capacities in excess of 40 mgd. Thorough characterization of the subsurface materials at the well site allows the design of the collector well and laterals to be optimized for higher mechanical capacity. We recommend thorough well site characterization of existing and proposed collector wells to optimize the mechanical capacity and to take advantage of the maximum available aquifer yield.

7.3.8 Optimization of collector well operation

As we have previously discussed, to mitigate the risk and effects of clogging and compaction of riverbed sediments on the efficiency of the Well Field, the capacity of each collector well is limited by constraints on drawdown. To be conservative in our estimates of well field capacity, we limited drawdown *and* assumed that long-term yield would be reduced 25% because of clogging and compaction. For Alternative 80-A, our estimate of safe design capacity was reduced by another 5.7 mgd for this potential loss of aquifer yield.

We recommend installing pressure transducers in piezometers to allow for continuous monitoring of water levels. We also recommend that instrumentation and control systems of the Well Field be designed to provide data collection, alarms, and analysis of trends in the efficiency of each collector well. With this information, changes in the transmissivity of riverbed sediments may be estimated and monitored to ensure that Well Field operation is optimized for long-term capacity and efficiency.

A reliable water supply is needed for economic development in southern Indiana. The State has the potential to provide 75 mgd of drought-proof water to southern and central Indiana. Planning for the use of this valuable resource today will build the foundation needed to promote and sustain economic growth in the future.

References

- Bakker, M., Kelson, V., and Luther, K. (2005). Multiaquifer Analytic Element Modeling of Radial Collector Wells. *Ground Water*, (in press).
- BRAC (2010). Installation Action Plan, Fiscal Year 2010, Indiana Army Ammunition Plant. Technical report, US Army.
- Burgess and Niple (1995). Evaluation and testing of horizontal collector well nos. 4, 5, and 6 at Indiana Army Ammunition Plant. Technical report, Burgess and Niple Engineers Architects.
- Clark, G. and Larrison, D. (1980). The Indiana Water Resource. Technical report, Governor's Water Resource Study Commission, Indiana Department of Natural Resources.
- Curry, R. (2006). Charlestown State Park Waterworks Evaluation. Technical report, R.E. Curry and Associates. Report to Indiana Department of Natural Resources.
- Doherty, J. (2000). Model-independent parameter estimation. Computer software manual, Watermark Numerical Computing.
- Doherty, J. (2004). PEST - Model-Independent Parameter Estimation User Manual. Software manual.
- Fenelon, J. and Bobay, K. (1994). Hydrogeologic Atlas of Aquifers in Indiana. Water Resources Investigation 92-4142, U.S. Geological Survey.
- Gollnitz, W., Clancy, J., McEwen, J., and Garner, S. (2005). Riverbank filtration for IESWTR compliance. *Journal of the American Water Works Association*, 97(12):64–76.
- Gollnitz, W., Clancy, J., Whitteberry, B., and Vogt, J. (2003). RBF as a Microbial Treatment Process. *American Water Works Association*, 95(12):98–110.
- Gollnitz, W., Whitteberry, B., and Vogt, J. (2004). Riverbank Filtration: Induced Infiltration and Groundwater Quality. *American Water Works Association*, 96(12):98–110.
- Haitjema, H. M. (1995). *Analytic Element Modeling of Groundwater Flow*. Academic Press, San Diego, CA.
- Harbaugh, A., Banta, E., Hill, M., and McDonald, M. (2000). MODFLOW-2000, The U.S. Geological Survey Modular Ground-water Model - User Guide to Modularization Concepts and the Ground-water Flow Process. Open-File Report 00-92, U.S. Geological Survey.
- Hendricks, R. (1995). A preliminary assessment of hydrogeological significant solution and fracture features: Indiana Army Ammunition Plant, Charlestown, Clark County, Indiana. Technical report, Indiana Geological Survey.

- Hubbs, S., Ball, K., and Caldwell, T. (2006). Riverbank filtration: An evaluation of RBF hydrology and impacts on yield. Technical report, AWWARF.
- IDNR (1980). Ground-Water Availability. <http://www.in.gov/dnr/water/files/indiana-wa.pdf>. Accessed February 2011.
- IDNR (2009). Water Well Record Database. <http://www.in.gov/dnr/water/3595.htm>.
- Kazmann, R. (1948). River infiltration as a source of ground water supply. Paper 2339, American Society of Civil Engineers.
- Kelly, B. and Rylund, P. (2006). Water-quality changes caused by riverbank filtration between the Missouri River and three pumping wells of the Independence, Missouri, Well Field, 2003-05. SIR-2006-5174, U.S. Geological Survey.
- ORSANCO (2011). Clean metals sampling program. <http://www.orsanco.org/clean-metals>. Accessed 2011.
- Planert, M. and Williams, J. (1995). Ground water atlas of the United States, Segment 1 - California, Nevada. Hydrologic Investigations Atlas 730-B, U.S. Geological Survey.
- Raney (1965). Report on Ranney Well inspection for Olin Matheson Chemical Corporation, charlestown, indiana. Technical report, Ranney Water Systems, Inc.
- Raney (1979). Ranney Well Inspections for ICI Americas, Inc., Charlestown, Indiana. Technical report, The Ranney Company, a division of Layne-New York Company, Inc.
- Reynolds (2000). Inspection of radial collector wells, Charlestown, Indiana. Technical report.
- Reynolds (2011). Budgetary estimate for engineering & construction services, charlestown state park collector well field. e-mail correspondence.
- Risch, M. and Fowler, K. K. (2008). Mercury in precipitation in Indiana, January 2004-December 2005. Scientific Investigations Report 2008-5148, U.S. Geological Survey.
- Rumbaugh, J. and Rumbaugh, D. (2000-2007). *Guide to Using Groundwater Vistas*. Environmental Simulations, Inc.
- Schafer, D. C. (2006). Use of aquifer testing and groundwater modeling to evaluate aquifer/river hydraulics at Louisville Water Company, Louisville, Kentucky, USA. In *Proceedings of the NATO Advanced Research Workshop on Riverbank Filtration (2004)*, pages 179–198. Springer.
- Scharfenaker, M., Stubbart, J., and Lauer, W. C. (2006). Field Guide to SDWA regulations. American Water works Association.

- Schmidt, C., Lange, F., Brauch, H., and Kühn, W. (2003). Experiences with riverbank filtration and infiltration in Germany. In *Proceedings International Symposium on Artificial Recharge of Groundwater*, pages 115–141.
- URS (2003). Installation Groundwater - Site 90, Indiana Army Ammunition Plant, Phase II RCRA Facility Investigation. Technical report, URS Corporation.
- USEPA (1997). Mercury study report to Congress Volume III: fate and transport of mercury in the environment. Technical Report EPA-452/R-97-005, U.S. Environmental Protection Agency, Office of Air Quality Planning and Standards & Office of Research and Development.
- USGS (2011). IDEM Pesticide Study. USGS National Water Information System. <http://nwis.waterdata.usgs.gov/in/nwis/nwis>.
- Weiss, W., Bower, E., Ball, W., O'melia, C., Lechevallier, M., Aora, H., and Speth, T. (2003). riverbank Filtration- fate of DPB precursors and selected microorganisms. *American Water Works Association*, 95(10):68–80.
- WHPA (2009). Charlestown Water Supply Investigation. Technical report, Wittman Hydro Planning Associates, a division of Layne Christensen.
- WHPA (2010). Wellfield design and analysis of the sand-and-gravel aquifer at Charlestown State Park. Technical report, Wittman Hydro Planning Associates, a division of Layne Christensen.
- Williams, E. (1981). Fundamental concepts of well design. *Ground Water*, 19(5):527–542.

This page intentionally left blank

Appendix A - Supplemental Geophysical Survey Information

Land survey results

Based on where each actual field data point is measured and the finite-difference modeling methodology, the 2D modeled depth sections have the appearance of an inverted trapezoid. Note that the limited data overlap on the left and right edges of the individual model greatly affects the model resolution along those edges. As such, the accuracy of the model results in these areas is limited.

Overall, the quality of the land geophysical survey data was good. Some electrodes overlying existing well field water-transmission mains and paved roads were disconnected to improve overall data quality. Unfortunately, the precise location of transmission mains could not be determined in the majority of the study area. The location of the transmission lines are illustrated on the ERI profile line models by an anomalous low electrical-resistivity response shown as the light to dark blue gradient in Figures 31 to 38. Some of the water main interference on the data occurred in the deeper portions of the profiles or at the edges where resolution is poor due to limited data overlap.

The land ERI profile lines results were sufficient to adequately define the upper and lower boundaries of the sand and gravel aquifer. However, the modeled velocity depth cross section for seismic line SL2 (Figure 39) did not correlate well with ERI profile line R3 (which overlapped SL2) or nearby monitoring well bedrock depth data. The SL2 bedrock depth and layer velocity estimates were lower than expected, which was likely caused by the presence of a low-velocity layer composed of weathered bedrock that underlies the aquifer. This low velocity (low resistivity) layer correlates with ERI profile line R3 model results. The low velocity layer causes a *blind zone*, which tends to lower the estimated layer velocity and depth estimates.

The ERI profile line model and the modeled velocity depth cross section for seismic line SL1 (Figure 40) suggest that the western subsurface bedrock contact (i.e., base of the bluff) is near-vertical. This near-vertical bedrock contact trend is evident based on the western portion of SL1 modeled depth section which illustrates that the estimated bedrock depth below geophone 1 (which is approximately 75 ft from the toe of the bluff) is over 90 ft. This inferred trend is consistent with previous study results.

The land ERI and seismic line model results suggest that depth to bedrock in the survey area ranges from 80 ft to over 125 ft, which is consistent with the depth to bedrock recorded in monitoring well logs. Results also suggest that the bedrock surface is undulated, with the slope of the bedrock surface decreasing towards the Ohio River.

Additionally, the results suggest that the thickness of the gravel aquifer in most the survey area ranges between 25 ft and 120 ft. The estimated range in gravel aquifer thickness is also consistent with monitoring well log data. The electrical resistivity values for the gravel aquifer range from

approximately 100 ohm-meters to over 300 ohm-meters. Based on unconsolidated formation lithology from monitoring well logs, the lower electrical resistivity values suggest a higher silt and clay content, whereas the higher electrical resistivity values suggest that the aquifer is predominantly composed of medium to coarse sand and gravel with very low silt/clay content.

We can also infer that throughout the study area, a low electrical resistivity layer (10 ohm-meters to 50 ohm-meters) overlies the gravel aquifer. The shallow layer has thickness between 20 ft to more than 30 ft and is likely composed of silt and clay material from alluvial origin. This is consistent with well log data. Results indicate that the shallow layer can become thin in portions of the survey area. Where present, this layer is a confining layer to the underlying gravel aquifer.

Marine survey results

The water depth is illustrated on the ERI marine model profiles by a white line, and in the survey area it ranged from approximately 10 ft to 40 ft. The model results suggest that the penetration depth using the 6-meter electrode spacing (Figure 41) was between 40 ft to 50 ft, whereas the penetration depth with the 12-meter electrode spacing (Figure 42) was over 80 ft. Because of the relatively thick water column, the 12-meter electrode model profile lines provided better subsurface resolution compared to the 6-meter model profile line results.

The marine profile model results suggest that the Ohio River bed is comprised of an upper, relatively thin (approximately 5 to over 10 ft thick) layer of low electrical resistivity material (light blue-green color), which overlies a zone of unconsolidated material with a higher range of electrical resistivity values (dark green to red color). The upper low electrical resistivity material is most likely comprised of relatively impermeable unconsolidated material composed of silt, clay, sand, and gravel. The underlying zone of higher electrical resistivity material is likely composed of permeable unconsolidated formation ranging from fine to coarse sand and gravel (dark to light green) to more permeable medium to coarse sand and gravel (yellow to red). The underlying zone of higher electrical resistivity material appears to correlate with the onshore sand and gravel aquifer.

The marine model profile results also suggest that bedrock was not detected. Based on the onshore geophysical survey results and other available information, the depth to bedrock underlying the Ohio River in the survey area is approximately 120 ft below the water surface.

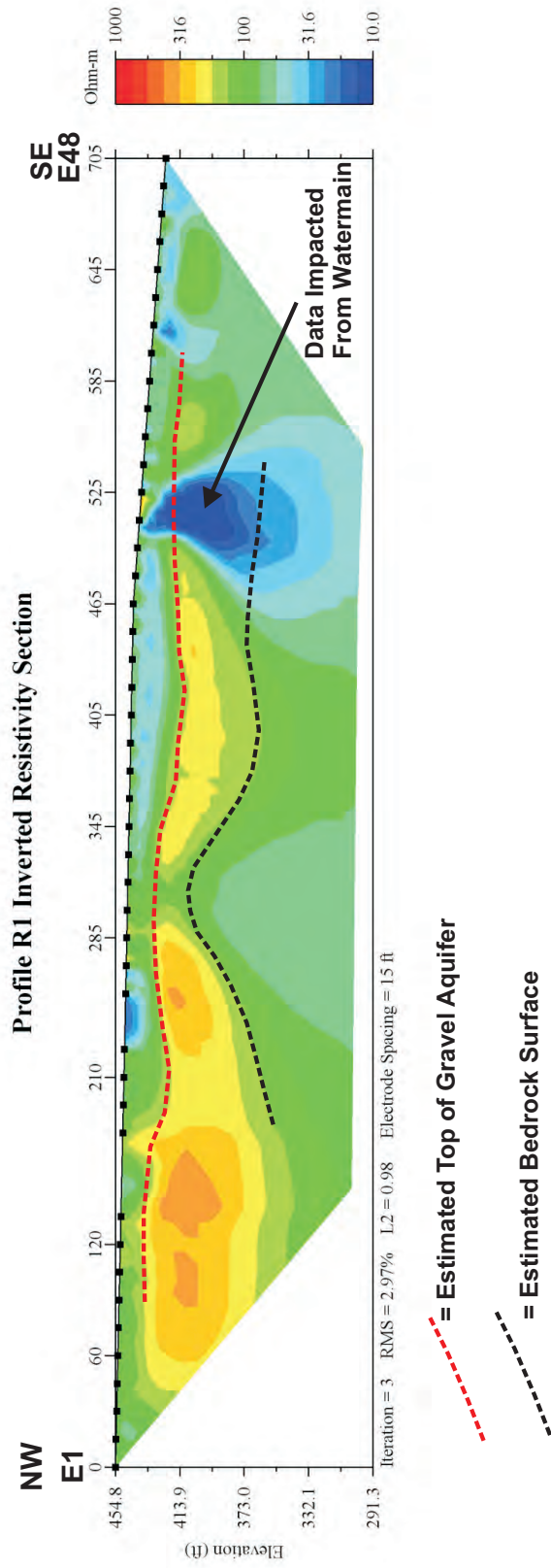


Figure 31: Land survey profile R1.

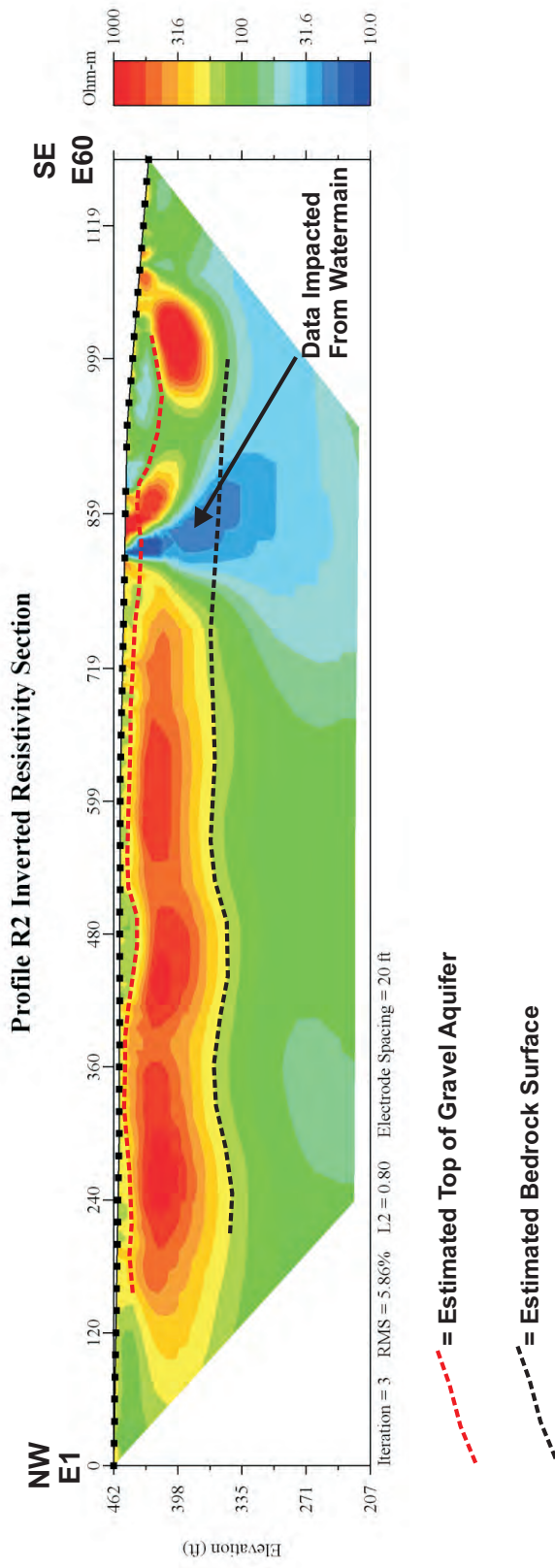


Figure 32: Land survey profile R2.

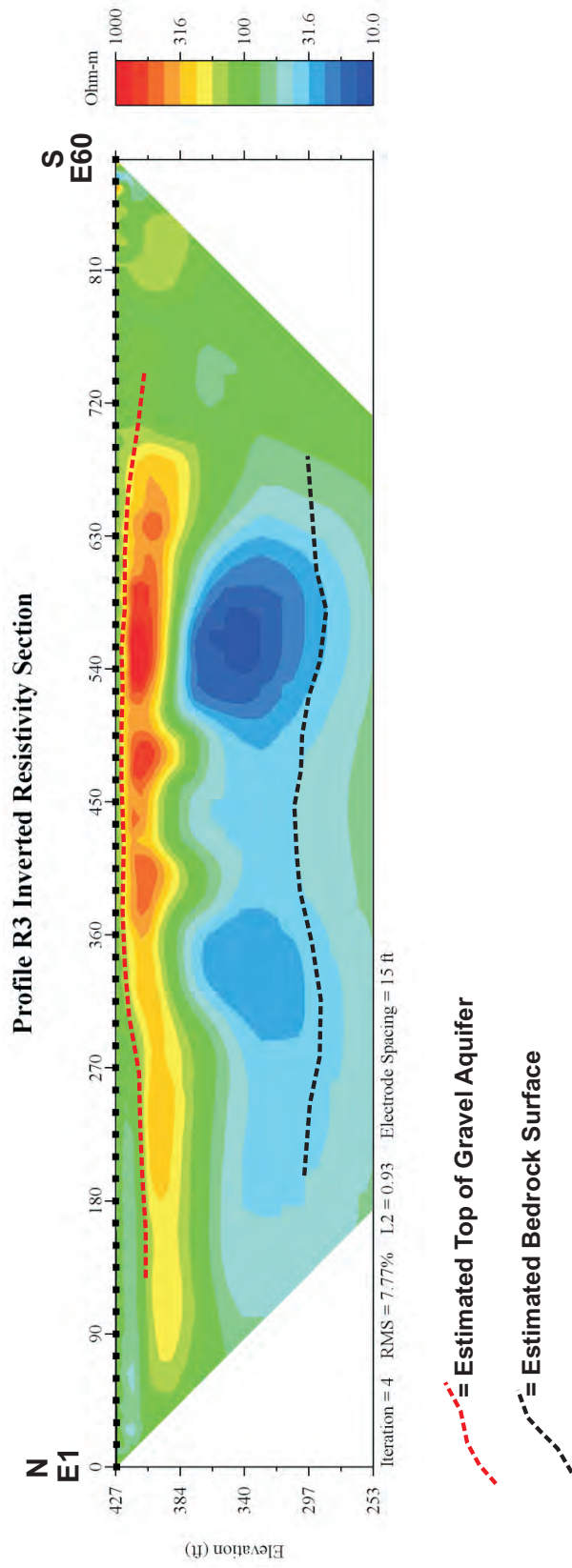


Figure 33: Land survey profile R3.

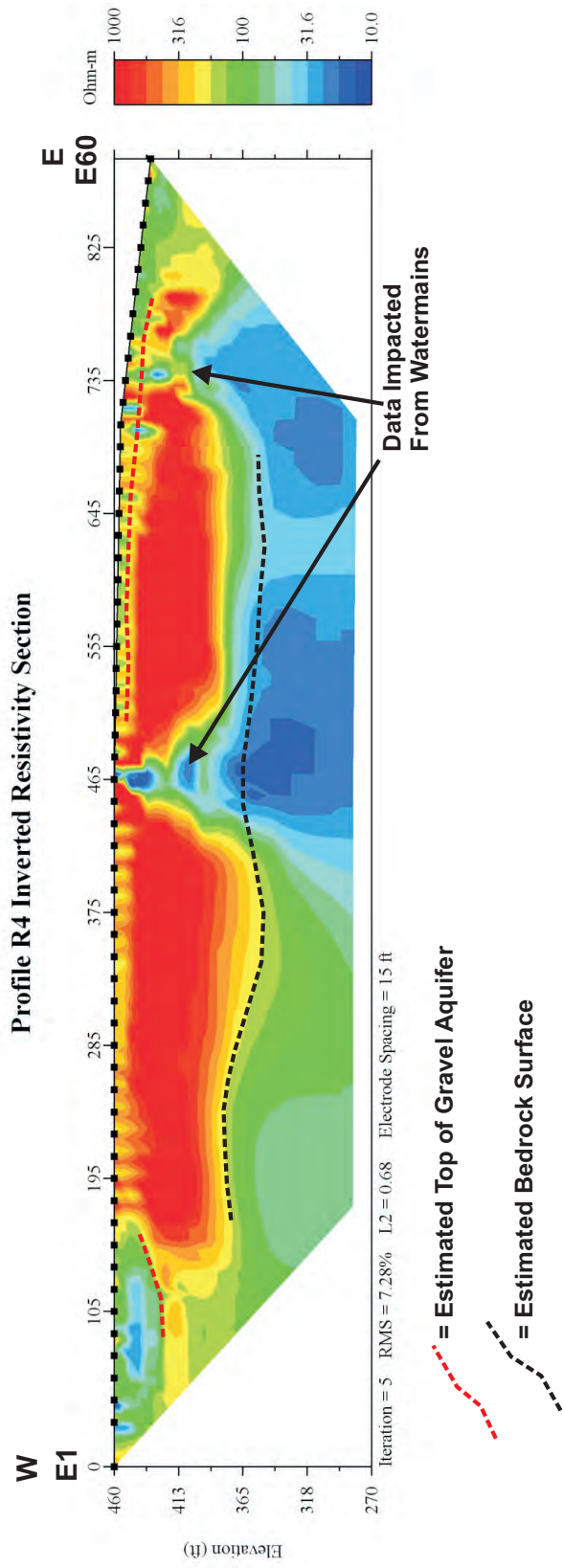


Figure 34: Land survey profile R4.

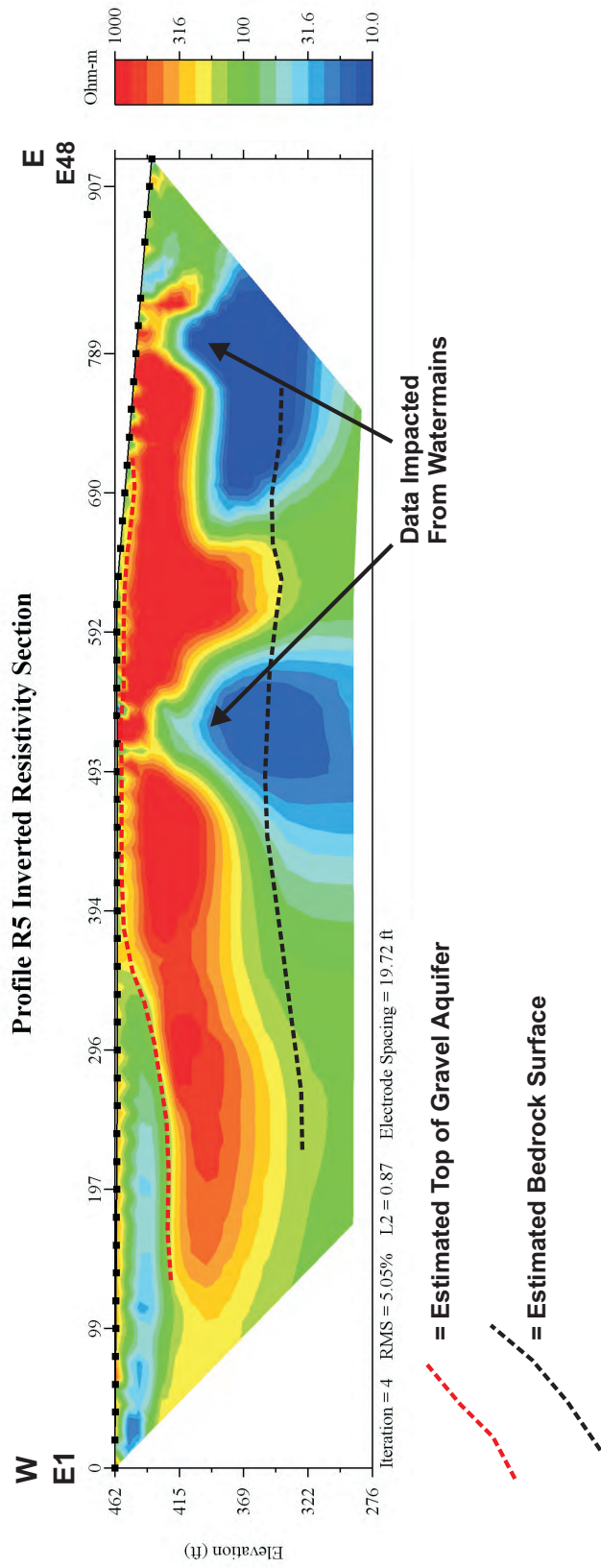


Figure 35: Land survey profile R5.

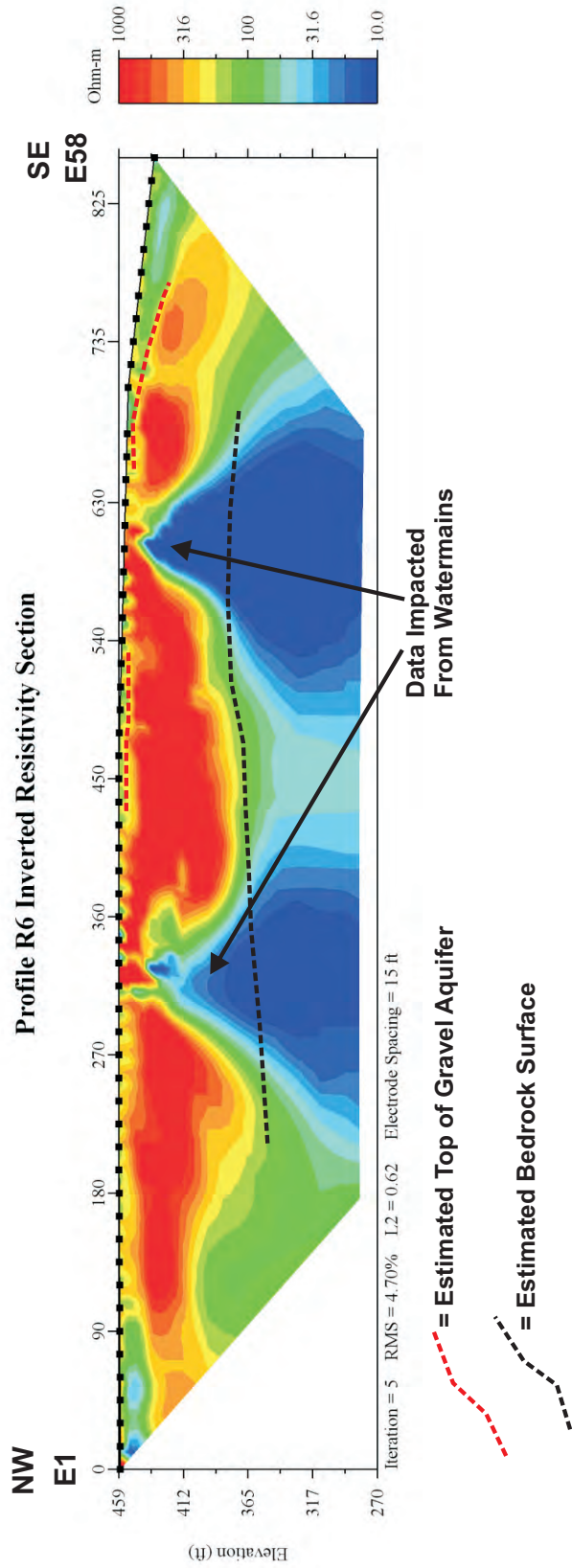


Figure 36: Land survey profile R6.

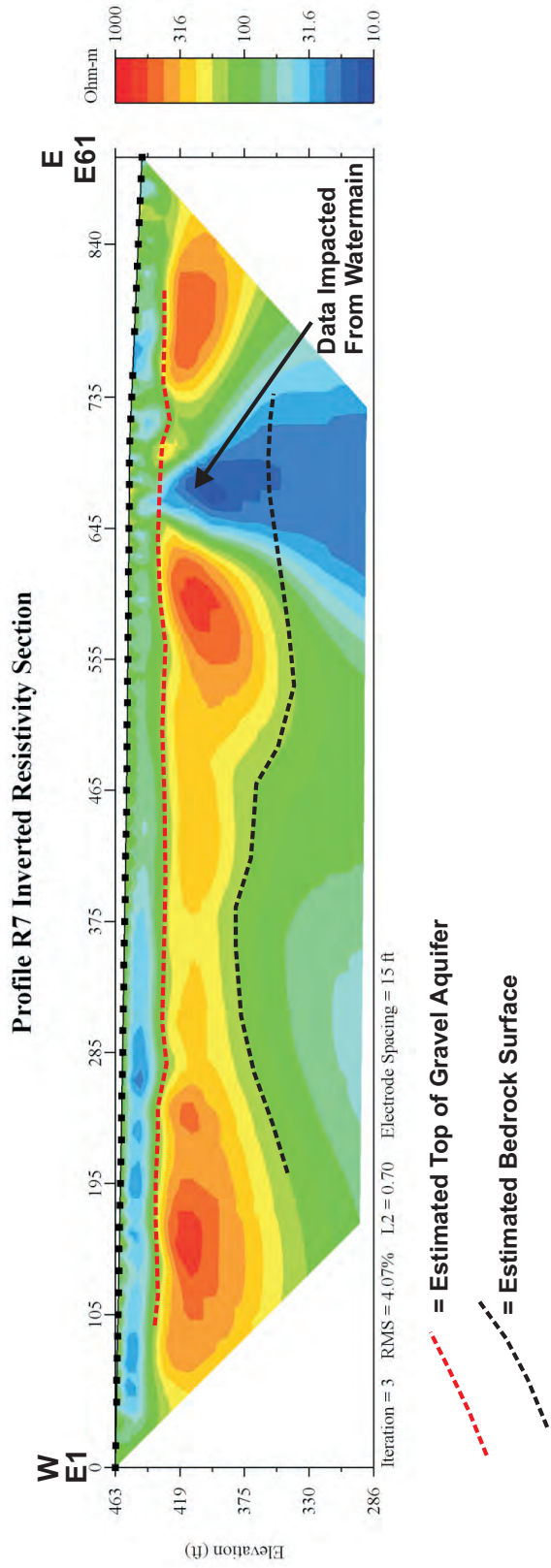


Figure 37: Land survey profile R7.

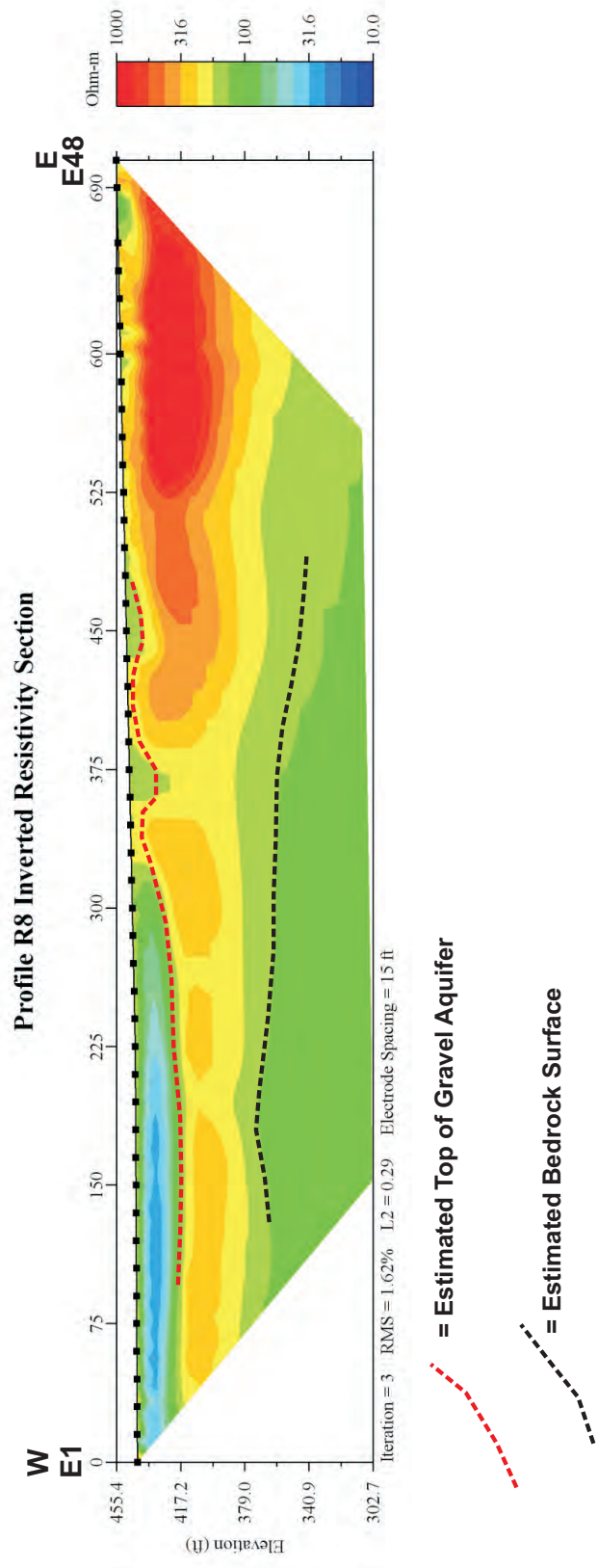


Figure 38: Land survey profile R8.

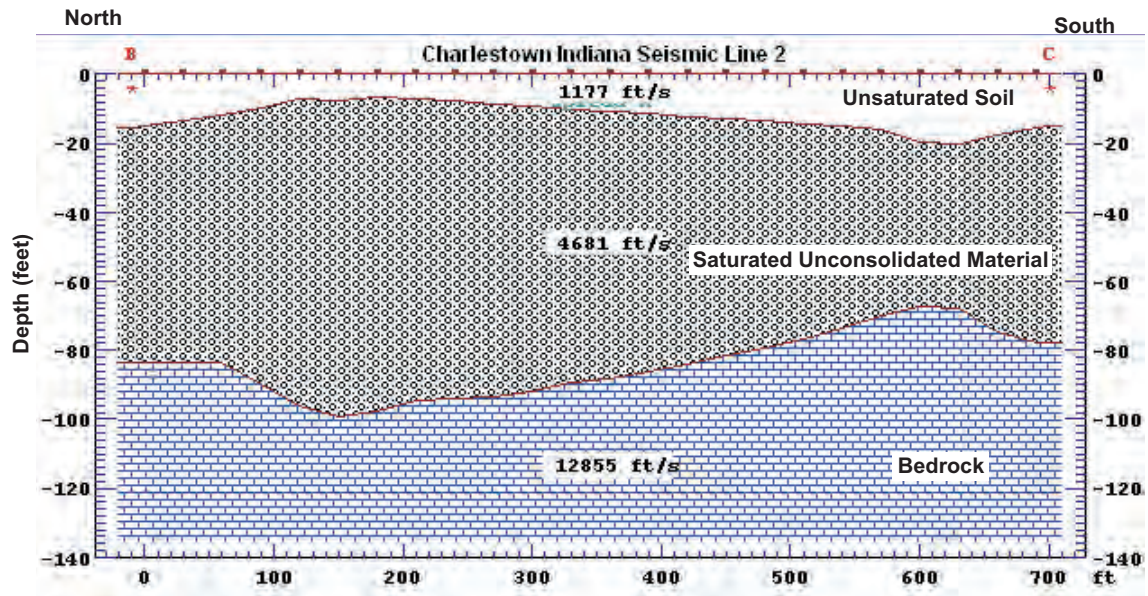


Figure 39: Seismic line SL2.

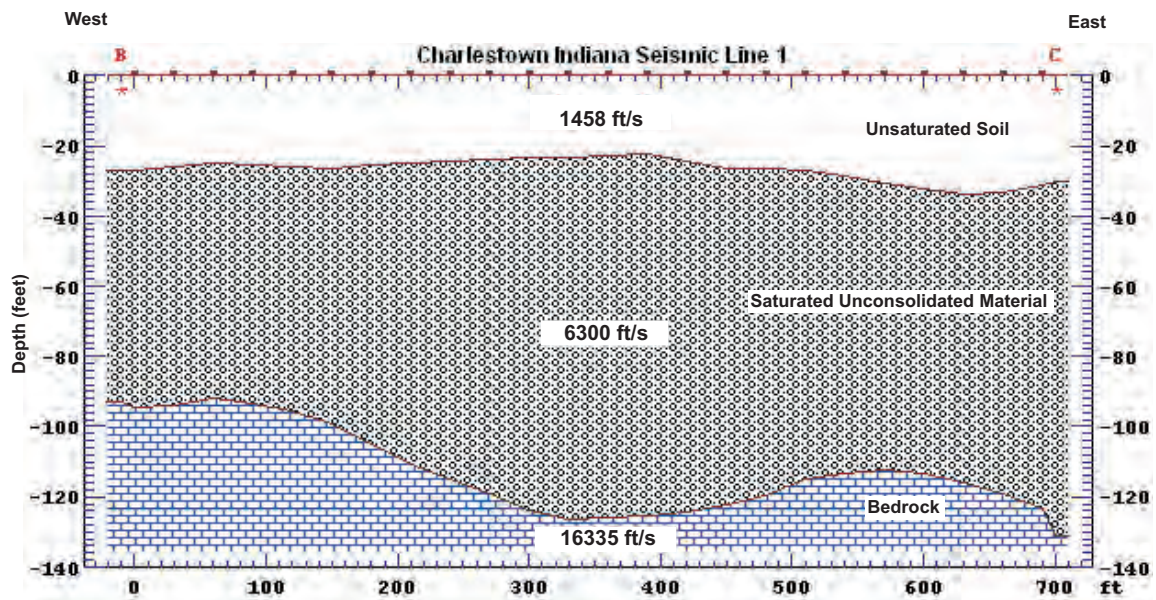


Figure 40: Seismic line SL1.

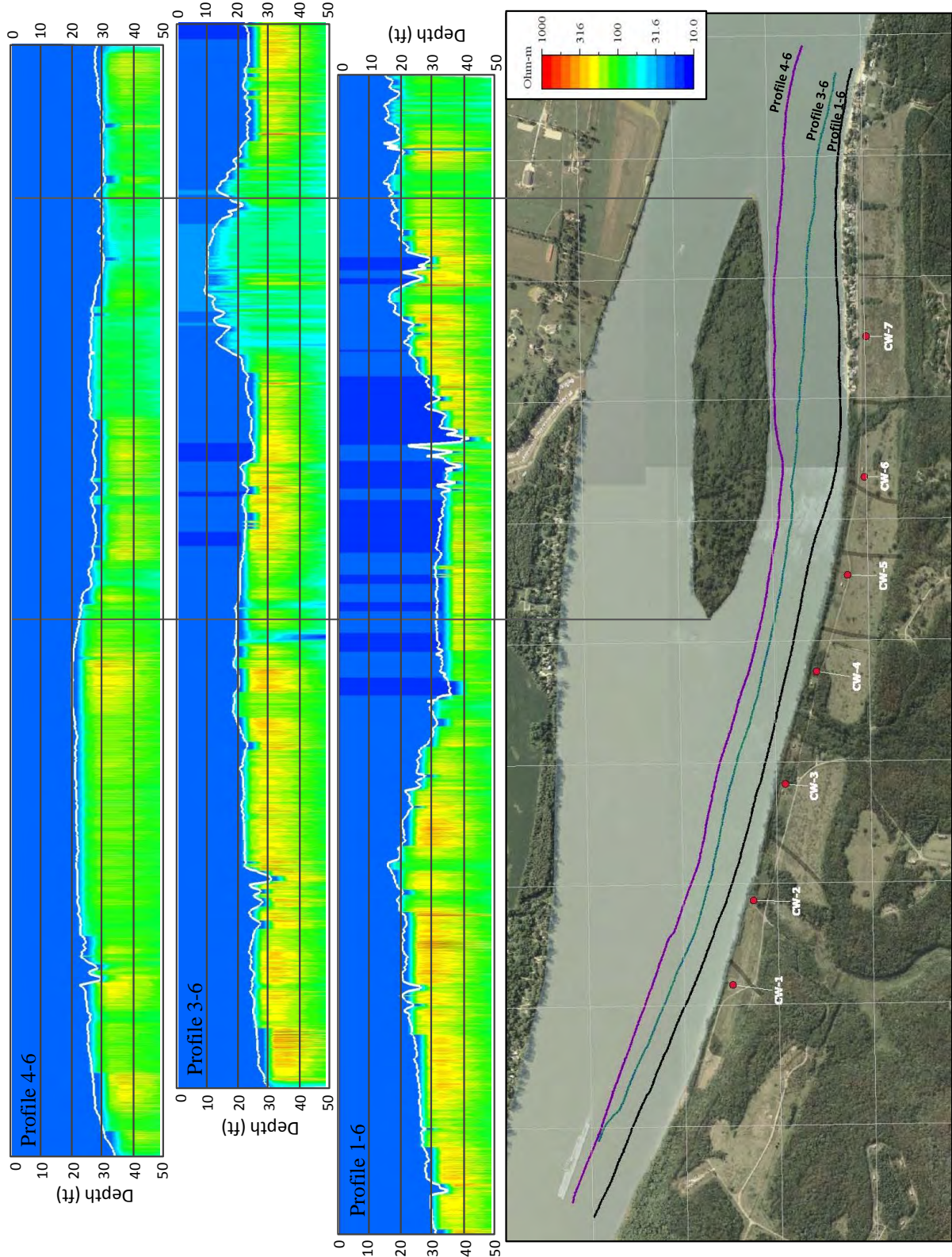


Figure 41: Marine survey 2-D sections of the 6-meter profile lines.

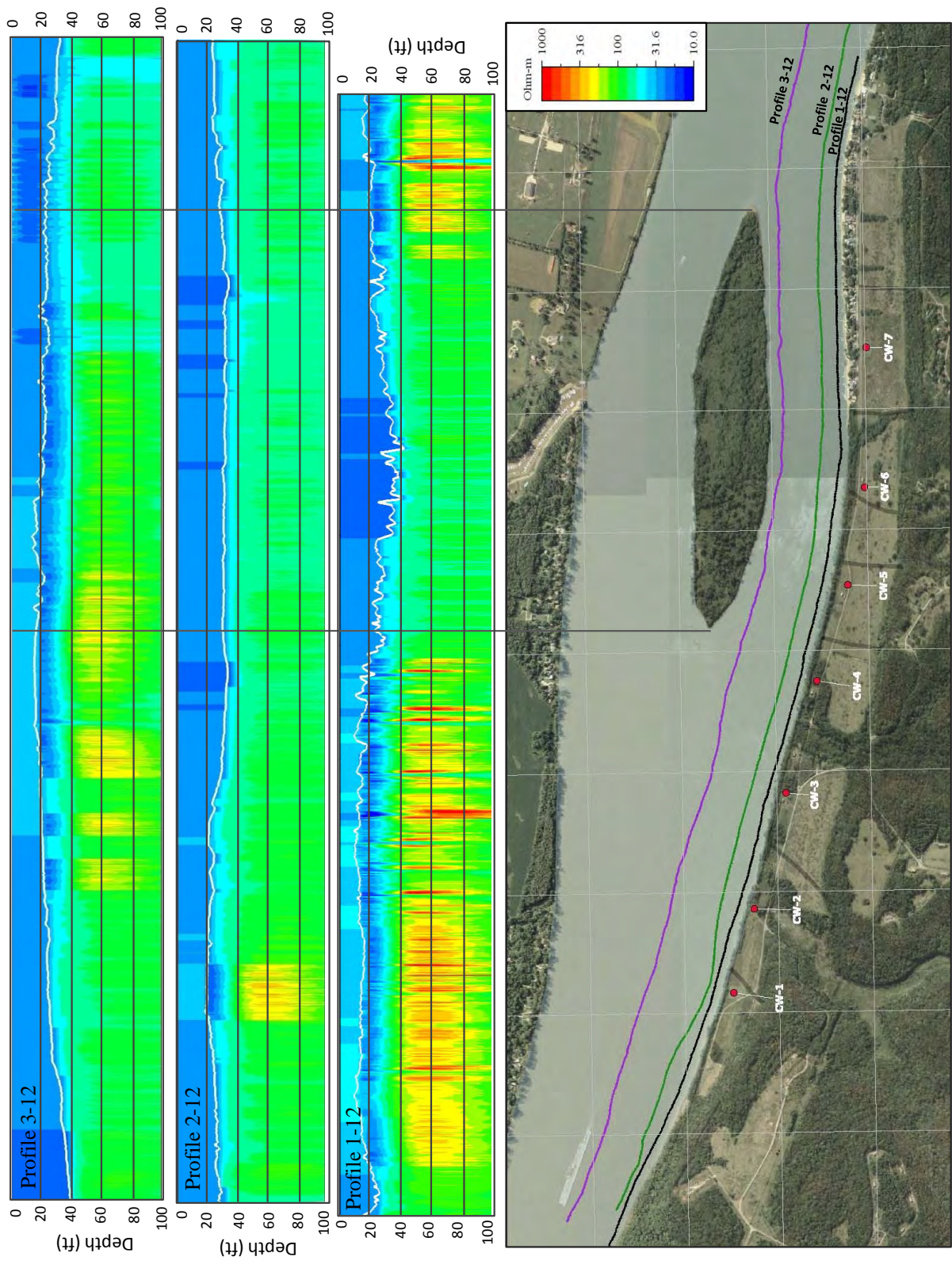


Figure 42: Marine survey 2-D sections of the 12-meter profile lines.

This page intentionally left blank

Appendix B - Predicting Collector Well Yields with MODFLOW

Introduction

A common use of groundwater flow models is for the design of new wells and well fields. Because the scale of the problem is large and great local-scale detail is not needed, typical models for well field design often use two-dimensional or quasi-three-dimensional models based on the Dupuit-Forchheimer (Dupuit) assumption. This approach offers a robust set of tools for simulating regional groundwater flow including interactions with surface waters, the potential for well interference, and varying aquifer properties and recharge rates. However, predicting the yield of a well at a particular operating water level or drawdown with a 2D model is complicated by a variety of hydraulic factors, including the effects of converging 3D flow to a partially-penetrating well screen, inefficiency at the screen itself, and the possibility of localized turbulent flow near the well. Since the Dupuit assumption does not account for these effects, it underestimates the operating drawdown at the well screen for a partially-penetrating well; depending on the ratio of the well screen height to the aquifer thickness, the error may be very large. Thus, when the yield of a well is computed, given the operating water level in the wells, a Dupuit model can greatly overpredict the yield of the well.

For design purposes, this is unacceptable – a means for predicting well yields in an accurate, appropriately conservative manner is needed. A simple way to predict vertical well yield using the Dupuit assumption is to assume a well “efficiency” that is based on previous experience. If Q is the well yield predicted by the Dupuit assumption, a well with 70% efficiency, will achieve $0.7 \times Q$ at any given drawdown in the well screen. More rigorous approaches such as the general well-loss equation (Jacob, 1947; modified by Rorabaugh, 1953), allow the user to develop a factor that includes corrections for the model cell size, a resistive “skin effect” at the well perimeter, and turbulent flow near the well. This approach is used to parameterize multiple-aquifer wells using the drawdown-limited, multi-node well (MNW) package for MODFLOW (USGS, 2002).

Design of angled or horizontal well screens is additionally complicated by the difficulty of simulating horizontal, or nearly horizontal, screens in a numerical model grid. In plan view, a vertical well appears as a “point sink” in an analytical solution or as a single cell of a numerical model while a horizontal screen has a linear geometry, and will likely extend over several neighboring cells. Also, when the well screens do not align with rows or columns in a numerical model, it is not immediately obvious how to enter the well’s configuration into the model, or how small the model cells must be to achieve a reliable yield estimate. Furthermore, it is necessary to include the effects of converging 3D flow to the lateral well screens, and since each well is different, it is not clear how to assign a simple well efficiency. Finally, in the case of horizontal collector wells, the model must account for interactions between the well screens, which depend on the layout of the lateral screens and therefore will differ among wells. This paper presents a method for simulating the yield

of angled or horizontal well screens in numerical groundwater flow models, specifically using the USGS code MODFLOW. Although the method presented here is suitable for angled well screens, galleries, or drains, this paper focuses on the simulation of horizontal collector wells; the text refers only to horizontal screens.

Previous Work

In the Analytic Element Method (AEM), the simulation of horizontal well screens is facilitated by the availability of line elements that accurately represent the geometry of well screens. Bakker et al. (2005) divided each well screen into a collection of horizontal, quasi-three-dimensional, Bessel line sink elements. By assigning the proper boundary conditions along the lateral screens, the code simulates groundwater flow to a collector well. Their code is based on TimML, a Bessel AEM code that allows for variable aquifer properties in horizontal layers. However, a major computational effort is required for the Bessel elements; for field applications, a regional 2D model is often used to derive boundary conditions for a local 3D TimML model. Detailed analysis of 3D flow near the collector well laterals, including pathline tracing, is supported. It is noted that the collector well element in TimML is covered by U.S. Patent number 7,769,574, held by Layne Christensen Company.

For 2D AEM models, Haitjema et al. (2010) provide a methodology for representing converging 3D flow to horizontal well screens in a 2D model. Their approach uses an entry resistance to express the effects of 3D converging flow to the lateral screens represented by 2D line-sink elements. This formulation is suitable for inclusion in regional models; however it does not allow for the detailed 3D pathline tracing offered by the Bessel code TimML. This formulation makes it possible to reliably predict yields to horizontal wells, collector wells, angled wells, and galleries in regional 2D AEM models by entering drain elements configured using the appropriate resistance. It has been demonstrated to provide yield estimates that compare well with 3D TimML models.

In MODFLOW, explicitly simulating groundwater flow to an arrangement of angled or horizontal lateral screens is more difficult, owing to the challenge of representing the screens with rectangular cells. It is possible to use a numerical model grid with very small cells, e.g. using the MODFLOW multiple-node well (MNW) package. Furthermore, the use of the MNW package requires the modeler to choose an appropriate, and *a priori* unknown, entry resistance parameter for the well screens. However, the USGS offers no guidance on developing the so-called cell-to-well conductance for horizontal wells when using MNW to simulate horizontal wells. The resulting model requires large data management and computational efforts, and even so, results depend on the modeler's selected entry resistance.

Clearly, a simpler and more robust modeling technique is needed for predicting collector well yields.

This paper presents a methodology that applies the resistance formulation of Haitjema et al. within a MODFLOW model. Although it is intuitive that the resistance formulation is appropriate for any model code that can simulate horizontal groundwater flow at a regional scale, it is less clear how the resistance should be entered into the model. The formulation provided here is based on the AEM scheme: each lateral screen is subdivided into a collection of segments, and each segment is represented by one or more drains using the MODFLOW DRN package. The scheme used does not require that the laterals lie along rows or columns in the MODFLOW grid. Instead, a drain conductance is applied in each cell that adjoins the segment, using an interpolation scheme.

Mathematical Formulation

In general, it is very unlikely that the lateral screens of a collector well will coincide with the rows or columns of the numerical model grid. A common strategy for dealing with this problem is to make the grid cells small enough that an arrangement of small cells that lie along the lateral will mimic the geometry of the lateral. The result is similar to a "raster" representation of a line on a computer display (see Figure 45). While a sufficiently small model grid can accurately represent the geometry of the lateral, this strategy inevitably leads to a very fine model grid, typically requiring cells on the scale of 1 m or smaller. Additionally, it is necessary to include detailed vertical discretization at a large cost in data management and model performance. This level of detail yields very accurate flow fields, however, it is unclear how to compute the entry resistance of the small cells that represent the lateral (USGS, 2002). Furthermore, this level of grid resolution is inappropriate for inclusion in a regional groundwater flow model.

For design purposes, it is rarely necessary to simulate details of the local flow field; the objective is more often to predict the design yield of the collector well, assuming an operating water level in the well caisson. It is therefore advantageous to make use of a model grid with larger cells, and if possible to apply the Dupuit assumption. The formulation is presented in two steps: (1) development of a general conceptual formulation for simulating collector well laterals; and (2) implementation of the conceptual formulation using MODFLOW. The general conceptual formulation is presented in more detail by Haitjema et al. (2010), and is summarized here.

Conceptual formulation

Haitjema et al. offers a methodology for including 3D effects at collector wells in a 2D AEM model. Figure 43 illustrates the conceptual formulation for a collector well model. It is noted that a similar organization is used in TimML. The collector well is composed of M laterals arranged about a central caisson as shown in Figure 43. Lateral $m = 1 \dots M$ is subdivided into N segments, each of which is represented by a single first-order line-sink element. It is noted that the sink density σ_j ,

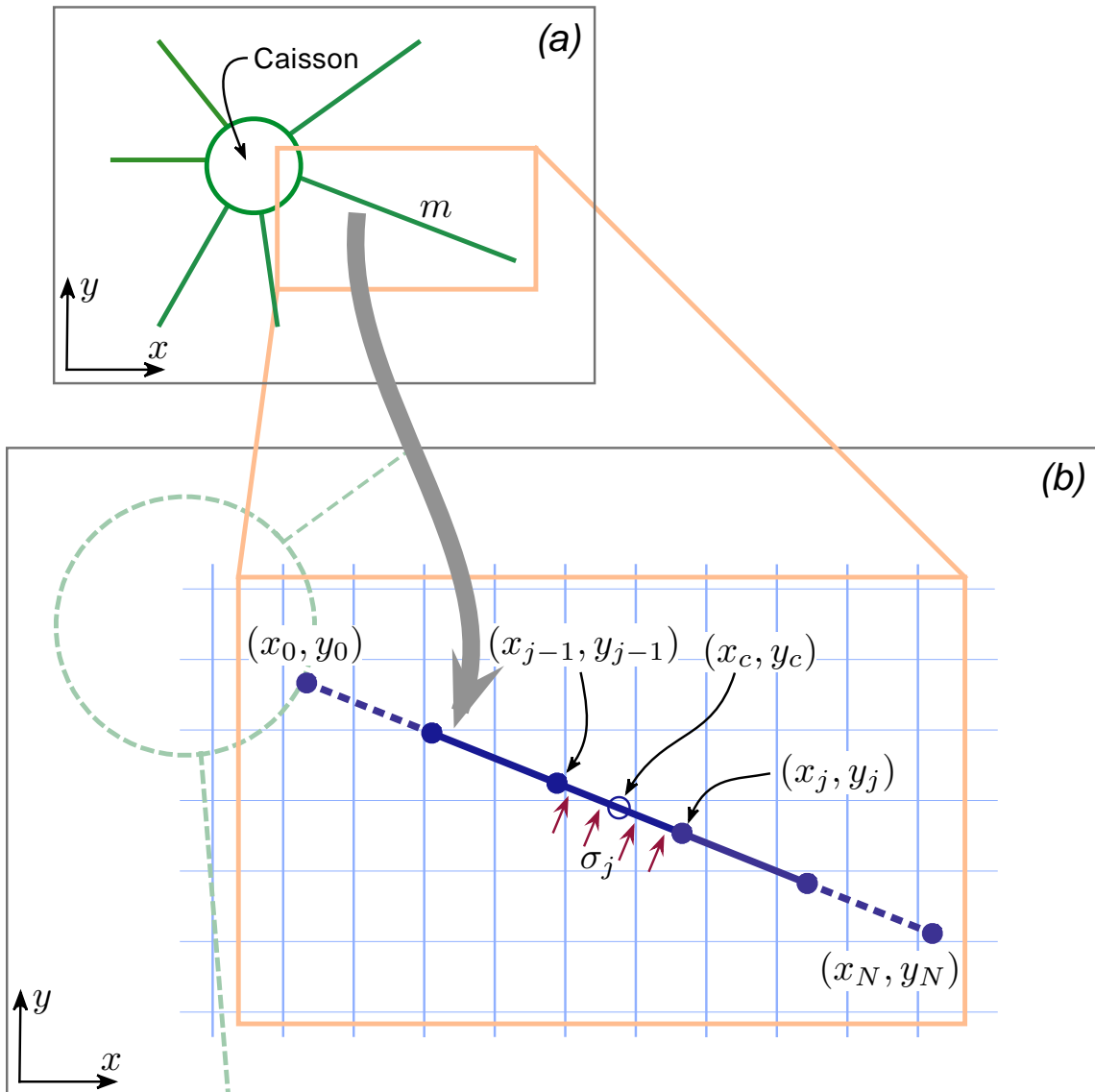


Figure 43: (a) Plan view of a collector well with six laterals. (b) Detail of a lateral m , divided into segments; each segment j may have a different sink density σ_j .

defined as the amount of water entering the lateral per unit length, is not necessarily constant along the lateral. This arises due to interference effects and the geometry of the lateral relative to other features in the model. For clarity, the illustrated case uses five segments to represent a lateral. In practice, ten or more segments should be used to represent variations in the sink density along the length of the lateral. Each segment $j = 1 \dots N_m$ has length L_j , width w_j , screen radius r_j , and extends from (x_{j-1}, y_{j-1}) to (x_j, y_j) . A collocation point is assigned at the center of the segment (x_c, y_c) . As shown below, the value for w_j may be selected arbitrarily. For segment j , the sink density is given as

$$\sigma_j = \frac{w_j}{c_j}(h_a - h_j) \quad (10)$$

where h_a is the (*a priori* unknown) Dupuit-Forchheimer head in the aquifer at (x_c, y_c) ; h_j is the head inside the lateral at the center of the segment; and c_j is a resistance parameter. In general, the head inside the lateral may change along its length in order to account for head losses due to pipe friction. Bakker et al. (2005) used a Moody friction factor to include pipe friction in the 3D TimML code. Although this offers a complete simulation of well performance, it is unnecessary for design purposes. Thus, for this analysis it is assumed that the head is constant along the lateral, and equal to the head in the caisson.

As shown in (10), the resistance c_j relates the flow rate into the segment to the difference between the head inside the lateral and the vertically-averaged head in the aquifer (Dupuit assumption) at the center of the segment. This may be done with any head-dependent flux boundary condition; for pumping wells a drain is the most convenient.

The availability of an appropriate formula for c_j makes it possible to approximate the effects of partial penetration within a 2D model. In some cases, collector well laterals are installed such that they extend beneath nearby surface waters, and in such cases the resistance factor should account for this. Haitjema offers expressions for both cases. For a lateral that does not lie beneath surface waters, the lateral resistance is given as

$$c_j = -\frac{w_j}{2\pi\bar{K}} \ln \left\{ 4 \sin \left(\frac{\pi r_j}{2H} \right) \sin \left(\pi \frac{h + r_j/2}{H} \right) \right\} \quad (11)$$

where H is the saturated thickness of the aquifer at $z = z_c$; h is the elevation of the centerline of the lateral above the aquifer base; and \bar{K} is the scaled aquifer hydraulic conductivity $\bar{K} = \sqrt{K_h K_v}$, where K_h and K_v are the horizontal and vertical hydraulic conductivity, respectively.

For a lateral that lies beneath surface waters, two resistances must be accounted for, first the resistance of the stream bed itself, and second the equivalent Dupuit resistance due to converging flow at the lateral beneath the streambed. The resistance of the stream bed is computed as $c_b = \delta/k_s$, where δ is the thickness and k_s is the vertical hydraulic conductivity of the streambed sediments, respectively. It is noted that c_b is the reciprocal of the MODFLOW “leakance” for inundated cells

modeled using the river (RIV) package. The equivalent Dupuit resistance for a lateral segment is

$$c_j = c_2 - \frac{\lambda w}{2T} \quad (12)$$

where λ is the representative leakage length \sqrt{Tc} . The value c_2 is given by

$$c_2 = \frac{w}{\bar{K}} \sum_{n=0}^{\infty} \left[\frac{1}{\alpha_n} \frac{\cos(\alpha_n(h/H))}{1 + \varepsilon/(\alpha_n^2 + \varepsilon^2)} \cos\left(\alpha_n \frac{h + r_w}{H}\right) \right] \quad (13)$$

where ε is defined as

$$\varepsilon = \frac{H}{\bar{K}c_b} \quad (14)$$

and α_n are the roots of

$$\alpha \tan \alpha = \varepsilon \quad (15)$$

It is noted that the width parameter w_j in (11) and (13) is canceled algebraically in the calculation of the sink density (10). Thus, any non-zero value may be used; by convention $w_j = 1$.

It is instructive to observe that c_j is primarily a function of the location of the lateral in the vertical section and the radius of the lateral. This is not surprising; the objective is to represent the effects of vertically converging flow. It is also noted for a particular lateral radius r_w , the choice of the lateral elevation will affect the resulting resistance (see Figure 44). The resistance due to converging flow is smallest at the center of the aquifer, and increases as the lateral is placed closer to the aquifer top or bottom. This behavior results from interactions with no-flow conditions at the top and bottom of the saturated thickness. While it is intuitive that the most hydraulically desirable location is at the center of the aquifer, raising the lateral elevation might limit the well's yield because it reduces the available operating drawdown (Moore et al., 2011). Field conditions also often require that the laterals be installed at an elevation that is less desirable.

The above formulations for c_j are only strictly valid for single layer Dupuit models, and assumes that the aquifer is of infinite extent, the lateral arm is infinitely long, regional flow is normal to the arm, and that no other features within $1.5H$ cause vertical flow. However, they have been shown to be accurate when used in AEM models in the manner described in this paper (see Haitjema et al., 2010). It is a useful approximation for evaluating drain conductances.

Finite-difference implementation

As previously discussed, the MODFLOW MNW package may be used to simulate horizontal wells or collector wells, however there is currently no guidance about how the entry resistance of the lateral screens should be computed. In the MNW package, a collector well would be configured

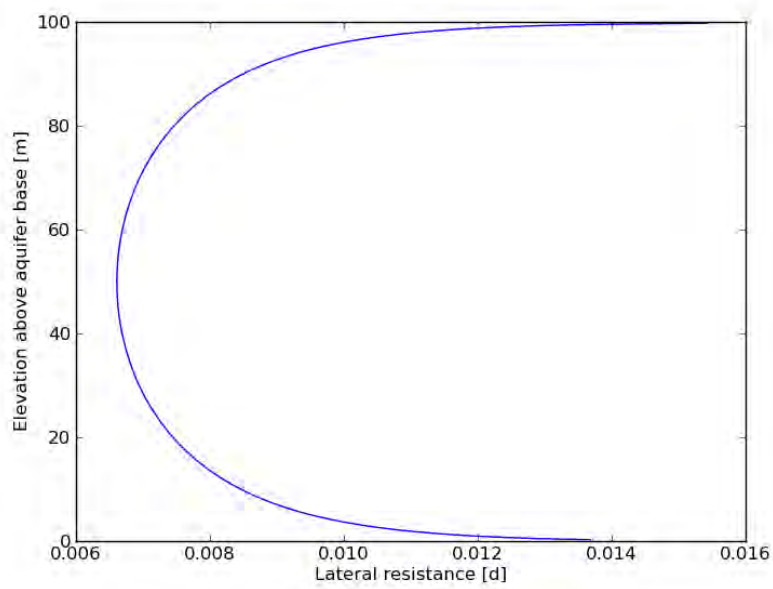


Figure 44: Resistance c [d] as a function of the elevation of a lateral with radius $r_w = 0.5$ m in an aquifer of thickness 100 m, where $\bar{K} = 100$ m/d.

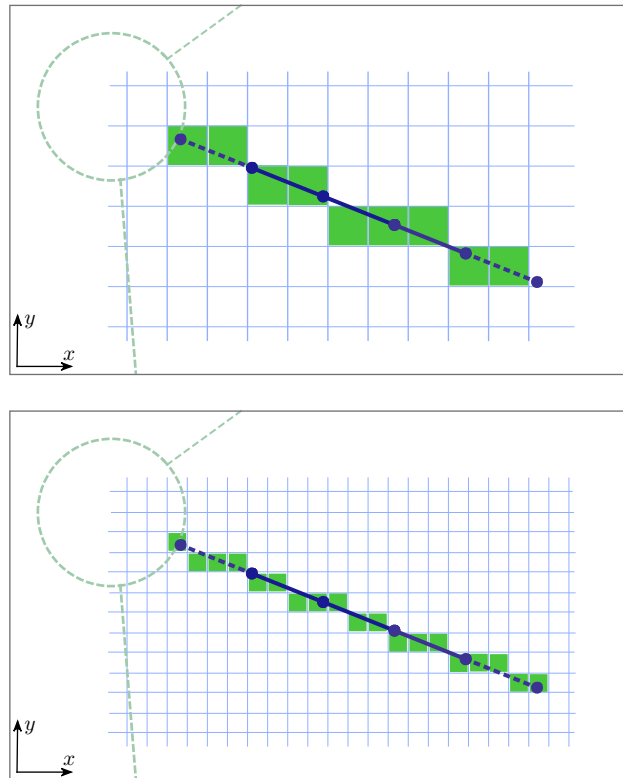


Figure 45: Selecting cells for a coarse representation (top) and a finer resolution (bottom) of a collector well lateral using the MODFLOW MNW package. Note that the aquifer would require detailed vertical discretization, with the cells all lying within the layer that contains the lateral.

by selecting a collection of small cells that approximate the geometry of each lateral, as shown in Figure 45. In practice, small cells on the order of 1 m might be required to achieve suitable accuracy in the geometry of the well. Furthermore, the model would require a substantial degree of vertical discretization, with similarly small layer thicknesses.

For the purpose of estimating the yield of horizontal well screens given the head inside the lateral, the Haitjema formulation has been demonstrated to be effective in Dupuit models, at least in AEM codes. For a similar implementation in MODFLOW, it is necessary to determine how to select the appropriate cells and what their sizes should be. It is possible to implement the same organization of the AEM collector well model discussed above in MODFLOW, however an interpolation scheme is necessary. Figure 46 illustrates the procedure. Similarly as in the AEM formulation, the lateral is divided into a series of segments. In the AEM code, each segment was a single line sink. In the MODFLOW formulation, each segment is modeled using a collection of drains, using the MODFLOW DRN package. The formulation of the drain conductances follows.

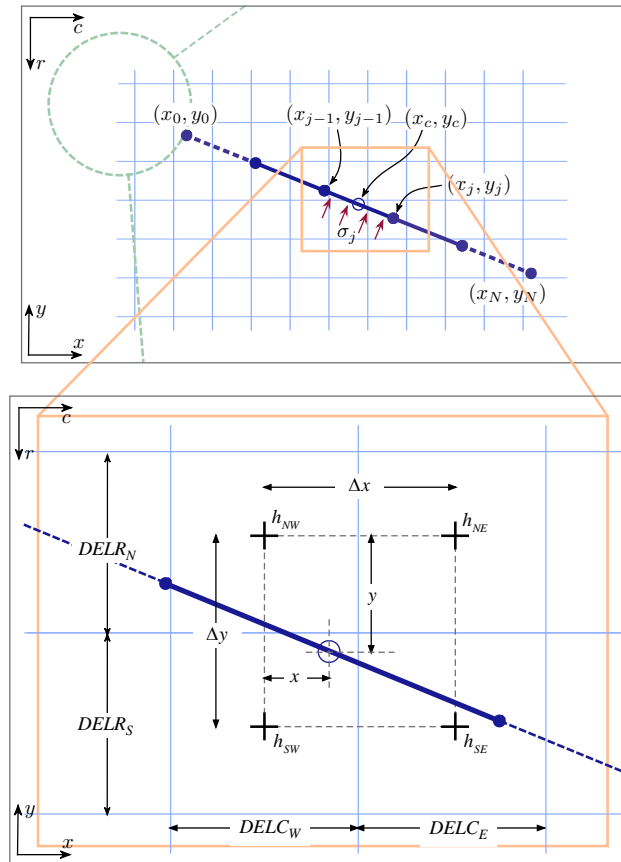


Figure 46: Calculating drain conductances for the collector well model.

The flow rate into segment j is computed according to (10), based on the head at the center of the segment. Recalling that the length of segment j is L_j and choosing $w_j = 1$, the flow rate into the segment is $L_j\sigma_j$, or

$$Q_j = \frac{L_j}{c_j}(h_a - h_j) \quad (16)$$

where h_a is the Dupuit-Forchheimer head in the aquifer at the center of the segment.

In general, the center of segment j is located within a rectangular region bounded by the centers of four neighboring cells. The cells are located in rows N and M and columns W and E , and here are labeled NW , NE , SW , and SE . The *a priori* unknown heads at the four cell centers are h_{NW} , h_{NE} , h_{SW} , and h_{SE} . The center of the segment lies at a distance x east of the column center of cells NW and SW , and at a distance y south of the row center of cells NW and NE . The column widths for columns W and E are $DEL C_W$ and $DEL C_E$, and the row heights for rows N and S are $DEL R_N$ and $DEL R_S$, respectively. Using a bi-linear interpolation scheme, the modeled head at the center of the lateral is

$$h_a = (1 - u)(1 - v)h_{NW} + u(1 - v)h_{NE} + (1 - u)v h_{SW} + uv h_{SE} \quad (17)$$

where

$$u = \frac{x}{\Delta x} \quad (18)$$

and

$$v = \frac{y}{\Delta y} \quad (19)$$

where $\Delta x = \frac{1}{2}(DEL C_W + DEL C_E)$ and $\Delta y = \frac{1}{2}(DEL R_N + DEL R_S)$. Combining (16) and (17), the rate of groundwater flow into the segment is

$$Q_j = COND_{NW}(h_{NW} - h_j) + COND_{NE}(h_{NE} - h_j) + COND_{SW}(h_{SW} - h_j) + COND_{SE}(h_{SE} - h_j) \quad (20)$$

where

$$\begin{aligned} COND_{NW} &= \frac{L_j}{c_j}(1 - u)(1 - v) \\ COND_{NE} &= \frac{L_j}{c_j}u(1 - v) \\ COND_{SW} &= \frac{L_j}{c_j}(1 - u)v \\ COND_{SE} &= \frac{L_j}{c_j}uv \end{aligned} \quad (21)$$

Each term in expression (20) is recognizable as the flow rate into a drain cell using the MODFLOW DRN package with drain conductances calculated as shown in (21). DRN entries are made in cells *NW*, *NE*, *SW*, and *SE*, for all non-zero drain conductance values. The model was implemented and tested as described below.

Laterals that lie beneath surface waters

In the validation example, it was not necessary to include the possibility that a lateral would lie beneath an inundated cell. It was necessary to modify the collector well preprocessor described above to handle this eventuality. As discussed above, Haitjema (2005) offers an expression for the lateral resistance for a segment that beneath a surface water body. That conductance requires information about the geometry of the lateral screen and the entry resistance of the overlying surface water body. In a MODFLOW model, the interaction between surface waters and groundwater is simulated using the RIV (river) package. Because many collector wells are installed with laterals that extend beneath nearby surface waters, the collector well preprocessor was modified to include this eventuality. The RIV input file is read by the preprocessor. For each lateral segment, it is determined whether the center of the segment lies in a MODFLOW cell that contains a RIV entry. After McDonald and Harbaugh (xxxx), the RIV cell conductance for an inundated cell can be computed as

$$COND = \frac{K_V}{D} \times DELR \times DELC \quad (22)$$

where K_V is the vertical hydraulic conductivity of the streambed sediments, D is the thickness of the sediments, and $DELR$ and $DELC$ are the row and column dimensions of the cell, respectively. Noting that the resistance of the streambed sediments in (13) is given as $c_s = D/K_V$, the streambed resistance is computed from the RIV conductance,

$$c_s = \frac{DELR \times DELC}{COND} \quad (23)$$

using this value of c_s , the lateral resistance is computed using (13).

Implementation and Validation

The collector well formulation was implemented using a new preprocessor code. The preprocessor requires three MODFLOW input files: (1) the discretization (DIS) input file; (2) the layer-property flow (LPF) package input¹; and (3) the river (RIV) package input file. Three support files are also

¹It is noted that the preprocessor could be re-coded for use with the block-centered flow (BCF) or hydrologic unit flow (HUF) package.

```

# Four-pointed star configuration
# caisson label caisson-radius
caisson "Star4" 0.0
  # lateral length orientation radius blank elev
  lateral 100.0 0.0 0.5 0.0 40.0
  lateral 100.0 90.0 0.5 0.0 40.0
  lateral 100.0 180.0 0.5 0.0 40.0
  lateral 100.0 270.0 0.5 0.0 40.0

```

Figure 47: Input file for collector wells.

required: an input file that contains a description of the geometry of each collector well design that is to be used in the model; a file that contains georeferencing information for coordinate-to-grid transformation; and a file that contains the selected well design, location, orientation, and design water level in each collector well. The location of the collector well caisson is provided in spatial coordinates, e.g. from a GIS. The coordinate transformation file tells the preprocessor where the lower-left corner of the grid is located and the rotation of the grid, if any. The preprocessor was developed specifically for a project that used a steady model with a single time step to predict yields of wells, depending on their designs; thus the current version of the preprocessor creates a DRN package input file that assumes the well will be active throughout the model simulation. The modeler can easily change the DRN input to select specific time steps that should include the collector well. A sample input file for a collector well is shown in Figure 47.

The collector well formulation was tested by solving a problem containing a collector well in a uniform flow field using a single-layer MODFLOW model and a detailed three-dimensional TimML model. The model domain is illustrated in Figure 48 . The overall model domain is a square, 4000 ft (1219.2 m) on a side. The aquifer is 100 ft (30.48 m) thick, with a horizontal base at $z = 0$, horizontal hydraulic conductivity $K_h = 100 \text{ ft/d}$ (30.48 m/d), and vertical hydraulic conductivity $K_v = 10 \text{ ft/d}$ (3.05 m/d). No-flow conditions are imposed at the north and south edges of the grid, and a uniform flow field is imposed by placing a head-specified condition with water level $h = 200 \text{ ft}$ (60.96 m) at the east edge and a row of wells at the west edge such that an inflow rate $10 \text{ ft}^2/\text{d}$ ($3.048 \text{ m}^3/\text{d}$) per unit length is imposed. This yields an ambient hydraulic gradient of 0.001 declining from west to east in the model. During the validation runs, it was necessary to examine the effect of MODFLOW cell size on the simulated yield; thus the actual flow rate into each well along the west edge of the model was recalculated for each simulation.

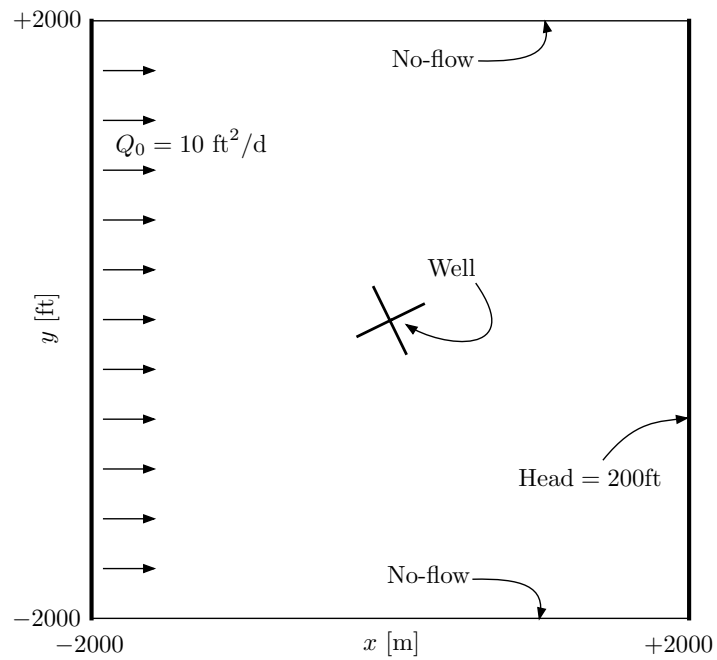


Figure 48: The validation model domain. Ambient groundwater flow is from left to right. The collector well is installed with the orientation of the laterals 30 degrees counterclockwise of the grid orientation.

Table 18: Relationship between the simulated collector well yield and cell size, as compared to the 3D analytic element solution.

Code	MODFLOW		Flow to		Difference
	cell size		collector well		from 3D AEM
	[m]	[ft]	[m ³ /d]	[ft ³ /d]	[%]
TimML	—	—	1371.2	48425	—
MODFLOW	60.96	200	1463.7	51695	+6.7
MODFLOW	30.48	100	1425.7	50347	+4.0
MODFLOW	15.24	50	1397.7	49361	+1.9
MODFLOW	7.62	25	1384.0	48877	+0.9
MODFLOW	3.81	12.5	1377.5	48645	+0.4
MODFLOW	1.91	6.5	1374.1	48528	+0.2

The collector well is configured with laterals 40 ft (12.19 m) above the aquifer base. Four laterals are used, equally spaced at 90° angles about the caisson. For the test problem, the caisson was omitted, with a radius of 0. The lateral screens are assumed to extend 100 ft (30.48 m), beginning at the caisson wall. The center of the caisson is placed at the origin. In all simulations, the centers of the east and west edges are at positions $x = \pm 2000$ ft (± 609.6 m), respectively. At the north and south edges of the model, the active area of the model ranges from $y = -1000$ ft (-609.6 m) to $y = +1000$ ft ($+609.6$ m).

A TimML simulation was executed using comprehensive no-flow, head-specified, and discharge-specified conditions configured to match the flow field described above. The collector well was modeled using the proprietary Bessel collector well model (Bakker, 2005), with 50 segments per lateral. MODFLOW simulations were executed using regular grids with cell sizes of 200 ft (60.96 m), 100 ft (30.48 m), 50 ft (15.24 m), 25 ft (7.62 m), 12.5 ft (3.81 m) and 6.25 ft (1.91 m). For each simulation, the preprocessor was used to generate appropriate drain cells, based on 50 segments per lateral. For each simulation, the operating head in the collector laterals was set to 200 ft (60.96 m).

Table 18 provides the results. The difference between the fully 3D simulation and the single-layer MODFLOW simulation is about 1% for cell sizes smaller than 25 ft (7.62 m), and as the grid cell size is reduced, the predicted yield converges on the AEM solution. It may be surprising that a small error is obtained with such large cells in a single-layer model; at this grid resolution, only 4-5 MODFLOW cells would be needed to simulate an entire lateral. However, a more detailed examination illustrates why this occurs. Haitjema et al. (2001) demonstrated that the error in the flux to a head-dependent-flux boundary in MODFLOW is small if the cell size is on the order of the

representative leakage length λ ,

$$\lambda = \sqrt{Tc} \quad (24)$$

From (11), the test problem yields a value of $\lambda = 16.7$ ft (5.09 m). The cell size is on the order of λ , so small errors are expected.

It is noted that this formulation for the collector well provides a result that differs from the fully 3D AEM solution by about 6.5% when the grid cells are large enough to contain the entire collector. It is likely that this results from two factors. First, the laterals are modeled by many short segments that capture some knowledge of the head differences in the model. Second, the Dupuit potentiometric surface in the vicinity of a collector well tends to be “dish-shaped”, since the laterals spread out the infiltration into the well over a large area. As a result, the bilinear head interpolation scheme provides a fairly accurate approximation of the actual Dupuit head distribution near the well.

Furthermore, this analysis is based on the assumption that the aquifer may be satisfactorily represented in a single layer. Most collector wells are installed in shallow, unconsolidated aquifers. Although the aquifer may well be stratified, with a vertically varying hydraulic conductivity, in most cases the contrast in hydraulic conductivity would be assumed to be small, and a single-layer model is likely to be adequate.

Conclusions

This work demonstrates that it is possible to predict the yield for radial collector wells, given the operating drawdown in the well, in a 2D MODFLOW model. The effects of converging flow at the lateral are replaced by an appropriate entry resistance, in a manner similar to the 2D analytic element model of Haitjema et al. (2010). Yield estimates in the MODFLOW model compare very closely to those obtained from a detailed, 3D analytic element model.

The methodology used to implement the collector well laterals in MODFLOW relies on an innovative strategy: instead of simply dividing the laterals into cells that approximate the lateral geometry, the lateral is divided into segments. Each segment is represented by up to four neighboring drain cells, using the DRN package. The conductance for each drain is derived from the geometry of the segment in the vertical section, and the proximity of the center of the segment to the centers of the neighboring cells, using a bi-linear interpolation scheme. The author is unaware of another MODFLOW package that interpolates cell-by-cell heads in this manner. Further research is warranted; a similar approach might be used to represent narrow surface waters that overlie only a small portion of a cell, e.g. small streams. In that case, the conductances for neighboring RIV cells could be similarly computed based on similar analytic approximations for the effects of converging flow and the streambed sediment properties. If properly implemented, this approach might reduce the errors that often arise from up-scaling or down-scaling model cell sizes in MODFLOW.

The solution presented here is appropriate for estimating the yield of collector wells, and may be extended in a similar manner to angled wells, horizontal wells, drains, or galleries. Currently, the collector well model is suitable only for yield estimation, based on an operating water level in the well. In addition, the effects of the well on the regional aquifer system will be properly accounted for. However, the method is suitable for the implementation of discharge-specified wells, including the effects of head losses due to friction within the laterals as flow moves to the caisson. If such a package were implemented, it would be suitable for predicting regional effects of pumping, however the level of discretization is not suitable for accurate simulation of particle trajectories, e.g. using MODPATH. Even so, if a detailed local model were needed, e.g. for a contaminant-transport model, a model constructed using this method would be appropriate as the basis for a detailed, fully 3D model, perhaps using the multi-node well (MNW) package.

Appendix C - Comparison with Kazmann Yield Model

Sixty-three years ago, Kazmann REF investigated the yield of the seven collector wells based on four years of production data collected after the wells had been installed at the INAAP. After review of plant operational records, Kazmann extracted steady-state drawdowns at each collector well caisson due to pumping a single collector well at 10 mgd. Kazmann's data (Table 19), provides drawdown at each caisson caused by any single collector well in the field being pumped at 10 mgd. The values presented in the table are based on a water temperature of 68.5° F.

Kazmann's model can be used to estimate total drawdown at each caisson for any combination of pumping, if the relationship between pumping rate and drawdown is assumed to be linear over the range of pumping rates investigated, and the groundwater flow system behaves linearly. The values of drawdown in the table are simply weighted according to the pumping rate of each well and superimposed for each collector well that is pumping. We made a comparison of the yields predicted by the Predictive Model developed for this study, and Kazmann's linear model for a given drawdown in each caisson; the drawdown varies between wells from about 20-30 ft. The comparison is summarized in Table 20.

This comparison of model results is included for completeness. As many of the operational conditions represented by Kazmann's model are 65-70 years old, it would be unwise to use his results blindly to evaluate aquifer yield. In particular, the conditions of the river bed may have changed since the 1940's, caused by maintenance of the shipping lane along the west side of the river. However, the comparison does indicate that the conditions in the aquifer are similar to those in the 1940's. In particular, the distribution of the total yield between the collector wells compare well, with the highest yields occurring at wells 1, 6, and 7. The difference in computed yields for individual wells range from +1.9 to -1.6 mgd, however, the difference in total well field yield for the given drawdowns is +0.9 mgd – less than a 2% difference in total well field yield.

Table 19: Kazmann's linear model. Drawdown (ft) caused by pumping each collector well individually at 10 mgd.

drawdown at CW -	Collector well being pumped						
	1	2	3	4	5	6	7
1	20.0	5.5	2.0	-	-	-	-
2	6.5	22.0	6.0	2.5	-	-	-
3	3.2	4.3	24.0	5.0	1.5	-	-
4	1.9	2.1	4.3	22.3	2.8	1.1	-
5	-	1.4	2.2	4.3	17.6	2.7	1.7
6	-	-	-	1.8	2.8	14.5	3.4
7	-	-	-	-	1.4	2.4	10.8

Table 20: Comparison of results from the Predictive Model and Kazmann's linear model.

CW	Drawdown in caisson (ft)	Predictive Model yield (mgd)	Kazmann Model yield (mgd)	Difference (mgd)
1	28.3	12.4	11.4	+1.0
2	28.7	8.2	7.5	+0.7
3	27.7	8.1	7.2	+0.9
4	19.6	3.0	4.6	-1.6
5	20.2	3.7	5.2	-1.5
6	24.1	9.4	9.9	-0.5
7	26.5	23.6	21.7	+1.9
Total		68.4	67.5	+0.9

Appendix D - Alternative Analysis

Alternatives

For each alternative, the conceptual layout (Figures 49 to 64) and detailed modeling results (Tables 21 to 36) are presented below. For each scenario, we used PEST in predictive uncertainty mode to find the 95% confidence interval for the theoretical yield of the well field; the theoretical well field yield (i.e., the individual well yields summed over all wells) was minimized and maximized during the uncertainty analysis. For example, the confidence interval for the 10 mgd scenario A is shown in Table 21. Columns 3 through 5 of the table present the theoretical yield for each individual well operated in the scenario, and the total theoretical yield of the well field is presented in the final row of the table. For this scenario, the calibrated or “best-fit” theoretical yield of the well field is 17.9 mgd; the minimum end of the confidence interval is 16.6 mgd and the maximum end is 19.3 mgd. Because the confidence interval is based on the total well field yield, the minimum and maximum values of theoretical yields for each individual well may appear reversed in the table. For example, in Table 21 the values reported in the minimum and maximum columns for CW-1 are 10.8 mgd and 10.3 mgd, respectively. This apparent discrepancy is a result of adjusting parameters that increase or decrease the degree of well interference when maximizing or minimizing the total yield of the well field. The minimum and maximum values reported for each individual well do not represent confidence intervals on the individual well yields, and should not be interpreted that way. Rather, they simply show the behavior of individual wells in the well field when confidence intervals are placed on the total well field yield. For each scenario, we also report the *mechanical capacity* (column 2) and the *design capacity* (column 6) for each well. As discussed previously, the *design capacity* is the smaller of the *mechanical capacity* and the *theoretical yield*.

Finally, in the last column of each table we report a *sustainable capacity*. When large volumes of water are pumped in the near vicinity of the river, the potentiometric head beneath the river sediments may fall to a level that is sufficient to cause plugging or compaction of the bed sediments, reducing the hydraulic conductivity and induced recharge rate, and thus reducing the yield of wells. This has been studied across the river and southwest of the Charlestown site at a collector well operated by Louisville (KY) Water Works and at other sites. Hubbs et al. (2006) indicates that the reduction in yield due to sediment plugging can be expected to be in the range of 65-80% when overpumping the aquifer. We have limited the possibility of overpumping by imposing the operational constraint on each collector well of a minimum head in the caisson of 399.5 ft msl. As discussed previously, this minimum elevation represents a 20 ft drawdown in the aquifer and is approximately 10-15 ft above the streambed. This prevents the possibility of the heads beneath the river being drawn down below the elevation of the streambed. Further, each of the existing collector wells in the State Park were historically pumped to levels significantly below 399.5 ft. Both the

Table 21: Results of modeling for 10 mgd, alternative A. All values are in millions of gallons per day (mgd).

Well CW-	Mechanical capacity	Theoretical yield			Design capacity	Sustainable capacity
		Minimum	Best-fit	Maximum		
1	4.9	10.8	10.5	10.3	4.9	4.9
2	4.9	5.7	7.4	9.0	4.9	4.9
3	–	–	–	–	–	–
4	–	–	–	–	–	–
5	–	–	–	–	–	–
6	–	–	–	–	–	–
7	–	–	–	–	–	–
8	–	–	–	–	–	–
9	–	–	–	–	–	–
Total	9.8	16.6	17.9	19.3	9.8	9.8

operational constraint and the historical record at the site provide confidence that the effects of plugging and compaction of the streambed sediments can be minimized. For our purposes, we assume that there is the potential for plugging that would lead to a reduction of 25% in the capacity of the largest wells at the Park – the wells for which the theoretical yield is greater than 10 mgd. Therefore, we define the *sustainable capacity* to be an adjusted design capacity based on a 25% reduction in theoretical yield for collector wells 1, 6, 7, 8, and 9.

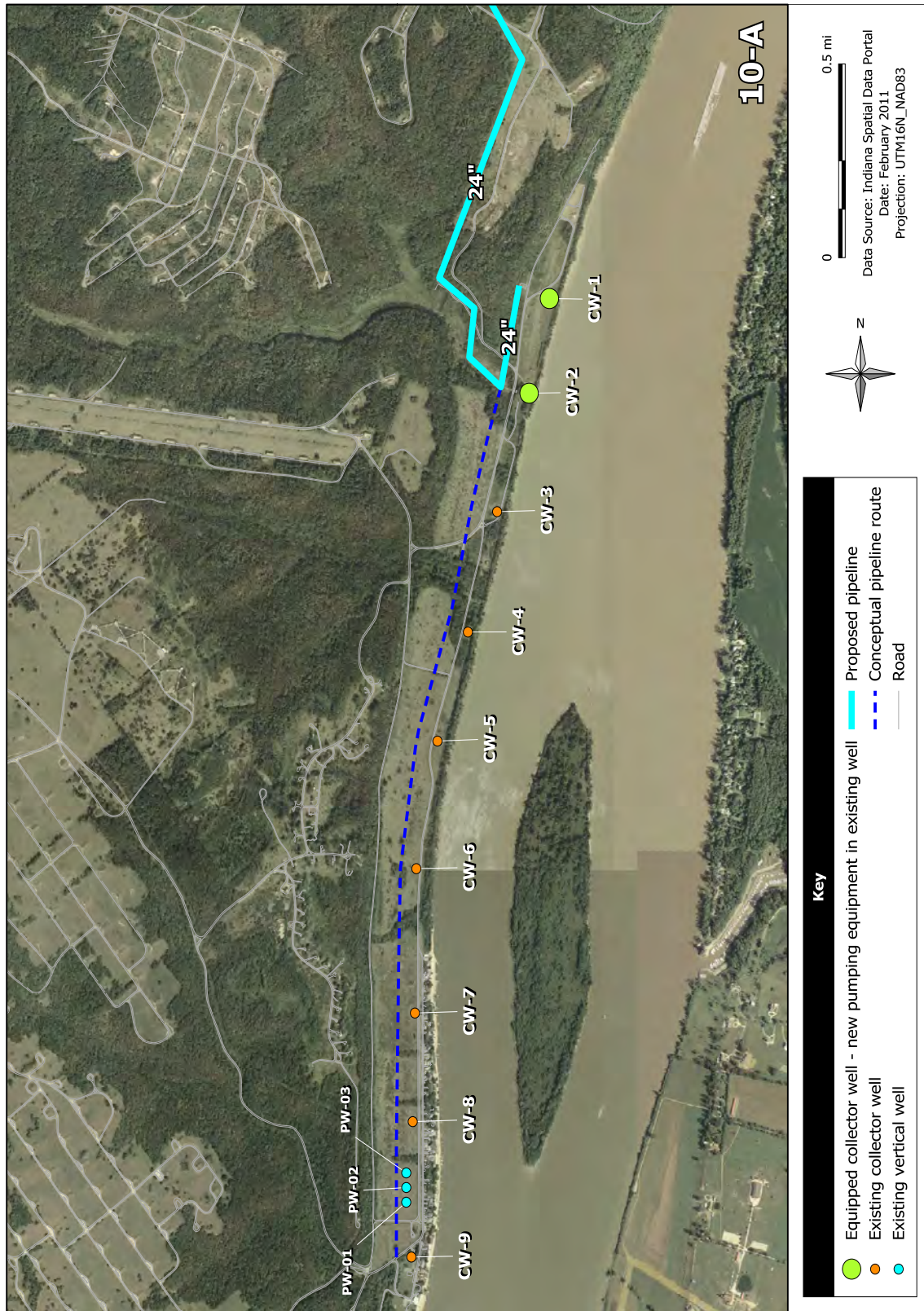


Figure 49: Conceptual layout of Alternative 10-A

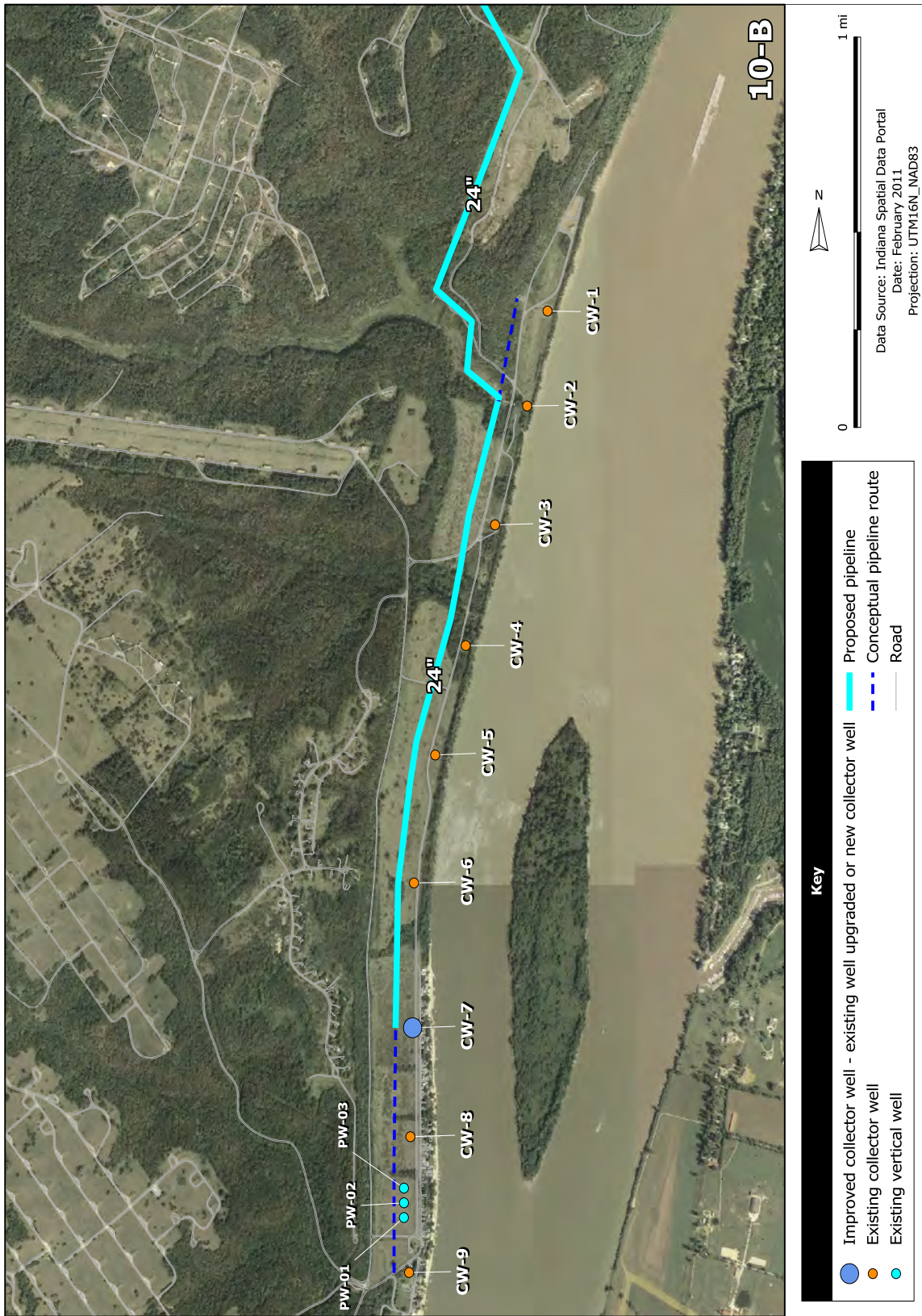


Figure 50: Conceptual layout of Alternative 10-B

Table 22: Results of modeling for 10 mgd, scenario B. All values are in millions of gallons per day (mgd).

Well CW-	Mechanical capacity	Theoretical yield			Design capacity	Sustainable capacity
		Minimum	Best-fit	Maximum		
1	–	–	–	–	–	–
2	–	–	–	–	–	–
3	–	–	–	–	–	–
4	–	–	–	–	–	–
5	–	–	–	–	–	–
6	–	–	–	–	–	–
7	15.0	18.7	22.1	27.1	15.0	15.0
8	–	–	–	–	–	–
9	–	–	–	–	–	–
Total	15.0	18.7	22.1	27.1	15.0	15.0

Table 23: Results of modeling for 20 mgd, scenario A. All values are in millions of gallons per day (mgd).

Well CW-	Mechanical capacity	Theoretical yield			Design capacity	Sustainable capacity
		Minimum	Best-fit	Maximum		
1	4.9	11.2	10.2	9.1	4.9	4.9
2	4.9	5.7	6.6	8.1	4.9	4.9
3	5.6	5.7	6.8	8.8	5.6	5.6
4	–	–	–	–	–	–
5	5.0	4.6	4.6	5.1	4.6	4.6
6	–	–	–	–	–	–
7	–	–	–	–	–	–
8	–	–	–	–	–	–
9	–	–	–	–	–	–
Total	20.4	27.2	28.2	31.1	20.0	20.0

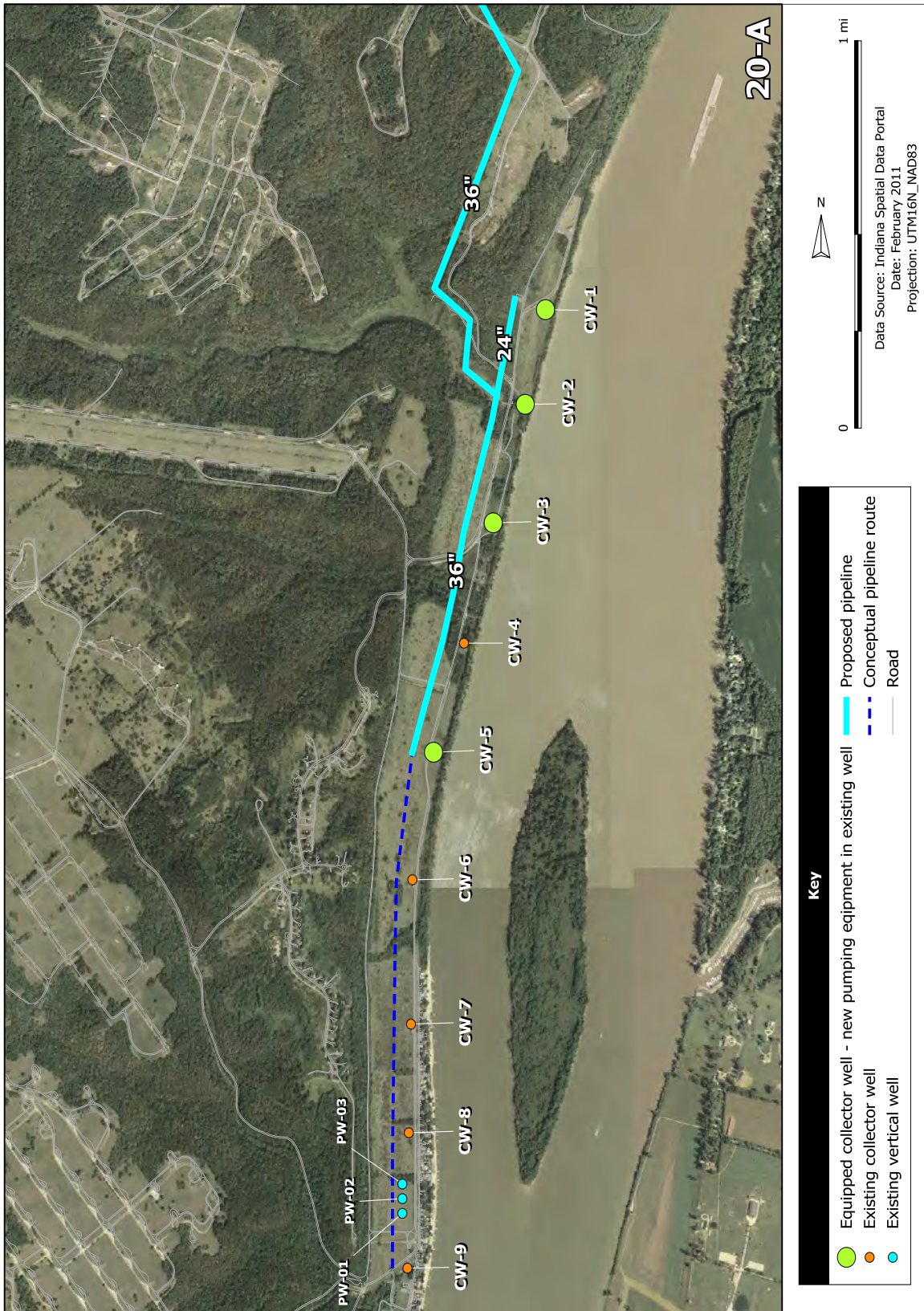


Figure 51: Conceptual layout of Alternative 20-A

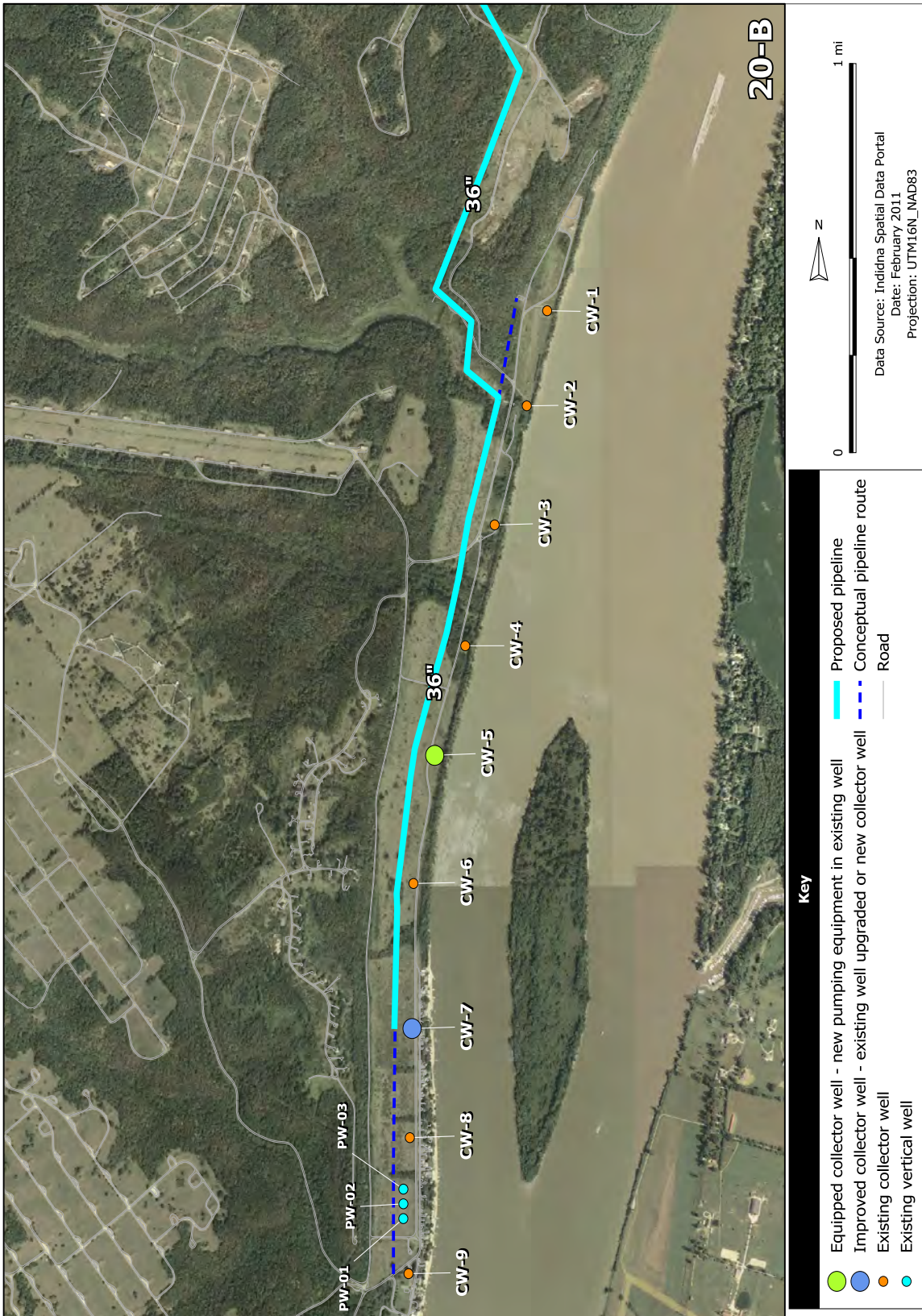


Figure 52: Conceptual layout of Alternative 20-B

Table 24: Results of modeling for 20 mgd, scenario B. All values are in millions of gallons per day (mgd).

Well CW-	Mechanical capacity	Theoretical yield			Design capacity	Sustainable capacity
		Minimum	Best-fit	Maximum		
1	–	–	–	–	–	–
2	–	–	–	–	–	–
3	–	–	–	–	–	–
4	–	–	–	–	–	–
5	5.8	4.5	4.7	5.2	4.7	4.7
6	–	–	–	–	–	–
7	15.0	18.6	22.1	27.1	15.0	15.0
8	–	–	–	–	–	–
9	–	–	–	–	–	–
Total	20.8	23.1	26.8	32.3	19.7	19.7

Table 25: Results of modeling for 30 mgd, scenario A. All values are in millions of gallons per day (mgd).

Well CW-	Mechanical capacity	Theoretical yield			Design capacity	Sustainable capacity
		Minimum	Best-fit	Maximum		
1	15.0	10.7	10.2	10.2	10.2	7.7
2	4.9	6.2	6.5	6.6	4.9	4.9
3	5.6	6.1	6.5	6.6	5.6	5.6
4	5.0	3.6	3.6	3.6	3.6	3.6
5	5.8	4.1	4.1	3.8	4.1	4.1
6	4.5	3.0	9.1	14.8	4.5	4.5
7	–	–	–	–	–	–
8	–	–	–	–	–	–
9	–	–	–	–	–	–
Total	40.8	33.7	40.0	45.6	32.9	30.4

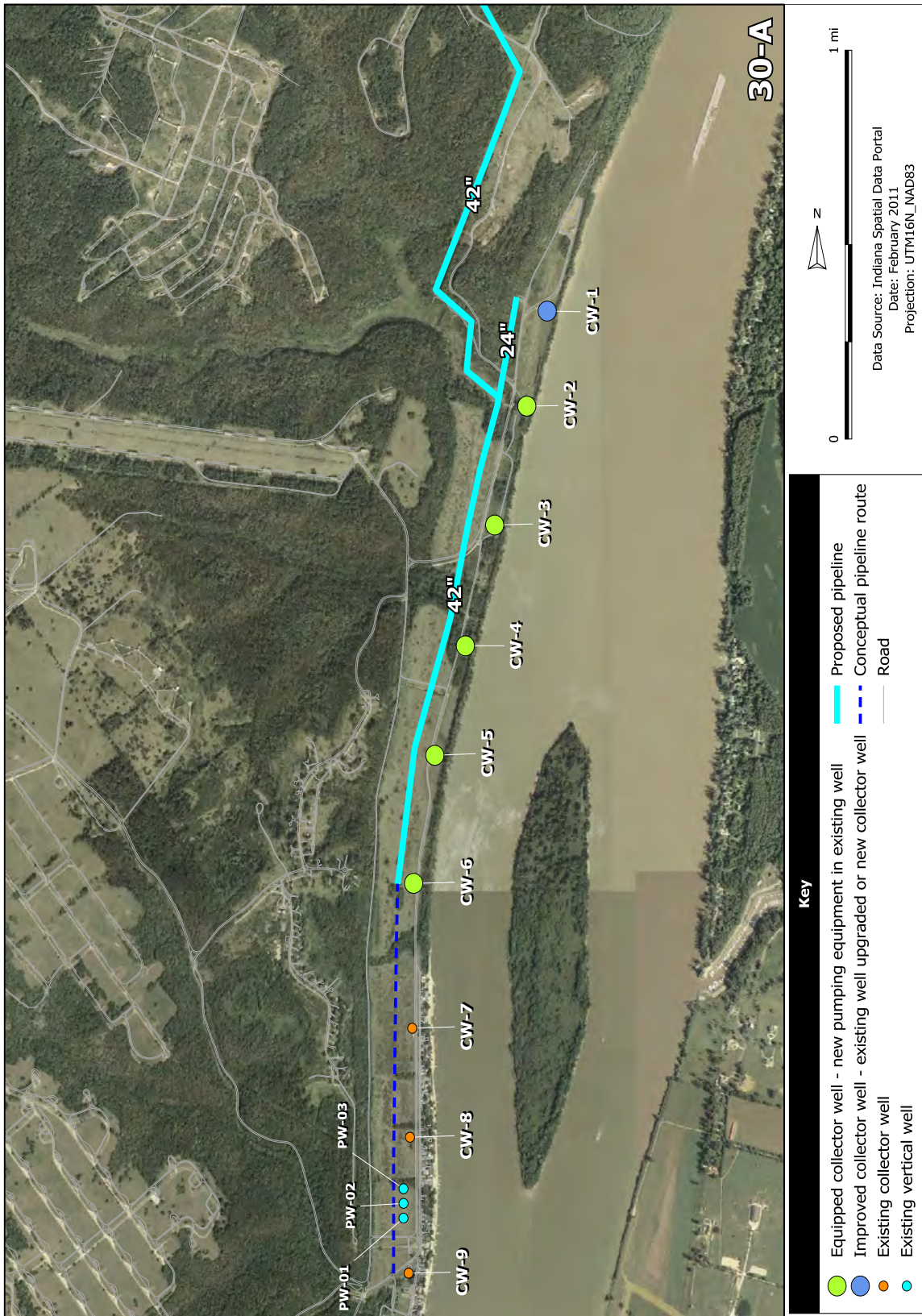


Figure 53: Conceptual layout of Alternative 30-A

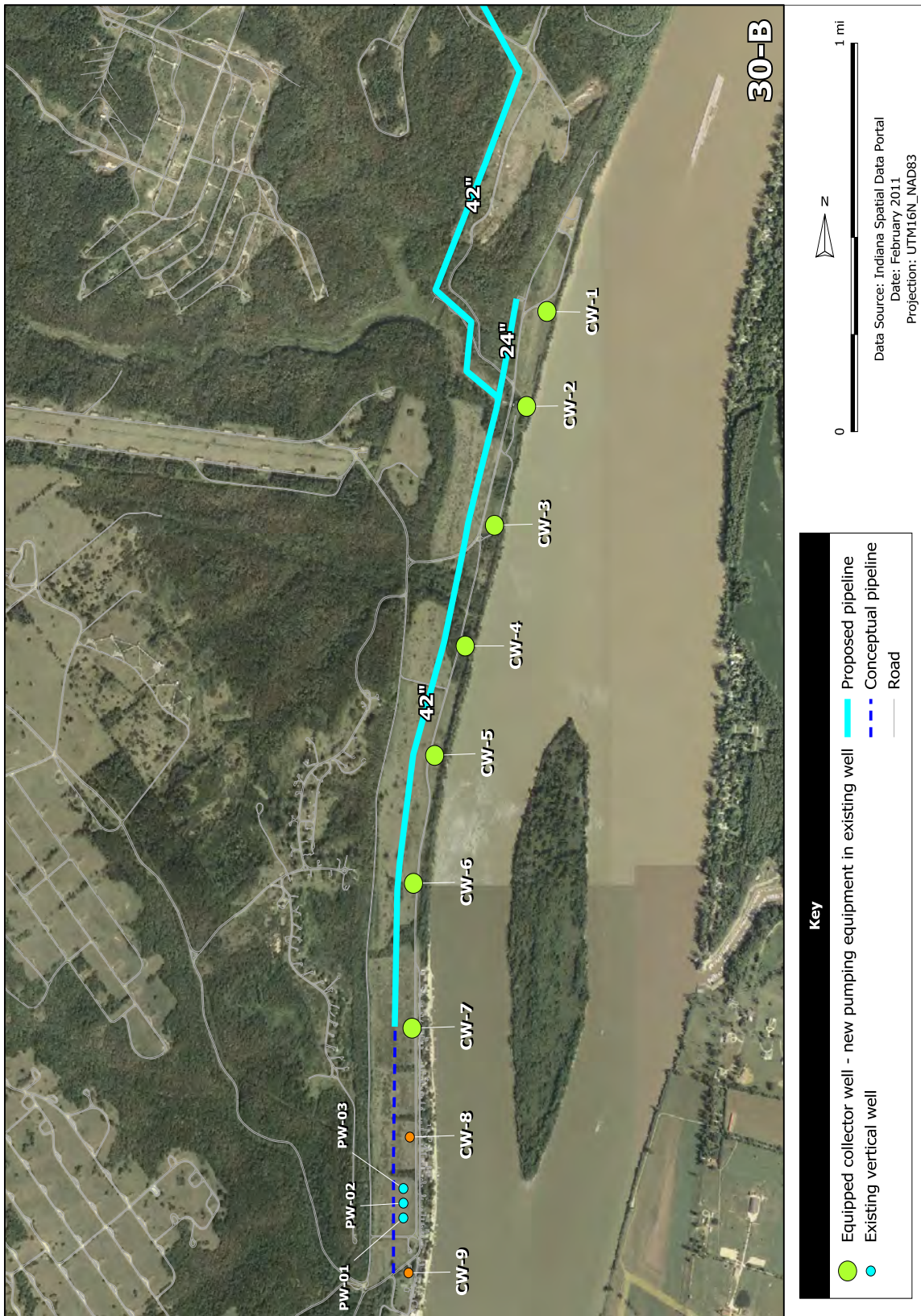


Figure 54: Conceptual layout of Alternative 30-B

Table 26: Results of modeling for 30 mgd, scenario B. All values are in millions of gallons per day (mgd).

Well CW-	Mechanical capacity	Theoretical yield			Design capacity	Sustainable capacity
		Minimum	Best-fit	Maximum		
1	4.9	10.4	10.2	10.2	4.9	4.9
2	4.9	6.4	6.5	6.6	4.9	4.9
3	5.6	6.4	6.5	6.6	5.6	5.6
4	5.0	3.6	3.6	3.6	3.6	3.6
5	5.8	4.1	4.0	3.8	4.0	4.0
6	4.5	3.5	8.5	13.2	4.5	4.5
7	5.1	19.1	19.9	19.9	5.1	5.1
8	–	–	–	–	–	–
9	–	–	–	–	–	–
Total	35.7	53.5	59.3	63.9	32.6	32.6

Table 27: Results of modeling for 30 mgd, scenario C. All values are in millions of gallons per day (mgd).

Well CW-	Mechanical capacity	Theoretical yield			Design capacity	Sustainable capacity
		Minimum	Best-fit	Maximum		
1	–	–	–	–	–	–
2	–	–	–	–	–	–
3	–	–	–	–	–	–
4	–	–	–	–	–	–
5	–	–	–	–	–	–
6	–	–	–	–	–	–
7	15.0	28.6	20.4	32.2	15.0	15.0
8	–	–	–	–	–	–
9	15.0	16.0	30.6	25.8	15.0	15.0
Total	30.0	44.6	51.0	58.0	30.0	30.0

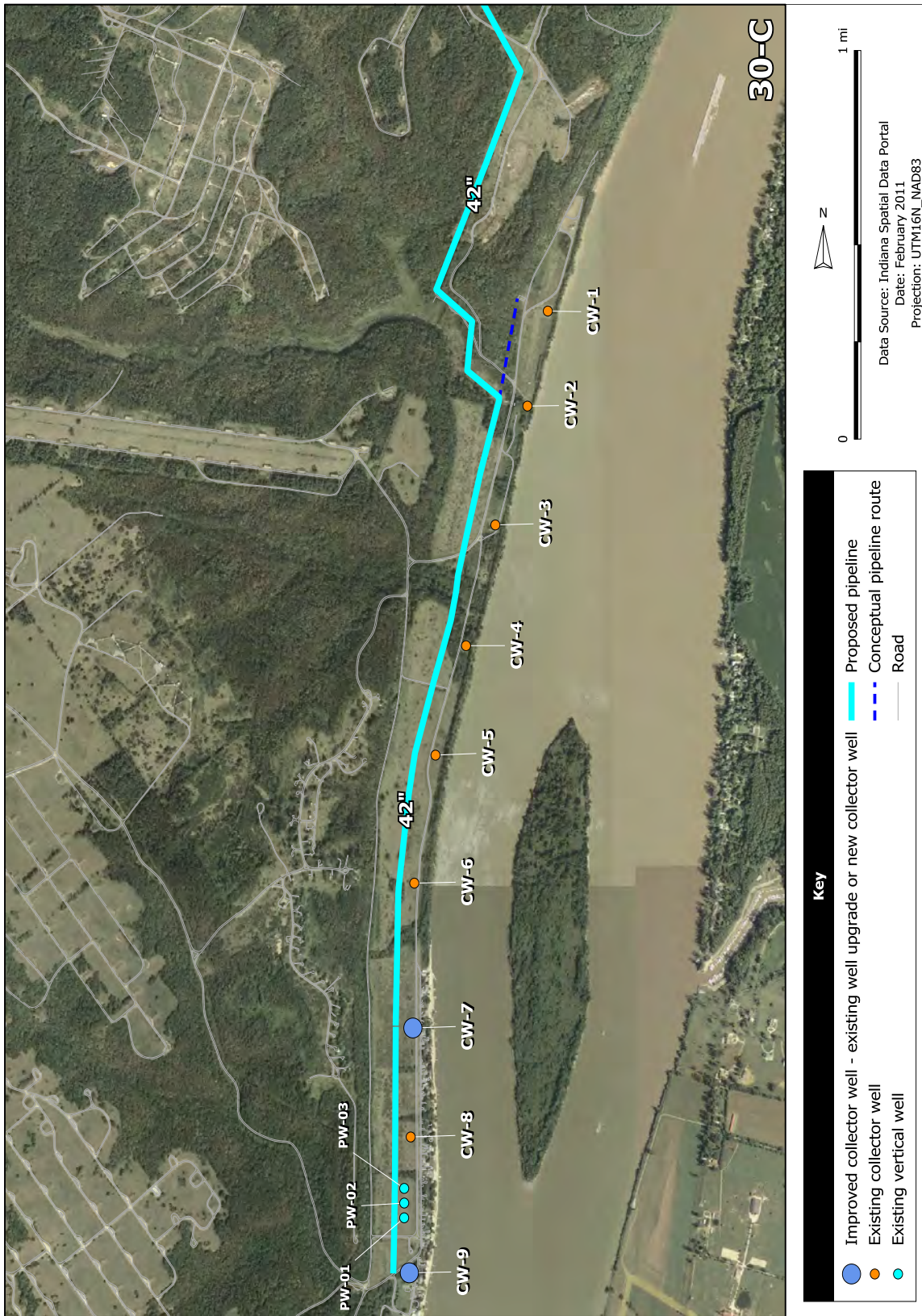


Figure 55: Conceptual layout of Alternative 30-C

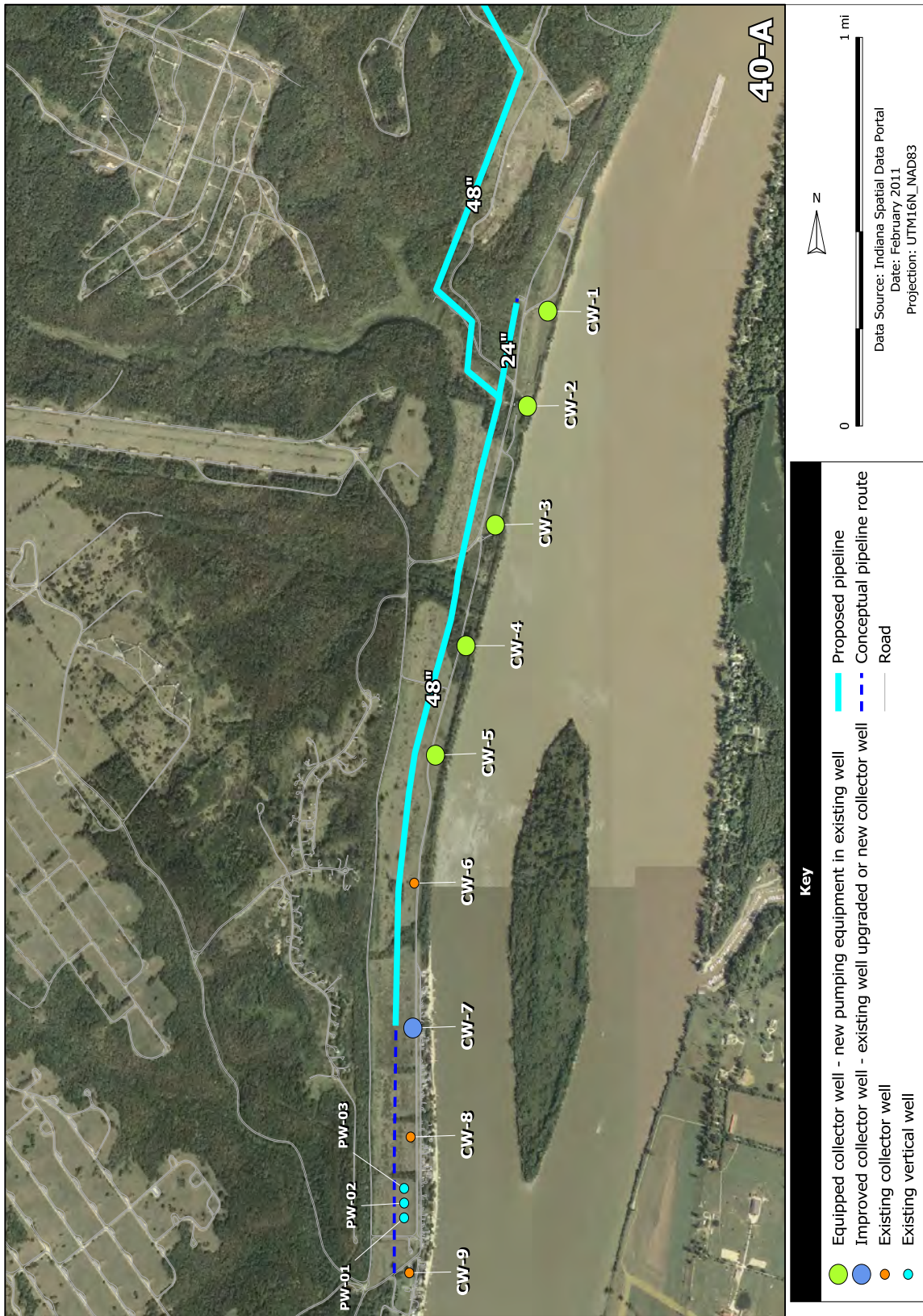


Figure 56: Conceptual layout of Alternative 40-A

Table 28: Results of modeling for 40 mgd, scenario A. All values are in millions of gallons per day (mgd).

Well CW-	Mechanical capacity	Theoretical yield			Design capacity	Sustainable capacity
		Minimum	Best-fit	Maximum		
1	4.9	10.3	10.2	9.7	4.9	4.9
2	4.9	6.5	6.5	7.3	4.9	4.9
3	5.6	6.4	6.5	7.3	5.6	5.6
4	5.0	3.6	3.7	4.0	3.7	3.7
5	5.8	4.3	4.3	4.9	4.3	4.3
6	–	–	–	–	–	–
7	15.0	21.7	22.0	25.8	15.0	15.0
8	–	–	–	–	–	–
9	–	–	–	–	–	–
Total	36.2	52.8	53.2	59.0	38.4	38.4

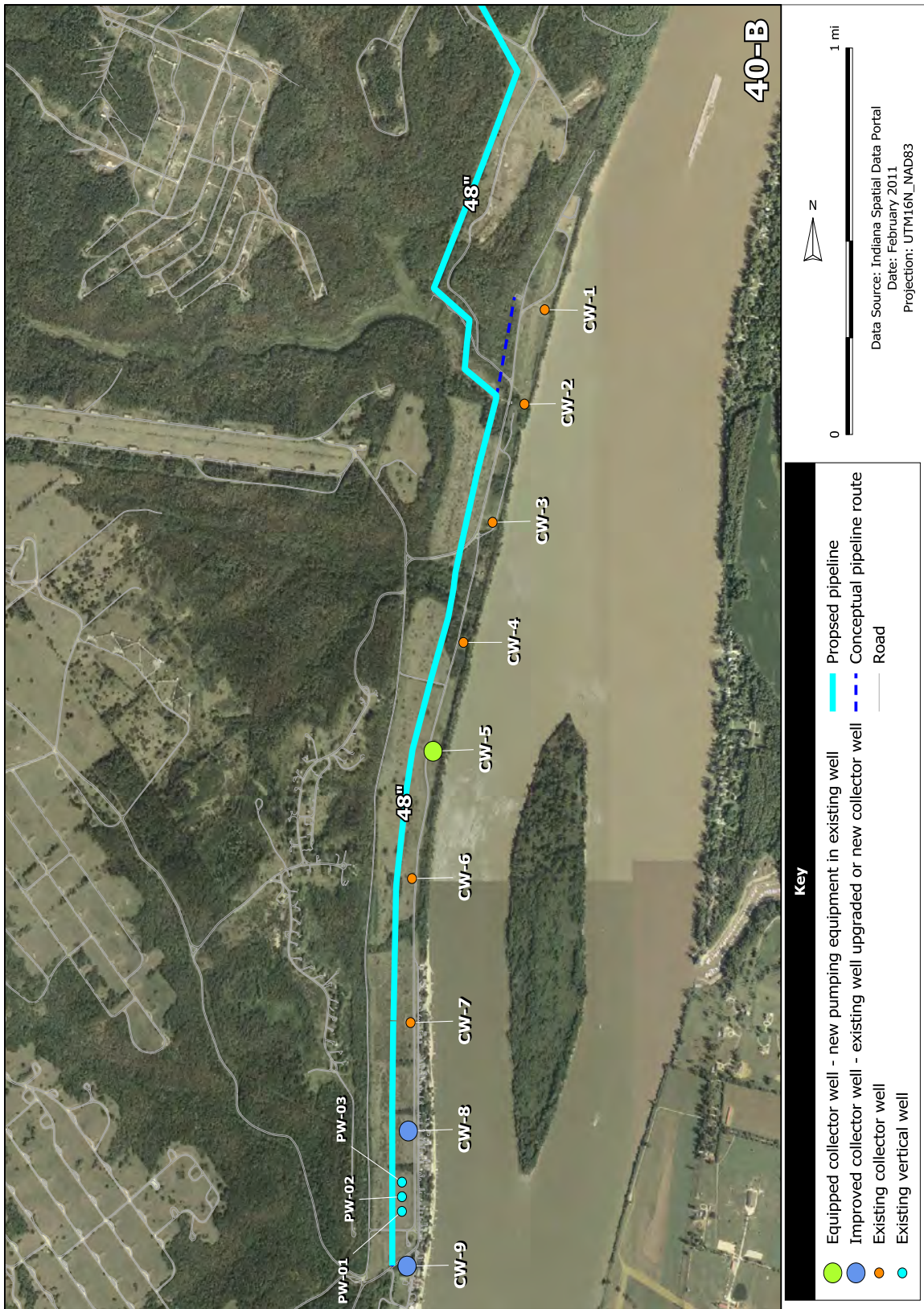


Figure 57: Conceptual layout of Alternative 40-B

Table 29: Results of modeling for 40 mgd, scenario B. All values are in millions of gallons per day (mgd).

Well CW-	Mechanical capacity	Theoretical yield			Design capacity	Sustainable capacity
		Minimum	Best-fit	Maximum		
1	–	–	–	–	–	–
2	–	–	–	–	–	–
3	–	–	–	–	–	–
4	–	–	–	–	–	–
5	5.8	4.6	4.7	4.9	4.7	4.7
6	–	–	–	–	–	–
7	–	–	–	–	–	–
8	15.0	23.3	26.6	33.5	15.0	15.0
9	15.0	24.1	27.1	31.2	15.0	15.0
Total	35.8	52.1	58.4	69.7	34.7	34.7

Table 30: Results of modeling for 50 mgd, scenario A. All values are in millions of gallons per day (mgd).

Well CW-	Mechanical capacity	Theoretical yield			Design capacity	Sustainable capacity
		Minimum	Best-fit	Maximum		
1	15.0	10.4	10.2	10.0	10.2	7.7
2	4.9	6.4	6.5	6.9	4.9	4.9
3	5.6	6.4	6.5	6.8	5.6	5.6
4	5.0	3.6	3.6	4.2	3.6	3.6
5	5.8	4.0	4.0	3.7	4.0	4.0
6	15.0	3.2	10.3	33.8	10.3	7.7
7	15.0	20.2	21.3	22.9	15.0	15.0
8	–	–	–	–	–	–
9	–	–	–	–	–	–
Total	66.3	54.2	62.4	88.3	53.6	48.5

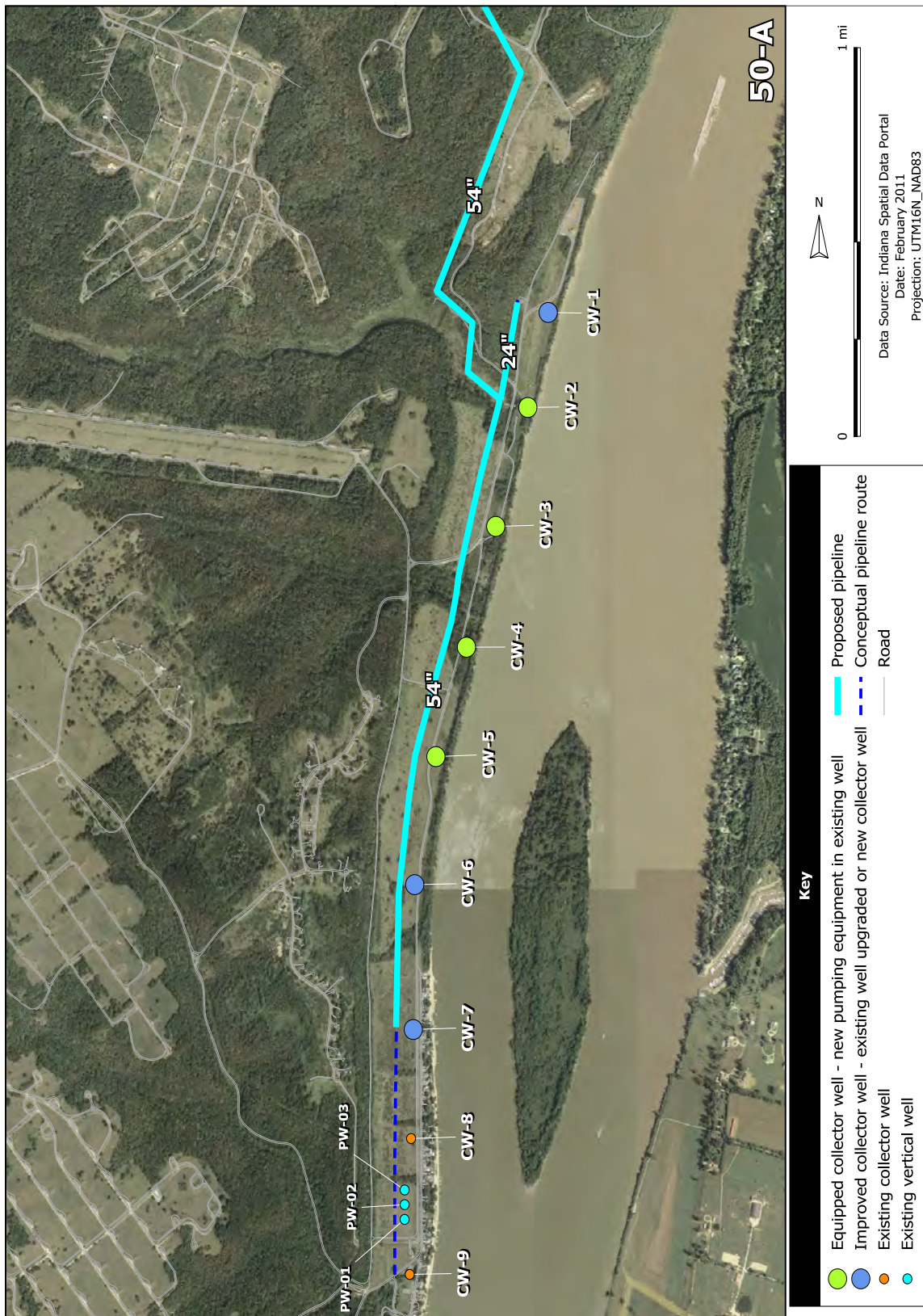


Figure 58: Conceptual layout of Alternative 50-A

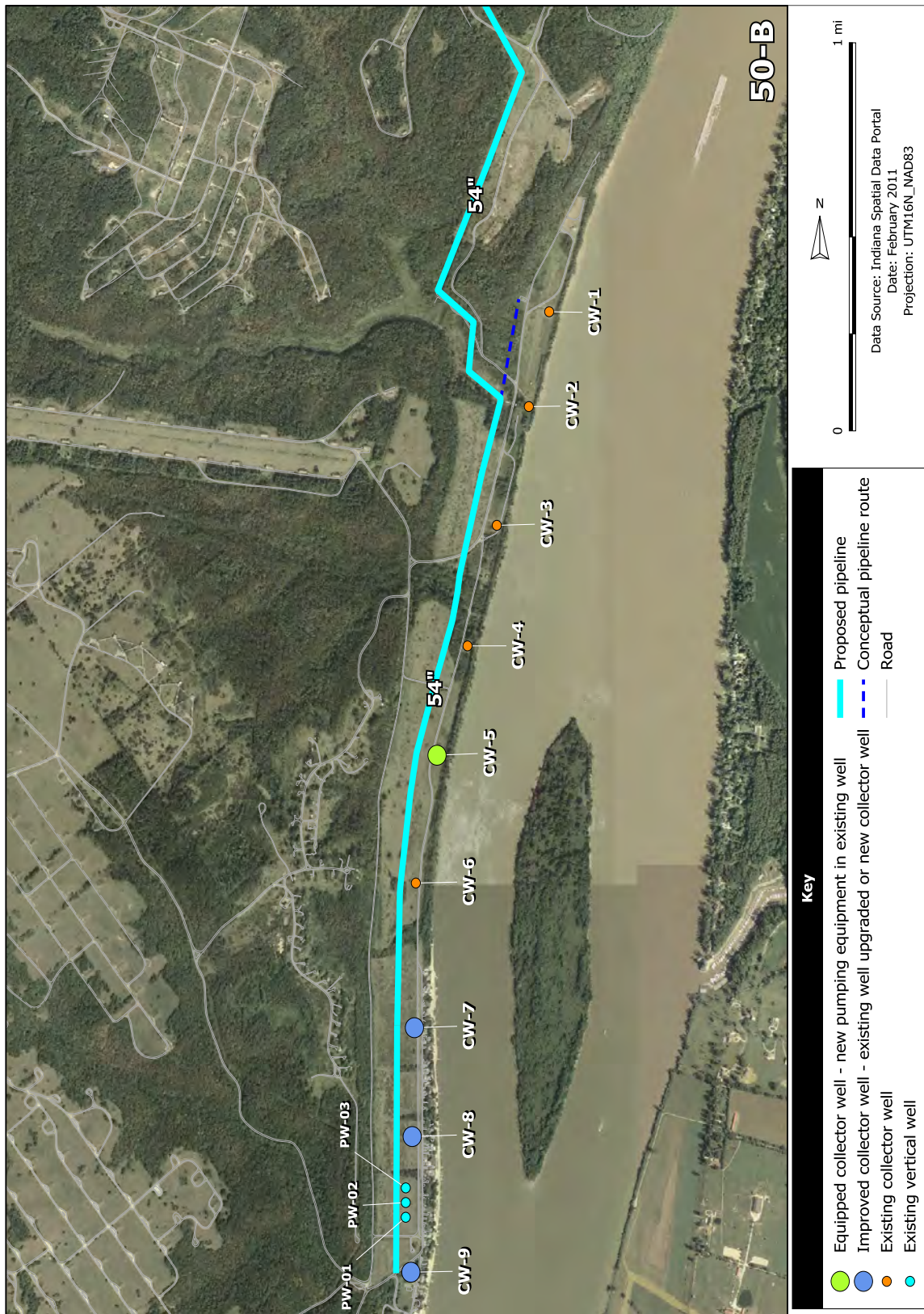


Figure 59: Conceptual layout of Alternative 50-B

Table 31: Results of modeling for 50 mgd, scenario B. All values are in millions of gallons per day (mgd).

Well CW-	Mechanical capacity	Theoretical yield			Design capacity	Sustainable capacity
		Minimum	Best-fit	Maximum		
1	–	–	–	–	–	–
2	–	–	–	–	–	–
3	–	–	–	–	–	–
4	–	–	–	–	–	–
5	5.8	4.6	4.7	4.8	4.7	4.7
6	–	–	–	–	–	–
7	15.0	11.8	15.9	23.8	15.0	11.9
8	15.0	18.8	22.2	31.3	15.0	15.0
9	15.0	24.3	26.4	31.5	15.0	15.0
Total	50.8	59.5	69.2	91.4	49.7	46.6

Table 32: Results of modeling for 50 mgd, scenario C. All values are in millions of gallons per day (mgd).

Well CW-	Mechanical capacity	Theoretical yield			Design capacity	Sustainable capacity
		Minimum	Best-fit	Maximum		
1	–	–	–	–	–	–
2	–	–	–	–	–	–
3	–	–	–	–	–	–
4	–	–	–	–	–	–
5	–	–	–	–	–	–
6	15.0	4.0	10.6	14.3	10.6	8.0
7	15.0	13.3	15.3	16.2	15.0	11.5
8	15.0	21.1	22.2	23.6	15.0	15.0
9	15.0	25.8	26.4	27.3	15.0	15.0
Total	60.0	64.2	74.5	81.4	55.6	49.5

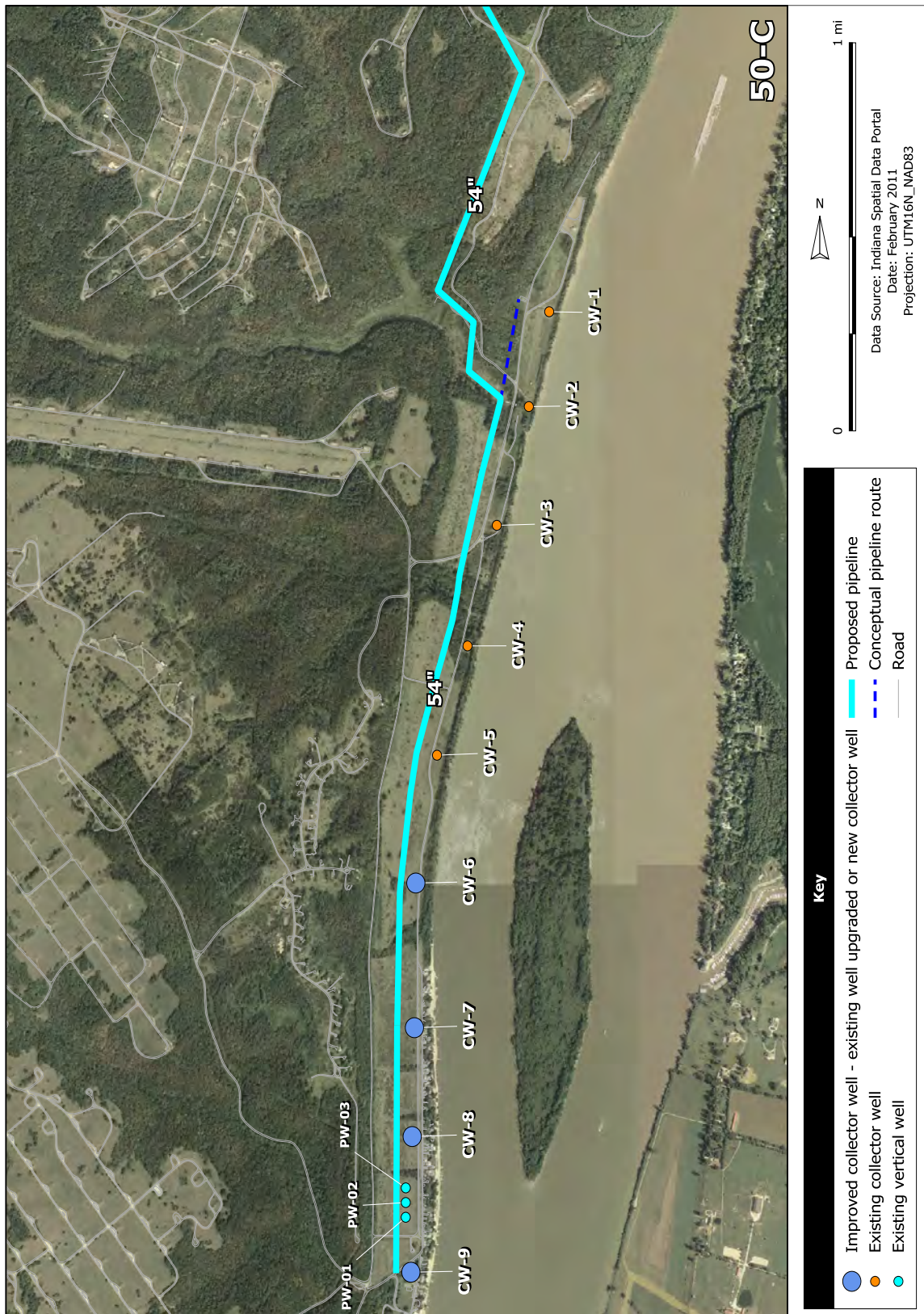


Figure 60: Conceptual layout of Alternative 50-C

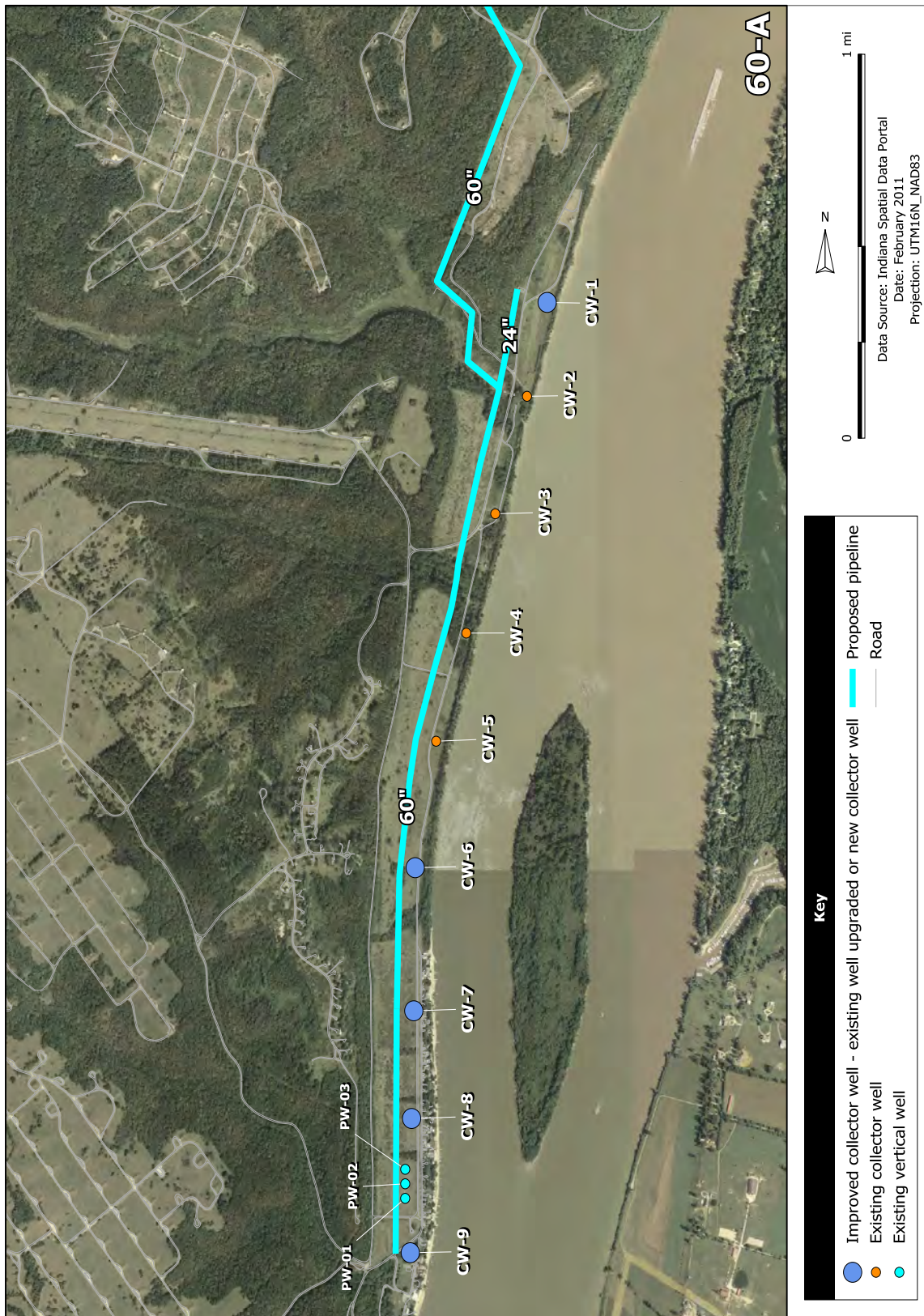


Figure 61: Conceptual layout of Alternative 60-A

Table 33: Results of modeling for 60 mgd, scenario A. All values are in millions of gallons per day (mgd).

Well CW-	Mechanical capacity	Theoretical yield			Design capacity	Sustainable capacity
		Minimum	Best-fit	Maximum		
1	15.0	11.8	11.8	11.9	11.8	8.9
2	–	–	–	–	–	–
3	–	–	–	–	–	–
4	–	–	–	–	–	–
5	–	–	–	–	–	–
6	15.0	4.8	10.6	15.0	10.6	8.0
7	15.0	13.1	15.3	16.2	15.0	11.5
8	15.0	20.8	22.2	23.6	15.0	15.0
9	15.0	25.6	26.4	27.3	15.0	15.0
Total	75.0	76.1	86.3	94.0	67.4	58.4

Table 34: Results of modeling for 60 mgd, scenario B. All values are in millions of gallons per day (mgd).

Well CW-	Mechanical capacity	Theoretical yield			Design capacity	Sustainable capacity
		Minimum	Best-fit	Maximum		
1	–	–	–	–	–	–
2	–	–	–	–	–	–
3	5.6	7.1	7.1	7.3	5.6	5.6
4	5.0	3.6	3.7	3.8	3.7	3.7
5	5.8	4.3	4.3	4.5	4.3	4.3
6	–	–	–	–	–	–
7	15.0	15.3	15.9	23.6	15.0	11.9
8	15.0	21.7	22.2	31.2	15.0	15.0
9	15.0	26.1	26.4	31.4	15.0	15.0
Total	61.4	89.6	90.9	101.8	58.6	55.5

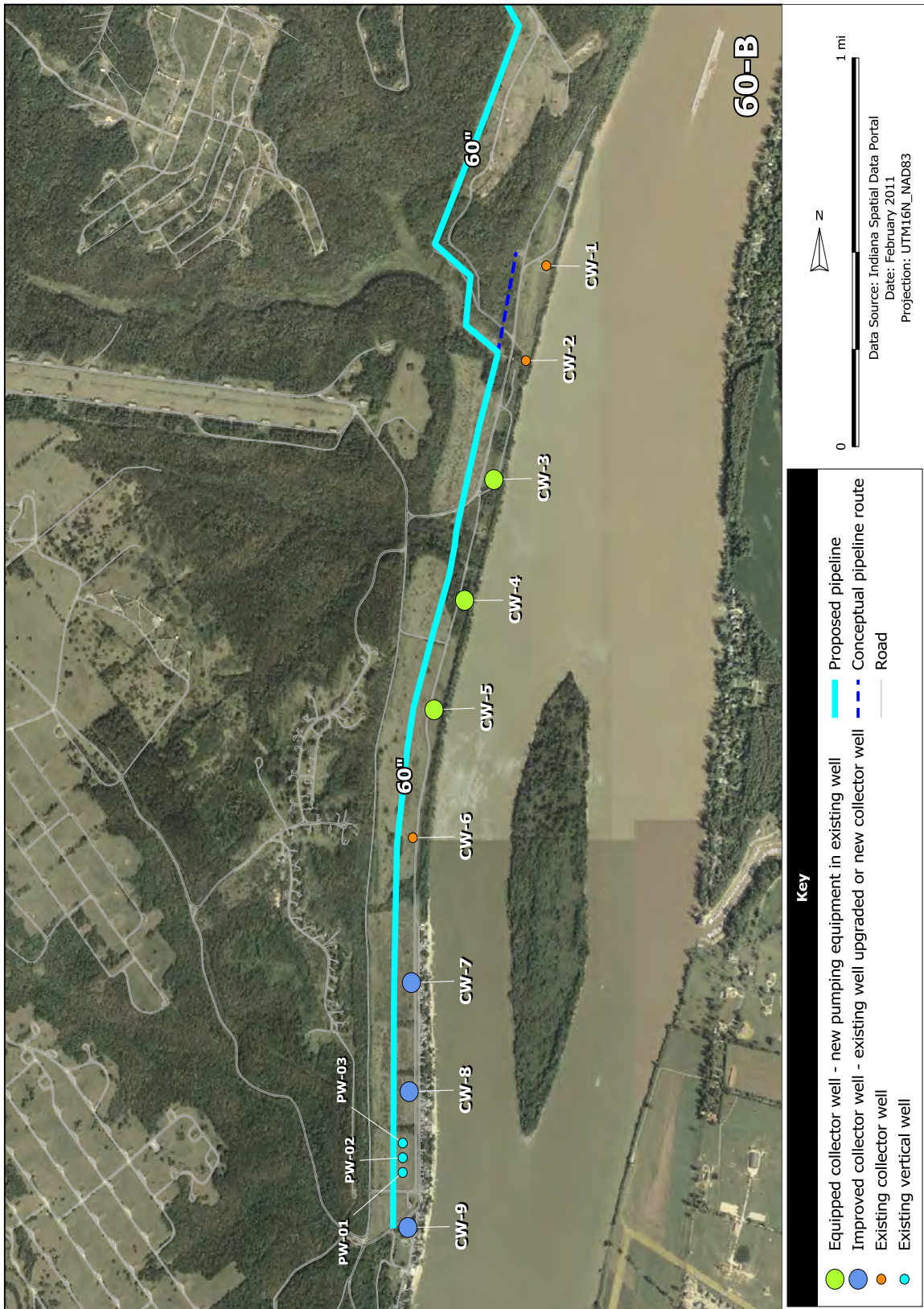


Figure 62: Conceptual layout of Alternative 60-B

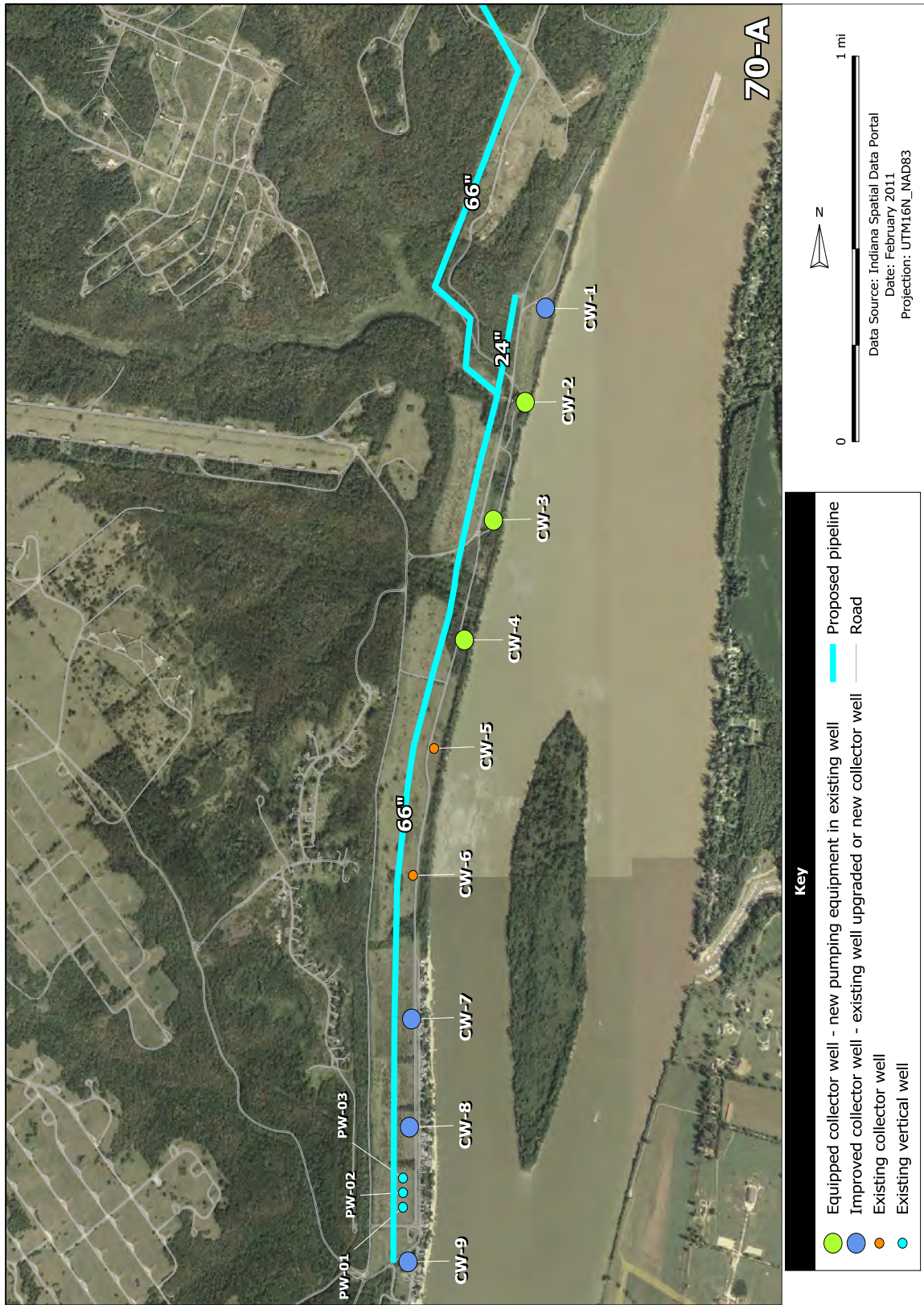


Figure 63: Conceptual layout of Alternative 70-A

Table 35: Results of modeling for 70 mgd, scenario A. All values are in millions of gallons per day (mgd).

Well CW-	Mechanical capacity	Theoretical yield			Design capacity	Sustainable capacity
		Minimum	Best-fit	Maximum		
1	15.0	10.6	10.2	10.0	10.2	7.7
2	4.9	6.2	6.5	6.9	4.9	4.9
3	5.6	6.2	6.5	6.9	5.6	5.6
4	5.0	4.0	3.9	3.9	3.9	3.9
5	–	–	–	–	–	–
6	–	–	–	–	–	–
7	15.0	11.7	16.0	23.7	15.0	12.0
8	15.0	18.7	22.2	31.2	15.0	15.0
9	15.0	24.2	26.4	31.4	15.0	15.0
Total	75.5	81.6	91.7	114.0	69.6	64.1

Table 36: Results of modeling for 80 mgd, scenario A. All values are in millions of gallons per day (mgd).

Well CW-	Mechanical capacity	Theoretical yield			Design capacity	Sustainable capacity
		Minimum	Best-fit	Maximum		
1	15.0	10.8	10.2	10.0	10.2	7.7
2	4.9	6.2	6.5	6.8	4.9	4.9
3	5.6	6.1	6.5	6.8	5.6	5.6
4	5.0	3.7	3.6	3.9	3.6	3.6
5	5.8	4.1	4.0	3.3	4.0	4.0
6	15.0	5.3	10.2	30.5	10.2	7.7
7	15.0	11.1	15.2	21.4	15.0	11.3
8	15.0	18.7	22.1	30.4	15.0	15.0
9	15.0	24.2	26.4	30.9	15.0	15.0
Total	96.3	90.2	104.7	144.0	80.5	74.8

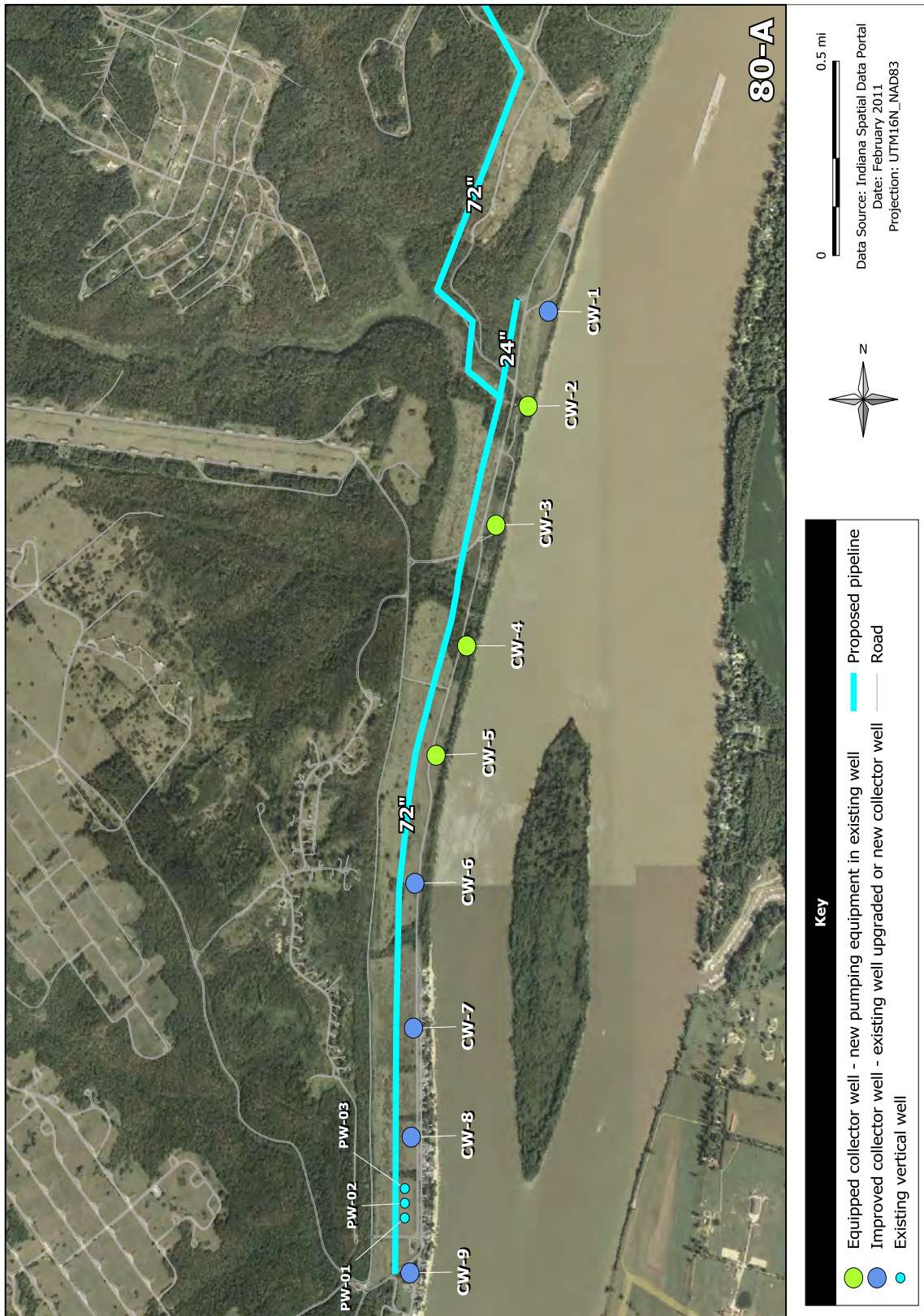


Figure 64: Conceptual layout of Alternative 80-A

Cost estimating

The conceptual cost estimates presented in this report are preliminary in nature and based on limited available information. Conceptual level cost estimates have an estimated accuracy of +40%/-20%. For our conceptual cost estimates, we assumed the following:

- the diameter of pipe used in each alternative is the smallest standard pipe diameter that results in water velocity of 5 ft/sec or less at the nominal capacity (10 mgd, 20 mgd, etc.) of the applicable scenario
- the full length of the well field main is sized for the full capacity of the wells in any given alternative, the diameter is not reduced through the well field
- existing concrete caissons are in adequate condition to allow cleaning, repairs, installation of new pumping equipment, improvement with the installation of additional laterals, and construction of new pump houses.
- existing well houses are not in condition to be improved, and would be demolished and replaced with prefabricated metal buildings.
- none of the existing pumping equipment and related switchgear is usable and will be removed in its entirety and replaced with new equipment.
- existing electrical services are not usable and will be demolished or abandoned and replaced with new wiring, conduit, and equipment.
- none of the existing cast iron pipelines can economically be used. We recommend the installation of new pipelines for the redevelopment of the well field.
- the costs to refurbish and equip an existing collector well include improvements as indicated in Figure 28.
- the costs to refurbish and improve (additional laterals) an existing collector well include improvements as indicated in Figure 29.

The following cost estimates were developed by Reynolds, Inc. (Reynolds, 2011) and used as the basis for the conceptual cost estimates of each alternative. Costs include design and construction, and are estimated to be generally accurate to +40%/-20%.

- Refurbish and equip an existing collector well, 5 mgd pumping capacity - \$4,950,000
- Refurbish and improve an existing collector well, 10 mgd pumping capacity - \$5,523,000

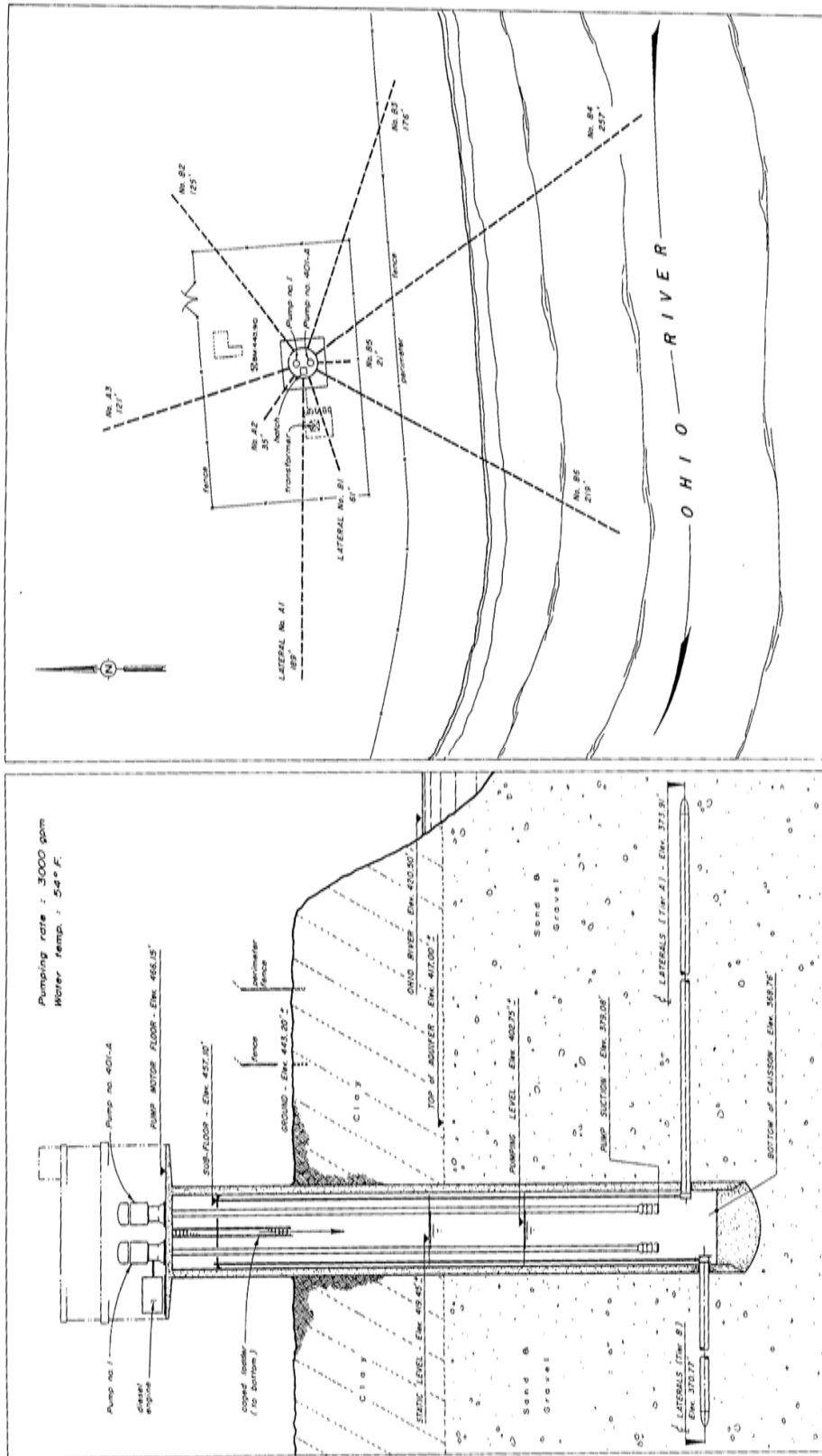
- Refurbish and improve an existing collector well, 15 mgd pumping capacity - \$6,721,000
- Construct a new collector well, 15 mgd pumping capacity - \$6,980,000
- Construct a surface water treatment facility, 10 mgd capacity - \$35,000,000
- Construct a surface water treatment facility, 40 mgd capacity - \$120,000,000
- Construct a surface water treatment facility, 80 mgd capacity - \$160,000,000
- Construct pipelines: 24-inch \$144/ft, 36-inch \$220/ft, 42-inch \$280/ft, 48-inch \$340/ft, 54-inch \$370/ft, 60-inch \$400/ft, 66-inch \$450/ft, 72-inch \$515/ft

Appendix E - Infrastructure Evaluation

Photographs and section and plan views of existing collector wells CW-1 to CW-7 are presented below. The report for the inspection of the caisson of CW-6 is also included.



Figure 65: Collector Well CW-1

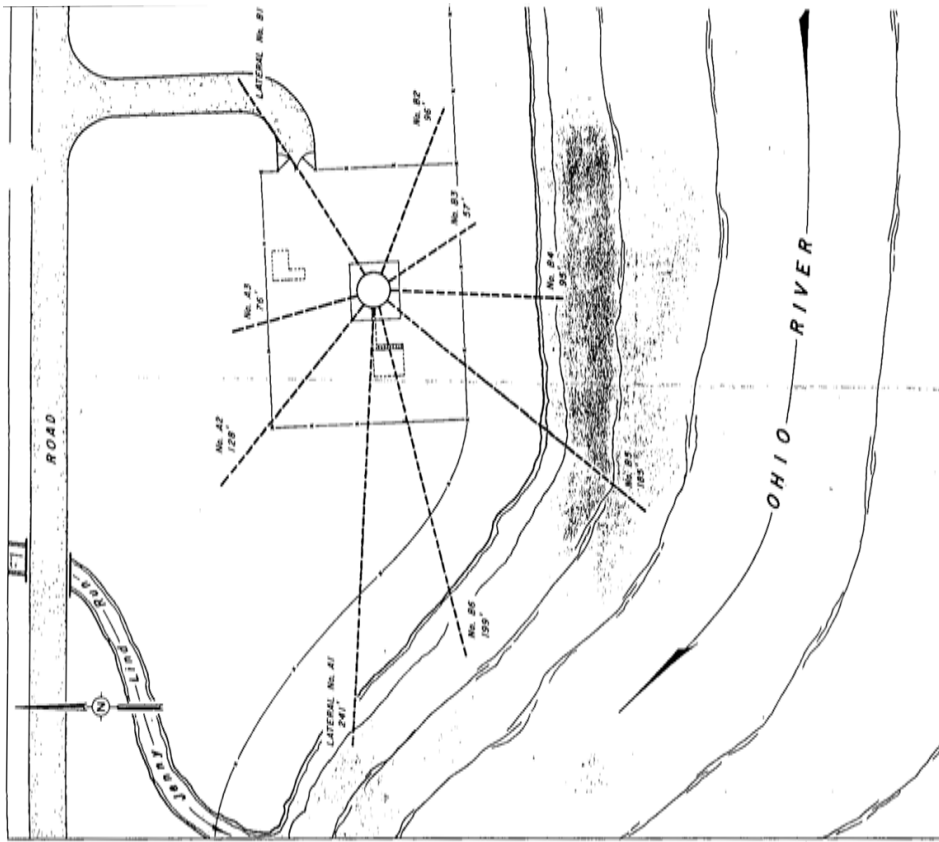


Dwg. No. 1C1-2
SECTION and PLAN VIEWS
of COLLECTOR No. 1

Figure 66: CW-1 Plan & Section (Ranney, 1979)



Figure 67: Collector Well CW-2



Dwg. No. ICI - 3
SECTION and PLAN VIEWS
of COLLECTOR No. 2

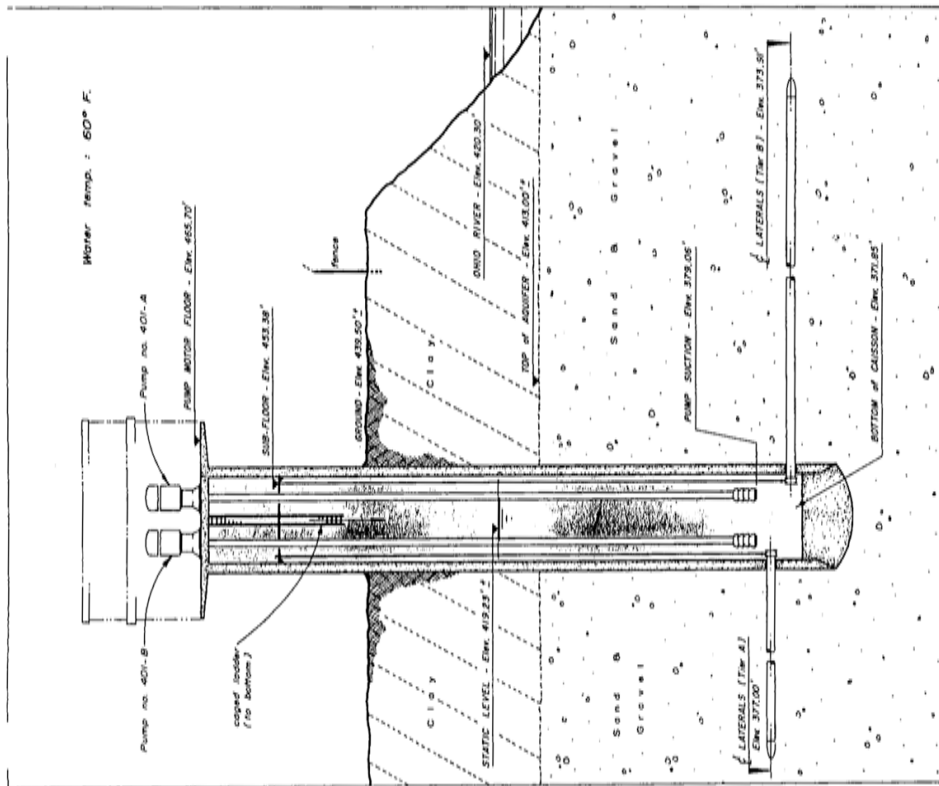
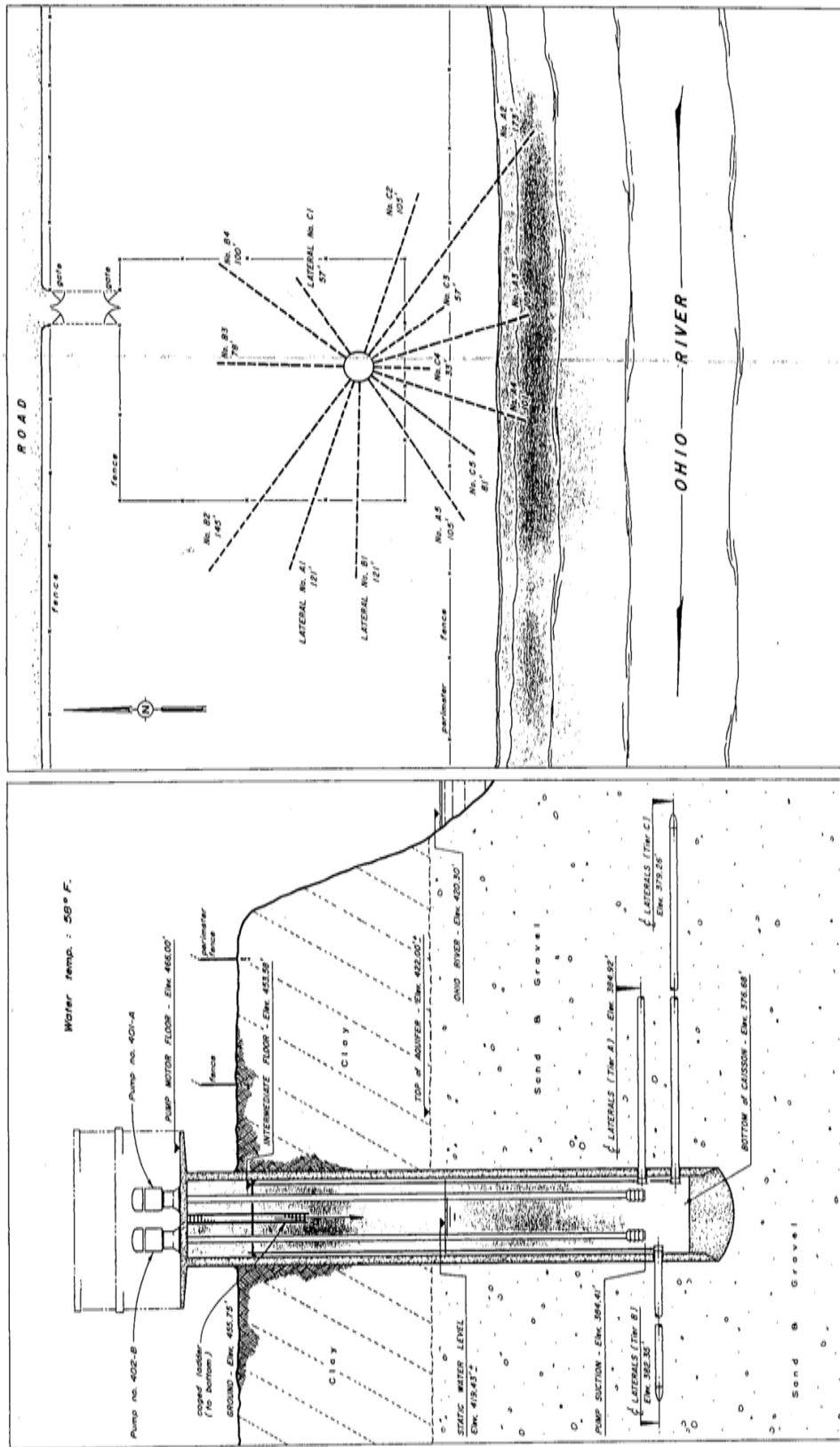


Figure 68: CW-2 Plan & Section (Ranney, 1979)



Figure 69: Collector Well CW-3



Dwg. No. ICI - 4
SECTION and PLAN VIEWS
of COLLECTOR No. 3

Figure 70: CW-3 Plan & Section (Ranney, 1979)



Figure 71: Collector Well CW-4



Figure 73: Collector Well CW-5



Figure 75: Collector Well CW-6

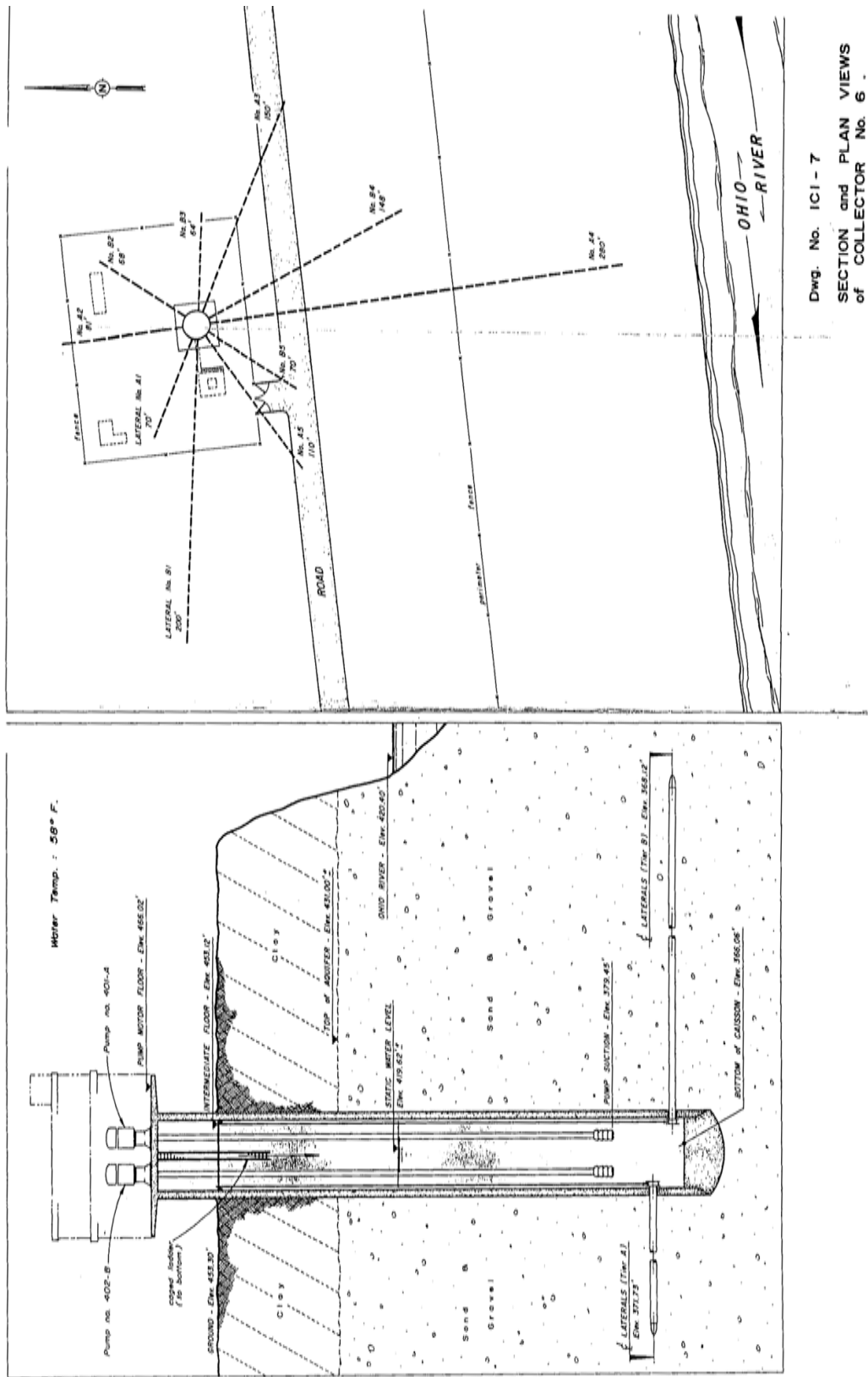
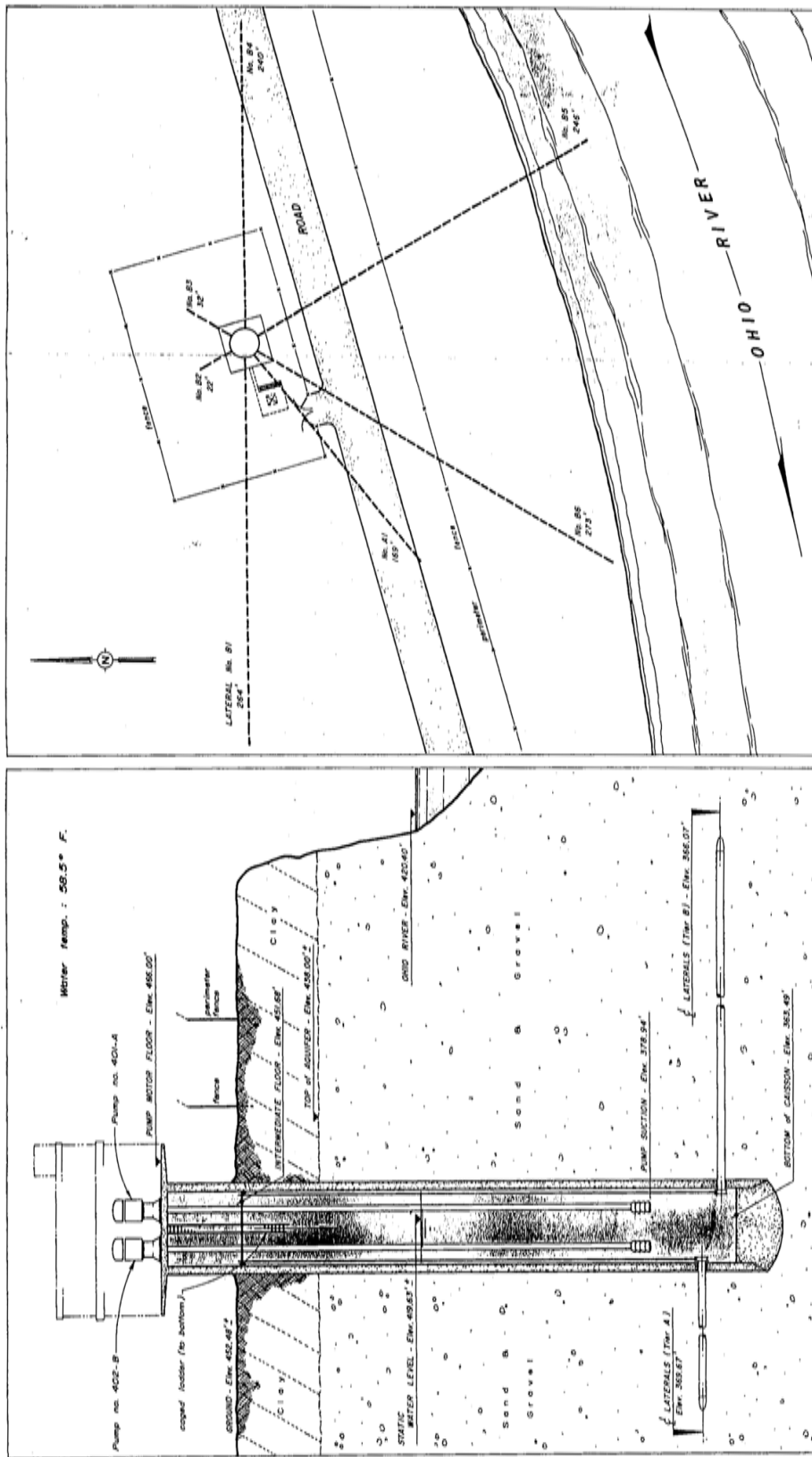


Figure 76: CW-6 Plan & Section (Ranney, 1979)



Figure 77: Collector Well CW-7



Dwg. No. ICI - 8
SECTION and PLAN VIEWS
of COLLECTOR No. 7.

Figure 78: CW-7 Plan & Section (Ranney, 1979)

This page intentionally left blank



6360 Huntley Road • Columbus, OH 43229 • 614.888.6263

MEMORANDUM

To: Dan Haddock / Layne Hydro
From: Matt Reed / Ranney Collector Wells
CC: Mark Nilges & Sam Stowe / Ranney Collector Wells
Re: Collector Well 6 Caisson Concrete Testing, Indiana Army Ammunition Plant, Charlestown, Indiana
Date: February 4, 2011
Attachments: 1) HC Nutting Report of Underwater Concrete Assessment, March 2, 2011
2) HC Nutting Inspection DVD

Pursuant your request, Ranney Collector Wells mobilized equipment, personnel and subcontractors to the Indiana Army Ammunition Plant, Charlestown, Indiana to perform an underwater assessment of the concrete caisson at Collector Well 6. The assessment was undertaken to determine the extent of concrete deterioration described in previous inspections and documented in a June 1995 report entitled "Evaluation and Testing of Horizontal Collector Well Nos. 4,5 and 6 at Indiana Army Ammunition Plant" completed by Burgess & Niple, Limited for Indiana-American Water Company.

The 1995 report referenced above describes surficial deterioration of concrete near the base of the caisson. The deterioration is described as including areas of pitting that were "soft and chalky". The report also describes a three-foot long crack, 1 to 1.5 inches wide and three inches deep. Because of the reported extent of this deterioration, it was proposed that the concrete be examined specifically to confirm the structural integrity of the caisson.

Background

Collector Well 6 was constructed in 1941 as part of the water supply for the Indiana Army Ammunition Plant. Previous inspections of the well indicate the caisson is approximately 100 feet in overall length, with an inside diameter of 13 feet. The caisson walls are reported to be 18 inches thick.

Ten laterals are located equally in two tiers at the base of the caisson and are constructed of 8-inch diameter slotted steel pipe. Total lateral length is reported to be 1241 feet. A third tier of ports is located above the two lateral tiers, but was not used. In 1994, the well had a calculated design yield of between 4 and 8 million gallons per day (based upon entrance velocity criteria), although the aquifer at Collector Well 6 is reported to potentially yield in excess of 13 million gallons per day.

Field and Testing Activities

Personnel and equipment mobilized to Collector Well 6 on February 16, 2011 and a temporary pump was set in the well. That pump was operated at approximately 800 gallons per minute for four hours on February 17, 2011 to remove stagnant water from the caisson and improve underwater visibility. The pumped water was discharged on the ground adjacent to the well.



6360 Huntley Road • Columbus, OH 43229 • 614.888.6263

After pumping, a diver from HC Nutting entered the well and performed an inspection on the sections of the caisson below water level. That inspection was remotely witnessed by Ranney personnel experienced in caisson construction and general concrete installation. A video obtained by the diver during the inspection is attached to this memorandum.

Diving personnel returned to the well on February 26 and February 27, 2011 to collect core samples of the concrete in areas selected during the February 17 inspection. The cores were transported to the HC Nutting Laboratory where they were subjected to testing pursuant ASTM Method C-42 (compressive strength). After each core was extracted, the cored area was patched with hydraulic cement.

The concrete cores were collected in three areas:

- Core C-1. Collected from an area at the interface between honeycombed concrete and concrete with a “normal” appearance,
- Core C-2. Collected from an area of honeycombed concrete, and
- Core C-3. Collected from an area of concrete with a “normal” appearance.

A more complete description of the cores is included in the HC Nutting report attached to this memorandum.

Results

As noted above, a video of the inspection dive is included with this memorandum. The inspection documented a number of areas in the bottom ten feet of the caisson where the concrete was pitted or “honeycombed”. While the crack noted in the 1994 report as existing between laterals 13 and 14 and eight feet above the caisson floor was not identified, a linear area of deteriorated concrete (possibly a cold joint) was located in the general vicinity that may have previously been mistaken for a crack.

Visual inspection of Cores C-1 and C-3 indicate the concrete appears to be in good condition. Compressive strength testing indicates the concrete at Cores C-1 and C-3 have strengths in excess of 7500 pounds per square inch (psi).

Visual inspection of Core C-2 indicates the honeycombing is extensive at the core surface and extends approximately two inches from the interior caisson surface. The honeycombing does not extend to rebar encountered in the core. Beyond the honeycombing, the concrete appears to be in good condition. The testing on Core C-2 was not completed because rebar encountered in the core invalidates the test assumptions.

Conclusions and Recommendations

Based upon the results of the inspection, it appears that the lower portion of the Collector Well 6 caisson is structurally sound. While there are a number of areas with surficial deterioration, including honeycombing and a possible cold joint, the blemishes appear to be surficial and do not seriously compromise the overall strength of the concrete. As a result, it appears there is no



6360 Huntley Road • Columbus, OH 43229 • 614.888.6263

structural damage to the Collector Well 6 caisson that would impede the coring of ports for new laterals to replace or supplement the existing laterals.

March 2, 2011



Ranney Collector Wells
Mr. Matthew Reed
6360 Huntley Road
Columbus, Ohio 43229
(614) 888-6263
(614) 888-9208 fax
mtreed@ranneymethod.com

**RE: Report of Underwater Concrete Assessment
Wells #6
Charlestown, Indiana
Terracon Project No. N1111031**

Dear Mr. Reed:

As requested, diving personnel from H.C. Nutting, A Terracon Company (HCN) traveled to the above-mentioned project site to perform an underwater assessment of the interior of the concrete collector well.

Prior to performing the inspection, the dive team had the opportunity to review a previous inspection report from Burgess and Niple, Limited dated June 1995. This report discusses two prior underwater inspections; the most recent performed in March of 1995, and one performed in July of 1994. In both reports it was mentioned that the internal exposed concrete caisson surface was "pitted". In the March 1995 report, the diver stated the "entire underwater portion of the concrete caisson to be pitted with ¼ to 2-½ inch deep pits. The pitted areas were noted to be "soft and chalky". Furthermore, it denotes a crack roughly 8 feet above the well bottom and varied in width from 1 to 1-½ inches and at least 3 inches in depth.

The July 1994 report mentioned "the lower 6 to 7 feet of the caisson indicated some signs of surficial deterioration" with numerous areas of small pits, ¼ inch in and ½ inch deep. A larger deteriorated area near lateral No. 11 was roughly 10" x 6-½" and up to 1 inch deep. During our inspection, we observed the above mentioned areas and assessed the present condition.



H.C. Nutting, a Terracon Company, 611 Lunken Park Drive, Cincinnati, Ohio 45226
P [513] 321-5816 F [513] 321-4540

Geotechnical



Environmental



Construction Materials



Facilities

UNDERWATER OBSERVATION

Upon reaching the bottom of the concrete collector well caisson, HCN divers observed the numerous areas of rock pockets or honeycombing in which coarse aggregate without surrounding fines or cement past was noted, indicating poor consolidation. The largest area was estimated to be approximately 2 feet in length, 12 inches in height and a maximum depth of 3 inches. We assume that the rock pockets or honeycombed areas are what the previous inspection noted as “pitted”. The depth of water within the well was 49 feet at the time of the inspection. The worst or wide spread areas are confined to the last ten feet of the well (39 to 49 feet in depth); however, other areas of isolated rock pockets or honeycombing were observed at lesser depths between 0 and 39 feet.

We were unable to locate the crack noted in the March 1995 report in which the diver describes a crack roughly 8 feet above the well bottom and varied in width from 1 to 1-½ inches and at least 3 inches in depth. The area could possibly be a rough cold or construction joint that was observed in that approximate area.

In general observation of the interior concrete surfaces, the areas of rock pockets or honeycombing were noted to be “soft and chalky” the aggregate could be chipped away easily, however the other areas of solid concrete were noted to be hard & sound. When scarified or scraped with an “awl” type tool with moderate pressure only a 1/16 inch gouge was present. Moreover, hammer soundings were performed randomly along the concrete surface from the bottom of the well to approximately 1 foot above of the water line, as well as around the worst areas of rock pockets or honeycombing to detect potential voids within the structure. No areas of unsound concrete (delaminations, voids, etc.) were able to be detected.

CORING OPERATION

HCN used an underwater pneumatic core drill and specialized core bit to cut and extract three cores from the interior concrete wall. The cores were extracted from approximately the last five feet (near the bottom) of the well.

Core C-1, with the well plan view figuratively representing the face of an analog clock, with 12 o'clock designated as the point of the interior well ladder. C-1 was cut and extracted from the vertical wall in approximately the 7 o'clock position, approximately 4 feet above the well floor. C-1 was extracted at the interface of a honeycombed area and concrete considered “good”. Upon extraction, the core hole was patched using fast setting hydraulic cement, however the patch is purely cosmetic.

C-1 was subjected to a laboratory compressive strength in accordance to ASTM C-42.

Please see the information regarding the core description and compressive strength found in appendix 1.

Core C-2, with the well plan view figuratively representing the face of an analog clock, with 12 o'clock designated as the point of the interior well ladder. C-2 was cut and extracted from the vertical wall in approximately the 7 o'clock position approximately 6 inches from C-1 and approximately 4 feet from the well floor. C-2 was extracted from within the boundaries of a honeycombed area. Upon extraction, the core hole was patched using fast setting hydraulic cement, however the patch is purely cosmetic.

C-2 was unsuitable to perform laboratory compressive strength in accordance to ASTM C-42, due to the presence of reinforcing steel bars in the core and the inability to achieve a minimum 1:1 ratio of length to diameter..

Please see the information regarding the core description and compressive strength found in appendix 1.

Core C-3, with the well plan view figuratively representing the face of an analog clock, with 12 o'clock designated as the point of the interior well ladder. C-3 was cut and extracted from the vertical wall in approximately the 1 o'clock position approximately 3 feet from the well floor. C-3 was extracted from an area that showed no visible signs of distress. Upon extraction, the core hole was patched using fast setting hydraulic cement, however the patch is purely cosmetic.

C-3 was subjected to a laboratory compressive strength in accordance to ASTM C-42.

Please see the information regarding the core description and compressive strength found in appendix 1.

INTERIOR WELL COMPONENTS

With exception of the interior well ladder, the interior well components, i.e., pump columns and valves were found to be moderately to heavily corroded and pitted.

The timber pump column support bracing was found to be in good condition with no visible sign of rot or decay.

CLOSING

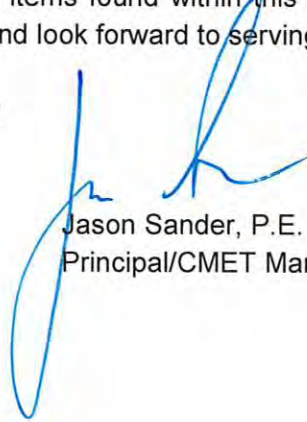
We trust that this information meets your current needs. Please contact us should you have any questions or need any clarifications of items found within this report. It has been a pleasure assisting you in regard to this project, and look forward to serving you again in the future.

Respectfully submitted,

H.C. NUTTING, A Terracon Company



Brad Walden
Diving Services Manager



Jason Sander, P.E.
Principal/CMET Manager

Attachments: Appendices 1 & 2

APPENDIX 1
CORE DESCRIPTION

C-1 CORE DESCRIPTION

Cut and extracted on February 26, 2011

Length: 8 ½ inches

Nominal Diameter: 3 ¾ inches

Maximum Coarse Aggregate Size: 1-½ inches, consisting of natural gravel sub-rounded to subangular. Moderately to tightly packed.

Concrete appears overall in good condition. Concrete appears to be well consolidated the entire length of the extracted core with no dominant particle orientation or aggregate segregation, but with a subtle particle orientation at a low angle to the core axis.

Coarse aggregate consist predominantly of Limerock (Limestone/Dolomite) with subordinate sandstone and chert. Particles are fresh, moderately hard to hard, tough and moderately dense to dense. Particles appear to be durable.

Fine aggregate is natural sand and was not examined in detail.

Moderate amount of entrapped ovoid air voids (1/8 inch maximum size) was noted.

No concrete reinforcing steel was observed in the extracted core.

C-1 was subjected to a laboratory compressive strength in accordance to ASTM C-42. The corrected compressive strength of the specimen was 7,730 psi. Please see attached Laboratory Data Sheet for additional Information.



C-2 CORE DESCRIPTION

Cut and extracted on February 26, 2011

Length: 6-3/4 inches

Nominal Diameter: 3-3/4 inches

Maximum Course Aggregate Size: 1-1/2 inches, consisting of natural gravel sub-rounded to subangular. Moderately to tightly packed.

Concrete appears overall in fair condition. A rock pocket, i.e., all coarse aggregate without surrounding fines or cement paste was noted on the core surface. The rock pocket extends into the core about 2 inches from the surface. Beyond that, the concrete is uniform and similar in characteristic and composition to C-1.

Fine aggregate is natural sand and was not examined in detail.

Minor amount of entrapped ovoid air voids (5/8 inch maximum size) was noted.

Concrete reinforcing steel was observed in the extracted core. All observed bars were noted to be 3/4 inch diameter or #6 bars. The reinforcing steel shows no signs of corrosion and is surrounded entirely by paste matrix.

The first bar was observed at 2-1/4 inches from the face, while the second bar was 3-3/4 inches and the third bar noted at 4-1/4 inches from the face.

C-2 was not suitable for to perform a laboratory compressive strength in accordance to ASTM C-42 because of the reinforcing steel in the sample.



C-3 CORE DESCRIPTION

Cut and extracted on February 27, 2011

Length: 10-¼ inches

Nominal Diameter: 3-¾ inches

Maximum Coarse Aggregate Size: 1-¾ inches, consisting of natural gravel sub rounded to sub angular. Moderately to tightly packed.

Concrete appears overall in good condition and is similar in composition and characteristic to C-1.

Minor amount of entrapped ovoid air voids (1/8 inch maximum size) was noted.

Concrete reinforcing steel was not observed in the extracted core.

C-3 was subjected to a laboratory compressive strength in accordance to ASTM C-42. The corrected compressive strength of the specimen was 8,500 psi. Please see attached Laboratory Data Sheet for additional Information



APPENDIX 2
CORE REPORT



CORE REPORT - ASTM C-42

Client:	<u>Ranney Collector Wells</u>	Order No.	<u>N1111031</u>
Project:	<u>Diving – Charlestown, Indiana</u>	Date Typed:	<u>3-2-11</u>
	<u>(Well #6)</u>	Date Drilled:	<u>2-26 & 2-27-11</u>

Description of Pavement or Structure: Vertical well of concrete collector well, Well #6

Lab No.	1458	1459		
Identification	C-1	C-3		
Location of Core				
Condition of Core	Good	Good		
Length of Core (Approx)	10"	10"		
Thickness Required				
Depth of Reinforcement	N/A	N/A		
Type of Coarse Agg.	N/A	N/A		
Mixture Used	Unknown	Unknown		
Condition of Sub Soil	N/A	N/A		
Date Concrete Placed	N/A	N/A		
COMPRESSION TESTS				
Date Tested	3-2-11	3-2-11		
Weight, Lbs.	7.10	6.96		
Age of Concrete				
Length of Core (in.)	7.49	7.42		
Diameter of Core (in.)	3.70	3.70		
Area of Core (sq.in.)	10.75	10.75		
Capped Length (in.)	7.829	7.644		
Ratio Length to Dia.	2.13	2.07		
Correction Factor	---	---		
Total Load, Lbs.	83,162	91,170		
Uncorrected Strength (psi)	7,734	8,479		
Corrected Strength (psi)	7,730	8,500		

Remarks:

HCN / a Terracon Company



H.C. Nutting, a Terracon Company. 611 Lunken Park Drive. Cincinnati, Ohio 45226
P [513] 321-5816 F [513] 321-0294 terracon.com

